



<https://theses.gla.ac.uk/>

Theses Digitisation:

<https://www.gla.ac.uk/myglasgow/research/enlighten/theses/digitisation/>

This is a digitised version of the original print thesis.

Copyright and moral rights for this work are retained by the author

A copy can be downloaded for personal non-commercial research or study, without prior permission or charge

This work cannot be reproduced or quoted extensively from without first obtaining permission in writing from the author

The content must not be changed in any way or sold commercially in any format or medium without the formal permission of the author

When referring to this work, full bibliographic details including the author, title, awarding institution and date of the thesis must be given

Enlighten: Theses

<https://theses.gla.ac.uk/>  
[research-enlighten@glasgow.ac.uk](mailto:research-enlighten@glasgow.ac.uk)

THE STRUCTURE OF SYMMETRIC PERIODIC SOLUTIONS  
OF THE RESTRICTED THREE-BODY PROBLEM

by

Iain A. Robin, B.Sc.

Thesis submitted to the  
University of Glasgow  
for the degree of  
Ph.D.

Department of Astronomy,  
University of Glasgow,  
Glasgow, G12 8QQ.

October, 1980

ProQuest Number: 10760462

All rights reserved

INFORMATION TO ALL USERS

The quality of this reproduction is dependent upon the quality of the copy submitted.

In the unlikely event that the author did not send a complete manuscript and there are missing pages, these will be noted. Also, if material had to be removed, a note will indicate the deletion.



ProQuest 10760462

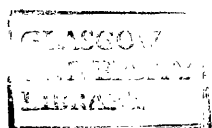
Published by ProQuest LLC (2018). Copyright of the Dissertation is held by the Author.

All rights reserved.

This work is protected against unauthorized copying under Title 17, United States Code  
Microform Edition © ProQuest LLC.

ProQuest LLC.  
789 East Eisenhower Parkway  
P.O. Box 1346  
Ann Arbor, MI 48106 – 1346

Thesis  
6310  
Copy 1.



to my wife, Elizabeth,

and my parents

O LORD, our Lord,  
how majestic is your name in all the earth!  
You have set your glory  
above the heavens.  
From the lips of children and infants  
you have ordained praise  
because of your enemies,  
to silence the foe and the avenger.

When I consider your heavens,  
the work of your fingers,  
the moon and the stars,  
which you have set in place,  
what is man that you are mindful of him,  
the son of man that you care for him?  
You made him a little lower than the heavenly beings  
and crowned him with glory and honour.

You made him ruler over the works of your hands;  
you put everything under his feet:  
all flocks and herds,  
and the beasts of the field,  
the birds of the air,  
and the fish of the sea,  
all that swim the paths of the seas.

O LORD, our Lord,  
how majestic is your name in all the earth!

Psalm 8  
(New International  
Version)

## PREFACE

This thesis presents the results of a numerical investigation into the structure of symmetric periodic solutions of the restricted three-body problem, and in particular, the relationships between families of planar and three-dimensional periodic orbits, and between families in the circular and elliptic versions of the restricted problem. The numerical techniques used in the determination of families and series of symmetric periodic orbits in each of the different versions of the problem are also described.

Chapters 1 and 2 and the first five sections of Chapter 3 form an introduction to the restricted problem, with emphasis on periodic orbits and their properties, such as symmetry and stability. The remaining section of Chapter 3 is concerned with bifurcations of planar with three-dimensional periodic orbits. Chapter 4 deals with numerical techniques for determining periodic orbits; in Chapters 5 - 8, various aspects of the structure and classification of symmetric periodic solutions are discussed, and numerical examples are given to illustrate each of these aspects. The original material contained in this thesis begins with Section 3.6 of Chapter 3, and includes Chapter 4 (with the exception of Section 4.2), together with Chapters 5 - 8. The bulk of the content of Chapters 4 and 5 has been published in the journal "Celestial Mechanics", Vol. 21, pp. 395 - 434 (with Dr. V. Markellos); a second paper presenting some of the results given in Chapter 7 has been accepted for publication in the same journal.

The numbering of tables, figures and equations in this thesis follows the usual decimal notation indicating the chapter to which each belongs. Computer plots of representative periodic orbits belonging to the families discussed in Chapters 5 - 8 are given in the Appendix, and are numbered A1, A2, A3... etc.

I would like to take this opportunity to thank a number of people who have helped me in the course of my work. I am grateful for financial support in the form of a Research Studentship provided by the Science Research Council. It is my pleasure to thank my supervisors, Prof. A.E. Roy and Prof. P.A. Sweet, for their help and encouragement over the last three years; special thanks go to Dr. (now Prof.) V.V. Markellos for numerous invaluable discussions and for suggesting many

of the topics upon which the work of this thesis is based. The assistance of Dr. P. Rosenberg of the University of Glasgow in providing the necessary numerical integration routines, and general advice on the running of computer programs, is appreciated. I would like to record my gratitude to Mrs. L. Williamson for her efficient typing of most of the tables, and to Mrs. M. Morris and Mr. P. McHaffie for preparing the diagrams. Last, but not least, thanks go to my wife Elizabeth for typing this thesis.

## CONTENTS

	Page
SUMMARY	1
1. THE RESTRICTED PROBLEM	3
1.1 Introduction	3
1.2 Applications	7
1.3 Equations of Motion	9
1.4 The State Vector	19
1.5 Jacobi Integral	21
1.6 Lagrange Solutions	23
2. PERIODIC ORBITS	27
2.1 Introduction	27
2.2 Definition and Classification	30
2.3 Periodicity Conditions	32
2.4 Symmetry Classes	38
2.5 Families and Series of Periodic Orbits	41
2.6 Strömngren Classification	43
3. STABILITY, SELF-RESONANCE AND BIFURCATION	46
3.1 Introduction	46
3.2 Variational Equations	47
3.3 Variations with respect to the Parameters	51
3.4 Stability	54
3.5 Bifurcation	61
3.6 Vertical Bifurcations of Symmetric Periodic Orbits	65
4. NUMERICAL TECHNIQUES	77
4.1 Introduction	77
4.2 Calculation of the Variational Matrix	79
4.3 Differential Correction	82
4.4 Predictor Algorithms	87
4.5 Selection of Family Parameter	93
4.6 Numerical Determination of Vertical Branches	96

	Page
5. VERTICAL BRANCHES OF FAMILY $f$ IN THE SUN-JUPITER CASE OF THE CIRCULAR RESTRICTED PROBLEM	101
5.1 Introduction	101
5.2 Simply-Symmetric Branches	106
5.3 Doubly-Symmetric Branches	115
5.4 Stability of Branch Orbits	121
5.5 Remarks	125
6. CONTINUATION OF PERIODIC ORBITS FROM THE CIRCULAR INTO THE ELLIPTIC RESTRICTED PROBLEM	128
6.1 Introduction	128
6.2 Planar Orbits	131
6.3 Three-Dimensional Orbits	134
6.4 Numerical Examples	136
6.5 Remarks	143
7. VERTICAL BIFURCATION SERIES	148
7.1 Introduction	148
7.2 Numerical Determination	150
7.3 Results: Circular Restricted Problem	157
7.4 Results: Elliptic Restricted Problem	164
7.5 Further Results	172
8. BIFURCATION IN THREE DIMENSIONS	178
8.1 Introduction	178
8.2 Numerical Results	179
8.3 Remarks	184
9. SUGGESTIONS FOR FURTHER WORK	186
10. REFERENCES	189
11. APPENDIX: ORBIT PLOTS	192

## SUMMARY

This thesis is concerned with the structure of symmetric periodic solutions of the restricted three-body problem, in the cases of planar and three-dimensional motion of the massless third particle, and for circular and elliptic motion of the two massive primaries. Particular emphasis is placed on the relationships existing between families of periodic orbits in the different versions of the problem, and on numerical methods of continuing periodic orbits in the simplest version of the restricted problem, the planar circular case, into the more general versions of the problem.

The restricted three-body problem is introduced in Chapter 1; applications to actual physical systems are discussed, and a derivation of the equations of motion in their usual form is offered. The Jacobi integral and the Lagrange equilibrium solutions are also obtained for later reference. Chapter 2 deals with periodic orbits and their significance from both the theoretical and practical points of view; symmetry properties and periodicity conditions are discussed in terms of the two possible types of "mirror configuration" in the restricted problem. The existence of monparametric sets or families of periodic orbits in both the circular and elliptic versions of the restricted problem, for a fixed value of the mass parameter of the primaries, is discussed in this chapter, and Strömberg's and Hénon's explorations of the planar circular problem are briefly reviewed.

A first-order treatment of variations in a periodic orbit resulting from small changes in the initial conditions is given in Chapter 3, and this is used to establish the usual linear stability criterion. Variations resulting from small changes in the parameters  $\mu$  (mass parameter) and  $e$  (orbital eccentricity) of the primaries are also introduced for use in subsequent chapters. The bifurcation, or branching, of families of periodic orbits (for fixed  $\mu$ ) is discussed in general terms, with a more detailed analysis in the particular case of "vertical" bifurcations, that is, bifurcations of planar with three-dimensional periodic orbits. Numerical techniques for establishing families of three-dimensional symmetric periodic orbits are described in Chapter 4, with particular reference to the numerical determination of "vertical branches", or families of three-dimensional orbits generated from vertical bifurcations.

The results of a numerical investigation of the vertical branches of Strömberg's family  $f$ , in the Sun-Jupiter case ( $\mu = 0.00095$ ) of the circular problem, are given in Chapter 5 to illustrate the foregoing discussion. Examples corresponding to each kind of vertical bifurcation, and all possible symmetry classes, are given. The results confirm the prediction that families of three-dimensional orbits bifurcating vertically from the plane occur in pairs, and the predicted relationship between symmetry properties and multiplicity is observed. With a single exception, the vertical branches investigated are found to connect the families of retrograde and of direct satellite orbits about the less-massive primary (Jupiter).

The continuation of periodic orbits of the circular restricted problem into the elliptic case is discussed in Chapter 6. Three-dimensional as well as planar periodic orbits are considered, and it is shown that for any commensurability in the period with that of the primaries, two families of periodic orbits of the elliptic problem can always be obtained from a commensurable orbit of the circular problem. To illustrate the discussion, numerical examples are presented for each type of commensurability, including orbits of both simple and double symmetry.

Chapter 7 deals with the numerical determination of series of vertical bifurcation orbits, for which the vertical stability index  $a_v$  is kept constant and the mass parameter  $\mu$  is allowed to vary. The importance of this type of series (from any orbit of which may be generated either one or two entire families of three-dimensional periodic orbits), with regard to the structure of symmetric periodic solutions, is discussed, and numerical examples in both the circular and elliptic cases of the restricted problem are offered, together with an instance of the continuation of planar periodic orbits of the elliptic restricted problem into three dimensions.

Chapter 8 presents the results of a preliminary investigation into the phenomenon of three-dimensional bifurcation: that is, the intersection of two families of periodic orbits in three dimensions. Numerical examples given in this chapter include a family of three-dimensional orbits which appears to terminate in a planar orbit with consecutive collisions, and a family originating from a quadruple bifurcation in three dimensions.

## 1. THE RESTRICTED PROBLEM

### 1.1 Introduction

The restricted three-body problem is perhaps the most celebrated problem of dynamics, and has occupied an important place in the development of dynamical and mathematical techniques for over two centuries. Simple in its formulation, yet of great complexity in the structure of its solutions, the restricted problem has absorbed the interest of great mathematicians such as Euler, Lagrange, Jacobi, Poincaré and Birkhoff. The restricted problem rests on the firm foundation of classical Newtonian physics (Newton's laws of motion and of gravitation) and so presents an appealing purity and simplicity not often found in other fields of intellectual endeavour.

One way of defining the restricted three-body problem would be to start with what is usually referred to as the "N-body problem", the problem of the motion of N massive particles under the sole influence of their mutual gravitational interactions, following Newton's famous law, which states that the force of attraction between any two bodies (in the point-mass approximation) is proportional to each of their masses and inversely proportional to the square of the distance between them. Thus each of the N bodies is attracted by the N-1 others, and experiences an acceleration proportional to the vector sum of the N-1 forces. For arbitrary values of N, the problem is extremely complicated, and it has been found that only for  $N = 2$  is it possible to obtain a complete analytical solution; the addition of one further particle to the system renders the problem non-integrable and discouragingly complicated. (The two-body problem is said to be "integrable" because it possesses a sufficient number of integrals of the motion to allow the state of the system to be determined at any epoch given only the values of the integrals; a "non-integrable" problem is one for which an insufficient number of integrals exists to allow the direct determination of the exact state of the system at an arbitrary epoch). A considerable reduction in the complexity of the "general" three-body problem results when the mass of one of the three particles is taken to be so small that it has no effect on the motion of the other two. The two massive particles, referred

to as the "primaries", then behave as a two-body system, and their motion can be determined; it remains only to find the motion of the third body of infinitesimal mass. This modification of the three-body problem, still non-integrable, is termed the "restricted" problem.

The most general form of the restricted problem is usually considered to be the "three-dimensional elliptic restricted problem"; "three-dimensional" refers to the orbit of the third body, and "elliptic" to the orbit of the primaries. It is well known that there are three categories of solutions of the two-body problem: elliptic, parabolic and hyperbolic, according as the total energy of the system is negative, zero or positive, respectively. In the restricted problem, the primaries are conventionally taken to move in an elliptic relative orbit; the cases of parabolic and hyperbolic motion of the primaries would not be expected to result in "interesting" solutions for the motion of the third particle, except perhaps during a finite time interval around the instant of pericentre passage of the primaries. Virtually all applications of the restricted problem in celestial mechanics involve an elliptical orbit of the primaries, and it is obvious that periodic solutions of the restricted problem can only occur in the elliptic case.

There are two important simplifications of the three-dimensional elliptic restricted problem. The first of these results when the eccentricity of the elliptic orbit of the primaries is taken to be zero, and is referred to as the "circular restricted problem". There are several important differences between the circular (zero eccentricity) and elliptic (non-zero eccentricity) cases, the most important of which is that there exists an integral of the circular problem (the Jacobi integral), while no integral exists for the elliptic problem. Because of its greater simplicity and the small eccentricities normally encountered in applications, the circular problem has received much more attention than the elliptic case.

The second important simplification is termed the "planar restricted problem", and arises because of the property that if at any instant the massless third body lies in the orbital plane of the primaries,

with its velocity vector also in the plane, its subsequent motion will be confined to that plane. It is therefore possible to consider only planar motion of the third body in the plane of the primaries (or "horizontal" plane). In many applications of the restricted problem, the actual motion is almost two-dimensional, and the planar approximation is therefore quite a good one.

The "circular" and "planar" simplifications can be applied independently, resulting in a total of four versions of the restricted problem: the planar circular case, the three-dimensional circular case, the planar elliptic case and, finally, the three-dimensional elliptic case. Of these four versions, the planar circular restricted problem is the simplest and has been most extensively explored. A special case of the circular restricted problem (in two or three dimensions), known as Hill's problem, is concerned with the motion of the third body in the vicinity of one of the primaries, in the limit as the mass of the primary is reduced to zero; the scale of length is adjusted in such a way that this does not degenerate into the restricted two-body problem. In all of these different versions of the restricted problem, the fundamental property of non-integrability remains.

The restricted three-body problem has its origins in the work of Euler on the classic problem of the motion of the Moon under the gravitational influences of the Earth and Sun (the lunar problem), and was first formulated in a paper published in 1772. In the same year, Lagrange discovered particular solutions (equilibrium solutions) valid in both the restricted and general three-body problems. A major advance was made in 1836 by Jacobi, who discovered the integral of the circular restricted problem which now bears his name. This integral was used by Hill in 1878 in connection, once again, with the lunar problem. In 1899, Poincaré showed that no other integrals of the restricted problem existed, and made many other important contributions to the study of the problem. It was Poincaré who first used the term "restreint" (restricted) to signify this particular case of the three-body problem, and a great deal of modern work in many areas of the restricted problem is based on his ideas.

Numerical study of the restricted problem began with Darwin at

the end of the 19th century, and Moulton and his school at the beginning of the 20th. Because of the laboriousness of hand calculation, this early work was limited in scope and in accuracy; yet important advances were made, and many of the principal classes of periodic orbits of the planar circular problem were computed. Progress was also made, at about this time, in the sphere of regularisation, a mathematical technique which removes the singularities of the equations of motion (corresponding to the positions of the two primaries). Several regularisation methods have been devised, and were applied not only in the analytical study of the restricted problem, but also in numerical work, resulting in improved accuracy of integration of orbits involving close approaches to one or other of the primaries, and allowing numerical solutions to be continued through collision with one or other of the primaries. During the 1920's and 30's, Strömberg and his co-workers at the Copenhagen Observatory carried out a detailed numerical investigation of the planar circular restricted problem, mainly in the case of equal masses of the primaries (often referred to as the "Copenhagen problem").

With the rise of the electronic computer in the 1950's and 60's, it became possible to perform fast, accurate numerical integrations of the equations of motion of the restricted problem. Particular interest in the Earth-Moon case was stimulated by the need to compute spacecraft trajectories for lunar missions; numerical studies were also carried out on periodic orbits in the vicinity of the Lagrange equilateral triangle equilibrium points  $L_4$  and  $L_5$ . With the aid of the electronic computer it became possible to tackle the three-dimensional restricted problem, and to calculate the stability properties of periodic orbits, exercises previously beyond the practical limits of hand-calculation. The digital computer has nowadays become an indispensable research tool in the study of the restricted problem; the numerical approach to the problem has almost become an experimental science, its results being used to construct and test various theories about the structure and properties of the solutions (periodic and non-periodic) of the restricted problem.

## 1.2 Applications

The assumptions of the restricted three-body problem (point masses, Newtonian gravitational attraction, and no external forces acting, such as aerodynamic drag) confine its sphere of applicability to astronomical systems consisting of massive bodies separated by distances much greater than their physical dimensions. Various modifications of the restricted problem have been studied, taking into account the effects of tidal forces or of a resisting medium, or other departures from point-mass gravitational attraction, but we shall restrict our attention to the "pure" problem.

The origins of the restricted problem lie in studies of the lunar problem. The motion of the Moon is almost entirely controlled by the gravitational attractions of the Sun and the Earth, the other planets exerting only a feeble influence; a simple calculation shows that the Sun attracts the Moon twice as strongly as does the Earth, and although the gravitational force due to the Sun is largely cancelled out by the centrifugal force due to the motion of the Earth-Moon system about the Sun, the Moon's orbit around the Earth is subject to large solar perturbations. The restricted problem is applied to the Earth-Moon-Sun system by taking the Earth and Sun to be the two massive primaries, the Moon then being represented by the massless third body. This model neglects a number of effects, such as lunar perturbations of the Earth's orbit around the Sun, and departures from strict point-mass gravitation caused by tidal forces. In the Earth-Moon-Sun system these effects are appreciable, and the restricted problem (usually the special case known as Hill's problem) represents only an approximate first step in the full lunar problem.

The classic application of the restricted problem within the Solar System is that of the motion of a minor body (an asteroid or satellite) in the Sun-Jupiter system. Jupiter is the most massive body in the Solar System apart from the Sun, outweighing all the other planets put together, and has an important influence on the motions of the asteroids, most of which orbit the Sun in a belt between the orbits of Mars and Jupiter. The asteroids have negligible masses compared with Jupiter or the Sun, and the assumptions of the restricted problem are valid to a very high accuracy in this application. The famous "Kirkwood Gaps" are gaps in the distribution of asteroid mean motions which correspond closely

to commensurabilities with the mean motion of Jupiter; there are also groups of asteroids which cluster around certain commensurable values of the mean motion, such as the Trojan family at the 1:1 commensurability. The discovery of the Trojan asteroids close to the  $L_4$  and  $L_5$  Lagrange equilateral triangle equilibrium points has stimulated detailed study of the solutions of the restricted problem in the vicinity of these two points. The restricted problem has also been applied to the outer satellites of Jupiter, which experience such large solar perturbations as to depart appreciably from Keplerian motion around the planet. The circular restricted problem in either two or three dimensions is the main tool for the study of the orbits of these bodies, but investigation of the hypothesis that some of Jupiter's outer satellites (particularly the retrograde ones) are captured asteroids has to start with the elliptic restricted problem, because capture cannot occur under the assumptions of the circular problem.

Other Solar System applications of the restricted problem have been made, with varying degrees of validity, usually involving the Sun and a planet as the primaries, and another planet or a (natural) satellite as the third body of the system. With the advent of rockets and interplanetary spacecraft, there has been revived interest in the use of the restricted problem for calculating space probe trajectories; <sup>the</sup> negligible mass of a man-made spacecraft compared with the natural bodies of the Solar System ensures that one of the main assumptions of this model is satisfied to high accuracy. The main interest has been in the trajectories of lunar probes, with the Earth and Moon as the two massive primaries, and more recently there have been proposals to place spacecraft, or even inhabited space colonies, at the equilateral triangle equilibrium points of the Earth-Moon system.

Applications of the restricted three-body problem outside the Solar System, though rather limited, include (a) investigation of the possibility of planets in binary star systems, (b) the use of zero-velocity surfaces and "Roche lobes" in the study of close binary star systems, and (c) analysis of the stability of star clusters against disruption by gravitational perturbations of the Galaxy. The relatively narrow range of normal stellar masses means that triple star systems must be modelled by the general, rather than the restricted, three-body problem.

The restricted three-body problem has been studied not only in its applications, as listed above, but also as a pure dynamical problem. Because of the simplicity of its formulation, and because of the large

amount of effort that has been expended in the analytical and numerical investigation of its solutions, it is a proving ground for mathematical techniques and dynamical theories, many of which are transferable to other types of problem.

While the results presented in this thesis are intended to illustrate certain general characteristics of the overall structure of symmetric periodic solutions of the restricted problem, and do not necessarily correspond to any actual astronomical system, a substantial proportion pertain to the Sun-Jupiter case (mass parameter  $\mu = 0.00095$ ) of the problem and correspond to retrograde orbits around the planet Jupiter of similar dimensions to the orbits of the natural retrograde satellites.

### 1.3 Equations of Motion

In this section, a fairly detailed derivation of the equations of motion of the restricted three-body problem is presented for the general case of an elliptical orbit of the primaries, and three-dimensional motion of the third body. This is not intended to be in any way an original presentation, following as it does the standard derivations of, for example, Kopal and Lyttleton (1963) and Szebehely (1967). The object is to show how the equations are obtained for the general case, at the same time introducing the various coordinate systems and the notation used throughout this thesis. The equations of motion, in their final form, are readily simplified in the case of a circular orbit of the primaries, and for planar motion of the third body. Firstly, the differential equations of motion of the restricted three-body problem will be derived (in "physical" or "dimensional" units).

Since the motion of the two primaries is known, the expression "equations of motion of the restricted problem" really means the equations of motion of the third body of the system, that is, the particle of infinitesimal mass. Let the masses of the two primaries be  $m_1$  and  $m_2$ , and let the mass of the third particle,  $m_3$ , be sufficiently small compared with both  $m_1$  and  $m_2$  as to have a negligible effect on the orbits of the primaries. Let  $O$  be the centre of mass, or barycentre, of the primaries and  $OXYZ$  a fixed Cartesian coordinate system with origin at  $O$ , such that the  $X$  and  $Y$  axes lie in the plane of the primaries, the direction  $\vec{OX}$  being defined as the direction from  $O$  to the position of pericentre of the primary of mass  $m_2$ . (If the orbits of the primaries about the barycentre  $O$  are circular, the precise directions of axes  $X$  and  $Y$  in the plane are arbitrarily defined). Since the primaries

form a closed two-body system, OXYZ is an inertial coordinate system.

Let the position vectors of bodies  $m_1$ ,  $m_2$  and  $m_3$  referred to this coordinate system be respectively  $\underline{R}_1$ ,  $\underline{R}_2$  and  $\underline{R}$ ; defining  $(\hat{X}, \hat{Y}, \hat{Z})$  to be unit vectors in the directions of the three inertial axes, the position vectors can be written in component form

$$\begin{aligned} \underline{R}_1 &= X_1 \hat{X} + Y_1 \hat{Y} + Z_1 \hat{Z} \quad , \\ \underline{R}_2 &= X_2 \hat{X} + Y_2 \hat{Y} + Z_2 \hat{Z} \quad , \\ \underline{R} &= X \hat{X} + Y \hat{Y} + Z \hat{Z} \quad . \end{aligned} \tag{1.1}$$

Since the primaries move in the (X,Y)-plane, we can at once write  $Z_1 \equiv 0$ ,  $Z_2 \equiv 0$ . The distance  $D = |\underline{R}_1 - \underline{R}_2|$  between the primaries at any epoch is given by

$$D = \frac{a(1-e^2)}{1+e\cos\theta} \quad , \tag{1.2}$$

where  $a$  and  $e$  are respectively the semi-major axis and eccentricity of the relative orbit of the primaries, and  $\theta$  is the true anomaly at the epoch. Note that for zero eccentricity,  $D = a$  (constant). Now by definition of the barycentre, we have

$$m_1 \underline{R}_1 + m_2 \underline{R}_2 = \underline{Q} \quad . \tag{1.3}$$

Thus

$$D = \left(1 + m_1/m_2\right) |\underline{R}_1| \quad . \tag{1.4}$$

Defining the MASS PARAMETER  $\mu$  by

$$\mu = \frac{m_2}{m_1 + m_2} \quad , \tag{1.5}$$

we obtain

$$\begin{aligned} R_1 &= |\underline{R}_1| = \mu D \\ R_2 &= |\underline{R}_2| = (1-\mu) D \quad . \end{aligned} \tag{1.6}$$

It follows from the definition of the coordinate system OXYZ that the polar angle of vector  $\underline{R}_2$  with respect to the X-axis is equal to the true anomaly  $\theta$  of the primaries (see Figure 1.1). We can therefore write

$$\begin{aligned} \underline{R}_1 &= -\mu D (\hat{X} \cos\theta + \hat{Y} \sin\theta) \\ \underline{R}_2 &= (1-\mu) D (\hat{X} \cos\theta + \hat{Y} \sin\theta) \quad . \end{aligned} \tag{1.7}$$

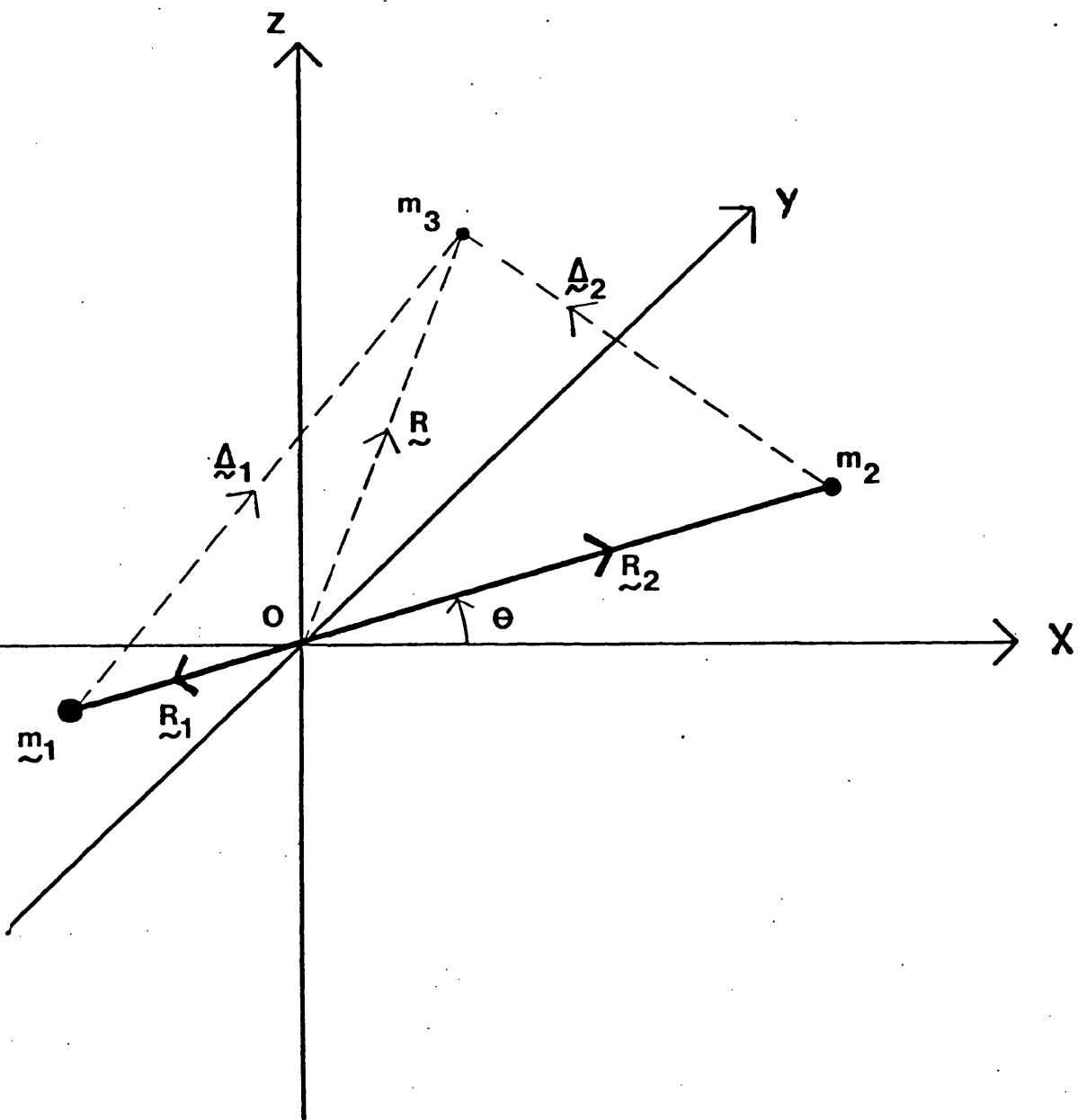


Figure 1.1 : The inertial coordinate system OXYZ. The primaries  $m_1$  and  $m_2$  orbit the barycentre O in the (X,Y) plane.

These two equations give the positions  $R_1$  and  $R_2$  of the two primaries in terms of the true anomaly  $\theta$  (recall that  $D$  is a function of  $\theta$ ). In principle,  $\theta$  can be computed for any epoch by means of Kepler's Equation, although in practice this is inconvenient and time-consuming. It will be shown later that this difficulty can be avoided by introducing a rotating coordinate system and by using  $\theta$ , instead of the epoch  $t$ , as the independent variable in the equations of motion.

The equations of motion of the third body, of mass  $m_3$ , can be expressed in vector form as

$$m_3 \ddot{R}^* = F_1 + F_2, \quad (1.8)$$

where  $\ddot{R}^* = \frac{d^2 R}{dt^2}$  is the acceleration vector as measured with respect to inertial coordinates, and  $F_1, F_2$  are the forces of gravitational attraction acting on  $m_3$  due to primaries  $m_1, m_2$  respectively. Defining the vectors  $\Delta_1, \Delta_2$  by

$$\begin{aligned} \Delta_1 &= R - R_1, \\ \Delta_2 &= R - R_2, \end{aligned} \quad (1.9)$$

the forces  $F_1$  and  $F_2$  are given by Newton's law of gravitational attraction (written in vector form):

$$\begin{aligned} F_1 &= \frac{Gm_1 m_3}{\Delta_1^2} \left( -\frac{\Delta_1}{\Delta_1} \right), \\ F_2 &= \frac{Gm_2 m_3}{\Delta_2^2} \left( -\frac{\Delta_2}{\Delta_2} \right), \end{aligned} \quad (1.10)$$

where  $\Delta_1 = |\Delta_1|$ ,  $\Delta_2 = |\Delta_2|$ , and  $G$  is the Newtonian gravitational constant.

Dividing through Equation (1.8) by  $m_3$ , and inserting Equations (1.10), we have

$$\ddot{R}^* + \frac{Gm_1}{\Delta_1^3} \Delta_1 + \frac{Gm_2}{\Delta_2^3} \Delta_2 = 0. \quad (1.11)$$

The vector equation (1.11) may be written in component form

$$\left. \begin{aligned} \ddot{X}^* + \frac{Gm_1}{\Delta_1^3} (X-X_1) + \frac{Gm_2}{\Delta_2^3} (X-X_2) &= 0 \\ \ddot{Y}^* + \frac{Gm_1}{\Delta_1^3} (Y-Y_1) + \frac{Gm_2}{\Delta_2^3} (Y-Y_2) &= 0 \\ \ddot{Z}^* + G \left( \frac{m_1}{\Delta_1^3} + \frac{m_2}{\Delta_2^3} \right) Z &= 0 \end{aligned} \right\} \quad (1.12)$$

where dots denote differentiation with respect to the time  $t$ ,

$$\begin{aligned} \Delta_1^2 &= (X-X_1)^2 + (Y-Y_1)^2 + Z^2, \\ \Delta_2^2 &= (X-X_2)^2 + (Y-Y_2)^2 + Z^2, \end{aligned} \tag{1.13}$$

and  $(X_1, Y_1)$ ,  $(X_2, Y_2)$  are the non-zero components of vectors  $\underline{R}_1, \underline{R}_2$  as given by Equations (1.7). These are the equations of motion of the three-dimensional elliptic restricted problem, with respect to inertial coordinates and in terms of physical or dimensional quantities (that is, quantities which can be specified in any self-consistent system of units).

This form of the equations of motion is perfectly usable for numerical integrations, but it is advantageous to carry out certain transformations which cast the equations into a more convenient form. Firstly, a new coordinate system is introduced which rotates synchronously with the primaries; secondly, the dimensional coordinates are replaced by a dimensionless set by choosing an appropriate unit of length; and thirdly, a new choice of independent variable is made. The end result of these operations will be that (i) the primaries are at fixed locations in the new coordinate system, rather than tracing out elliptical paths about the barycentre, (ii) the actual physical dimensions of the three-body system do not enter into the new equations, reflecting the fact that they have no real dynamical significance, (iii) Kepler's Equation does not have to be solved in order to integrate the equations of motion, and (iv) the new equations are particularly convenient for use in the determination of periodic orbits.

Let us introduce the Cartesian coordinate system  $O\xi\eta\zeta$  with origin at  $O$ , such that the  $\xi$ -axis is in the direction of the instantaneous position of primary  $m_2$  and the  $\zeta$ -axis coincides with the  $Z$ -axis of the inertial coordinate system (see Figure 1.2). This new coordinate system therefore rotates non-uniformly with the primaries  $m_1$  and  $m_2$ , which simply oscillate on the  $\xi$ -axis at periodically varying distances  $R_1$  and  $R_2$  from the origin, as given by Equations (1.6) and (1.2). The transformation between coordinate system  $OXYZ$  and  $O\xi\eta\zeta$  is

$$\left. \begin{aligned} \xi &= X \cos \theta + Y \sin \theta \\ \eta &= -X \sin \theta + Y \cos \theta \\ \zeta &= Z, \end{aligned} \right\} \tag{1.14}$$

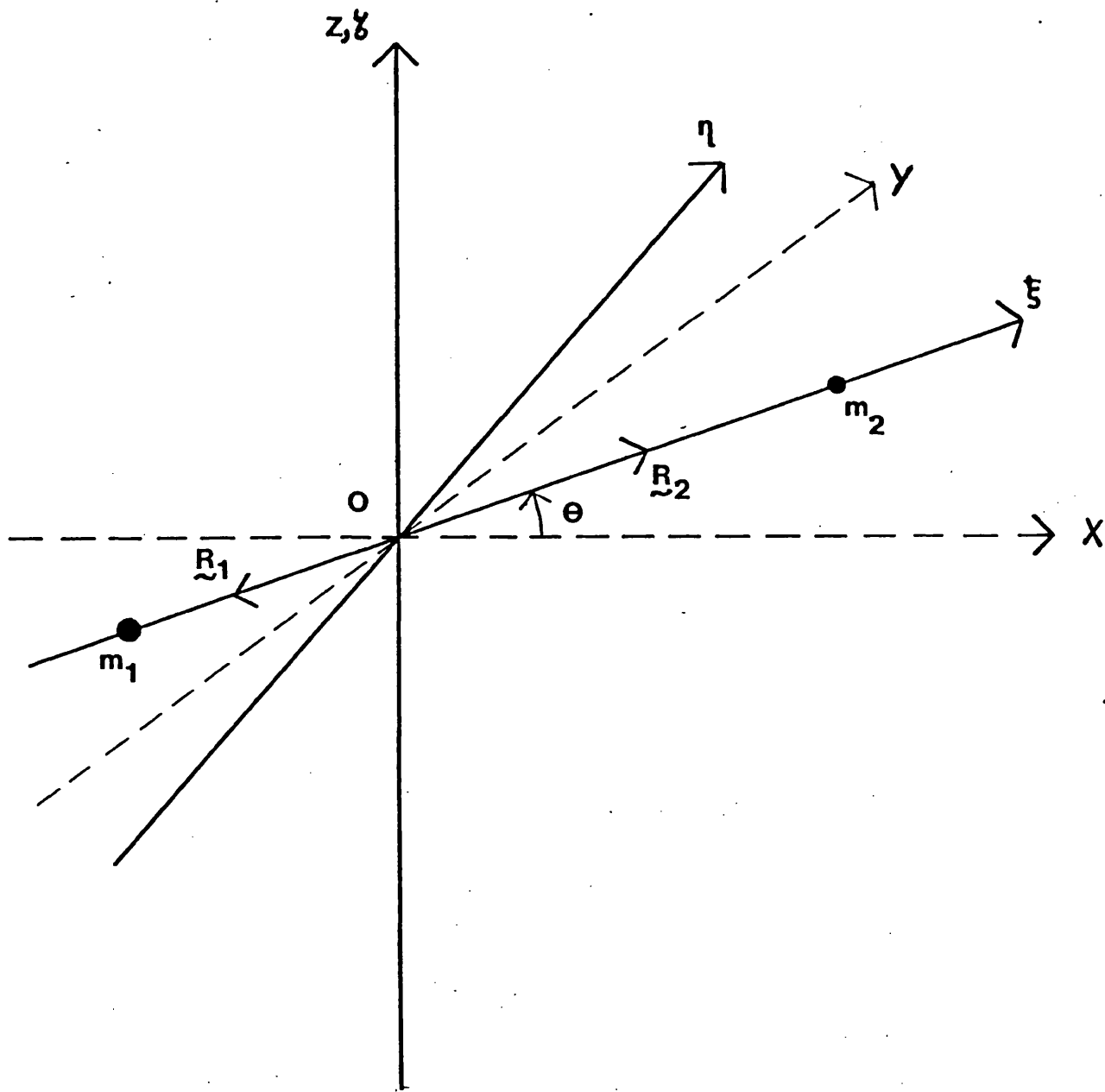


Figure 1.2 : The rotating coordinate system  $O\xi\eta\zeta$ . The  $\xi$  and  $\eta$  axes rotate with the primaries in the  $(X,Y)$  plane; the  $\zeta$  and  $Z$  axes coincide.

and the vector  $\underline{R}$  can be expressed as

$$\underline{R} = \xi \hat{\xi} + \eta \hat{\eta} + \zeta \hat{\zeta}, \quad (1.15)$$

where  $(\hat{\xi}, \hat{\eta}, \hat{\zeta})$  are unit vectors in the directions of the three axes of the rotating coordinate system. The instantaneous angular velocity  $\underline{\omega}$  of the system  $O\xi\eta\zeta$  with respect to the inertial system  $OXYZ$  is equal to the orbital angular velocity of the primaries:

$$\underline{\omega} = \omega \hat{Z} = \omega \hat{\zeta}, \quad (1.16)$$

where

$$\omega = d\theta/dt. \quad (1.17)$$

The acceleration vector  $\underline{\ddot{R}}$  of the third body of the system as measured with respect to this rotating reference frame is given by the Coriolis Theorem:

$$\underline{\ddot{R}} = \underline{\ddot{R}}^* - \underline{\omega} \times (\underline{\omega} \times \underline{R}) - 2\underline{\omega} \times \underline{\dot{R}} - \dot{\underline{\omega}} \times \underline{R}. \quad (1.18)$$

In this equation, unstarred derivatives are those measured in the rotating system; the first term on the right-hand side is the inertial acceleration, given by Equation (1.11), the remaining terms being respectively the centrifugal force and Coriolis force terms, and a term resulting from the non-uniform angular velocity of the rotating coordinate system. Since  $\underline{\omega}$  varies only in magnitude, and not in direction, we can write

$$\dot{\underline{\omega}} = \dot{\omega} \hat{\zeta} \quad (1.19)$$

and Equation (1.18) becomes

$$\underline{\ddot{R}} = \underline{\ddot{R}}^* + \omega^2 (\zeta \hat{\xi} + \eta \hat{\eta}) + 2\omega (\dot{\eta} \hat{\xi} - \dot{\xi} \hat{\eta}) + \dot{\omega} (\eta \hat{\xi} - \xi \hat{\eta}). \quad (1.20)$$

Substituting for  $\underline{\ddot{R}}^*$  from Equation (1.11), we obtain the vector equation of motion of the body  $m_3$  with respect to the rotating coordinate system:

$$\underline{\ddot{R}} + \frac{Gm_1}{\Delta_1^3} \underline{\Delta}_1 + \frac{Gm_2}{\Delta_2^3} \underline{\Delta}_2 - (\omega^2 \xi + 2\omega \dot{\eta} + \dot{\omega} \eta) \hat{\xi} - (\omega^2 \eta - 2\omega \dot{\xi} - \dot{\omega} \xi) \hat{\eta} = \underline{0}, \quad (1.21)$$

where

$$\begin{aligned} \underline{\Delta}_1 &= (\xi + R_1) \hat{\xi} + \eta \hat{\eta} + \zeta \hat{\zeta}, \\ \underline{\Delta}_2 &= (\xi - R_2) \hat{\xi} + \eta \hat{\eta} + \zeta \hat{\zeta}, \end{aligned} \quad (1.22)$$

and  $R_1, R_2$  are given by Equation (1.6).

The next step is to carry out a further transformation, from the coordinate system  $O\xi\eta\zeta$  to a new coordinate system  $Oxyz$ , defined by:

$$\left. \begin{aligned} x &= \xi/D \\ y &= \eta/D \\ z &= \zeta/D. \end{aligned} \right\} \quad (1.23)$$

This new dimensionless coordinate system has as unit of length the distance  $D$  between the primaries, as given by Equation (1.2). Because the coordinate system  $Oxyz$  rotates with the primaries, and has a unit of length which varies periodically with the period of the primaries, it is often referred to as the "barycentric rotating-pulsating" system. In the circular restricted problem the unit of length  $D$  is a constant. Note that the transformed coordinates of the primaries are  $x_1 = -R_1/D = -\mu$ ,  $y_1 = z_1 = 0$ , and  $x_2 = R_2/D = 1-\mu$ ,  $y_2 = z_2 = 0$ ; both primaries are therefore at fixed locations in the transformed system (see Figure 1.3).

The position vector  $\underline{R}$  of the third body is transformed to

$$\underline{r} = \underline{R}/D, \quad (1.24)$$

and since the unit vectors  $(\hat{x}, \hat{y}, \hat{z})$  in the directions of the axes of the rotating-pulsating coordinate system are identical to  $(\hat{\xi}, \hat{\eta}, \hat{\zeta})$ , we can write

$$\underline{r} = x\hat{x} + y\hat{y} + z\hat{z} = \frac{1}{D} (\xi\hat{\xi} + \eta\hat{\eta} + \zeta\hat{\zeta}). \quad (1.25)$$

The vectors  $\underline{\Delta}_1$  and  $\underline{\Delta}_2$  are transformed to

$$\begin{aligned} \underline{r}_1 &= \underline{\Delta}_1/D = (x+\mu)\hat{x} + y\hat{y} + z\hat{z}, \\ \underline{r}_2 &= \underline{\Delta}_2/D = (x-1+\mu)\hat{x} + y\hat{y} + z\hat{z}. \end{aligned} \quad (1.26)$$

The final step in the procedure is to introduce a change of independent variable in the equations of motion from the epoch  $t$  to the true anomaly  $\theta$  of the primaries, by means of the relation

$$\frac{d}{dt} = \frac{d\theta}{dt} \frac{d}{d\theta} = \omega \frac{d}{d\theta}. \quad (1.27)$$

Note that for the circular restricted problem,  $\omega$  is constant. Let  $\alpha$  be an arbitrary dimensional coordinate, and define the dimensionless variable

$$\bar{\alpha} = \alpha/D. \quad (1.28)$$

The time derivative of  $\alpha$  is

$$\dot{\alpha} = \omega \frac{d}{d\theta} (D\bar{\alpha}) = \omega (D'\bar{\alpha} + D\bar{\alpha}'). \quad (1.29)$$

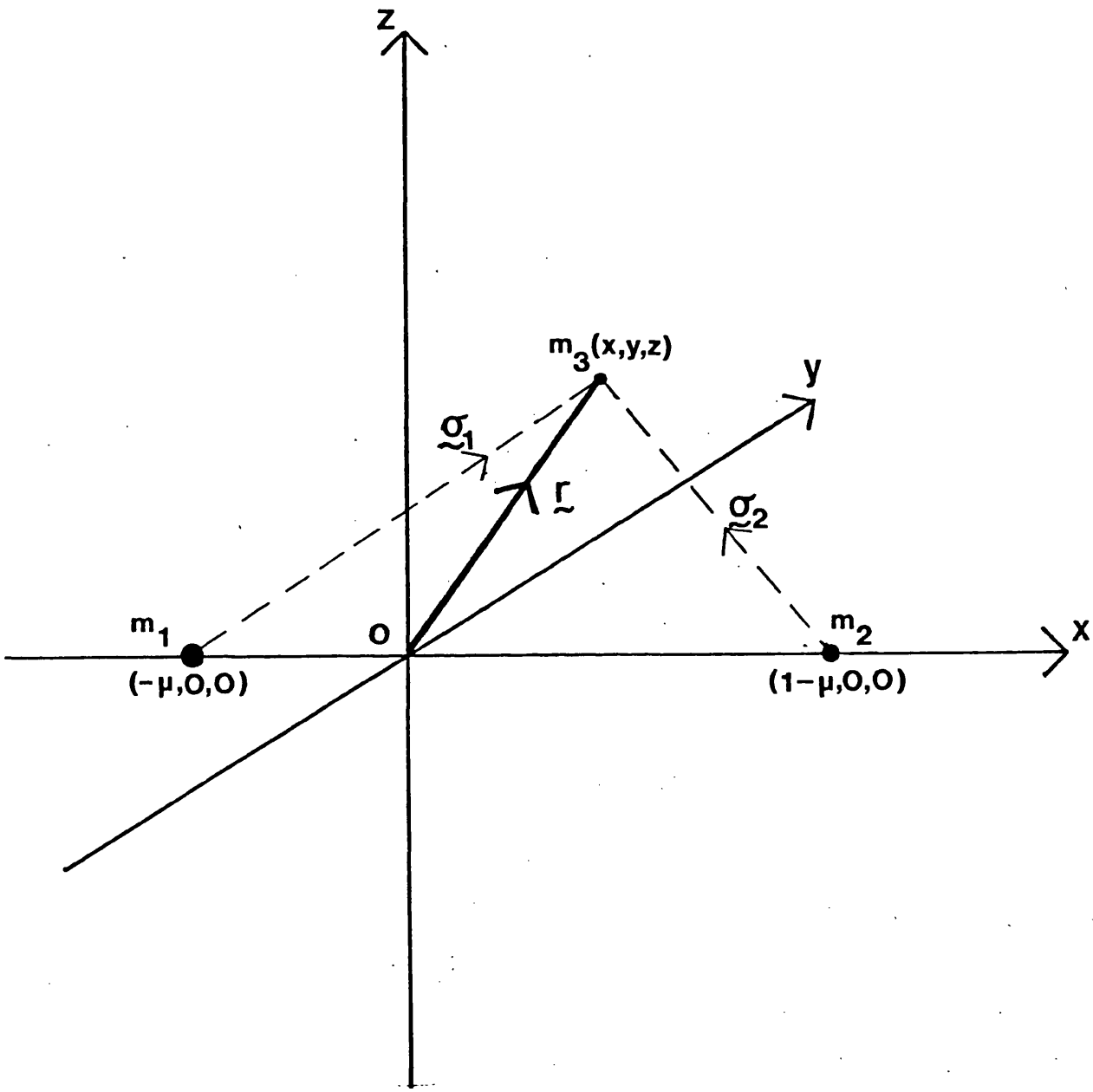


Figure 1.3 : The dimensionless rotating-pulsating coordinate system Oxyz. The primaries  $m_1$  and  $m_2$  have fixed positions on the x axis; the distance between the primaries is taken as the unit of length.

From Equation (1.2),

$$D' = \frac{a(1-e^2)e \sin \theta}{(1+e \cos \theta)^2} = \frac{De \sin \theta}{1+e \cos \theta}, \quad (1.30)$$

where the prime denotes differentiation with respect to  $\theta$ , and so

$$\dot{\alpha} = \omega D \left( \alpha' + \bar{\alpha} \left( \frac{e \sin \theta}{1+e \cos \theta} \right) \right). \quad (1.31)$$

Differentiating once more with respect to  $t$ , we obtain

$$\begin{aligned} \ddot{\alpha} = & (\dot{\omega} D + \omega^2 D') \left( \alpha' + \bar{\alpha} \left( \frac{e \sin \theta}{1+e \cos \theta} \right) \right) \\ & + \omega^2 D \frac{d}{d\theta} \left( \alpha' + \bar{\alpha} \left( \frac{e \sin \theta}{1+e \cos \theta} \right) \right). \end{aligned} \quad (1.32)$$

Now the angular momentum integral for the primaries can be written

$$\omega D^2 = h \quad (\text{constant}). \quad (1.33)$$

Differentiating with respect to  $t$ , and using Equation (1.30), we get

$$\dot{\omega} = -2\omega^2 \left( \frac{e \sin \theta}{1+e \cos \theta} \right), \quad (1.34)$$

and Equation (1.32) becomes

$$\ddot{\alpha} = \omega^2 D \left( \alpha'' + \left( \frac{e \cos \theta}{1+e \cos \theta} \right) \alpha' \right). \quad (1.35)$$

We now have to perform the transformations defined in Equations (1.23) and (1.27) to the equations of motion (1.21). This is done by applying the general formulae (1.31) and (1.35) to the components of Equation (1.21), noting that

$$\frac{Gm_1}{\Delta_1^3} = \frac{G(m_1+m_2)(1-\mu)}{D^3 \sigma_1^3} = \left( \frac{\omega^2}{1+e \cos \theta} \right) \left( \frac{1-\mu}{\sigma_1^3} \right), \quad (1.36)$$

and

$$\frac{Gm_2}{\Delta_2^3} = \left( \frac{\omega^2}{1+e \cos \theta} \right) \left( \frac{\mu}{\sigma_2^3} \right), \quad (1.37)$$

where  $\sigma_1 = |\sigma_1|$ ,  $\sigma_2 = |\sigma_2|$

After some reduction, we obtain the equations of motion of the three-dimensional elliptic restricted problem with respect to rotating-pulsating coordinates  $(x, y, z)$ , in component form:

$$\begin{aligned} x'' - 2y' &= \left( \frac{1}{1+e\cos\theta} \right) \left\{ \left( 1 - \frac{1-\mu}{\sigma_1^3} - \frac{\mu}{\sigma_2^3} \right) x - \mu(1-\mu) \left( \frac{1}{\sigma_1^3} - \frac{1}{\sigma_2^3} \right) \right\}, \\ y'' + 2x' &= \left( \frac{1}{1+e\cos\theta} \right) \left( 1 - \frac{1-\mu}{\sigma_1^3} - \frac{\mu}{\sigma_2^3} \right) y, \\ z'' + z &= \left( \frac{1}{1+e\cos\theta} \right) \left( 1 - \frac{1-\mu}{\sigma_1^3} - \frac{\mu}{\sigma_2^3} \right) z. \end{aligned} \quad (1.38)$$

From Equations (1.26), we have

$$\begin{aligned} \sigma_1^2 &= (x+\mu)^2 + y^2 + z^2, \\ \sigma_2^2 &= (x-1+\mu)^2 + y^2 + z^2. \end{aligned} \quad (1.39)$$

Note that for non-zero values of the primary orbit eccentricity  $e$ , the right-hand sides of Equations (1.38) have an explicit dependence on the true anomaly  $\theta$ ; this has important dynamical consequences, as we shall see later. All of the quantities appearing in these equations are dimensionless; the two basic parameters are  $\mu$ , the mass parameter, and  $e$ , the eccentricity of the relative orbit of the primaries. From its definition in Equation (1.5), we see that  $\mu$  can have any value between 0 and 1 (since  $m_1$  and  $m_2$  must be non-negative);  $\mu = 0$  when  $m_2$  is zero, while  $\mu = \frac{1}{2}$  for equal masses of the primaries. Usually  $m_2$  is taken to be the less massive of the two primaries, so that  $0 \leq \mu \leq \frac{1}{2}$ , values greater than  $\mu = \frac{1}{2}$  being essentially redundant (Equations (1.38) and (1.39) are unaltered if  $\mu$  is replaced by  $1-\mu$ ). However, it is sometimes more convenient, for the sake of continuity, to allow  $\mu$  to have any value in the range  $[0,1]$ .

The equations of motion of the three-dimensional circular restricted problem are obtained simply by setting  $e=0$  in Equations (1.38), with the result that the factor  $(1+e\cos\theta)^{-1}$  becomes unity, eliminating the explicit appearance of the independent variable in the equations of motion. The planar restricted problem corresponds to the case  $z \equiv 0$ ; the third of Equations (1.38) reduces to an identity and the first two define the motion in the horizontal plane.

#### 1.4 The State Vector

The state vector, which we shall denote by  $\underline{s}$ , is a vector in the six-dimensional phase space (coordinate-velocity space) of the restricted problem, describing the state of the third body of the system at any instant. It is a convenient form of notation which will be used extensively throughout this thesis; in this section the notation will be introduced and the equations of motion (1.38) expressed in terms of  $\underline{s}$ .

The state vector has components

$$\begin{aligned} s_1 &= x; & s_2 &= y; & s_3 &= z; \\ s_4 &= x'; & s_5 &= y'; & s_6 &= z', \end{aligned} \quad (1.40)$$

where  $(x, y, z)$  are the components of the third body with respect to the rotating-pulsating coordinate system, and primes denote differentiation with respect to  $\theta$ , the true anomaly of the primaries. The notation

$$\begin{aligned} \underline{s}_0 &= (s_{01}, s_{02}, s_{03}, s_{04}, s_{05}, s_{06}) \\ &= (x_0, y_0, z_0, x'_0, y'_0, z'_0) \end{aligned} \quad (1.41)$$

will be used to denote the value of the state vector at the initial epoch, when the true anomaly of the primaries has the value  $\theta_0$ . The expression "initial conditions" will be employed to mean the components of  $\underline{s}_0$ . Since the three differential equations of motion (1.38) are of second order, a unique solution is specified once the values of the six initial conditions  $(x_0, y_0, z_0, x'_0, y'_0, z'_0)$  have been given.

An alternative formulation of the equations of motion (1.38), in terms of the state vector, is

$$\underline{s}' = \underline{f}(\underline{s}; \theta), \quad (1.42)$$

where the vector function  $\underline{f}$  has components

$$\begin{aligned} f_1 &= s_1, \\ f_2 &= s_2, \\ f_3 &= s_3, \\ f_4 &= 2s_5 + E \left\{ A s_1 + \mu(1-\mu)(\sigma_1^{-3} - \sigma_2^{-3}) \right\}, \\ f_5 &= -2s_4 + E A s_2, \\ f_6 &= (EA-1) s_3, \end{aligned} \quad (1.43)$$

and

$$\begin{aligned} A(s_1, s_2, s_3) &= 1 - \frac{1-\mu}{\sigma_1^3} - \frac{\mu}{\sigma_2^3}, \\ E(\theta) &= (1 + e \cos \theta)^{-1}. \end{aligned} \quad (1.44)$$

From Equations (1.39) and (1.40),

$$\begin{aligned} \sigma_1^2 &= (s_1 + \mu)^2 + s_2^2 + s_3^2, \\ \sigma_2^2 &= (s_1 - 1 + \mu)^2 + s_2^2 + s_3^2. \end{aligned} \quad (1.45)$$

Thus the three second-order equations (1.38) have been replaced by six first-order equations (1.42); these will be used in preference to the original equations.

### 1.5 Jacobi Integral

Let  $\Omega$  be a function of the three coordinates  $(x, y, z)$  of the third body of the system (with respect to the rotating-pulsating coordinate system) defined by

$$\Omega(x, y, z) = \frac{1}{2}(x^2 + y^2 + z^2) + \frac{1-\mu}{\sigma_1} + \frac{\mu}{\sigma_2} + \frac{1}{2}\mu(1-\mu), \quad (1.46)$$

or, equivalently, by

$$\Omega = (1-\mu)\left(\frac{1}{\sigma_1} + \frac{\sigma_1^2}{2}\right) + \mu\left(\frac{1}{\sigma_2} + \frac{\sigma_2^2}{2}\right). \quad (1.47)$$

It can be shown by inspection that the equations of motion (1.38) may be written

$$\left. \begin{aligned} x'' - 2y' &= \left(\frac{1}{1+\epsilon\cos\theta}\right) \frac{\partial\Omega}{\partial x}, \\ y'' + 2x' &= \left(\frac{1}{1+\epsilon\cos\theta}\right) \frac{\partial\Omega}{\partial y}, \\ z'' + z &= \left(\frac{1}{1+\epsilon\cos\theta}\right) \frac{\partial\Omega}{\partial z}. \end{aligned} \right\} \quad (1.48)$$

The total derivative of  $\Omega$  with respect to  $\theta$  is

$$\begin{aligned} \Omega' &= \frac{\partial\Omega}{\partial x} x' + \frac{\partial\Omega}{\partial y} y' + \frac{\partial\Omega}{\partial z} z' \\ &= (1+\epsilon\cos\theta)(x''x' + y''y' + z''z' + z'z), \end{aligned} \quad (1.49)$$

by Equations (1.48). We therefore have

$$\Omega' = \frac{1}{2}(1+\epsilon\cos\theta) \frac{d}{d\theta} (x'^2 + y'^2 + z'^2 + z^2). \quad (1.50)$$

Now

$$\left(\frac{\Omega}{1+\epsilon\cos\theta}\right)' = \frac{\Omega'}{1+\epsilon\cos\theta} + \frac{\Omega \epsilon \sin\theta}{(1+\epsilon\cos\theta)^2}. \quad (1.51)$$

Combining Equations (1.50) and (1.51) and integrating, we obtain

$$\frac{\Omega}{1+\epsilon\cos\theta} = \frac{1}{2}(x'^2 + y'^2 + z'^2 + z^2) + \int \frac{\Omega \epsilon \sin\theta}{(1+\epsilon\cos\theta)^2} d\theta. \quad (1.52)$$

Along a particular solution of the equations of motion, the following invariant relation must therefore hold for all values of  $\theta$ :

$$\frac{\Omega}{1+e\cos\theta} - \frac{1}{2}(x'^2 + y'^2 + z'^2 + z^2) - \int_{\theta_0}^{\theta} \frac{\Omega e \sin\theta}{(1+e\cos\theta)^2} d\theta = \frac{1}{2}C, \quad (1.53)$$

where C is a constant whose value can be determined from the initial conditions (the values of x,y,z,x',y' and z' at  $\theta = \theta_0$ ). This invariant relation is not an integral of the elliptic restricted problem, because of the appearance of the non-integrated term involving  $\Omega$ . The main practical value of Equation (1.53) is as a check on the accuracy of numerical integrations of the equations of motion.

In the circular restricted problem, however,  $e = 0$  and the non-integrated term vanishes, with the important result that Equation (1.53) becomes an integral:

$$2\Omega - (x'^2 + y'^2 + z'^2 + z^2) = C. \quad (1.54)$$

The constant of integration, C, is known as the JACOBI CONSTANT, after the mathematician who first discovered the integral. This is the only integral of the circular restricted problem, as has been shown by Poincaré, and replaces the energy and angular momentum integrals of the general three-body problem, which are no longer valid in the restricted problem. The left-hand side of Equation (1.54) can be divided into two terms, one of which,  $2\Omega - z^2$ , involves only the coordinates, while the other,  $x'^2 + y'^2 + z'^2$  (the square of the speed of the third body with respect to rotating axes), involves only the first derivatives of the coordinates. The Jacobi constant C is uniquely defined only within an additive constant, according to the definition of the function  $\Omega$ . Since only the partial derivatives of  $\Omega$  with respect to the coordinates feature in the equations of motion (1.48), the addition of an arbitrary constant is permissible and the value of C will alter correspondingly. The constant  $\frac{1}{2}\mu(1 - \mu)$  has been inserted into Equation (1.46) to allow the more compact expression (1.47) to be written. This definition of the function  $\Omega$ , and consequently of the Jacobi constant, follows the recommendation of Szebehely in his book "Theory of Orbits". It is important to note that not all authors employ this definition and it is often necessary to transform published numerical results to achieve consistency. The "rotating-pulsating" coordinate system Oxyz, as defined in Section 1.3, and (where applicable) the Jacobi constant, as defined in this section, will be used throughout this thesis.

The form of the Jacobi integral (Equation (1.54)) leads to the introduction of an important set of surfaces in coordinate space, usually referred to as zero-velocity surfaces. For a given value of the Jacobi constant, say  $C^*$ ,

the zero-velocity surfaces comprise those points  $(x,y,z)$  which satisfy

$$2\Omega(x,y,z) - z^2 = C^* . \quad (1.55)$$

Clearly, if the third body of the system has the value  $C^*$  of the Jacobi constant, its velocity at all points on these surfaces is zero. This has important consequences for qualitative studies of the motion of the third body, for the zero-velocity surfaces are effectively barriers to the massless particle through which it cannot pass. Motion is possible only within those regions of coordinate space, bounded by the zero-velocity surfaces, for which

$$x'^2 + y'^2 + z'^2 = 2\Omega - z^2 - C^* > 0 ; \quad (1.56)$$

Those regions of coordinate space for which  $2\Omega - z^2 - C^* < 0$  are referred to as "forbidden regions". In the planar circular restricted problem, the zero-velocity surfaces reduce to zero-velocity curves in the  $(x,y)$ -plane, and these curves are often termed "Hill curves" after the mathematician who first made use of the Jacobi integral in connection with the problem of the stability of the Earth-Moon system.

An extensive discussion of zero-velocity curves and their significance is given in Szebehely (1967).

## 1.6 Lagrange Solutions

We now present a brief derivation of the equilibrium solutions of the restricted problem usually named after their discoverer, Lagrange. An equilibrium solution is one for which the coordinates  $(x,y,z)$  of the massless third body, with respect to the barycentric rotating-pulsating coordinate system, are constant; the velocity components  $(x',y',z')$  and acceleration components  $(x'',y'',z'')$  of the massless body in this coordinate system must therefore all vanish. The procedure for finding the equilibrium solutions is straightforward: taking the equations of motion (1.38), we set  $x' = y' = z' = 0$ ,  $x'' = y'' = z'' = 0$  and solve for  $x,y$  and  $z$ . If such solutions exist, they are the coordinates of points having the property that if the massless body is at rest at such a point, it experiences no net force and therefore remains in equilibrium at that point.

Equations (1.39) show that if the coordinates  $(x,y,z)$  are all constant,

then so are the distances  $\sigma_1$  and  $\sigma_2$  of the third body from the two primaries. (Recall that the coordinate system has unit of length D, the distance between the primaries, which varies periodically with  $\theta$ ; thus, if  $\sigma_1$  and  $\sigma_2$  are constant, the distances  $\Delta_1$  and  $\Delta_2$  measured with respect to a fixed unit of length actually pulsate in a periodic fashion). Taking the third of Equations (1.38), and setting  $z'' = 0$ , we obtain

$$\left[ \left( \frac{1}{1+e\cos\theta} \right) \left( 1 - \frac{1-\mu}{\sigma_1^3} - \frac{\mu}{\sigma_2^3} \right) - 1 \right] z = 0. \quad (1.57)$$

Now the expression in square brackets can only vanish, for all values of  $\theta$ , for  $e = 0$  and  $\sigma_1 \rightarrow \infty$ ,  $\sigma_2 \rightarrow \infty$ : this is the trivial case where the massless body lies infinitely distant from the primaries and so experiences no attractive forces, clearly not a true equilibrium solution; we conclude that any non-trivial equilibrium points must lie in the plane of the primaries ( $z = 0$ ).

Setting  $x' = x'' = y' = y'' = 0$  in the first two of Equations (1.38), we obtain

$$\left( \frac{1}{1+e\cos\theta} \right) \left\{ \left( 1 - \frac{1-\mu}{\sigma_1^3} - \frac{\mu}{\sigma_2^3} \right) x - \mu(1-\mu) \left( \frac{1}{\sigma_1^3} - \frac{1}{\sigma_2^3} \right) \right\} = 0, \quad (1.58)$$

$$\left( \frac{1}{1+e\cos\theta} \right) \left( 1 - \frac{1-\mu}{\sigma_1^3} - \frac{\mu}{\sigma_2^3} \right) y = 0, \quad (1.59)$$

and we seek solutions  $(x,y)$  valid for all values of  $\theta$ . From Equation (1.59) we have either

$$y = 0 \quad (1.60)$$

or

$$1 - \frac{1-\mu}{\sigma_1^3} - \frac{\mu}{\sigma_2^3} = 0. \quad (1.61)$$

The solutions corresponding to  $y = 0$  are referred to as the COLLINEAR EQUILIBRIUM POINTS, since they are collinear with the two primaries. For  $y = z = 0$ , Equations (1.39) give

$$\begin{aligned} \sigma_1 &= |x+\mu|, \\ \sigma_2 &= |x-1+\mu|, \end{aligned} \quad (1.62)$$

and from Equation (1.58) the collinear equilibrium points have  $x$ -coordinates satisfying

$$x - \frac{(1-\mu)(x+\mu)}{|x+\mu|^3} - \frac{\mu(x-1+\mu)}{|x-1+\mu|^3} = 0. \quad (1.63)$$

In each of the three intervals  $I_1 : (x < -\mu)$ ,  $I_2 : (-\mu < x < 1-\mu)$  and  $I_3 : (x > 1-\mu)$ , Equation (1.63) becomes a different quintic in  $x$ . For  $0 < \mu \leq \frac{1}{2}$ , each of these three quintics has one and only one real root in the corresponding interval on the  $x$ -axis; consequently, there are three collinear equilibrium points, usually denoted by  $L_1, L_2$  and  $L_3$ , one occurring in each of the three intervals  $I_1, I_2$  and  $I_3$ , that is, one situated between the primaries, and the other two on either side of the primaries, as shown schematically in Figure 1.4. (A fuller discussion of the collinear equilibrium points and numerical methods of solving the quintics are given by Szebehely (1967)).

The remaining equilibrium solutions are those for which Equation (1.61) is valid. Equation (1.58) then gives

$$\frac{1}{\sigma_1^3} - \frac{1}{\sigma_2^3} = 0, \quad (1.64)$$

or  $\sigma_1 = \sigma_2$ ; substituting into (1.61) we obtain

$$\sigma_1 = \sigma_2 = 1. \quad (1.65)$$

There are only two points in the  $(x,y)$ -plane for which Equation (1.65) is valid: these are the EQUILATERAL TRIANGLE EQUILIBRIUM POINTS, designated  $L_4$  and  $L_5$ , each of which forms an equilateral triangle with the two primaries.

There is no standard system for labelling the five Lagrange equilibrium points, except that  $L_1 - L_3$  are always the collinear points and  $L_4, L_5$  the equilateral triangle points. Indeed, the choices of origin and orientation of the rotating coordinate system of the restricted problem vary between different authors, despite attempts to standardise the notation. The designations indicated in Figure 1.4 will be adhered to throughout this thesis.

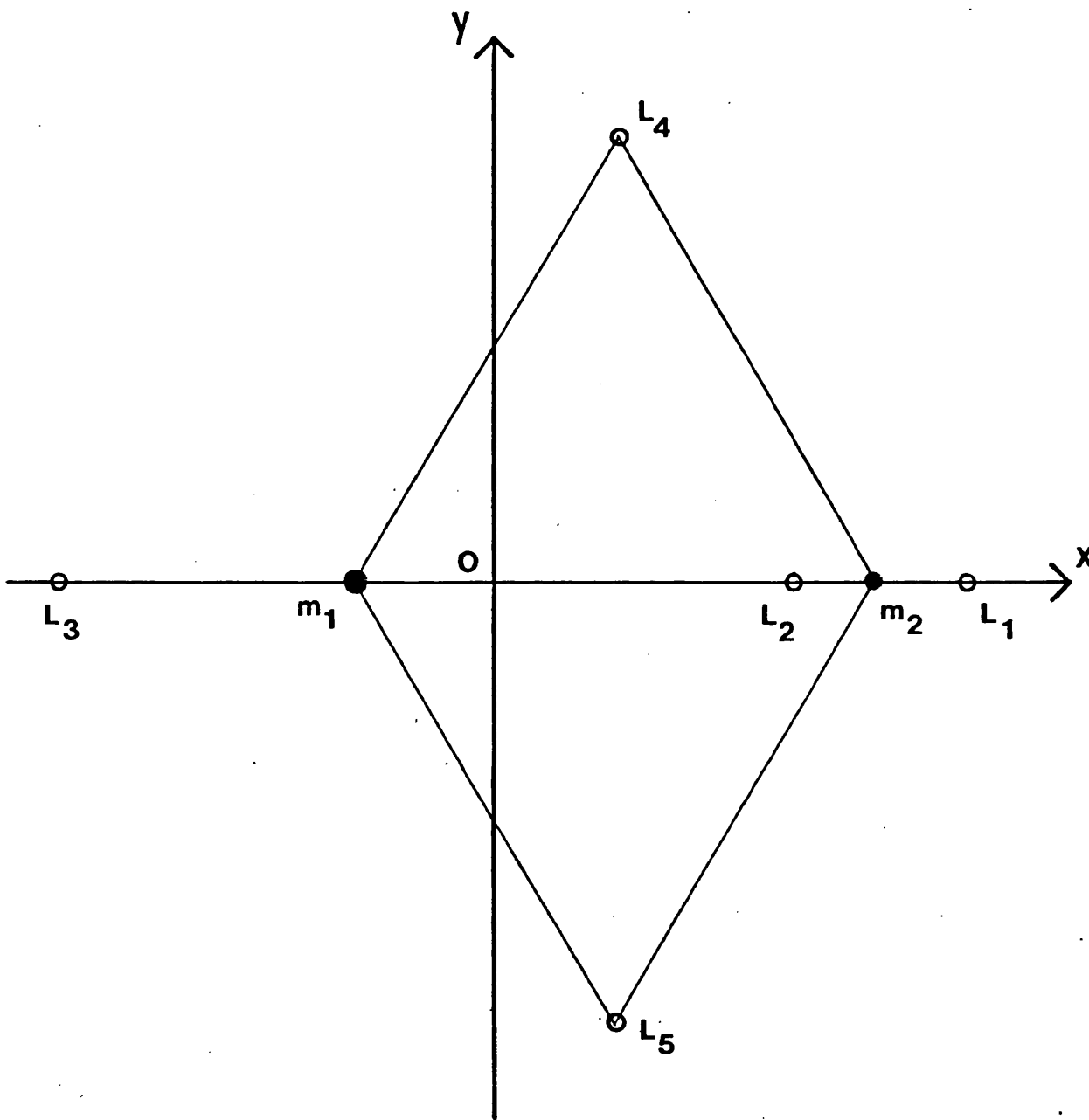


Figure 1.4 : Schematic diagram of the locations of the five Lagrange equilibrium points in the  $(x,y)$  plane.

## 2. PERIODIC ORBITS

### 2.1 Introduction

The existence of periodic orbits of the restricted three-body problem, that is, orbits which repeat themselves after certain fixed periods of time, with respect to a suitable coordinate system, has been established mathematically by a number of methods, such as the method of analytical continuation, the process of equating Fourier coefficients, the application of fixed point theorems, and the method of power series. An example of the first method is the analytical continuation of orbits of the restricted two-body problem (the problem of the motion of a body of infinitesimal mass under the gravitational attraction of a single massive primary) into the circular restricted three-body problem, the mass of the second primary being increased from zero to non-zero values. Poincaré's work in this area led to his classification of the periodic orbits of the restricted problem into three "kinds": the first kind (première sorte) are those generated by analytical continuation of circular two-body orbits in the plane of the primaries, the second kind (deuxième sorte) are generated from elliptical orbits in the plane, and the third kind (troisième sorte) from elliptical orbits inclined to the plane of the primaries. Analytical and numerical continuation will be referred to in subsequent chapters, with particular emphasis on methods of numerical continuation.

The importance of periodic orbits in the study of the restricted problem has long been recognised. Because the restricted problem is non-integrable, the only orbits for which complete information is available are asymptotic, periodic or almost-periodic orbits; for non-periodic motion, the behaviour over intervals of time tending to infinity is completely unknown, since numerical integration can only be carried on for a finite time. The practical importance of periodicity is therefore that if the motion is known over a finite interval (the period of the orbit), then the solution is available, in principle to arbitrary precision, from  $t = -\infty$  to  $t = +\infty$ . In his classic "Méthodes Nouvelles", Poincaré (1899) advanced the opinion that the study of periodic orbits was indeed the only opening through which it would be feasible to explore the three-body problem. His famous conjecture, which has since been proved subject to appropriate assumptions, states that given a particular solution of the circular restricted problem, a periodic solution (generally of very long period) can always be found such that the difference between the solutions is arbitrarily small for any desired time

interval. Schwarzschild's (1898) version of this conjecture uses the terminology of phase space: in an arbitrarily close neighbourhood of any point in the phase space there is a point representing a periodic orbit, in general of very long period. Thus, rather than being "exotic" or untypical kinds of solutions, periodic solutions are in fact dense in the global set of solutions of the restricted problem.

The motivation for studying periodic orbits stems not only from their "practical" and "representational" significance, as already mentioned, but also from certain other important properties, which include the following:

- (i) periodic orbits of the circular problem can often be obtained by analytical continuation from two-body orbits, or from linearised solutions at the Lagrange equilibrium points, and this analytical continuation approach can be further applied to generate three-dimensional periodic orbits and periodic orbits of the elliptic restricted problem, from planar periodic orbits of the circular problem;
- (ii) periodic orbits can be established numerically in continuous sets or "families" which, for a given value of the mass parameter  $\mu$ , are monoparametric (see Section 2.5);
- (iii) the existence of "bifurcation orbits", with certain well-defined stability properties, allows exploration of the periodic solutions of the restricted problem to be carried out in a systematic, methodical way;
- (iv) rigorous criteria can be established for the linear stability of periodic orbits (stability with respect to small perturbations);
- (v) nearly-periodic phenomena are widely observed in nature, and in particular the orbits of nearly all of the various bodies of the Solar System can be approximated by periodic orbits, frequently with periods which are mutually commensurable.

The importance of periodic orbits is not confined to the study of the restricted three-body problem, and many of the points listed above apply equally to the periodic orbits of other non-integrable dynamical systems of two or three degrees of freedom. However, as the subtitle of Szebehely's

book "Theory of Orbits", viz. "The Restricted Problem of Three Bodies", indicates, the study of orbits (particularly periodic ones, for the reasons already given) and of the restricted problem, is inextricably linked, and the analytical and numerical techniques developed primarily for the purpose of attacking the restricted problem are applicable to many other dynamical problems.

The analytical and numerical approaches to the determination of periodic orbits are essentially complementary. Since the restricted problem is non-integrable, arbitrary solutions can only be determined by numerical methods; however, rigorous proofs of existence, and other properties of periodic orbits, can only be achieved by analytical theory. It is important to recognise the fundamental limitations of the numerical approach to the restricted problem. Numerical integration of the equations of motion can only give an approximation to the exact solution, because the differential equations themselves are not in fact integrated; rather, they are replaced by finite difference equations with solutions which may have completely different characteristics from the original differential equations. The numerical approach relies heavily on analytical theorems of existence, continuity, etc. for its validity; but in return, it offers a wealth of results which may stimulate further analytical development and a greater understanding of the structure of the set of periodic solutions unattainable by purely analytical methods.

Attention has, in the past, focused almost exclusively on the periodic orbits of the planar circular case of the restricted problem, although in recent years there has been increasing interest in the three-dimensional, and to a lesser extent the elliptic, cases. The main theme of this thesis is the structure of periodic solutions of the restricted problem in all of its manifestations, and particularly the relationships which exist between periodic orbits of the planar and three-dimensional cases, and between periodic orbits of the circular and elliptic cases. The approach taken in this chapter is therefore general in character, dealing with such topics as periodicity and symmetry in the context of three-dimensional orbits of the circular and elliptic problems; mention will be made, where appropriate, of the simplifications arising in the case of planar orbits. Section 2.6 deals with the Strömberg classification of periodic orbits in the planar circular problem, and is therefore specific to that particular case; as we shall see in later chapters, however, the basic Strömberg nomenclature can be generalised to allow the classification of <sup>families of</sup> three-dimensional periodic orbits, as well as orbits of the elliptic problem.

## 2.2 Definition and Classification

The definition of a periodic orbit of the restricted three-body problem given in the previous section can be expressed in mathematical form in terms of the position vector  $\underline{r}(\theta) = (x(\theta), y(\theta), z(\theta))$  of the massless third body with respect to the barycentric rotating-pulsating coordinate system. A periodic orbit is any solution  $\underline{r}(\theta)$  of the equations of motion (1.38) which, for all values of  $\theta$ , satisfies

$$\underline{r}(\theta + T) = \underline{r}(\theta), \quad (2.1)$$

where  $T$ , a positive constant, is the PERIOD of the solution. This definition of periodicity, it should be noted, means periodicity with respect to the rotating-pulsating coordinate system, and does not necessarily involve periodicity with respect to an inertial frame of reference. An important distinction arises here between the circular ( $e = 0$ ) and elliptic ( $e > 0$ ) versions of the restricted problem, as we shall see.

Differentiation of Equation (2.1) with respect to  $\theta$  yields

$$\underline{r}'(\theta + T) = \underline{r}'(\theta). \quad (2.2)$$

Equations (2.1) and (2.2) can be combined, using the state vector  $\underline{s} = (\underline{r}, \underline{r}')$ , to give

$$\underline{s}(\theta + T) = \underline{s}(\theta), \quad (2.3)$$

which, upon differentiation, yields

$$\underline{s}'(\theta + T) = \underline{s}'(\theta). \quad (2.4)$$

Now the equations of motion of the restricted problem, in state vector form, are (Equation (1.42))

$$\underline{s}' = \underline{f}(\underline{s}; \theta). \quad (2.5)$$

From Equations (2.3), (2.4) and (2.5) it is found that for a periodic orbit, the function  $\underline{f}$  satisfies

$$\underline{f}(\underline{s}(\theta); \theta + T) = \underline{f}(\underline{s}(\theta); \theta). \quad (2.6)$$

The part of  $\underline{f}$  explicitly dependent upon the independent variable  $\theta$  is the factor  $E(\theta) = (1 + e \cos \theta)^{-1}$  (Equations (1.43) and (1.44)). Equation (2.6) shows that

$$E(\theta + T) = E(\theta), \quad (2.7)$$

for all values of  $\theta$ , is a necessary condition for periodicity with period  $T$ . For the circular restricted problem ( $e = 0$ ),  $E(\theta) = 1$  and Equation (2.7) is satisfied for any value of  $T$ . In the elliptic problem, however,  $e \neq 0$ , and, by Equations (2.7) and (1.44), the period  $T$  must satisfy

$$T = 2k\pi \quad (2.8)$$

for some (positive) integer  $k$ . This shows that in the circular restricted problem, periodic orbits of arbitrary period may, in principle, exist, while in the elliptic restricted problem, only periodic orbits of period equal to an integer multiple of  $2\pi$  (the period of the primaries) can exist.

The transformation from dimensional inertial coordinates  $(X, Y, Z)$  to rotating-pulsating coordinates  $(x, y, z)$ , defined by Equations (1.14) and (1.23), can be written in matrix form

$$\begin{pmatrix} x \\ y \\ z \end{pmatrix} = \frac{1}{D(\theta)} \begin{pmatrix} \cos\theta & \sin\theta & 0 \\ -\sin\theta & \cos\theta & 0 \\ 0 & 0 & 1 \end{pmatrix} \begin{pmatrix} X \\ Y \\ Z \end{pmatrix}, \quad (2.9)$$

where  $D(\theta)$ , given by Equation (1.2), is periodic in  $\theta$  with period  $2\pi$ . The inverse transformation is

$$\begin{pmatrix} X \\ Y \\ Z \end{pmatrix} = D(\theta) \begin{pmatrix} \cos\theta & -\sin\theta & 0 \\ \sin\theta & \cos\theta & 0 \\ 0 & 0 & 1 \end{pmatrix} \begin{pmatrix} x \\ y \\ z \end{pmatrix}. \quad (2.10)$$

It is clear from Equation (2.10) that a periodic solution  $x(\theta), y(\theta), z(\theta)$  with respect to rotating-pulsating coordinates, with period  $T$ , will transform to a periodic solution  $X(\theta), Y(\theta), Z(\theta)$  with respect to the inertial coordinate system if and only if  $T = 2k\pi$ , for some integer  $k$ . All periodic orbits of the elliptic problem are therefore periodic with respect to both rotating and non-rotating frames, while in the circular problem an orbit which is periodic in the rotating frame will not in general be periodic in the inertial frame, unless the period satisfies Equation (2.8).

Any periodic orbit of the restricted problem can be classified according to the following general scheme:

- (a) planar or three-dimensional;
- (b) circular or elliptic problem;
- (c) symmetric or asymmetric.

The properties (a) and (b) have already been discussed; the symmetry property (c) will be dealt with in Section 2.3. The three properties (a), (b) and (c) are all independent, and consequently there are eight

categories of periodic orbits within this classification scheme. Of the eight categories, four (those consisting of symmetric periodic orbits) are of interest in this thesis, while the other four categories (consisting of asymmetric periodic orbits) will not be considered. In principle, the orbits of actual astronomical systems would be more accurately approximated by asymmetric than by symmetric periodic orbits; however, from the computational point of view, it is much easier to determine symmetric orbits, and it is reasonable to suppose that we may arrive at general conclusions with regard to orbital stability of natural systems by investigating symmetric periodic orbits alone. The definition (2.1) of periodicity is the most general statement of the property, and applies to both symmetric and asymmetric orbits, as well as to both planar and three-dimensional orbits, and to both the circular and elliptic versions of the restricted problem. We shall see in the next section that symmetric periodic orbits are a special case with the additional property of symmetry, just as planar orbits are a special case where the motion is confined to the horizontal plane, and the circular problem is a special case where the eccentricity of the primary orbit is zero; each of these special cases has particular properties which do not apply in the more general case, such as the Jacobi integral of the circular problem.

An important and useful property of periodic orbits is that the various categories defined above are not disjoint, but are connected together through certain orbits (bifurcation orbits) which are effectively common to two (or possibly more) different categories. In subsequent chapters we shall see how families of planar and families of three-dimensional periodic orbits connect through vertical bifurcation orbits, and how families of periodic orbits in the circular and elliptic cases of the restricted problem connect through commensurable orbits. Since this thesis is concerned only with symmetric periodic orbits, bifurcations of families of symmetric with asymmetric periodic orbits, and of families of different categories of asymmetric orbits, will not be considered. Recent contributions have been made on these topics by Message (1970), Message and Taylor (1978), Taylor (1979), and Markellos (1977a, 1977b, 1978).

### 2.3 Periodicity Conditions

In the previous section, the basic definition of a periodic orbit (Equation (2.1)) was stated in terms of the position vector  $\underline{x}$  of the massless body. Since a unique solution of the equations of motion is specified by

the initial values  $(x_0, y_0, z_0, x'_0, y'_0, z'_0)$  of the position and velocity vector components, the problem of the numerical determination of a periodic orbit is equivalent to that of finding a set of initial conditions  $\underline{s}_0$ , such that upon integration of Equation (1.42) from  $\theta = \theta_0$  to  $\theta = \theta_0 + T$ , for some positive  $T$ , the state vector satisfies

$$\underline{S}(\underline{s}_0; \theta_0; \theta_0 + T) - \underline{s}_0 = \underline{Q}. \quad (2.11)$$

The six components of Equation (2.11) form a system of six simultaneous equations in the six unknown initial conditions, and the period, also unknown; hence, this system is underdetermined, with one degree of freedom, and we may apply an arbitrary constraint, such as fixing the value of one of the initial conditions. A great deal of effort has been devoted to the problem of solving the system (2.11) and to ways of simplifying it. One obvious simplification is to consider only planar periodic orbits, reducing the dimensionality from 3 to 2, so that Equation (2.11) becomes a fourth-order rather than a sixth-order system; indeed, most of the literature of periodic orbits is concerned with planar periodic orbits, almost entirely in the circular restricted problem. Another important simplification of the problem is achieved by making use of the symmetry properties of solutions of the restricted three-body problem, as we shall see.

The relationship between symmetry and periodicity in the general N-body problem can be expressed in terms of "mirror configurations", as defined by Roy and Ovenden (1955). There are two kinds of mirror configuration, one associated with reflection in a plane, which we denote type (P), and the other associated with reflection in an axis, which we denote type (A). These two types of mirror configuration can be defined as configurations in the  $6N$ -dimensional phase space which are invariant under certain transformations. A type (P) mirror configuration is invariant under the transformation which reflects the  $N$  position vectors and  $N$  velocity vectors in an arbitrary plane in three-dimensional coordinate space and reverses the signs of the velocity components; a type (A) mirror configuration is invariant under the transformation which reflects the position and velocity vectors of all  $N$  particles in an arbitrary axis, and again reverses the signs of the velocity components. In a type (P) mirror configuration, therefore, all of the  $N$  particles lie in a common plane, with every velocity vector normal to the plane; in a type (A) mirror configuration, all of the bodies lie on a common axis, with their velocity vectors all perpendicular to the axis (but not necessarily parallel). The two types of mirror

configuration are depicted schematically in Figures 2.1 and 2.2. Note that only the directions of the velocity vectors are constrained, and not their magnitudes.

It can be shown, by a simple argument, that the orbits of the  $N$  bodies prior to the occurrence of a type (P) mirror configuration are the mirror images of the orbits after the epoch of the mirror configuration, under reflection in the plane of the mirror configuration; similarly, the orbits before and after the occurrence of a type (A) mirror configuration are images of one another under reflection in the axis of the mirror configuration. The Periodicity Theorem of Roy and Ovenden (1955) states that any solution of the equations of motion of an  $N$ -body system in which two mirror configurations occur at distinct epochs is periodic. This sufficient (but not necessary) condition for periodicity also confers symmetry on the orbits of the  $N$  bodies because of the "mirror image" property; the type of symmetry depends on which of the two possible kinds of mirror configuration occur in the orbit: that is, whether they are both of type (P), both of type (A), or one of each type.

Having discussed mirror configurations and periodicity in the context of the general  $N$ -body problem, let us now apply these considerations to the determination of periodic orbits of the restricted <sup>three-body</sup> problem. First of all, we state the conditions which must be satisfied for the occurrence of each type of mirror configuration. From the specifications of the two possible types of mirror configuration already given, these conditions may be stated as follows:

Type (P) A type (P) mirror configuration occurs if and only if the massless particle of the system of three bodies is in the  $(x,z)$ -plane (the plane defined by the line joining the two massive primaries and the axis about which the primaries revolve in their orbit), with its instantaneous velocity vector perpendicular to that plane; in addition, if the relative orbit of the primaries is elliptic, with eccentricity  $e > 0$ , the primaries must be located at either periapsis or apoapsis.

Type (A) A type (A) mirror configuration occurs if and only if the massless particle is on the  $x$ -axis (the axis of the primaries), with its instantaneous velocity vector perpendicular to

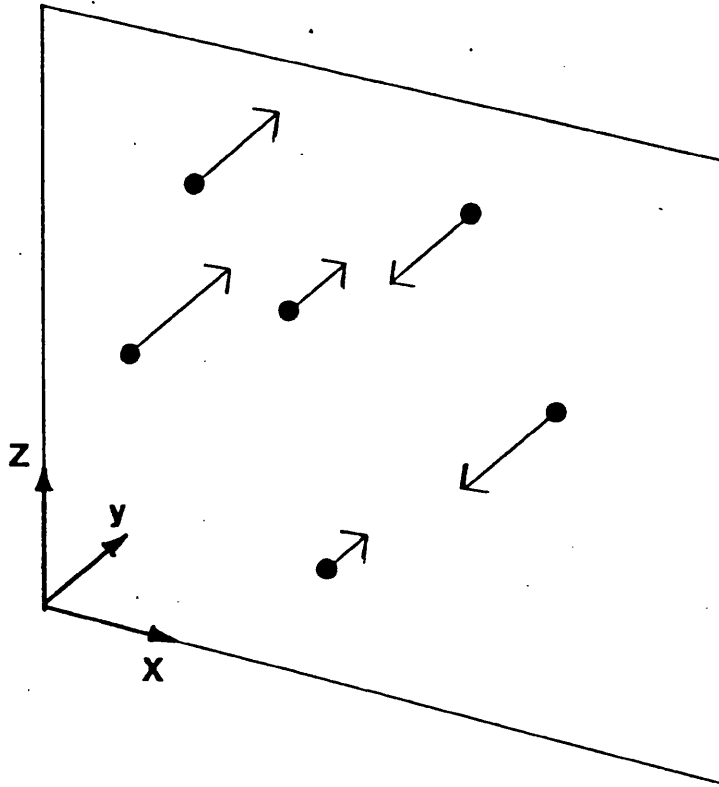


Figure 2.1 : Schematic representation of a type (P) mirror configuration. The  $N$  particles all lie in a common plane  $(x,z)$ , with their velocity vectors normal to the plane.

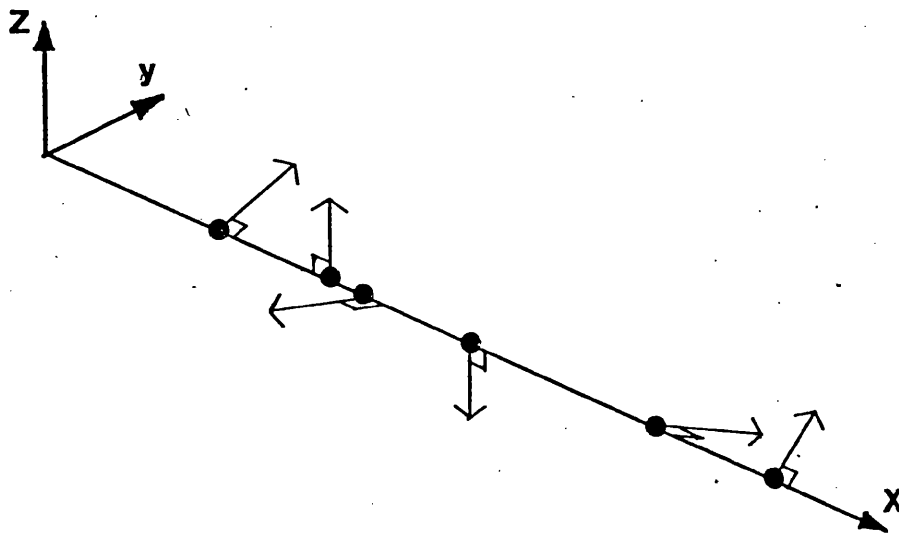


Figure 2.2 : Schematic representation of a type (A) mirror configuration. The  $N$  particles all lie on a common axis  $(x)$ , with their velocity vectors perpendicular to the axis.

that axis; again, if the primary orbit is non-circular, the primaries must be located at one or other of the apses of their relative orbit.

It should be noted that the two types of mirror configuration in the restricted three-body problem differ only in terms of the position and velocity of the massless third body. For both types of mirror configuration, the instantaneous velocity vectors of the primaries with respect to their centre of mass must be perpendicular to the axis joining them, in order to satisfy the perpendicularity requirement on the velocity vectors of all three bodies. In the case of a circular relative orbit of the primaries (the circular restricted problem), the orbital velocities of the primaries are always at right angles to their radius vectors, and so this requirement is satisfied at all epochs; in the case of elliptic motion of the primaries, the velocities are perpendicular to the radius vectors only at the instants when the primaries are at periapsis or at apoapsis.

There is no distinction between the two types of mirror configuration in the planar restricted problem; a mirror configuration occurs when the third body is located on the axis of the primaries, with its velocity vector directed at right angles to the axis (that is, in the y-direction). In the planar case of the elliptic restricted problem, the requirement that the primaries be located at either periapsis or apoapsis still applies.

The conditions stated above for the two types of mirror configuration in the restricted problem can be expressed in terms of the components  $(x, y, z, x', y', z')$  of the state vector  $\underline{s}$ , as follows:

$$\text{Type (P) mirror configuration : } y = x' = z' = 0; \quad (2.12)$$

$$\text{Type (A) mirror configuration : } y = z = x' = 0. \quad (2.13)$$

In both cases, the remaining three components of  $\underline{s}$  ( $x, z$  and  $y'$  for type (P);  $x, y'$  and  $z'$  for type (A)) are not constrained by the mirror configuration conditions, and may therefore have arbitrary values. The additional requirement that the primaries must be located at periapsis or apoapsis in the elliptic restricted problem can be expressed in terms of the true anomaly  $\theta$  of the primaries:

$$\theta = K\pi, \quad (2.14)$$

where  $K$  is an integer.

In the planar restricted problem, we have  $z = z' = 0$  by definition, and the conditions (2.12) and (2.13) reduce to

$$y = x' = 0, \quad (2.15)$$

the remaining non-zero components  $x$  and  $y'$  of the state vector being unconstrained.

From Equations (2.12) and (2.13), we can write down the form of the initial conditions corresponding to the two types of mirror configuration:

$$\underline{s}_0 = (x_0, 0, z_0, 0, y'_0, 0) \quad [\text{TYPE (P)}]; \quad (2.16)$$

$$\underline{s}_0 = (x_0, 0, 0, 0, y'_0, z'_0) \quad [\text{TYPE (A)}]. \quad (2.17)$$

For an elliptic orbit of the primaries, a mirror configuration can only occur at the initial epoch if the corresponding value of the true anomaly satisfies

$$\theta_0 = K_0 \pi, \quad (2.18)$$

where  $K_0$  is an integer, which can, without loss of generality, be taken to be either  $K_0 = 0$  (periapsis) or  $K_0 = 1$  (apoapsis). The initial value of  $\theta$  can be taken to be  $\theta_0 = 0$  in the circular restricted problem, again without loss of generality, by an appropriate choice of the direction of the  $x$ -axis.

By the Periodicity Theorem, an orbit with initial conditions satisfying either Equation (2.16) or Equation (2.17), with an appropriate value of  $\theta_0$ , will be periodic if at some later epoch (the "final" epoch) the state vector again satisfies the conditions for a mirror configuration (Equation (2.12) or (2.13)), the true anomaly  $\theta_1$  of the primaries at the final epoch also satisfying Equation (2.14) if the orbital eccentricity of the primaries is non-zero. Referring to the fact that in the circular problem there is no constraint on  $\theta_0$  and  $\theta_1$  (except that  $\theta_1 \neq \theta_0$ ), while in the elliptic problem  $\theta_0$  and  $\theta_1$  must be integer multiples of  $\pi$ , Broucke (1969) calls the condition for periodicity in the circular case the "weak periodicity criterion", and that for the elliptic case the "strong periodicity criterion". Writing the formal solution of the equations of motion (1.42) (in state vector notation) as

$$\underline{z} = \underline{z}(\underline{s}_0; \theta_0; \theta), \quad (2.19)$$

and taking the initial conditions  $\underline{s}_0$  in the form (2.16) or (2.17), the "weak periodicity criterion" for a symmetric periodic orbit of the circular restricted problem can be stated as either

$$\underline{S}(\underline{s}_0; \theta_0; \theta_1) = (x, 0, z, 0, y', 0), \quad (2.20)$$

or

$$\underline{S}(\underline{s}_0; \theta_0; \theta_1) = (x, 0, 0, 0, y', z'), \quad (2.21)$$

depending on the type of mirror configuration occurring at the final epoch, with  $\theta_0 = 0$  and  $\theta_1 > 0$ . The "strong periodicity criterion" for a symmetric orbit of the elliptic restricted problem consists of the weak periodicity criterion plus the requirements

$$\begin{aligned} \theta_0 &= 0 \text{ or } \pi, \\ \theta_1 &= \theta_0 + k\pi, \end{aligned} \quad (2.22)$$

where  $k = K - K_0$  is a positive integer.

(Note: In subsequent chapters of this thesis, the term "periodicity conditions" will be used in preference to "periodicity criterion").

#### 2.4 Symmetry Classes

In the previous section, the existence of different classes of three-dimensional symmetric periodic orbits in the general N-body problem, according to the types of mirror configuration occurring at the "initial" and "final" epochs, was alluded to. We shall now examine the classification of symmetry properties on this basis in more detail, confining our attention to the particular case of interest, namely the restricted three-body problem.

By the Periodicity Theorem, an orbit of the restricted problem is both symmetric and periodic if it satisfies the conditions for a mirror configuration at two distinct epochs. There are four ways in which this can be achieved, corresponding to the four combinations (P) - (P), (A) - (A), (P) - (A) and (A) - (P) of types of mirror configuration occurring at the two epochs. We have already seen that any orbit in which a type (P) mirror configuration occurs is symmetrical with respect to the plane of the mirror configuration (the (x,z)-plane), and that similarly any orbit in which a

type (A) mirror configuration takes place is symmetrical with respect to the axis of the mirror configuration (the x-axis). An orbit in which both types of mirror configuration take place must, therefore, possess symmetry with respect to both the (x,z)-plane and the x-axis (and consequently the (x,y)-plane, as well). Thus, three classes of symmetric periodic orbits can be distinguished, corresponding to the combinations of mirror configurations

- (i) (P) - (P)
- (ii) (A) - (A)
- (iii) (P) - (A) and (A) - (P).

(Symmetry classes (i),(ii) and (iii) listed here correspond respectively to the classes (A),(B) and (C) defined by Goudas (1961)). Orbits of class (i) are called "plane symmetric", and orbits of class (ii) "axisymmetric"; the orbits belonging to classes (i) and (ii), which possess only one type of symmetry, are collectively referred to as "simply symmetric". There is no essential difference between orbits for which the sequence of mirror configurations is (P) - (A) and those for which it is (A) - (P) (the choice of "initial" mirror configuration is an arbitrary one); consequently, both of these cases are taken together in class (iii) of "doubly symmetric" periodic orbits. (Since this class of orbits actually possesses three kinds of symmetry - symmetry with respect to the (x,y)- and (x,z)-planes, and the x-axis - it should strictly be termed "triply symmetric"; but the term "doubly symmetric" is the conventional one).

Because of the fact that there is no distinction between the two types of mirror configuration in the planar restricted problem, there is only one type of symmetry, namely symmetry with respect to the x-axis; this is the degenerate form of all three kinds of three-dimensional symmetry when the motion of the third body is confined to the plane of the primaries. This general property of symmetry with respect to the x-axis should not be confused with the special symmetry, with respect to the y-axis, of a certain class of periodic orbits of the Copenhagen problem ( $\mu = \frac{1}{2}$ , that is, the case of equal masses of the primaries) which no longer holds for values of  $\mu \neq \frac{1}{2}$ .

From the computational point of view, symmetric periodic orbits have the convenient property that they can be determined by numerical integration over only half or quarter of the orbital period, rather than requiring integration over the full period, thus saving a substantial amount of computer time. In order to show this, let us denote by  $C_0$  and  $C_1$  respectively the mirror

configurations occurring at  $\theta = \theta_0$  and  $\theta = \theta_1$  (the initial and final epochs), defining a certain periodic orbit. (Note that it is assumed that  $C_1$  is the first mirror configuration to be encountered after the system has passed through configuration  $C_0$ ). For orbits of simple symmetry (mirror configurations  $C_0$  and  $C_1$  of the same type), the motion following configuration  $C_1$  is simply the mirror image, in either the  $(x,z)$ -plane or the  $x$ -axis, as appropriate, of the part of the orbit between  $C_0$  and  $C_1$ . The massless body will therefore return to the original configuration  $C_0$ , completing one orbital period, after a further interval equal to that between  $C_0$  and  $C_1$ , and so the period of the orbit is given by

$$T = 2(\theta_1 - \theta_0) \quad [\text{SIMPLE SYMMETRY}]; \quad (2.23)$$

in other words, the interval  $\theta_1 - \theta_0$  between successive mirror configurations in a periodic orbit of simple symmetry is equal to half the orbital period. For a doubly-symmetric orbit, the situation is slightly different. If we assume, without loss of generality, that  $C_0$  is a type (A) and  $C_1$  a type (P) mirror configuration, it is clear that the segment  $C_0C_1$  of the orbit has mirror image  $C_1C_2$  in the  $(x,z)$ -plane, where  $C_2$ , another mirror configuration occurring at a further interval  $\theta_1 - \theta_0$  after  $C_1$ , is the image of the starting configuration  $C_0$  in the  $(x,y)$ -plane. Since  $C_0$  and  $C_2$  differ in the sign of the  $z$ -velocity of the massless particle, they are not identical, and so periodicity is not achieved. In fact the orbit is described over one full orbital period only after a further interval, equal to the interval from  $C_0$  to  $C_2$ , when the particle returns to the starting configuration  $C_0$ . In one complete description of the orbit, four different mirror configurations take place at intervals of one quarter of the period: two of these are of type (P) and the other two of type (A), the members of each pair of mirror configurations being images of one another under reflection in the  $(x,y)$ -plane (the plane of the primaries). Thus the period of a doubly-symmetric periodic orbit is given by

$$T = 4(\theta_1 - \theta_0) \quad [\text{DOUBLE SYMMETRY}], \quad (2.24)$$

and the interval between mirror configurations  $C_0$  and  $C_1$ , defining the orbit, is equal to a quarter of the period.

For symmetric periodic orbits of the elliptic restricted problem, the interval  $\theta_1 - \theta_0$  between successive mirror configurations must be equal to an integer multiple of  $\pi$ , as was shown in Section 2.2. Equations (2.23)

and (2.24) show that simply-symmetric periodic orbits of the elliptic problem have periods of  $2k\pi$  ( $k = 1, 2, 3, \dots$ ), while doubly-symmetric periodic orbits can only have periods equal to  $4k\pi$  ( $k = 1, 2, 3, \dots$ ). This means that periodic orbits of class (iii) (double symmetry) are less common in the elliptic problem than in the circular case; this will be discussed further in another chapter.

Since only "simple" symmetry, with respect to the x-axis, is found in the planar restricted problem, mirror configurations always occur at intervals of half the orbital period. In the planar elliptic case, there exist symmetric periodic orbits with periods of  $2k\pi$  for all positive integral values of  $k$ .

## 2.5 Families of Periodic Orbits

So far in this chapter, we have been discussing the properties of individual periodic orbits, with reference to broad classification schemes. In this section, we shall consider an important aspect of the structure of symmetric periodic orbits, namely their occurrence in infinite numbers as members of continuous sets in which a smooth transition of characteristic properties (for example, initial conditions, period, stability) is evident between neighbouring orbits. We shall see that these sets, or FAMILIES (or in some cases, SERIES) are, for a fixed value of the mass parameter of the primaries, monoparametric: in other words, a member of a given family of periodic orbits can be uniquely specified by the value of a single parameter. Although only symmetric periodic orbits will be considered, the argument can easily be generalised to include asymmetric periodic orbits.

It will be found very useful in this section and elsewhere to employ a uniform notation for the periodicity conditions of a symmetric periodic orbit. Equations (2.16) and (2.17), giving the form of the initial conditions  $\underline{s}_0 = (s_{01}, s_{02}, s_{03}, s_{04}, s_{05}, s_{06}) = (x_0, y_0, z_0, x'_0, y'_0, z'_0)$  for a mirror configuration of type (P) and of type (A) respectively, can be written in the common form

$$\underline{s}_0 = (s_{01}, s_{05}, s_{0i}) , \quad (2.25)$$

where the subscript  $i = 3$  for a type (P) and  $i = 6$  for a type (A) mirror configuration at the initial epoch, and the zero components of  $\underline{s}_0$  have been omitted. Similarly, Equations (2.12) and (2.13) can be combined in the form

$$s_2 = s_4 = s_j = 0, \quad (2.26)$$

where  $j = 6$  for a type (P) and  $j = 3$  for a type (A) mirror configuration. In this notation, the periodicity conditions (2.20) and (2.21) for a symmetric periodic orbit (in the "weak" form) can be expressed as

$$\begin{aligned} S_2 (s_{01}, s_{05}, s_{0i}; \theta_0; \theta_1) &= 0, \\ S_4 (s_{01}, s_{05}, s_{0i}; \theta_0; \theta_1) &= 0, \\ S_j (s_{01}, s_{05}, s_{0i}; \theta_0; \theta_1) &= 0. \end{aligned} \quad (2.27)$$

Let us first of all consider the system of equations (2.27) as applied to periodic orbits of the circular restricted problem. In this case, as we have seen,  $\theta_0$  can be taken to be zero and, from the discussion of the previous section,  $\theta_1$  must be equal to half or quarter of the orbital period  $T$ , according as the orbit is simply or doubly symmetric. The periodicity conditions (2.27) therefore form a system of three simultaneous equations in four unknowns: the initial conditions  $(s_{01}, s_{05}, s_{0i})$ , and  $\theta_1$ , or, equivalently, the period  $T$ . Now for a given value of the mass parameter  $\mu$  in the circular restricted problem, the values of  $s_{01}, s_{05}$  and  $s_{0i}$  (the other three initial conditions having the value zero), and of  $T$ , specify a unique periodic solution of the equations of motion; these four unknowns are subject to three constraints (Equations (2.27)), and therefore have one degree of freedom. Since all four of these quantities may vary in a continuous fashion (by the continuity property of the solutions of the differential equations of motion), we conclude that solutions of the periodicity conditions occur in monoparametric sets.

Periodic orbits of the elliptic restricted problem must satisfy the "strong" periodicity conditions, and so the values of  $\theta_0$  and  $\theta_1$  in Equations (2.27) are subject to the constraints (2.22). By the continuity property of solutions of the differential equations of motion, and therefore of solutions of Equations (2.27), it is clear that periodic orbits of the elliptic problem represented by neighbouring points in the phase space must have the same values of  $\theta_0$  and  $\theta_1$ . In other words, since the period of a periodic orbit in the elliptic problem can only have the discrete values  $2k\pi$  ( $k = 1, 2, 3, \dots$ ) and cannot vary in a continuous fashion as in the circular problem, once the values of  $\mu$  and  $e$  have been specified the non-zero initial conditions  $(s_{01}, s_{05}, s_{0i})$  are uniquely determined by Equations (2.27). This means that for given values of the parameters  $\mu$  and  $e$ , periodic orbits occur as discrete entities and not in continuous families, as in the circular problem. However, if only the mass parameter  $\mu$  is kept fixed and the eccentricity  $e$  of the orbit of the primaries is

allowed to vary, we see that families of periodic orbits can be said to exist in the elliptic problem, parametrised by the eccentricity of the primaries. The foregoing discussion shows that if we take the restricted three-body problem in the general sense, rather than in a particular application corresponding to given values of the parameters  $\mu$  and  $e$ , the structure of symmetric periodic solutions is characteristically biparametric. In the circular restricted problem, the two parameters controlling the structure are  $\mu$  and  $T$ , and in the elliptic problem they are  $\mu$  and  $e$ .

No specific mention has been made so far in this section of planar periodic orbits. If the periodicity conditions (2.27) are applied to planar orbits, we automatically have  $s_{0i} = 0$  and  $s_j = 0$ . Thus, one of the three periodicity conditions disappears, while one of the unknowns ( $s_{0i}$ ) assumes a fixed (zero) value; there is no net effect on the number of degrees of freedom of the system of equations. The conclusions presented above are therefore equally valid in the planar and three-dimensional versions of the restricted problem, as might be expected, since the planar restricted problem is simply a special case of the more general three-dimensional restricted problem.

## 2.6 Strömberg Classification

In the 1920's and 1930's a very thorough investigation of the periodic orbits of the planar circular restricted problem, mainly in the so-called Copenhagen case ( $\mu = \frac{1}{2}$ ), was carried out by Strömberg and his co-workers at the Copenhagen Observatory. Strömberg (1933) introduced a classification of the main families of periodic orbits of Poincaré's first generation ("première genre"), consisting for the most part of simple-periodic (one-revolution) orbits. This classification is widely used in the literature of periodic orbits, and will be employed frequently in this thesis; it is therefore worthwhile including a brief discussion of the scheme for reference purposes.

The Strömberg classification is based on two simple characteristics of the generating orbits from which the various families of periodic orbits can be obtained. The generating orbits are either infinitesimal orbits about one of the primaries or one of the five equilibrium points, or two-body orbits around both of the primaries, and can be either direct (having the same sense of rotation as the orbit of the primaries) or retrograde (having the opposite sense of rotation to that of the primaries). For a

typical orbit of one of Strömberg's families, the definitions of the two characteristics "centre of orbital motion" and "sense of rotation" are not always clear-cut, and apply rigorously only to the generating orbits themselves; thus Strömberg's simple classification does not truly reflect the complexity of the structure of periodic orbits of the planar circular problem, but is, nevertheless a useful scheme which can be successfully applied (with slight modifications) in cases other than the Copenhagen ( $\mu = \frac{1}{2}$ ) case of the restricted problem.

With the notation of Figure 1.4 for the Lagrange equilibrium points (Section 1.6), the most important Strömberg classes are as follows:

- (a) retrograde periodic orbits around  $L_1$  (direct orbits non-existent)
- (b) retrograde periodic orbits around  $L_3$  (direct orbits non-existent)
- (c) retrograde periodic orbits around  $L_2$  (direct orbits non-existent)
- (d) periodic orbits around  $L_4$  (non-existent for  $\mu = \frac{1}{2}$ )
- (e) periodic orbits around  $L_5$  (non-existent for  $\mu = \frac{1}{2}$ )
- (f) retrograde periodic orbits around  $m_2$
- (g) direct periodic orbits around  $m_2$
- (h) retrograde periodic orbits around  $m_1$
- (i) direct periodic orbits around  $m_1$
- (k) periodic orbits around both primaries : synodically direct
- (l) periodic orbits around both primaries : synodically retrograde,  
sidereally direct
- (m) periodic orbits around both primaries : retrograde with respect to  
both rotating and fixed axes.

All of these classes, with the exception of d and e, consist of periodic orbits symmetrical with respect to the x-axis. The distinction between classes k,l and m arises from the fact that the sense of rotation of the massless particle is not necessarily the same with respect to the fixed (or "sidereal") coordinate system OXYZ and the rotating (or "synodical") coordinate system Oxyz. If the mean motion of the primaries about the barycentre, with respect to the fixed axes, is denoted by  $n_0$ , and that of the third body in its two-body generating orbit around the two primaries is denoted by  $n$ , then classes k,l and m correspond to the cases  $n > n_0$ ,  $0 < n < n_0$  and  $n < 0$ , respectively.

Because of the invariance of the equations of motion of the planar restricted problem under the exchange  $\mu \leftrightarrow 1 - \mu$ , combined with a  $180^\circ$

rotation of the x and y coordinate axes about the origin O, several of the Strömberg classes of periodic orbits are not independent, but have a pairwise correspondence under this transformation. It is easily seen that families a and b, d and e, f and h, and g and i, are essentially identical apart from a  $180^\circ$  rotation of the coordinate system, if the mass parameter  $\mu$  is considered to take all possible values between 0 and 1. It is possible to distinguish between families a and b, f and h, and g and i if  $\mu$  is taken to be less than  $\frac{1}{2}$ , so that  $m_2$  can be chosen as the less massive of the two primaries; families d and e, however, are always equivalent, because as a result of the symmetry property of the restricted problem, asymmetric periodic orbits occur in mirror image pairs with respect to the x-axis.

Among the twelve "natural" classes of periodic orbits listed above, our attention in later chapters will be focused particularly on the "retrograde satellite orbits" of family f, and to a lesser extent on the "direct satellite orbits" of family g. (The primary  $m_2$  is usually taken to be the less massive of the two, as remarked earlier, and for small values of the mass parameter  $\mu$ , the orbits of family f correspond to periodic satellite orbits around a planet; the more massive primary  $m_1$  then represents the Sun). Family f, especially in the Sun-Jupiter case ( $\mu = 0.00095$ ) of the restricted problem, is of interest for a number of reasons: for example, it has been found (e.g. Hénon, 1965b; Markellos, 1974b; Benest, 1976, 1977) that the orbits of family f remain stable at large distances from the primary  $m_2$ , unlike the orbits of class g, and this may be related to the observation that Jupiter's outermost group of satellites, which experience very large solar perturbations, all have retrograde motion, while all of the direct satellites have much smaller orbits (e.g. Hunter, 1967).

The study of the periodic orbits of the Copenhagen category begun by Strömberg and his school was continued by Hénon (1965a,b), resulting in the discovery of several new classes of periodic orbits. Hénon (1969) also explored the periodic orbits of Hill's problem ( $\mu = 0$ ), which bear a close resemblance to certain classes of periodic orbits of the restricted problem for small values of  $\mu$ , and investigated the stability properties of periodic orbits of the main families of the restricted problem for all values of the mass parameter (Hénon and Guyot, 1970; Hénon, 1973a, 1974).

### 3. STABILITY, SELF-RESONANCE AND BIFURCATION

#### 3.1 Introduction

In this chapter, some properties of periodic orbits, both individually and collectively, will be discussed. The discussion centres around the question of the variation in a given periodic orbit resulting from a small change in its initial conditions; as we shall see, this is closely connected with the usual definition of stability (in the linear sense) in dynamics and in mathematics, and also has an important bearing on the structure of periodic orbits, through the phenomenon of bifurcation.

The main objective of research into the restricted problem is not only to map out the global set of solutions, but also to determine their stability properties, and the importance of stability in the overall structure of periodic orbits is underlined by the predictions of linearised analytical theory, confirmed by extensive numerical investigations, of the occurrence of bifurcations for particular values of the linear stability indices (see Section 3.5).

The concept of stability with respect to small disturbances, or perturbations, is a natural one. A dynamical system is said to be in a stable configuration if, upon being subjected to a small external disturbance, it tends to return to the original configuration; an unstable configuration, on the other hand, is one in which a small disturbance leads to greater and greater departures from the original configuration. This definition is most easily thought of in terms of static configurations, or states of equilibrium; for example, a disc lying flat on a table (stable equilibrium) or standing upright on its edge (unstable equilibrium). More generally, we can define stability with respect to small perturbations for dynamical systems constantly in motion; we then have to measure the departure from a reference orbit (or solution), rather than a fixed configuration, resulting from an imposed perturbation at some epoch. In practice, this can only be done for a periodic orbit, from which the departure of a perturbed orbit over arbitrary time intervals can be determined by considering the departure over a finite interval (the orbital period).

In Section 3.2, the variational equations are obtained: these describe, to first order, the effect of a small perturbation on a given solution of the equations of motion. The first-order variational equations are applied

to the question of linear stability in Section 3.4. Section 3.3 deals with variations with respect to the parameters  $\mu$  and  $e$  of the restricted problem, which although not connected with the discussion of stability, are important in the determination of families (or series) of periodic orbits in which one or both of these parameters vary; this will be taken up in Chapter 4. Section 3.5 gives an outline of the phenomenon of bifurcation, in general terms, with reference to bifurcations of planar periodic orbits with three-dimensional periodic orbits ("vertical" bifurcations). This type of bifurcation is discussed in some detail for the case of symmetric orbits in Section 3.6.

Throughout this chapter, it is important to remember that a linear stability analysis of a nonlinear system neglects <sup>terms</sup> of second and higher orders in the Taylor series expansion, on the assumption that these are small compared with the first-order terms. This assumption can be examined either by actually calculating the higher-order contributions or by comparing the linear theory with the results of numerical integrations. For example, the prediction of the occurrence of a bifurcation for certain values of the linear stability parameters can be tested by attempting to find numerically a periodic orbit belonging to the bifurcating family, and indeed there is ample evidence (such as that offered in this thesis) that the linear approximation is valid. However, it is known (e.g. Bray and Goudas, 1967) that periodic orbits found to be linearly stable may in fact be unstable because of third- or higher-order terms in the initial perturbation. References to stability of periodic orbits in this thesis should always be taken to mean linear stability.

### 3.2 Variational Equations

The equations of motion of the restricted problem can be written, as we saw in Section 1.4, in the state-vector form (Equation (1.42))

$$\dot{\underline{s}} = \underline{f}(\underline{s}; \theta) \quad (3.1)$$

with formal solution (Equation (2.19))

$$\underline{s} = \underline{\mathcal{L}}(\underline{s}_0; \theta_0; \theta) \quad (3.2)$$

Suppose that the solution corresponding to initial conditions  $\underline{s}_0 = (s_{01}, s_{02}, s_{03}, s_{04}, s_{05}, s_{06})$  at  $\theta = \theta_0$ , as given by Equation (3.2), is known;

this will be referred to as the "unperturbed" solution, or orbit. Let us consider an orbit in the neighbourhood of the known orbit, with initial conditions (at  $\theta = \theta_0$ ) given by

$$\underline{s}_0^* = \underline{s}_0 + \delta \underline{s}_0, \quad (3.3)$$

where the perturbation  $\delta \underline{s}_0$  has components  $\delta \underline{s}_0 = (\delta s_{01}, \delta s_{02}, \delta s_{03}, \delta s_{04}, \delta s_{05}, \delta s_{06})$ , which are all assumed to be small. The perturbed orbit is given by

$$\underline{s}^* = \underline{s}(\underline{s}_0^*; \theta_0; \theta). \quad (3.4)$$

The right-hand side of Equation (3.4) can be expanded in Taylor series about the unperturbed solution; if  $\delta \underline{s}_0$  is sufficiently small, terms in the expansion of second and higher order in the components of  $\delta \underline{s}_0$  may be neglected, and to first order we have

$$\underline{s}^* = \underline{s}(\underline{s}_0; \theta_0; \theta) + V(\underline{s}_0; \theta_0; \theta) \delta \underline{s}_0, \quad (3.5)$$

where the Jacobian matrix  $V$  is given by

$$V(\underline{s}_0; \theta_0; \theta) = [v_{ij}]_{6 \times 6} \quad (3.6)$$

and

$$v_{ij} = \frac{\partial s_i}{\partial s_{0j}} \quad (i, j = 1, 2, \dots, 6). \quad (3.7)$$

The partial derivatives  $v_{ij}$  are to be evaluated on the unperturbed orbit at true anomaly  $\theta$ . Defining the "variation" vector

$$\delta \underline{s} = \underline{s}^* - \underline{s}, \quad (3.8)$$

we have, by Equation (3.5)

$$\delta \underline{s} = V \delta \underline{s}_0. \quad (3.9)$$

Differentiating Equation (3.9) with respect to the independent variable  $\theta$ , we obtain

$$\delta \underline{s}' = V \delta \underline{s}_0 ; \quad (3.10)$$

the elements of  $V'$  are, by Equations (3.1) and (3.2),

$$\begin{aligned} v'_{ij} &= \sum_{k=1}^6 \frac{\partial f_i}{\partial s_k} \frac{\partial s_k}{\partial s_{0j}} \\ &= \sum_{k=1}^6 f_{ik} v_{kj} \quad (i, j = 1, 2, \dots, 6), \end{aligned} \quad (3.11)$$

where  $f_i$  is the  $i^{\text{th}}$  component of the vector function  $\underline{f}$  (given by Equations (1.43)) and

$$f_{ik} = \frac{\partial f_i}{\partial s_k} \quad (i, k = 1, 2, \dots, 6). \quad (3.12)$$

In matrix form, Equations (3.11) can be written

$$V' = FV \quad (3.13)$$

where

$$F = [f_{ik}]_{6 \times 6}. \quad (3.14)$$

Using Equations (3.9) and (3.13), Equation (3.10) becomes

$$\delta \underline{s}' = F \delta \underline{s}_0. \quad (3.15)$$

The vector equations (3.15) are known as the VARIATIONAL EQUATIONS of the unperturbed orbit, and have solutions given by Equations (3.9).

The matrix  $F$  is easily calculated from Equations (1.43) and (1.44), and is given by

$$F = \begin{pmatrix} 0 & 0 & 0 & 1 & 0 & 0 \\ 0 & 0 & 0 & 0 & 1 & 0 \\ 0 & 0 & 0 & 0 & 0 & 1 \\ f_{41} & f_{42} & f_{43} & 0 & 2 & 0 \\ f_{51} & f_{52} & f_{53} & -2 & 0 & 0 \\ f_{61} & f_{62} & f_{63} & 0 & 0 & 0 \end{pmatrix}, \quad (3.16)$$

where

$$\begin{aligned}
 f_{41} &= E \left[ A + \frac{3(1-\mu)(s_1+\mu)^2}{\sigma_1^5} + \frac{3\mu(s_1+\mu-1)^2}{\sigma_2^5} \right], \\
 f_{42} &= 3E s_2 \left[ \frac{(1-\mu)(s_1+\mu)}{\sigma_1^5} + \frac{\mu(s_1+\mu-1)}{\sigma_2^5} \right], \\
 f_{43} &= 3E s_3 \left[ \frac{(1-\mu)(s_1+\mu)}{\sigma_1^5} + \frac{\mu(s_1+\mu-1)}{\sigma_2^5} \right], \\
 f_{51} &= f_{42}, \\
 f_{52} &= E \left[ A + \frac{3(1-\mu)s_2^2}{\sigma_1^5} + \frac{3\mu s_2^2}{\sigma_2^5} \right], \\
 f_{53} &= 3E s_2 s_3 \left[ \frac{1-\mu}{\sigma_1^5} + \frac{\mu}{\sigma_2^5} \right], \\
 f_{61} &= f_{43}, \\
 f_{62} &= f_{53}, \\
 f_{63} &= -1 + E \left[ A + \frac{3(1-\mu)s_3^2}{\sigma_1^5} + \frac{3\mu s_3^2}{\sigma_2^5} \right].
 \end{aligned} \tag{3.17}$$

The functions  $A(s_1, s_2, s_3)$  and  $E(\theta)$  are given by Equations (1.44). The matrix  $F$  is a function of the coordinates  $(s_1, s_2, s_3) = (x, y, z)$  and of the independent variable  $\theta$ , and is evaluated on the unperturbed orbit.

It is clear from Equation (3.13) that each of the six column vectors of the matrix  $V$  is a solution of the variational equations (3.15). At the initial epoch ( $\theta = \theta_0$ ) the elements of  $V$  are given by

$$v_{ij}(s_0; \theta_0; \theta_0) = \left( \frac{\partial s_i}{\partial s_{0j}} \right)_{\theta=\theta_0} = \delta_{ij} \quad (i, j = 1, 2, \dots, 6), \tag{3.18}$$

where  $\delta_{ij}$  is the Kronecker delta, and so

$$V(s_0, \theta_0, \theta_0) = I_6, \tag{3.19}$$

where  $I_6$  is the 6x6 unit matrix. The column vectors of  $V$  are initially linearly independent, and therefore comprise a fundamental set of linearly independent solutions of the variational equations. The matrix  $V$  is therefore a fundamental matrix, known as the "variational matrix", or as the "principal fundamental matrix" (because it corresponds to the particular set of initial conditions (3.19)) and is characteristic of a given solution of the equations of motion. The system (3.13) of thirty-six simultaneous

first-order ordinary differential equations can be numerically integrated in conjunction with the equations of motion (3.1). The variational matrix  $V$  of a periodic orbit is of central importance in the determination of its stability properties, as we shall see in Section 3.4, and is also required in differential corrector and predictor schemes for establishing families of periodic orbits; this latter application will be dealt with in Chapter 4.

In the foregoing discussion, no assumptions were made about the periodicity or otherwise of the unperturbed orbit, and the results are applicable to general non-periodic motion. The case of periodic motion will be examined further in Section 3.4, in connection with the stability of periodic orbits.

### 3.3 Variations With Respect to the Parameters

The variational equations (3.15) discussed in the previous section, with solutions (3.9), involve the variation  $\delta \underline{s}$  in an orbit resulting from a small change  $\delta \underline{s}_0$  in the initial conditions  $\underline{s}_0$ . In this section, we consider variations in an orbit resulting from small changes in the values of the mass parameter  $\mu$  and orbital eccentricity  $e$  of the primaries, the initial conditions being kept fixed. The variations with respect to these two parameters are important in the analytical and numerical continuation of periodic orbits, and will be used in subsequent chapters in differential predictor/corrector methods for the numerical determination of periodic orbits belonging to families, or series, along which one or both of the parameters  $\mu, e$  varies in a continuous fashion.

We begin by writing Equation (1.42) (the equations of motion in state vector form) more fully to show the explicit dependence of function  $f$  upon the parameters  $\mu$  and  $e$ , as given by the Equations (1.43) and (1.44):

$$\underline{s}' = \underline{f}(\underline{s}; \theta; \mu; e). \quad (3.20)$$

This has the formal solution

$$\underline{s} = \underline{s}(\underline{s}_0; \theta_0; \theta; \mu; e), \quad (3.21)$$

again with explicit dependence upon  $\mu$  and  $e$ .

Let us consider the effect of a small increment  $\delta \mu$  in the mass parameter upon an orbit given by Equation (3.21), with initial conditions  $\underline{s}_0$  at  $\theta = \theta_0$ .

The "varied" orbit is given by

$$\underline{s}^* = \underline{s}(\underline{s}_0; \theta_0; \theta; \mu + \delta\mu; e), \quad (3.22)$$

and assuming  $\delta\mu$  to be sufficiently small, expansion about the original orbit to first order in  $\delta\mu$  gives

$$\underline{s}^* = \underline{s}(\underline{s}_0; \theta_0; \theta; \mu; e) + \delta\mu \frac{d}{d\mu} \underline{s}(\underline{s}_0; \theta_0; \theta; \mu; e). \quad (3.23)$$

The variation in the orbit is

$$\delta\underline{s} = \underline{s}^* - \underline{s} = \underline{v}_\mu \delta\mu, \quad (3.24)$$

where the vector  $\underline{v}_\mu$  stands for  $d\underline{s}/d\mu$ , evaluated on the original orbit. The corresponding equation for the variation resulting from an increment  $\delta e$  in the primary eccentricity is

$$\delta\underline{s} = \underline{v}_e \delta e, \quad (3.25)$$

where  $\underline{v}_e = d\underline{s}/de$ , again evaluated on the original orbit. The components of vectors  $\underline{v}_\mu$  and  $\underline{v}_e$  are

$$\left. \begin{aligned} v_{i\mu} &= \frac{d}{d\mu} s_i(\underline{s}_0; \theta_0; \theta; \mu; e) \\ v_{ie} &= \frac{d}{de} s_i(\underline{s}_0; \theta_0; \theta; \mu; e) \end{aligned} \right\} (i=1,2,\dots,6). \quad (3.26)$$

Using Equations (3.1) and (3.2), the total derivatives of  $v_{i\mu}$  and  $v_{ie}$  with respect to  $\theta$  are

$$\left. \begin{aligned} v'_{i\mu} &= \sum_{j=1}^6 \frac{\partial f_i}{\partial s_j} \frac{ds_j}{d\mu} + \frac{\partial f_i}{\partial \mu} \\ v'_{ie} &= \sum_{j=1}^6 \frac{\partial f_i}{\partial s_j} \frac{ds_j}{de} + \frac{\partial f_i}{\partial e} \end{aligned} \right\} (i=1,2,\dots,6). \quad (3.27)$$

The quantities  $\partial f_i / \partial s_j$  ( $i, j = 1, 2, \dots, 6$ ) in Equations (3.27) are the elements  $f_{ij}$  of the matrix  $F$ , given by Equation (3.16). If the terms  $\partial f_i / \partial \mu$  and  $\partial f_i / \partial e$  ( $i = 1, 2, \dots, 6$ ), arising from the explicit dependence of  $\underline{f}$  upon the parameters, are denoted by the elements  $f_{i\mu}$  and  $f_{ie}$  ( $i = 1, 2, \dots, 6$ )

of column vectors  $\underline{f}_\mu$  and  $\underline{f}_e$ , then Equations (3.27) can be written in the matrix form

$$\begin{aligned} \underline{v}_\mu' &= F \underline{v}_\mu + \underline{f}_\mu, \\ \underline{v}_e' &= F \underline{v}_e + \underline{f}_e, \end{aligned} \quad (3.28)$$

which differ from the variational equations (3.15) only in the terms  $\underline{f}_\mu$  and  $\underline{f}_e$ .

From Equations (1.43), the partial derivatives of the components of vector function  $\underline{f}$ , with respect to the parameters  $\mu$  and  $e$  (the components of vectors  $\underline{f}_\mu$  and  $\underline{f}_e$ ), are given by

$$\begin{aligned} f_{1\mu} &= f_{2\mu} = f_{3\mu} = 0, \\ f_{4\mu} &= E \left[ \left( \frac{1}{\sigma_1^3} - \frac{1}{\sigma_2^3} \right) (s_1 - 1 + 2\mu) + \frac{3(1-\mu)(s_1+\mu)^2}{\sigma_1^5} + \frac{3\mu(s_1+\mu-1)^2}{\sigma_2^5} \right], \\ f_{5\mu} &= E s_2 \left[ \frac{1}{\sigma_1^3} - \frac{1}{\sigma_2^3} + \frac{3(1-\mu)(s_1+\mu)}{\sigma_1^5} + \frac{3\mu(s_1+\mu-1)}{\sigma_2^5} \right], \\ f_{6\mu} &= E s_3 \left[ \frac{1}{\sigma_1^3} - \frac{1}{\sigma_2^3} + \frac{3(1-\mu)(s_1+\mu)}{\sigma_1^5} + \frac{3\mu(s_1+\mu-1)}{\sigma_2^5} \right]; \end{aligned} \quad (3.29)$$

$$\begin{aligned} f_{1e} &= f_{2e} = f_{3e} = 0, \\ f_{4e} &= -E^2 \cos \theta \left[ s_1 - \frac{(1-\mu)(s_1+\mu)}{\sigma_1^3} - \frac{\mu(s_1+\mu-1)}{\sigma_2^3} \right], \\ f_{5e} &= -AE^2 s_2 \cos \theta, \\ f_{6e} &= -AE^2 s_3 \cos \theta. \end{aligned} \quad (3.30)$$

It is clear that  $\underline{f}_\mu$  and  $\underline{f}_e$  are functions only of the coordinates  $(s_1, s_2, s_3) = (x, y, z)$ , the independent variable  $\theta$ , and the parameters  $\mu$  and  $e$ . The vectors  $\underline{v}_\mu$  and  $\underline{v}_e$  can be computed by numerical integration of Equations (3.28), in conjunction with the equation for the variational matrix  $V$ , and the equations of motion. Since the initial conditions  $\underline{s}_0$  are independent of  $\mu$  and  $e$ , the initial values of  $\underline{v}_\mu$  and  $\underline{v}_e$  are

$$\begin{aligned} \dot{x}_\mu (\theta = \theta_0) &= 0, \\ \dot{x}_e (\theta = \theta_0) &= 0. \end{aligned} \tag{3.31}$$

### 3.4 Stability

It was shown in Section 3.2 that the variation in an orbit (not necessarily periodic) due to a small change  $\delta s_0$  in the initial conditions is, to first order in  $\delta s_0$  (Equation (3.9))

$$\delta s = V(s_0; \theta_0; \theta) \delta s_0, \tag{3.32}$$

where the variational matrix  $V$  is given by (Equation (3.13))

$$V' = FV, \tag{3.33}$$

and the matrix  $F$  depends only on the coordinates  $\underline{x} = (x, y, z)$  and the independent variable  $\theta$  (and the parameters  $\mu$  and  $e$ ). If we take the unperturbed orbit to be a periodic orbit of period  $T$ , satisfying Equation (2.3) (not necessarily symmetric), then we have the important property that the matrix  $F$  is also periodic, with period  $T$  (recall that in the elliptic problem,  $T \approx 2k\pi$  for some integer  $k$ ).

The periodicity property of the matrix  $F$  for a periodic orbit implies that  $V(s_0; \theta_0; \theta + T)$  is a solution of Equation (3.33). But as we saw in Section 3.2, the variational matrix is a fundamental matrix of the variational equations; we may therefore write

$$V(s_0; \theta_0; \theta + T) = V(s_0; \theta_0; \theta) M, \tag{3.34}$$

where  $M$  is a non-singular constant matrix for a given periodic orbit. Setting  $\theta = \theta_0$  in Equation (3.34), we obtain

$$M = V(s_0; \theta_0; \theta_0 + T). \tag{3.35}$$

The matrix  $M$ , equal to the variational matrix computed over one orbital period (from  $\theta = \theta_0$  to  $\theta = \theta_0 + T$ ), is termed the MONODROMY MATRIX of the fundamental matrix  $V$  (Wintner, 1946).

Repeated application of Equation (3.34) shows that

$$V(\underline{s}_0; \theta_0; \theta + mT) = V(\underline{s}_0; \theta_0; \theta) M^m, \quad (3.36)$$

and so, by Equation (3.32), the departure of the varied orbit from the unperturbed periodic orbit after  $m$  orbital periods ( $\theta = \theta_0 + mT$ ) is

$$\delta \underline{s}_m = M^m \delta \underline{s}_0. \quad (3.37)$$

The matrix  $M$  is characteristic of a particular periodic orbit, and is independent of the choice of initial conditions  $\underline{s}_0$  or the corresponding value of the independent variable  $\theta_0$ ; the same matrix is always obtained by integrating Equation (3.33) over one orbital period, starting from an arbitrary point on the orbit. In the sequel, it will be found convenient to employ the notation

$$V(\alpha) = V(\underline{s}_0; \theta_0; \theta_0 + \alpha), \quad (3.38)$$

in which the initial conditions  $\underline{s}_0$  at  $\theta = \theta_0$  are understood to be those of an arbitrary point on the periodic orbit of interest.

Equation (3.37) shows that the monodromy matrix  $M = V(T)$  governs the behaviour of the varied orbit over arbitrary intervals of time. It is clear that if any one of the eigenvalues  $\lambda_i$  ( $i = 1, 2, \dots, 6$ ) of  $M$  is greater than unity in absolute value, the vector  $\delta \underline{s}_m$  will increase in magnitude (with respect to some appropriate norm) as  $m$  increases. The criterion for linear stability of the periodic orbit is therefore

$$|\lambda_i| \leq 1 \quad (i=1, 2, \dots, 6). \quad (3.39)$$

It can be shown that one of the properties of the monodromy matrix  $M$  is that its eigenvalues occur in reciprocal pairs (see, e.g. Pars, 1965; Katsiaris, 1973):

$$\begin{aligned} \lambda_4 &= 1/\lambda_1 \\ \lambda_5 &= 1/\lambda_2 \\ \lambda_6 &= 1/\lambda_3. \end{aligned} \quad (3.40)$$

Thus, the stability criterion (3.39) can only be satisfied if all of the

eigenvalues lie on the unit circle in the complex plane; if any pair of eigenvalues does not lie on the unit circle, the orbit is linearly unstable.

In the circular restricted problem, one pair of eigenvalues of the monodromy matrix has the value unity (see, e.g. Bray and Goudas, 1967, Sect. V). This property follows from the existence of the Jacobi integral, and from the fact that the equations of motion of the circular problem are autonomous (do not explicitly contain the independent variable  $\theta$ ). The stability of a periodic orbit of the circular problem therefore depends upon the values of the remaining two pairs of eigenvalues. The equations of motion of the elliptic restricted problem are non-autonomous, with the result that the Jacobi integral does not exist, and in general there is no longer a pair of unit eigenvalues.

An alternative, and generally more convenient, way of expressing the stability criterion (3.39) uses the three "stability indices"  $k_1, k_2$  and  $k_3$  instead of the three pairs of eigenvalues of the monodromy matrix. The stability indices are defined (following Katsiaris, 1973) by

$$\begin{aligned}
k_1 &= -(\lambda_1 + \lambda_4) = -(\lambda_1 + 1/\lambda_1) \\
k_2 &= -(\lambda_2 + \lambda_5) = -(\lambda_2 + 1/\lambda_2) \\
k_3 &= -(\lambda_3 + \lambda_6) = -(\lambda_3 + 1/\lambda_3),
\end{aligned}
\tag{3.41}$$

and the criterion for the stability of a periodic orbit can be stated as:

$ \begin{aligned} &k_1, k_2, k_3 \text{ all REAL;} \\ & k_i  \leq 2, \quad i = 1, 2, 3. \end{aligned} $
---

(3.42)

Because of the property (3.40) of the eigenvalues, the stability indices can be calculated directly from the coefficients of the sixth-order characteristic equation of the monodromy matrix,

$$\det(M - \lambda I_6) = 0, \tag{3.43}$$

without the necessity of computing the eigenvalues themselves (see, e.g. Katsiaris, 1973). The coefficients of the characteristic equation may be obtained by calculating the traces of successive powers of the monodromy matrix, and since the roots  $\lambda_i$  ( $i = 1, 2, \dots, 6$ ) of Equation (3.43) form

reciprocal pairs, only  $\text{Tr}(M)$ ,  $\text{Tr}(M^2)$  and  $\text{Tr}(M^3)$  need be evaluated. In the circular restricted problem the stability index corresponding to the pair of unit eigenvalues ( $\lambda_3$  and  $\lambda_6$ , say) has the value  $k_3 = -2$ ; the cubic equation in the  $k$ 's then reduces to a quadratic whose coefficients can be found from  $\text{Tr}(M)$  and  $\text{Tr}(M^2)$  only. The stability of a periodic orbit in the circular problem depends on the values of the two remaining stability indices  $k_1$  and  $k_2$  (or  $p$  and  $q$ , in the notation of Bray and Goudas, 1967), the roots of the quadratic.

The stability properties of a planar periodic orbit can be determined by the general method described above, in terms of the stability indices  $p$  and  $q$  (in the circular problem) or  $k_1, k_2$  and  $k_3$  (in the elliptic problem), but as we shall see, it is possible to treat the planar case of the restricted problem in a way which exploits the special properties of a planar orbit, and particularly of its monodromy matrix, and allows the stability of the orbit with respect to perturbations in the plane of the primaries, and perpendicular to the plane, to be examined separately. The stability indices calculated in this way will be used extensively in the subsequent chapters of this thesis, and in particular, the "vertical" stability index, measuring the stability of a periodic orbit with respect to perturbations acting out of the plane of the primaries, will be employed in connection with bifurcations of planar with three-dimensional periodic orbits. It is therefore worthwhile to examine the special case of planar orbits in more detail.

It can easily be shown that for planar periodic orbits ( $z(\theta) = z'(\theta) = 0$ ), the variational matrix has the form

$$V(\theta) = \begin{pmatrix} V_{11} & V_{12} & 0 & V_{14} & V_{15} & 0 \\ V_{21} & V_{22} & 0 & V_{24} & V_{25} & 0 \\ 0 & 0 & V_{33} & 0 & 0 & V_{36} \\ V_{41} & V_{42} & 0 & V_{44} & V_{45} & 0 \\ V_{51} & V_{52} & 0 & V_{54} & V_{55} & 0 \\ 0 & 0 & V_{63} & 0 & 0 & V_{66} \end{pmatrix}. \quad (3.44)$$

In this form,  $V$  can be separated into two submatrices,  $V_h(4 \times 4)$  and  $V_v(2 \times 2)$ , the former, comprising the sixteen non-zero elements of rows 1, 2, 4 and 5, corresponding to horizontal variations (due to perturbations acting in the plane of the primaries), and the latter, comprising the elements  $v_{33}, v_{36}, v_{63}$  and  $v_{66}$ , corresponding to vertical variations (due to perturbations acting perpendicularly to the plane of the primaries). Equation (3.13) can be

rewritten in terms of the two decoupled submatrices  $V_h$  and  $V_v$ , to give

$$V_h' = F_h V_h \quad (3.45)$$

and

$$V_v' = F_v V_v, \quad (3.46)$$

where

$$V_h = \begin{pmatrix} V_{11} & V_{12} & V_{14} & V_{15} \\ V_{21} & V_{22} & V_{24} & V_{25} \\ V_{41} & V_{42} & V_{44} & V_{45} \\ V_{51} & V_{52} & V_{54} & V_{55} \end{pmatrix}, \quad (3.47)$$

$$V_v = \begin{pmatrix} V_{33} & V_{36} \\ V_{63} & V_{66} \end{pmatrix}, \quad (3.48)$$

and  $F_h$  and  $F_v$  are the two decoupled submatrices of matrix  $F$  given by

$$F_h = \begin{pmatrix} 0 & 0 & 1 & 0 \\ 0 & 0 & 0 & 1 \\ f_{41} & f_{42} & 0 & 2 \\ f_{51} & f_{52} & -2 & 0 \end{pmatrix} \quad (3.49)$$

and

$$F_v = \begin{pmatrix} 0 & 1 \\ f_{63} & 0 \end{pmatrix}. \quad (3.50)$$

The initial values of the horizontal and vertical variational matrices are given by

$$\begin{aligned} V_h(0) &= I_4 \\ V_v(0) &= I_2, \end{aligned} \quad (3.51)$$

where  $I_4$  and  $I_2$  are respectively the 4x4 and 2x2 unit matrices.

The two stability indices  $k_1$  and  $k_2$  corresponding to the horizontal part of the variational matrix are solutions of the quadratic equation

$$k^2 - \alpha k + (\beta - 2) = 0, \quad (3.52)$$

where

$$\begin{aligned} \alpha &= -\text{Tr} [M_h], \\ \beta &= \frac{1}{2} \left( \text{Tr}^2 [M_h] - \text{Tr} [M_h^2] \right), \end{aligned} \quad (3.53)$$

and  $M_h$  is the horizontal part of the monodromy matrix  $M$ :

$$M_h = V_h(T) \quad (3.54)$$

(see Broucke, 1969; note the sign difference in the definition of the stability indices  $k_1$  and  $k_2$ ). For planar orbits of the circular restricted problem, the two unit eigenvalues of the full variational matrix  $V$  appear in the horizontal submatrix  $V_h$ , and so one of the roots of Equation (3.52) must be equal to -2. The remaining root is

$$k = 2 - \text{Tr} [M_h]. \quad (3.55)$$

The horizontal stability of a planar periodic orbit of the circular problem is therefore characterised by one stability index and in the elliptic problem by two stability indices. An alternative definition of the stability index  $k$  is given by Whittaker (1904) in terms of "normal displacements" from a periodic orbit. It is more usual, however, to employ the index

$$a = -\frac{1}{2}k = \frac{1}{2} \text{Tr} [M_h] - 1. \quad (3.56)$$

This definition of the horizontal stability index is equivalent to that given by Hénon (1965b), in terms of the "surface of section" method. The criterion for horizontal stability, in terms of the index  $a$ , is

$$|a| \leq 1. \quad (3.57)$$

Until relatively recently, the discussion of stability of periodic orbits of the planar circular restricted problem concerned only what we call horizontal stability, that is, stability with respect to perturbations acting in the plane of motion. Hénon (1973a,b) has pointed out that in

real situations where the planar restricted problem is a satisfactory model, it is necessary to take account of the effect of perturbations acting out of the plane of the primaries, and overall stability of a planar periodic orbit is obtained only when the orbit is both horizontally and vertically stable. Let us therefore consider now the question of vertical stability.

Denoting the elements of  $M_V$ , the vertical part of the monodromy matrix

$$M_V = V_V (T) \quad (3.58)$$

by

$$M_V = \begin{pmatrix} a_V & b_V \\ c_V & d_V \end{pmatrix} \quad (3.59)$$

(in the notation of Henon, *op. cit.*), the characteristic equation of  $M_V$  is

$$\lambda^2 - (a_V + d_V)\lambda + (a_V d_V - b_V c_V) = 0. \quad (3.60)$$

The roots  $\lambda_1, \lambda_2$  of this quadratic form a reciprocal pair and so the constant term is equal to unity (this is a particular case of the general "volume-preserving" property of the variational matrix,  $\det V = 1$ ; see, e.g. Siegel and Moser, 1971, p.142). The criterion for vertical stability ( $|\lambda_1| = |\lambda_2| = 1$ ) can therefore be expressed, following Zagouras and Markellos (1977), as

$$|s_V| \leq 1, \quad (3.61)$$

where

$$s_V = \frac{1}{2}(a_V + d_V). \quad (3.62)$$

(The stability parameter  $s_V$  should not be confused with the components  $s_1, s_2, \dots, s_6$  of the state vector  $\underline{s}$ ).

The vertical stability criterion (3.61) is applicable to planar periodic orbits of either the circular or elliptic cases of the restricted problem, and to both symmetric and asymmetric orbits. Since we are concerned only with the symmetric orbits, which have the special property

$$a_V = d_V \quad (3.63)$$

(Hénon, 1973b), the vertical stability criterion can be written as

$$|a_v| \ll 1. \tag{3.64}$$

In the sequel, the elements  $a_v, b_v, c_v$  and  $d_v$  of matrix  $M_v$  will be referred to as the "vertical stability indices"; the expression "vertical stability index", in the singular, will normally mean the index  $a_v$ .

### 3.5 Bifurcation

The phenomenon of bifurcation is characteristic of nonlinear systems, and can be defined as the occurrence of a qualitative change in the topological aspect of the phase trajectories representing the solutions of the differential equations at a critical or "bifurcation" value of some parameter (see, e.g. Chapter 7 of Minorsky, 1962). In the restricted three-body problem, bifurcation in this general sense occurs with the mass parameter  $\mu$  of the primaries as the "bifurcation parameter". In this section, however, we shall deal with bifurcations of families of periodic orbits, for fixed values of  $\mu$ , associated with critical values of the linear stability indices. A general discussion of this phenomenon is given in this section, with reference to the particular example of interest in this thesis, namely the bifurcation of families of planar with three-dimensional periodic orbits ("vertical" bifurcation). This latter topic will be explored in greater detail, in the case of symmetric periodic orbits, in Section 3.6.

We begin our discussion by considering solutions of the restricted three-body problem in the neighbourhood of a periodic solution of the most general type (three-dimensional, circular or elliptic case, not necessarily symmetric). In Section 3.4, the important result was established that after  $m$  periods of an unperturbed periodic orbit, the variation resulting from a small perturbation  $\delta s_0$  in the initial conditions is, to first order, given by (Equation (3.37))

$$\delta s_m = M^m \delta s_0, \tag{3.65}$$

where  $M$ , the monodromy matrix of the variational matrix  $V$ , is given by Equation (3.35). Since the unperturbed orbit, with basic period  $T$ , also has period  $mT$ , we see that in the linear approximation, the perturbed orbit will also be periodic, with period  $mT$ , if and only if

$$\delta \xi_m = \delta \xi_0, \quad (3.66)$$

or, by Equation (3.65),

$$(M^m - I_6) \delta \xi_0 = Q. \quad (3.67)$$

Equation (3.67) shows that there exists, in the neighbourhood of the unperturbed periodic orbit, a periodic orbit of period  $mT$ , with initial conditions  $\xi_0^* = \xi_0 + \delta \xi_0$ , if and only if there exists an eigenvector  $\delta \xi_0$  of  $M^m$  corresponding to a unit eigenvalue. The two orbits will not be distinct, however, if  $\delta \xi_0$  is an eigenvector corresponding to one of the pair of unit eigenvalues of  $M$  which always exist in the circular case of the restricted problem, neither of which results in a bifurcation. One of these unit eigenvalues arises, as has already been remarked, from the fact that the system is autonomous, and the corresponding eigenvector simply introduces a "phase shift" along the original orbit; the other unit eigenvalue arises from the existence of the Jacobi integral (e.g. Bray and Goudas, 1967; see also Markellos, 1974a). Those periodic orbits of the circular restricted problem for which  $M^m$  has a unit eigenvalue distinct from the pair just mentioned, and all periodic orbits of the elliptic restricted problem for which the monodromy matrix satisfies Equation (3.67), are referred to as "bifurcation orbits", because of the fact that it is possible to continue such an orbit in more than one direction, resulting in a bifurcation or "branching" of families of periodic orbits. The eigenvalues of the monodromy matrix  $M$  occur in reciprocal pairs, and so unit eigenvalues of  $M^m$ , if such exist, also appear in pairs. Consequently, a bifurcation orbit can always be continued in two periodicity-preserving directions different from that corresponding to continuation along the basic family to which it belongs.

The bifurcation condition (3.67) is satisfied if  $M$  has a pair of eigenvalues  $\lambda_a$  and  $\lambda_b$ , say, in a reciprocal relationship, which are  $m^{\text{th}}$  roots of unity:

$$\lambda_a = \lambda_b^{-1} = e^{2\pi i n/m}, \quad (3.68)$$

where  $n$  is any integer such that  $0 < n \leq m$ . By Equation (3.41), the corresponding stability index,  $k_a$  say, is given by

$$k_a = -(\lambda_a + \lambda_b) = -2 \cos\left(\frac{2\pi n}{m}\right). \quad (3.69)$$

Let us now consider the particular case of planar bifurcation orbits. As we have seen, the variational matrix  $V$  of a planar periodic orbit can be split into horizontal and vertical submatrices; planar orbits therefore exhibit two types of bifurcation, corresponding to the decoupled horizontal and vertical parts of the variational equation. Horizontal bifurcation, as the term implies, takes place in the plane of the primaries, the bifurcating families consisting only of planar periodic orbits. This phenomenon has been investigated by Markellos (1974a,b, 1975), in connection with the "horizontal branches" of family  $f$  in the Sun-Jupiter case of the restricted problem. Vertical bifurcation, involving vertical variations of a planar periodic orbit, is the bifurcation of a family of planar periodic orbits with a family (or families) of three-dimensional periodic orbits (see, e.g. Markellos and Kazantsis, 1977). This latter type of bifurcation is clearly of great importance in the overall structure of periodic orbits, and it is on this type that we shall concentrate in the remainder of this section.

The vertical part of the variational equations (3.15) can be written as

$$\begin{pmatrix} \delta s_3 \\ \delta s_6 \end{pmatrix}' = F_v \begin{pmatrix} \delta s_3 \\ \delta s_6 \end{pmatrix}, \quad (3.70)$$

where  $\delta s_3$  and  $\delta s_6$  are the "vertical" components  $\delta z$  and  $\delta z'$  of the variation vector  $\delta s$ , and the matrix  $F_v$  is given by Equation (3.50).

The solution of Equation (3.70) is

$$\begin{pmatrix} \delta s_3 \\ \delta s_6 \end{pmatrix} = V_v \begin{pmatrix} \delta s_{03} \\ \delta s_{06} \end{pmatrix}, \quad (3.71)$$

where  $\delta s_{03}$  and  $\delta s_{06}$  are the vertical components  $\delta z_0$  and  $\delta z'_0$  of the initial perturbation  $\delta s_0$ , the remaining components of which are taken to be zero.

Because of the decoupling of the horizontal and vertical variational equations, the vertical perturbations  $\delta s_{03}$  and  $\delta s_{06}$  do not cause any horizontal variation from the unperturbed periodic orbit.

Applying the general argument outlined above to the case of vertical bifurcation, the condition that a planar periodic orbit is a vertical bifurcation orbit is

$$(M_V^m - I_2) \begin{pmatrix} \delta s_{03} \\ \delta s_{06} \end{pmatrix} = \begin{pmatrix} 0 \\ 0 \end{pmatrix}, \quad (3.72)$$

where  $M_V$  is the monodromy matrix of  $V_V(\theta)$ , and  $m$  is a positive integer; the perturbed orbit is then a three-dimensional periodic orbit (with small departures from the horizontal plane, to permit the use of linearised equations) of period  $mT$ , where  $T$  is the period of the unperturbed planar orbit. A non-trivial solution ( $\delta s_{03}$  and  $\delta s_{06}$  not both zero) of Equation (3.72) exists if and only if the two eigenvalues  $\lambda_1$  and  $\lambda_2$  of  $M_V$  are  $m^{\text{th}}$  roots of unity. The condition for vertical bifurcation is therefore

$$s_V = \cos\left(\frac{2\pi n}{m}\right), \quad (3.73)$$

where  $s_V$  is given by Equation (3.62). A planar periodic orbit satisfying Equation (3.73) will be referred to as "vertical self-resonant". Clearly, all vertical self-resonant orbits are vertically stable; those orbits for which  $s_V = +1$  ( $m = n = 1$ ) and  $s_V = -1$  ( $m = 2, n = 1$ ), corresponding to the boundaries between the vertically stable and unstable segments of a family of planar orbits, will be referred to as "vertical-critical".

For a symmetric planar periodic orbit we have  $s_V = a_V$ , and the vertical self-resonance condition is

$$a_V = \cos\left(\frac{2\pi n}{m}\right). \quad (3.74)$$

### 3.6 Vertical Bifurcations of Symmetric Periodic Orbits

The discussion in the previous section concerning the bifurcation of periodic orbits did not involve any assumptions about symmetry properties. In this section we shall consider the phenomenon of vertical bifurcation of symmetric orbits in more detail, referring particularly to the relationships between the vertical stability indices of a vertical bifurcation orbit, and the symmetry properties of the three-dimensional periodic orbits generated from the bifurcation. The central idea in this discussion is the use of the variational matrix evaluated at the half-period ( $\theta = \theta_0 + T/2$ ) of the planar periodic orbit, rather than at the full period ( $\theta = \theta_0 + T$ , that is, the monodromy matrix), combined with the application of the Periodicity Theorem; this approach is based on the work of Hénon (1973b) and of Markellos (1980).

We begin by considering a symmetric periodic orbit of the planar restricted problem (circular or elliptic case), of period  $T$ ; if the primary orbit is elliptic then  $T = 2k\pi$  for some positive integer  $k$ . Let the two distinct mirror configurations of this orbit, that is, successive perpendicular crossings of the  $x$ -axis, occurring at  $\theta = \theta_0$  and  $\theta = \theta_0 + T/2$ , be denoted  $C_0$  and  $C_1$  respectively. By Equation (2.15), the initial conditions at  $\theta = \theta_0$  satisfy

$$\underline{s}_0 = (s_{01}, 0, 0, 0, s_{05}, 0). \quad (3.75)$$

Let us now consider the orbit resulting from small vertical perturbations  $\delta s_{03}$  and  $\delta s_{06}$  in this planar periodic orbit. The initial conditions of the perturbed orbit are

$$\underline{s}_0^* = (s_{01}, 0, \delta s_{03}, 0, s_{05}, \delta s_{06}). \quad (3.76)$$

In terms of the horizontal components ( $s_1, s_2, s_4, s_5$ ) of the state vector, the perturbed orbit is identical to the unperturbed one, while to first order in the perturbations, the vertical components of the state vector are given by Equations (3.71) and (3.48):

$$\begin{pmatrix} \delta s_3 \\ \delta s_6 \end{pmatrix} = \begin{pmatrix} v_{33} & v_{36} \\ v_{63} & v_{66} \end{pmatrix} \begin{pmatrix} \delta s_{03} \\ \delta s_{06} \end{pmatrix}. \quad (3.77)$$

We seek to establish periodicity conditions for the perturbed orbit in terms of the Periodicity Theorem, as in Section 2.3. From Equations (3.76), (2.16) and (2.17), the initial conditions of the perturbed orbit correspond to a mirror configuration if and only if

$$\delta s_{06} = 0 \quad (\text{Type (P)}), \quad (3.78)$$

or

$$\delta s_{03} = 0 \quad (\text{Type (A)}). \quad (3.79)$$

The perturbed orbit resulting from initial perturbations  $(\delta s_{03}, \delta s_{06})$  satisfying either of these conditions will be periodic if, at some later epoch  $\theta = \theta_1$  say, another mirror configuration is obtained. In the elliptic restricted problem,  $\theta_1$  must also satisfy Equation (2.22). Since the horizontal part of the motion is (to first order) unaffected, it is clear that a mirror configuration can only take place at those epochs corresponding to the occurrence of a mirror configuration in the unperturbed planar periodic orbit, that is, for values of  $\theta$  given by

$$\theta = \theta_0 + N \left( \frac{T}{2} \right), \quad (3.80)$$

where  $N$  is some positive integer. (Note that the condition (3.80) automatically satisfies Equation (2.22)). The further requirement which must be satisfied involves the vertical motion: by Equations (2.20) and (2.21), we must have either

$$\delta s_6 = 0 \quad (\text{Type (P)}), \quad (3.81)$$

or

$$\delta s_3 = 0 \quad (\text{Type (A)}). \quad (3.82)$$

Combining Equations (3.77) - (3.82), we see that the periodicity conditions of the perturbed orbit can be written in the form

$$\delta s_j = v_{ji} (NT/2) \delta s_{0i} = 0, \quad (3.83)$$

where  $i = 3$  for a type (P) and  $i = 6$  for a type (A) mirror configuration

at the initial epoch, while  $j = 6$  for a type (P) and  $j = 3$  for a type (A) mirror configuration at the final epoch (as in Section 2.5);  $\delta_{s_{0i}}$  is therefore the non-zero initial perturbation in each case ( $\delta_{s_{0i}} = 0$  is the trivial solution corresponding to the unperturbed orbit). Equation (3.83) shows that there exists a three-dimensional symmetric periodic orbit bifurcating from the planar periodic orbit if and only if one of the four elements ( $v_{33}, v_{36}, v_{63}, v_{66}$ ) of  $V_v(NT/2)$  vanishes, for some positive integer  $N$ . The four possible cases of vertical bifurcation are listed in Table 3.1.

Table 3.1

Case	Type of Mirror Configuration at:		Symmetry Class	i	j	Period
	Initial Epoch( $\theta_0$ )	Final Epoch( $\theta_1$ )				
1	P	P	Plane symmetric	3	6	NT
2	A	A	axisymmetric	6	3	NT
3	A	P	} doubly-symmetric	6	6	2NT
4	P	A		3	3	2NT

The table shows, for example, that a family of plane symmetric three-dimensional periodic orbits bifurcate from a planar periodic orbit for which  $v_{63}(NT/2) = 0$  for some  $N$ . The final column of the table gives the period of the three-dimensional orbits in the neighbourhood of the bifurcation, as given by Equations (2.23) and (2.24), with  $\theta_1 = \theta_0 + NT/2$  (Equation (3.80)).

As we saw in Section 3.4, the matrix  $V_v(\theta)$  has unit determinant for all values of  $\theta$ :

$$v_{33} v_{66} - v_{36} v_{63} = 1. \tag{3.84}$$

The terms  $v_{33}v_{66}$  and  $v_{36}v_{63}$  of this equation cannot both vanish, and so zero elements of  $V_v$  can only exist either singly, or as one of the diagonal pairs ( $v_{33}, v_{66}$ ) or ( $v_{36}, v_{63}$ ). Table 3.1 shows that in consequence of this fact, a vertical bifurcation orbit can only give rise either to a single family of three-dimensional orbits, corresponding to one and only one of Cases 1 - 4 of the table, or else to two families of three-dimensional orbits, corresponding to Cases 1 and 2 or to Cases 3 and 4 (that is, one family of plane symmetric and one of axisymmetric

orbits, or two families of doubly-symmetric orbits).

We recall the definition of the vertical stability indices (Equations (3.58) and (3.59)):

$$V_v(T) = \begin{pmatrix} a_v & b_v \\ c_v & d_v \end{pmatrix}. \quad (3.85)$$

Let the elements of the vertical variational matrix evaluated at the half-period ( $\theta = \theta_0 + T/2$ ) of the planar periodic orbit be denoted

$$V_v(T/2) = \begin{pmatrix} A_v & B_v \\ C_v & D_v \end{pmatrix}. \quad (3.86)$$

It is easily shown, using the symmetry property of the planar orbit, that the elements of  $V_v$  at the full period are related to those at the half-period by

$$\begin{pmatrix} a_v & b_v \\ c_v & d_v \end{pmatrix} = \begin{pmatrix} A_v D_v + B_v C_v & 2B_v D_v \\ 2A_v C_v & A_v D_v + B_v C_v \end{pmatrix} \quad (3.87)$$

(e.g. Hénon, 1973b). The important property  $a_v = d_v$  of a symmetric orbit has already been mentioned in the previous section. Using Equation (3.34) (as applied to the vertical part  $V_v$  of the variational matrix  $V$ ), the vertical variational matrix computed at  $\theta = \theta_0 + NT/2$  can be expressed in terms of its value at the half-period and at the full period. The resulting expression for  $V_v(NT/2)$  depends on whether  $N$  is odd ( $N = 2r + 1$ ) or even ( $N = 2r$ ):

$$\underline{N = 2r + 1} \quad V_v(NT/2) = V_v(T/2 + rT) = V_v(T/2) [V_v(T)]^r \quad (3.88)$$

$(r = 0, 1, 2, \dots);$

$$\underline{N = 2r} \quad V_v(NT/2) = V_v(rT) = [V_v(T)]^r \quad (3.89)$$

$(r = 0, 1, 2, \dots).$

Let us first of all suppose that one of the elements of  $V_v(T/2)$  vanishes

(that is, taking  $N = 2r + 1$  with  $r = 0$ ). By Equation (3.82), Cases 1 - 4 of Table 3.1 correspond respectively to

$$C_v = 0 ; B_v = 0 ; D_v = 0 ; A_v = 0 . \quad (3.90)$$

Now from Equations (3.84) and (3.87), the vertical stability index  $a_v$  is given by

$$a_v = 2A_v D_v - 1 = 2B_v C_v + 1 . \quad (3.91)$$

In each of the cases (3.90),  $|a_v| = 1$  : the planar orbit is vertical-critical. In the first two cases ( $C_v = 0$  and  $B_v = 0$ ),  $a_v$  has the value  $+1$ . This corresponds to the values  $m = 1$ ,  $n = 1$  in Equation (3.74), and will be referred to as a "simple bifurcation". The quantities  $B_v$  and  $C_v$  are independent, and in general, when one of these parameters is zero, the other will be non-zero; thus, a vertical-critical planar periodic orbit with  $a_v = +1$  generally gives rise to just one family of simply-symmetric three-dimensional periodic orbits, the symmetry class depending on which of  $B_v$  or  $C_v$  vanishes (axisymmetric or plane symmetric, respectively). Table 3.1 shows that in the neighbourhood of the bifurcation, the period of the three-dimensional orbits is (to first order) equal to  $T$ , the period of the planar orbit; in the elliptic problem the entire family of three-dimensional orbits has period exactly equal to  $T$ .

In the second two cases of (3.90),  $A_v = 0$  and  $D_v = 0$ , Equation (3.91) shows that  $a_v = -1$ , corresponding to the values  $m = 2$ ,  $n = 1$  in Equation (3.74): this is referred to as a "double bifurcation". The three-dimensional periodic orbits in the neighbourhood of the bifurcation have double the period of the planar orbit, and so also double the multiplicity (the multiplicity of an orbit being defined as half the number of crossings of the  $(x,z)$ -plane occurring in one period). Since  $A_v$  and  $D_v$  are independent, there is in general only one bifurcating family of doubly-symmetric periodic orbits originating from a vertical-critical orbit with  $a_v = -1$ . If  $D_v = 0$ , then the orbits near the bifurcation have their type (A) mirror configuration close to the configuration  $C_0$  of the planar orbit; if  $A_v = 0$ , then the type (A) mirror configuration is close to the configuration  $C_1$  of the planar orbit. The geometry of bifurcation from a vertical-critical orbit, in each of the four possible cases listed above, is depicted schematically in Figure 3.1.

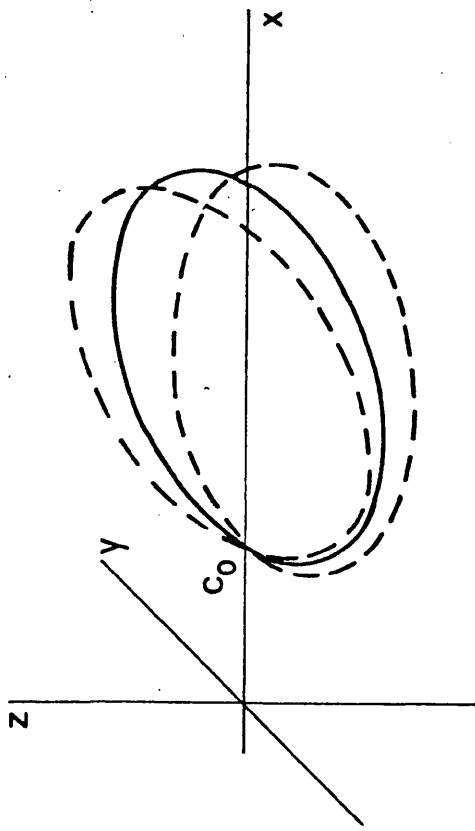
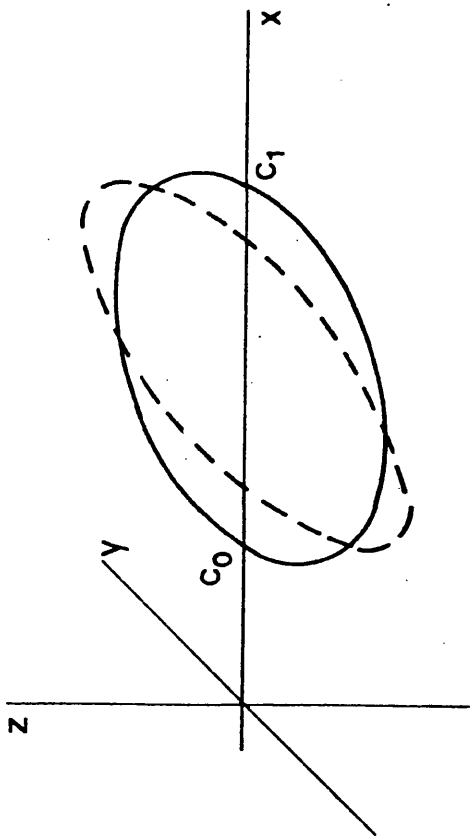
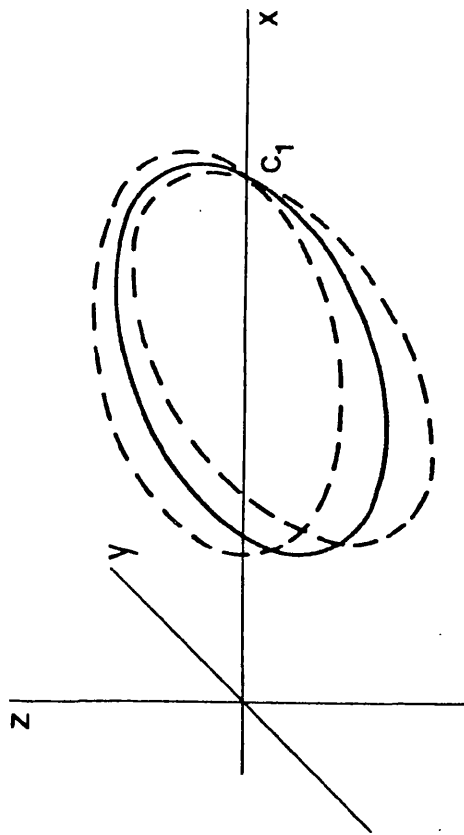
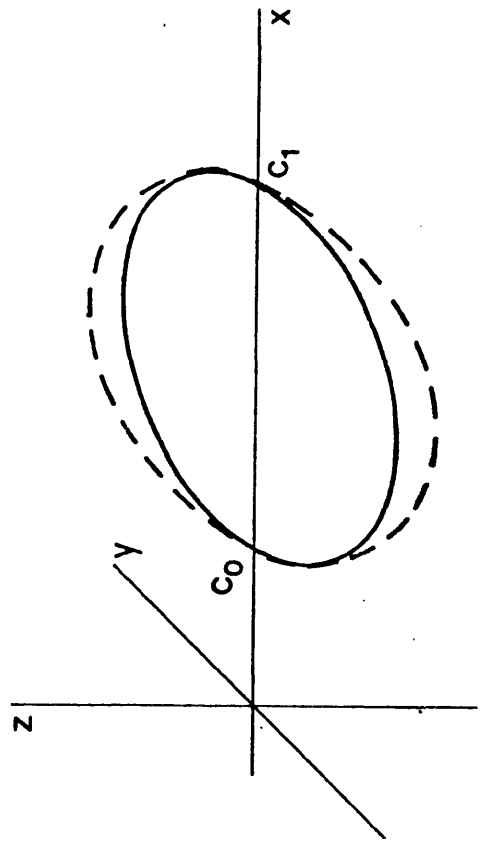


Figure 3.1 : Schematic shape of three-dimensional periodic orbits (broken lines) originating from vertical-critical orbits (solid lines) (after Hénon, 1973b).

Let us now suppose that all of the elements  $A_v, B_v, C_v$  and  $D_v$  of  $V_v(T/2)$  are non-zero, but that one of the elements of  $V_v(NT/2)$  vanishes, for some  $N > 1$ . Equation (3.91) shows that  $a_v$  cannot be equal to unity: we are no longer dealing with vertical-critical orbits, but with the more general vertical self-resonant orbits for which  $a_v$  is given by Equation (3.70), with  $m > 2$ . It is easily shown by induction that the vertical variational matrix  $V_v$  computed at  $\theta = \theta_0 + NT/2$  ( $N = 0, 1, 2, 3, \dots$ ) satisfies the following two equations:

$$V_v(T/2 + rT) = \begin{pmatrix} \alpha_r A_v & \beta_r B_v \\ \beta_r C_v & \alpha_r D_v \end{pmatrix} \quad (r \geq 0), \quad (3.92)$$

where  $\alpha_r$  and  $\beta_r$  are functions of  $A_v, B_v, C_v$  and  $D_v$ ;

$$V_v(rT) = \begin{pmatrix} \gamma_r & 2\delta_r B_v D_v \\ 2\delta_r A_v C_v & \gamma_r \end{pmatrix} \quad (r \geq 0), \quad (3.93)$$

where  $\gamma_r$  and  $\delta_r$  are functions of  $A_v, B_v, C_v$  and  $D_v$ . We may therefore state the following:

If the elements  $A_v, B_v, C_v$  and  $D_v$  of  $V_v(T/2)$  are all non-zero, then for all values of  $N > 1$ ,  $V_v(NT/2)$  has either no zero elements, or exactly two zero elements on the same diagonal.

This follows from Equation (3.84), together with Equation (3.93) for odd values of  $N$  ( $= 2r + 1, r = 1, 2, 3, \dots$ ), and Equation (3.94) for even values of  $N$  ( $= 2r, r = 1, 2, 3, \dots$ ), the important point being the appearance of the common factors  $(\alpha_r, \beta_r), (\gamma_r, \delta_r)$  in the diagonal pairs of elements; since  $A_v, B_v, C_v$  and  $D_v$  are assumed to be all non-zero, an element of  $V_v(NT/2)$  can only vanish if one of the functions  $\alpha_r, \beta_r, \gamma_r$  or  $\delta_r$  is zero.

We therefore have the important result that families of three-dimensional periodic orbits bifurcating from a vertical self-resonant periodic orbit for which  $N > 1$  (that is, excluding vertical-critical orbits) always occur in pairs, and as we have already seen, both families must consist either of simply-symmetric or of doubly-symmetric orbits.

Using Equations (3.34), (3.85) and (3.87), together with Equations (3.92) and (3.93), pairs of simultaneous recurrence relations can easily

be established for the functions  $\alpha_r$ ,  $\beta_r$ ,  $\gamma_r$  and  $\delta_r$ :

$$\left. \begin{aligned} \alpha_r &= a_v \alpha_{r-1} + (a_v - 1) \beta_{r-1} \\ \beta_r &= a_v \beta_{r-1} + (a_v + 1) \alpha_{r-1} \end{aligned} \right\}, \quad (3.94)$$

$$\left. \begin{aligned} \delta_r &= a_v \delta_{r-1} + (a_v^2 - 1) \gamma_{r-1} \\ \gamma_r &= a_v \gamma_{r-1} + \delta_{r-1} \end{aligned} \right\}. \quad (3.95)$$

Since  $|a_v| \neq 1$ , the  $\beta$ 's can be eliminated from Equations (3.94), and the  $\delta$ 's from Equations (3.95), giving

$$\left. \begin{aligned} \alpha_{r+1} - 2a_v \alpha_r + \alpha_{r-1} &= 0, \\ \gamma_{r+1} - 2a_v \gamma_r + \gamma_{r-1} &= 0. \end{aligned} \right\} \quad (3.96)$$

The general solutions of these two identical second-order recurrence relations are

$$\left. \begin{aligned} \alpha_r &= A e^{ir\phi} + B e^{-ir\phi}, \\ \gamma_r &= C e^{ir\phi} + D e^{-ir\phi}, \end{aligned} \right\} \quad (3.97)$$

where

$$\cos \phi = a_v, \quad (3.98)$$

and A, B, C, D are constants to be determined from the initial conditions

$$\alpha_0 = 1, \quad \alpha_1 = 2a_v - 1; \quad (3.99)$$

$$\gamma_0 = 1, \quad \gamma_1 = a_v. \quad (3.100)$$

Calculation of the four constants yields

$$\alpha_r = \frac{\sin(r+1)\phi - \sin r\phi}{\sin \phi}, \quad (3.101)$$

$$\gamma_r = \cos r\phi, \quad (3.102)$$

and the associated solutions for  $\beta_r$ ,  $\delta_r$  are

$$\beta_r = \frac{\sin(r+1)\phi + \sin r\phi}{\sin\phi}, \quad (3.103)$$

$$\delta_r = \frac{\sin r\phi}{\sin\phi}. \quad (3.104)$$

Let us consider the conditions for the occurrence of a pair of zero elements of the matrix  $V_v(NT/2)$ , for odd values of  $N = 2r + 1$  ( $r = 1, 2, 3, \dots$ ). It is clear from Equation (3.92) that this is the case if either  $\alpha_r$  or  $\beta_r$  vanishes, for some  $r > 0$ . By Equation (3.101), the function  $\alpha_r$  is equal to zero if and only if

$$\sin(r+1)\phi = \sin r\phi \quad (3.105)$$

and

$$\sin\phi \neq 0, \quad (3.106)$$

which is satisfied for

$$\phi = \left(\frac{2k+1}{2r+1}\right)\pi, \quad (3.107)$$

where  $k$  is an arbitrary integer, such that  $(2k + 1)(2r + 1)$  is not an integer. Substitution of the solutions (3.107) into Equation (3.98) gives

$$a_v = \cos\left(\frac{2k+1}{2r+1}\right)\pi, \quad (3.108)$$

with valid solutions for  $0 \leq k < r$ : this yields the complete set of  $r$  roots of  $\alpha_r$ , which is a polynomial in  $a_v$  of degree  $r$ . (A duplicate set of  $r$  solutions is obtained for  $r < k \leq 2r$ ). The zeroes of the function  $\beta_r$  are given by

$$\sin(r+1)\phi = -\sin r\phi, \quad (3.109)$$

such that

$$\sin \phi \neq 0, \tag{3.110}$$

with solutions

$$\phi = \frac{2k\pi}{2r+1}, \tag{3.111}$$

where k is once again an arbitrary integer. The corresponding values of the vertical stability index are

$$a_v = \cos\left(\frac{2k\pi}{2r+1}\right) \tag{3.112}$$

with valid solutions for  $0 < k \leq r$ , giving the complete set of r roots of  $\beta_r$ .

We now consider the conditions for the occurrence of a bifurcation for even values of  $N = 2r$  ( $r = 1, 2, 3, \dots$ ), that is, for the appearance of a pair of zero elements of  $V_v(rT)$ . This requires that either  $\gamma_r$  or  $\delta_r$  vanishes, for some  $r \geq 1$ . The first condition ( $\gamma_r = 0$ ) can, by Equation (3.102), be written

$$\cos r\phi = 0, \tag{3.113}$$

with solutions

$$\phi = \left(\frac{2k+1}{2r}\right)\pi, \tag{3.114}$$

where k is an arbitrary integer and we take  $0 \leq k < r$ , giving the complete set of r roots of the polynomial  $\gamma_r$ . The corresponding values of the vertical stability index are

$$a_v = \cos\left(\frac{2k+1}{2r}\right)\pi. \tag{3.115}$$

From Equation (3.104), the condition that  $\delta_r$  vanishes is

$$\phi = k\pi/r, \tag{3.116}$$

such that  $k/r$  is not an integer; thus

$$a_v = \cos\left(\frac{k\pi}{r}\right). \tag{3.117}$$

The complete set of roots of the polynomial  $\delta_r$ , of degree  $r-1$  in  $a_v$ , is given by  $0 < k < r$ .

Let us now relate these results to the vertical bifurcation condition (3.74) given in the previous section, namely

$$a_v = \cos\left(\frac{2\pi n}{m}\right), \tag{3.118}$$

where  $m$  and  $n$  are taken to be mutually prime integers with  $0 < n \leq m$ . The case  $n = m$  ( $a_v = +1$ ) is at once excluded from this discussion, since this is the case of a vertical-critical orbit, which has already been dealt with. From Equations (3.108), (3.112), (3.115) and (3.117), the condition for the occurrence of a bifurcation associated with the vanishing of one of the functions  $\alpha_r$ ,  $\beta_r$ ,  $\gamma_r$  and  $\delta_r$  (and therefore of one of the pairs of elements  $(v_{33}, v_{66})$ ,  $(v_{36}, v_{63})$  of the matrix  $V_v$ ) can be expressed in the form (3.118), with the values of the integers  $m$  and  $n$  in each case as given by the following table.

Table 3.2

Function	$m$	$n$
$\alpha_r$	$2(2r + 1)$	$2k + 1$
$\beta_r$	$2r + 1$	$k$
$\gamma_r$	$4r$	$2k + 1$
$\delta_r$	$2r$	$k$

The final entry of Table 3.2, corresponding to  $\delta_r = 0$ , is essentially

redundant, since all the possible combinations of values of  $m$  and of  $n$  can be constructed from the entries corresponding to the cases  $\alpha_r = 0$  and  $\delta_r = 0$ . This redundancy of solutions reflects the fact that a doubly-symmetric periodic orbit can be regarded as simply-symmetric if one of its symmetries is ignored; the bifurcation of doubly-symmetric orbits corresponding to  $v_{33}(NT/2) = v_{66}(NT/2) = 0$ , for some  $N \geq 1$  ( $\alpha_r$  or  $\gamma_r$  equal to zero), automatically gives  $v_{36}(N'T/2) = v_{63}(N'T/2) = 0$ , where  $N' = 2N$  is even (that is,  $\delta_{N'} = 0$ ). The occurrence of a bifurcation of genuinely simply-symmetric orbits is associated with the vanishing of the function  $\beta_r$ , for some  $r \geq 1$ .

The possible values of the integer  $m$  in Equation (3.118) in each case of Table 3.2 (with  $r = 1, 2, 3, \dots$ ) are

$$\begin{aligned} \alpha_r = 0 : \quad m &= 6, 10, 14, \dots \\ \beta_r = 0 : \quad m &= 3, 5, 7, \dots \\ \gamma_r = 0 : \quad m &= 4, 8, 12, \dots \end{aligned} \tag{3.119}$$

which together account for all integer values greater than 2; the values  $m = 1$  and  $m = 2$  apply to vertical-critical orbits. It is evident that an even value of  $m$  corresponds to the case of doubly-symmetric three-dimensional bifurcating orbits ( $v_{33} = v_{66} = 0$ ), while an odd value of  $m$  corresponds to a bifurcation with a family of simply-symmetric orbits ( $v_{36} = v_{63} = 0$ ). The following conclusion may therefore be stated:

A vertical self-resonant orbit, with vertical stability index  $a_v$  given by Equation (3.118), gives rise to one family of axisymmetric and one of plane symmetric three-dimensional orbits if  $m$  is odd, and to two families of doubly-symmetric orbits if  $m$  is even.

Numerical examples of the different types of vertical bifurcation predicted by the first-order theory are given in Chapter 5.

## 4. NUMERICAL TECHNIQUES

### 4.1 Introduction

In Chapters 1 and 2, emphasis was placed on the fact that the restricted three-body problem is non-integrable, in the sense that there is an insufficient number of integrals of the motion to allow a general solution to be expressed solely in terms of the values of the integrals, determined from the initial conditions. In practice, therefore, we must resort to numerical methods of integration in order to obtain a solution with arbitrary initial conditions. Numerical integration, nowadays performed with the aid of a digital computer, essentially involves replacing the exact differential equations of motion, of variation, etc. by finite difference equations approximating the exact equations to an accuracy which is usually controlled at each step of the integration. The overall accuracy of the numerical solution cannot normally be checked directly (except in the case of known analytical solutions, such as the Lagrange equilibrium solutions), although indirect tests can be carried out, the commonest method being to monitor at various points in the integration the value of the quantity  $C$  in the Jacobi invariant relation (Equation (1.47)), which is invariant along an exact solution of the elliptic restricted problem, and the first (and only) integral of the circular problem. It is important to note that satisfaction of this latter accuracy test is a necessary but not sufficient condition for overall accuracy of the solution.

In the essentially theoretical subject of the restricted three-body problem, the development of computer programs is analogous to the design of new equipment in an experimental field of research, and is worthy of attention in its own right; a substantial part of the present work was indeed concerned with program development and refinement. This chapter is concerned with a number of computational techniques and algorithms which can be used in the determination of families of symmetric periodic orbits, and in calculating orbital stability. The numerical integration itself will not be discussed in detail. The numerical results presented in this thesis were obtained using the methods described in this chapter, in conjunction with the EPISODE numerical integration package developed by Hindmarsh and Byrne (1975), based on a variable-step, variable-order Adams method, and adapted to

deal specifically with the integration of orbits by Dr. Paul Rosenberg of the University of Glasgow Computing Service.

In common with the majority of numerical integration facilities, the EPISODE package is designed to integrate systems of simultaneous first-order ordinary differential equations of the form

$$S_i' = f_i(\underline{S}; \theta) \quad (i=1,2,\dots,n), \quad (4.1)$$

where  $\theta$  is the independent variable, and  $\underline{S}$  is an n-dimensional vector of the quantities to be integrated. The equations of motion in terms of the state vector, and the equations of variation, can all be combined in this form. The first six components of the vector  $\underline{S}$  were taken to be the components of the state vector  $\underline{s}$ , and other components were used for the elements of the variational matrix  $V$ , the components of vectors  $\underline{y}_\mu$  and  $\underline{y}_e$ , and the Jacobi invariant  $C$ , the total number of elements being  $n = 6 + 36 + 6 + 6 + 1 = 55$ .

In the circular restricted problem, and in the integration of planar orbits, the system of differential equations is simplified, and  $n$  can be reduced from this maximum value. The various programs written for the determination of families of periodic orbits called the EPISODE integration package to generate a numerical solution of Equations (4.1) in the form

$$S_i = S_i(\underline{S}_0; \theta_0; \theta_f), \quad (4.2)$$

where  $\underline{S}_0 = (S_{01}, S_{02}, \dots, S_{0n})$  is the set of initial values of the components of  $\underline{S}$ , and  $\theta_0, \theta_f$  are respectively the initial and final values of the independent variable in the differential equations. The value of a parameter designated "EPS", which controlled the local truncation error in the first three components of  $\underline{S}$  (that is, the coordinates of the massless particle with respect to the rotating-pulsating coordinate system), was assigned at the outset, the most commonly-used value being  $10^{-11}$ . All calculations were carried out in Fortran double precision arithmetic, yielding an accuracy of approximately 16 decimal places.

Many of the numerical procedures described in this chapter are not only efficient for the determination of entire families of symmetric three-dimensional periodic orbits, but can easily be modified to be

applicable in the case of asymmetric periodic orbits of the planar restricted problem, which present the same degree of complexity in so far as numerical determination is concerned. As we shall see in a subsequent chapter, the algorithms can also be modified to allow the numerical determination of series (as opposed to families) of periodic orbits: that is, monoparametric sets of periodic solutions of the restricted problem in which the mass parameter, rather than being kept fixed, is allowed to vary, and some characteristic of the orbits is kept constant instead. In particular, we shall discuss in Chapter 7 the determination of series of vertical bifurcation orbits, having a fixed value of the vertical stability index  $a_v$ .

#### 4.2 Calculation of the Variational Matrix

It was shown in Chapter 2 that a symmetric periodic orbit can be computed by integrating over only a half or a quarter of the orbital period, according as the symmetry is simple or double, respectively. As we shall see in this section, orbital symmetry can also be employed in calculating the variational matrix  $V$  after one orbital period (in other words, the monodromy matrix  $M$ ), from its value at the half-period or quarter-period, as appropriate, without the need to integrate over the whole orbit. This well-known property of the variational matrix results in a 50% or even 75% saving in the computer time required to determine a symmetric periodic orbit and its stability properties (see, e.g. Bray and Goudas, 1967; Katsiaris, 1972; Zagouras and Markellos, 1977).

The transformations discussed in Section 2.3, associated with the two possible types of mirror configuration, can be represented by the diagonal matrices

$$\begin{aligned} P &= \text{diag} \{ 1, -1, 1, -1, 1, -1 \}, \\ A &= \text{diag} \{ 1, -1, -1, -1, 1, 1 \}, \end{aligned} \quad (4.3)$$

operating on the state vector  $g$ . The matrix  $P$  has the effect of reflecting the position and velocity vectors of the massless particle

in the  $(x,z)$ -plane, and changing the signs of the velocity components; the matrix A reflects in the x-axis, and reverses the velocity. A type (P) mirror configuration corresponds to invariance under the transformation represented by matrix P, that is

$$\underline{s} = P\underline{s}, \quad (4.4)$$

which gives Equation (2.16), while in a type (A) mirror configuration the state vector must satisfy

$$\underline{s} = A\underline{s}, \quad (4.5)$$

giving Equation (2.17). The two mappings represented by matrices P and A transform the variational matrix V to

$$U = PVP \quad (4.6)$$

and

$$W = AVA, \quad (4.7)$$

respectively. Because of the symmetry properties of the equations of motion of the restricted problem, the transformed variational matrices U and W still satisfy Equation (3.13), with the independent variable  $\theta$  replaced by  $2\theta_0 - \theta$ . Thus, for a periodic orbit which has a type (P) mirror configuration at  $\theta = \theta_0$  (that is,  $P\underline{s}_0 = \underline{s}_0$ ), the matrices U and V are related by

$$U(\psi) = V(-\psi), \quad (4.8)$$

where the shorthand notation  $V(\underline{s}_0; \theta_0; \theta_0 + \psi) = V(\psi)$  is once again employed for convenience. Equation (4.6) then gives

$$V(-\psi) = PV(\psi)P. \quad (4.9)$$

Now Equation (3.34), with  $\theta = -T/2$ , can be written as

$$V(T) = V^{-1}(-T/2) V(T/2); \quad (4.10)$$

using Equation (4.9) with  $\psi = T/2$ , and the property  $P^{-1} = P$ , we

obtain

$$V(T) = PV^{-1}(T/2)PV(T/2). \quad (4.11)$$

For a periodic orbit which has a type (A) mirror configuration at  $\theta = \theta_0$ , the analogous expression to Equation (4.9) is

$$V(-\psi) = AV(\psi)A, \quad (4.12)$$

and since  $A^{-1} = A$ , we have

$$V(T) = AV^{-1}(T/2)AV(T/2). \quad (4.13)$$

Equations (4.11) and (4.13) can be used to determine the monodromy matrix  $M = V(T)$  from  $V(T/2)$ , calculated over half of an orbit, for periodic orbits of simple symmetry (plane symmetric and axisymmetric, respectively). For doubly-symmetric periodic orbits, either Equation (4.9) or Equation (4.12) applies, depending on whether the initial mirror configuration is of type (P) or (A) respectively. In addition, because the half-period configuration in a doubly-symmetric orbit is identical to the initial configuration, apart from a reflection in the horizontal plane, the variational matrix satisfies

$$V(\psi + T/2) = DV(\psi)DV(T/2), \quad (4.14)$$

where  $D = \text{diag}\{1, 1, -1, 1, 1, -1\}$  is the matrix representing reflection in the (x,y)-plane. Equation (4.14), with  $\psi = -T/4$ , gives

$$V(T/4) = DV(-T/4)DV(T/2), \quad (4.15)$$

and the value of  $V(-T/4)$  can be obtained from either of Equations (4.9) or (4.12), as appropriate, with  $\psi = T/4$ . This establishes a relationship between  $V(T/2)$  and  $V(T/4)$  which, together with the relationship (4.11) or (4.13), as appropriate, between  $V(T)$  and  $V(T/2)$ , and the properties of matrices A, P and D

$$\left. \begin{aligned} AD &= DA = P \\ PD &= DP = A \\ AP &= PA = D \end{aligned} \right\} \quad (4.16)$$

yields the following expressions for the monodromy matrix  $V(T)$  in terms of  $V(T/4)$ :

Type (P) initial mirror configuration:

$$V(T) = [PV^{-1}(T/4)AV(T/4)]^2 ; \quad (4.17)$$

Type (A) initial mirror configuration:

$$V(T) = [AV^{-1}(T/4)PV(T/4)]^2 . \quad (4.18)$$

### 4.3 Differential Correction

Numerical integration of the equations of motion of the restricted three-body problem, from an arbitrary set of initial conditions, is an example of what is usually termed an initial-value problem. The numerical determination of a periodic orbit (symmetric or asymmetric), on the other hand, is an example of a boundary-value problem: that is, the problem of finding a set of initial conditions which, upon integration, yields a solution satisfying certain boundary conditions - in the case of a periodic orbit, the periodicity conditions. One of the most commonly-used methods of tackling a boundary-value problem is the differential correction approach, which assumes to start with that approximate values of the desired initial conditions are known. If the estimated values are sufficiently accurate, the departure of the corresponding solution from the exact boundary conditions will be small, and approximately linearly dependent upon the errors in the initial conditions. The system of linear equations expressing this dependence can be solved to provide estimated values of the errors in the initial conditions, which can then be "corrected" accordingly; the procedure is repeated in an iterative fashion until the boundary conditions are satisfied within some prescribed accuracy. In this section we examine how the differential correction method is applied in the numerical determination of symmetric periodic orbits, firstly in the circular restricted problem and secondly in the elliptic restricted problem.

In the circular restricted problem, the "weak" form of the periodicity conditions (Equation (2.27)) is applicable, and can be written as

$$\begin{aligned} S_2 (s_{01}, s_{05}, s_{0i} ; t) &= 0, \\ S_4 (s_{01}, s_{05}, s_{0i} ; t) &= 0, \\ S_j (s_{01}, s_{05}, s_{0i} ; t) &= 0, \end{aligned} \tag{4.19}$$

where the quantity  $\theta_0$ , which as we have seen can always be taken to be zero in the circular problem, has been omitted for clarity, and the symbol  $t$  has been used instead of  $\theta_1$ . We recall that for orbits of simple symmetry, the integration interval between successive mirror configurations is  $t = T/2$ , and for doubly-symmetric orbits,  $t = T/4$ , where  $T$  is the orbital period. The values of the subscripts  $i$  and  $j$  depend on the symmetry class, as in Table 3.1; the value of the mass parameter  $\mu$  is assumed to be fixed.

Suppose  $(s_{01}^*, s_{05}^*, s_{0i}^*)$  and  $t^*$  are approximate values of the initial conditions and integration interval of the sought periodic orbit, differing from the exact solutions  $(s_{01}, s_{05}, s_{0i}, t)$  of Equation (4.19) by the amounts

$$\left. \begin{aligned} \delta s_{01} &= s_{01} - s_{01}^* \\ \delta s_{05} &= s_{05} - s_{05}^* \\ \delta s_{0i} &= s_{0i} - s_{0i}^* \\ \delta t &= t - t^* \end{aligned} \right\} \tag{4.20}$$

which are assumed to be small. Approximate values for the "corrections"  $\delta s_{01}$ ,  $\delta s_{05}$ ,  $\delta s_{0i}$  and  $\delta t$  are now sought.

Numerical integration from initial conditions  $(s_{01}^*, s_{05}^*, s_{0i}^*)$  (the remaining three taken to be zero, as usual) at  $\theta = 0$  up to  $\theta = t^*$  yields final conditions

$$\begin{aligned} S_2^* &= S_2 (s_{01}^*, s_{05}^*, s_{0i}^* ; t^*) \\ S_4^* &= S_4 (s_{01}^*, s_{05}^*, s_{0i}^* ; t^*) \\ S_j^* &= S_j (s_{01}^*, s_{05}^*, s_{0i}^* ; t^*). \end{aligned} \tag{4.21}$$

Using Equations (4.20), the periodicity conditions (4.19) can be written as

$$\begin{aligned} S_2 &= S_2 (s_{01}^* + \delta s_{01}, s_{05}^* + \delta s_{05}, s_{0i}^* + \delta s_{0i}; t^* + \delta t) = 0 \\ S_4 &= S_4 (s_{01}^* + \delta s_{01}, s_{05}^* + \delta s_{05}, s_{0i}^* + \delta s_{0i}; t^* + \delta t) = 0 \\ S_j &= S_j (s_{01}^* + \delta s_{01}, s_{05}^* + \delta s_{05}, s_{0i}^* + \delta s_{0i}; t^* + \delta t) = 0. \end{aligned} \tag{4.22}$$

Expanding the right-hand sides of Equations (4.22) in Taylor series, to first order in the corrections, we obtain, using Equations (3.5)

$$\begin{aligned} s_2^* + v_{21} \delta s_{01} + v_{25} \delta s_{05} + v_{2i} \delta s_{0i} + f_2 \delta t &= 0 \\ s_4^* + v_{41} \delta s_{01} + v_{45} \delta s_{05} + v_{4i} \delta s_{0i} + f_4 \delta t &= 0 \\ s_j^* + v_{j1} \delta s_{01} + v_{j5} \delta s_{05} + v_{ji} \delta s_{0i} + f_j \delta t &= 0, \end{aligned} \quad (4.23)$$

where the  $v$ 's are elements of the variational matrix  $V$ , given by Equation (3.13), and the  $f$ 's components of vector  $f$ , that is, the derivatives  $\delta s_k / \delta \theta$ , all evaluated at  $\theta = t^*$  in the trial integration from initial conditions  $(s_{01}^*, s_{05}^*, s_{0i}^*)$ ; the values of these coefficients are therefore known.

The system (4.23) of three simultaneous equations, in the four unknowns  $\delta s_{01}$ ,  $\delta s_{05}$ ,  $\delta s_{0i}$  and  $\delta t$ , is the basic form of the differential corrector for the circular restricted problem. The system is under-determined, with one degree of freedom, allowing a further arbitrary constraint to be applied. This is usually done by setting one of the four corrections to zero, and solving for the other three. The choice of which of the correctors to set to zero, that is, which of the initial parameters  $(s_{01}, s_{05}, s_{0i}$  or  $t)$  to fix in value when the corrector is applied, can have an important effect on the convergence of the solution. This question is connected with the choice of "family parameter" in the predictor algorithm, and will be discussed further in Section 4.5. For the time being, in order to introduce the convention of interchangeable subscripts, allowing flexibility in the choice of the fixed parameter, let us rewrite Equations (4.23) in the form

$$\begin{aligned} v_{2K} \delta s_{0K} + v_{2L} \delta s_{0L} + v_{2M} \delta s_{0M} + f_2 \delta t &= -s_2^* \\ v_{4K} \delta s_{0K} + v_{4L} \delta s_{0L} + v_{4M} \delta s_{0M} + f_4 \delta t &= -s_4^* \\ v_{jK} \delta s_{0K} + v_{jL} \delta s_{0L} + v_{jM} \delta s_{0M} + f_j \delta t &= -s_j^*. \end{aligned} \quad (4.24)$$

The three subscripts  $K, L$  and  $M$  can be selected as any permutation of 1, 5 and  $i$  (recall that  $i = 3$  or  $6$ , depending on the type of initial mirror configuration, as in Table 3.1). Since  $K$  can always be selected appropriately, we can, without loss of generality, set

$$\delta s_{0K} = 0, \quad (4.25)$$

thus keeping  $s_{OK}$  fixed at the value  $s_{OK}^*$  in the corrector. The system (4.24) can then be solved for the corrections  $\delta s_{OL}$ ,  $\delta s_{OM}$  and  $\delta t$ , and improved values of the parameters  $s_{OL}$ ,  $s_{OM}$  and  $t$  obtained from Equations (4.20). Integration from the corrected initial conditions up to the corrected final epoch yields a new system of equations of the form (4.24), with smaller absolute values of the quantities  $s_2^*$ ,  $s_4^*$ ,  $s_j^*$  appearing on the right-hand side, if application of the corrector has been successful. The whole procedure is repeated in an iterative fashion until the final conditions satisfy the periodicity conditions within some specified accuracy. A suitable form of periodicity criterion is

$$\left( s_2^{*2} + s_4^{*2} + s_j^{*2} \right)^{1/2} < \epsilon, \quad (4.26)$$

where  $\epsilon$  is some (small) constant. (The results presented in this thesis were computed with a "periodicity accuracy"  $\epsilon = 10^{-8}$ ). Quadratic convergence of the corrector is obtained for sufficiently small periodicity errors (that is, each application of the corrector results, approximately, in a squaring of the error); starting with initial estimates of the orbital parameters with an accuracy of a few per cent, two or three applications of the corrector are usually sufficient, unless numerical difficulties associated with a highly unstable orbit or a close approach to one of the primaries arise.

The application of differential correction method to the determination of periodic orbits of the elliptic restricted problem is formally very similar to that for the circular case. The main difference is that the period of a periodic orbit in the elliptic problem can only take certain discrete values (equal to an integer multiple of the period of the primaries), and so must be kept fixed in the corrector process. With the addition of this constraint, the system of corrector equations (4.23) becomes completely determined, and unique solutions are obtained. In practice, estimates for the initial conditions of arbitrary periodic orbits of the elliptic problem are not available; however, as we saw in Chapter 2, families of periodic orbits can be established with either the mass parameter  $\mu$  or eccentricity  $e$  of the primaries as the parameter of the family.

We consider now the differential corrector algorithm which can be used to determine a periodic orbit belonging to a family parametrised

by the primary eccentricity, the mass parameter being kept fixed, as before. The periodicity conditions (2.27) are written in the form

$$\begin{aligned} S_2 (s_{01}, s_{05}, s_{0i}; e) &= 0 \\ S_4 (s_{01}, s_{05}, s_{0i}; e) &= 0 \\ S_j (s_{01}, s_{05}, s_{0i}; e) &= 0, \end{aligned} \quad (4.27)$$

indicating the explicit dependence upon the parameter  $e$ , which is allowed to vary. It is assumed that the (fixed) values of  $\theta_0$  and  $\theta_1$  are known a priori, and these are therefore omitted from Equations (4.27). The analogy between Equations (4.19) and (4.27) is obvious, and the corrector equations for the elliptic restricted problem may therefore be written

$$\begin{aligned} v_{21} \delta s_{01} + v_{25} \delta s_{05} + v_{2i} \delta s_{0i} + v_{2e} \delta e &= -s_2^* \\ v_{41} \delta s_{01} + v_{45} \delta s_{05} + v_{4i} \delta s_{0i} + v_{4e} \delta e &= -s_4^* \\ v_{j1} \delta s_{01} + v_{j5} \delta s_{05} + v_{ji} \delta s_{0i} + v_{je} \delta e &= -s_j^* . \end{aligned} \quad (4.28)$$

The quantity  $\delta e$  is the difference

$$\delta e = e - e^* \quad (4.29)$$

between the exact and estimated values of the eccentricity in the sought solution of Equations (4.27). The coefficients  $v_{2e}, v_{4e}$  and  $v_{je}$  of  $\delta e$  in Equations (4.28) are the components of the vector  $\underline{v}_e$  defined in Section 3.3 (that is, the derivatives  $ds_2/de, ds_4/de, ds_j/de$ ), evaluated at the final epoch ( $\theta = \theta_1$ ), and are calculated from Equations (3.25). The same considerations apply to the solution of Equations (4.28) as to Equations (4.23), and in the interchangeable-subscript notation, Equation (4.28) becomes

$$\begin{aligned} v_{2K} \delta s_{0K} + v_{2L} \delta s_{0L} + v_{2M} \delta s_{0M} + v_{2e} \delta e &= -s_2^* \\ v_{4K} \delta s_{0K} + v_{4L} \delta s_{0L} + v_{4M} \delta s_{0M} + v_{4e} \delta e &= -s_4^* \\ v_{jK} \delta s_{0K} + v_{jL} \delta s_{0L} + v_{jM} \delta s_{0M} + v_{je} \delta e &= -s_j^* . \end{aligned} \quad (4.30)$$

The selection of one of the parameters ( $s_{01}, s_{05}, s_{0i}, e$ ) to be kept fixed in the corrector is associated, as we have seen, with the choice of family parameter for the family of periodic orbits to be determined. If, as is frequently the case, a family of periodic orbits of the elliptic problem

is to be established by continuation from the circular problem, the primary eccentricity  $e$  is chosen as the parameter of the family, and we take

$$\delta e = 0 \tag{4.31}$$

in Equations (4.30). In other circumstances, such as in tracing out a family of three-dimensional periodic orbits bifurcating from a planar orbit (a "vertical branch"), it is more appropriate to fix one of the initial conditions, and Equation (4.25) is applicable. This will be discussed in Sections 4.5 and 4.6.

#### 4.4 Predictor Algorithms

By means of the differential correction method described in the previous section, the initial conditions and period (in the circular case) or the primary eccentricity (in the elliptic problem) of a three-dimensional symmetric periodic orbit can be found arbitrarily accurately in principle, on the assumption that the values of these parameters are known in the first place. The use of the corrector algorithm alone is sufficient to allow a number of representative periodic orbits to be found at intervals along a family, by incrementing one of the parameters ( $s_{01}, s_{05}, s_{0i}; t$ ) by a fixed amount between successive orbits, and taking the values of the other three parameters for the orbit just found as estimates for those of the next orbit. To start the whole process, the parameters of one orbit belonging to the family must be approximately known. This procedure, involving the use of the unaltered parameters of the previous orbit, is referred to as the "zeroth-order predictor" scheme. It is an inefficient procedure for tracing out a family of periodic orbits, usually requiring many iterations of the corrector in order to satisfy the periodicity criterion, and the interval between successive orbits along the family usually has to be made quite small to ensure convergence of the corrector.

At little cost in program complexity, and using information which is already available, a first- or second-order predictor scheme can be set up to produce accurate estimates of the initial conditions and period (eccentricity) for the next orbit along the family. Predictors of higher order than the second result in more accurate estimates of these parameters, reducing and sometimes eliminating the need for a corrector step, but have

the disadvantage of requiring either higher-order variations to be calculated, or more complicated starting procedures to be devised (see, e.g. Markellos et al., 1978). In this section, the first- and second-order predictors employed in obtaining the results given in this thesis are described. As in the previous section, we deal first of all with the circular restricted problem, and then make the necessary alterations for the elliptic case.

The first-order (linear) predictor algorithm is based on a slight modification of the differential correction method. Let us assume that the initial conditions  $(s_{01}^1, s_{05}^1, s_{0i}^1)$  and period  $T^1$  of an orbit satisfying the periodicity criterion (4.26) have been found; then, to an accuracy  $\epsilon$ , we have

$$\begin{aligned} S_2^1 &= S_2(s_{01}^1, s_{05}^1, s_{0i}^1; t^1) = 0 \\ S_4^1 &= S_4(s_{01}^1, s_{05}^1, s_{0i}^1; t^1) = 0 \\ S_j^1 &= S_j(s_{01}^1, s_{05}^1, s_{0i}^1; t^1) = 0, \end{aligned} \quad (4.32)$$

where as usual  $t^1 = T^1/2$  or  $T^1/4$ , depending on the orbital symmetry. Let  $(s_{01}^2, s_{05}^2, s_{0i}^2; t^2)$  be the corresponding parameters of a neighbouring orbit of the same family, such that the quantities

$$\begin{aligned} \Delta s_{01} &= s_{01}^2 - s_{01}^1 \\ \Delta s_{05} &= s_{05}^2 - s_{05}^1 \\ \Delta s_{0i} &= s_{0i}^2 - s_{0i}^1 \\ \Delta t &= t^2 - t^1 \end{aligned} \quad (4.33)$$

are small. The periodicity conditions for the second orbit can be written

$$\begin{aligned} S_2^2 &= S_2(s_{01}^1 + \Delta s_{01}, s_{05}^1 + \Delta s_{05}, s_{0i}^1 + \Delta s_{0i}; t^1 + \Delta t) = 0 \\ S_4^2 &= S_4(s_{01}^1 + \Delta s_{01}, s_{05}^1 + \Delta s_{05}, s_{0i}^1 + \Delta s_{0i}; t^1 + \Delta t) = 0 \\ S_j^2 &= S_j(s_{01}^1 + \Delta s_{01}, s_{05}^1 + \Delta s_{05}, s_{0i}^1 + \Delta s_{0i}; t^1 + \Delta t) = 0. \end{aligned} \quad (4.34)$$

Expanding in Taylor series to first order in the  $\Delta$ 's, and using Equations (4.32), we obtain the basic form of the linear predictor for the circular restricted problem:

$$\begin{aligned} v_{21} \Delta s_{01} + v_{25} \Delta s_{05} + v_{2i} \Delta s_{0i} + f_2 \Delta t &= 0 \\ v_{41} \Delta s_{01} + v_{45} \Delta s_{05} + v_{4i} \Delta s_{0i} + f_4 \Delta t &= 0 \\ v_{j1} \Delta s_{01} + v_{j5} \Delta s_{05} + v_{ji} \Delta s_{0i} + f_j \Delta t &= 0. \end{aligned} \quad (4.35)$$

The elements of the variational matrix  $V$  and components of the vector function  $f$  appearing as coefficients in these equations are those for the "known" orbit (superscript "1"), evaluated at  $\theta = t^1$ .

The system of three simultaneous equations (4.35) differs from the corrector equations (4.23) only in that the quantities corresponding to  $s_2^*$ ,  $s_4^*$  and  $s_j^*$  are zero; this is because both the "original" and "modified" orbits, in the present case, are periodic. Like the corrector system, Equations (4.35) have one degree of freedom, allowing an arbitrary constraint to be applied; this is usually done by assigning a fixed non-zero value to one of the  $\Delta$ 's. (Note that choosing any of the  $\Delta$ 's to be zero would result in the trivial solution  $\Delta s_{01} = \Delta s_{05} = \Delta s_{0i} = \Delta t = 0$ , merely reflecting the property of periodicity of the known orbit, except when the matrix of coefficients of the other  $\Delta$ 's is singular, in which case no solution exists). The parameter to which a fixed increment is given is termed the "family parameter". The choice of this parameter, from  $s_{01}$ ,  $s_{05}$ ,  $s_{0i}$  and  $t$ , can be important; if the selected family parameter has an extremum over the family being traced, so that the corresponding system of equations becomes singular or nearly-singular, the predictor-corrector scheme will break down completely and have to be restarted with a new choice of family parameter. In the next section, a simple criterion will be given for selecting the family parameter on a "local" basis, in such a way that these difficulties are avoided.

It will be found convenient in the sequel to rewrite Equations (4.35) in terms of the variable subscript notation introduced in the previous section:

$$\begin{aligned} V_{2K} \Delta s_{0K} + V_{2L} \Delta s_{0L} + V_{2M} \Delta s_{0M} + f_2 \Delta t &= 0 \\ V_{4K} \Delta s_{0K} + V_{4L} \Delta s_{0L} + V_{4M} \Delta s_{0M} + f_4 \Delta t &= 0 \\ V_{jK} \Delta s_{0K} + V_{jL} \Delta s_{0L} + V_{jM} \Delta s_{0M} + f_j \Delta t &= 0. \end{aligned} \tag{4.36}$$

As before, the subscripts  $K, L$  and  $M$  can be any permutation of the set  $(1, 5, i)$ . By suitably defining  $K$  we can, without loss of generality in the choice of family parameter among the three non-zero initial conditions, specify the value of the increment  $\Delta s_{0K}$  and solve Equations (4.36) for  $\Delta s_{0L}$ ,  $\Delta s_{0M}$  and  $\Delta t$ . This linear predictor algorithm has the advantage that knowledge of only one previous orbit of the family is required, and in some circumstances, as we shall see later, it is the only one usable.

It is often the case, however, that more than one orbit has previously been determined, and it is then possible to employ the more accurate second-order (quadratic) predictor, which we now consider.

The equation of the "family characteristic", defined as a curve in the four-dimensional space of the initial conditions  $(s_{01}, s_{05}, s_{0i})$  and integration interval  $t$ , each point of which represents an orbit belonging to the family, can be written in parametric form

$$\begin{aligned} S_{01} &= S_{01}(u) \\ S_{05} &= S_{05}(u) \\ S_{0i} &= S_{0i}(u) \\ t &= t(u), \end{aligned} \tag{4.37}$$

with respect to some parameter  $u$ . Suppose that two neighbouring orbits belonging to the family, corresponding to the values  $u_0$  and  $u_1$  of the parameter  $u$ , are known, such that

$$\Delta u = u_1 - u_0 \tag{4.38}$$

is small. Expanding the right-hand side of the first of Equations (4.37) to second order in  $\Delta u$ , we may write

$$S_{01}^0 = S_{01}^1 - \Delta u S_{01}^{1'} + \frac{1}{2} \Delta u^2 S_{01}^{1''}, \tag{4.39}$$

where  $S_{01}^0 = S_{01}(u_0)$ ,  $S_{01}^1 = S_{01}(u_1)$ , and the primes denote differentiation with respect to the parameter  $u$ , with similar expressions for  $S_{05}^0$ ,  $S_{0i}^0$  and  $t^0$ . The initial condition  $S_{01}^2$  of the orbit corresponding to

$$u = u_2 = u_1 + \Delta u \tag{4.40}$$

is given, to second order in  $\Delta u$ , by

$$S_{01}^2 = S_{01}^1 + \Delta u S_{01}^{1'} + \frac{1}{2} \Delta u^2 S_{01}^{1''}, \tag{4.41}$$

with similar expressions for  $S_{05}^2$ ,  $S_{0i}^2$  and  $t^2$ . From Equations (4.39) and (4.41) we have

$$\begin{aligned}
 s_{01}^2 &= s_{01}^0 + 2\Delta u s_{01}' \\
 s_{05}^2 &= s_{05}^0 + 2\Delta u s_{05}' \\
 s_{0i}^2 &= s_{0i}^0 + 2\Delta u s_{0i}' \\
 t^2 &= t^0 + 2\Delta u t' ,
 \end{aligned} \tag{4.42}$$

yielding predicted values for the initial conditions  $(s_{01}^2, s_{05}^2, s_{0i}^2)$  and integration interval  $t^2$  of the third orbit accurate to second order in the parameter increment  $\Delta u$ .

Now for each of the three orbits, corresponding to parameter values  $u_0, u_1$  and  $u_2$ , we have periodicity conditions of the form

$$\begin{aligned}
 s_2^\alpha &= S_2(s_{01}^\alpha, s_{05}^\alpha, s_{0i}^\alpha; t^\alpha) = 0 \\
 s_4^\alpha &= S_4(s_{01}^\alpha, s_{05}^\alpha, s_{0i}^\alpha; t^\alpha) = 0 \\
 s_j^\alpha &= S_j(s_{01}^\alpha, s_{05}^\alpha, s_{0i}^\alpha; t^\alpha) = 0 ,
 \end{aligned} \tag{4.43}$$

where  $\alpha$  takes the values 0, 1, 2. The right-hand sides of Equations (4.43) for orbits 0 and 2 can be expanded in Taylor series, to second order in  $\Delta u$ , about orbit 1:

$$\begin{aligned}
 s_2^0 &= s_2^1 - \Delta u (v_{21} s_{01}' + v_{25} s_{05}' + v_{2i} s_{0i}' + f_2 t') \\
 &\quad + \frac{1}{2} \Delta u^2 \left( \frac{\partial^2 s_2}{\partial s_{01}^2} s_{01}'' + \frac{\partial^2 s_2}{\partial s_{05}^2} s_{05}'' + \dots \right) ,
 \end{aligned} \tag{4.44}$$

$$\begin{aligned}
 s_2^2 &= s_2^1 + \Delta u (v_{21} s_{01}' + v_{25} s_{05}' + v_{2i} s_{0i}' + f_2 t') \\
 &\quad + \frac{1}{2} \Delta u^2 \left( \frac{\partial^2 s_2}{\partial s_{01}^2} s_{01}'' + \frac{\partial^2 s_2}{\partial s_{05}^2} s_{05}'' + \dots \right) ,
 \end{aligned} \tag{4.45}$$

with similar expressions for  $s_4^0, s_4^2, s_j^0$  and  $s_j^2$ . Subtraction of Equation (4.44) from (4.45) yields

$$s_2^2 - s_2^0 = 2\Delta u (v_{21} s_{01}' + v_{25} s_{05}' + v_{2i} s_{0i}' + f_2 t') = 0, \tag{4.46}$$

with similar expressions for the other two components,  $s_4$  and  $s_j$ . For the three orbits to be distinct, we must have  $\Delta u \neq 0$ ; comparison of Equation (4.46), and the corresponding equations for the 4 and j components, with Equations (4.36), shows that the two systems of equations are identical. Solution of the system of linear equations (4.36), with known coefficients, therefore yields the derivatives  $s_{01}^{1'}$ ,  $s_{05}^{1'}$ ,  $s_{0i}^{1'}$  and  $t^{1'}$  along the family

characteristic. The values of the derivatives are accurate to second order, and can be substituted into Equations (4.42) to yield predicted values of the initial conditions and integration interval of orbit 2 accurate to  $O(\Delta u^2)$ . This quadratic predictor algorithm requires only the values of the initial parameters  $(s_{01}^0, s_{05}^0, s_{0i}^0, t^0)$  of orbit 0, together with the derivatives  $s_{01}^{1/}, s_{05}^{1/}, s_{0i}^{1/}, t^{1/}$  calculated from the elements of the variational matrix of orbit 1, and which are needed in the linear predictor anyway.

Since the quadratic predictor achieves an improved accuracy for the predicted initial parameters of the next orbit along a family at virtually no cost in terms of extra calculations, it is clearly preferred over the linear predictor. However, the quadratic predictor requires that:

- (i) two previous orbits must be known;
- (ii) the interval in the parameter  $u$  between orbits 0 and 1, and between orbits 1 and 2, must be equal.

The first requirement fails to be satisfied only when the second orbit of a family is sought. The second requirement ensures that the terms involving  $\Delta u^2$  in Equations (4.44) and (4.45) cancel in Equation (4.46), so that second derivatives of the form  $\partial^2 s_\alpha / \partial s_{0\beta} \partial s_{0\gamma}$  (the elements of the second-order variational matrix) do not have to be computed. As we shall see in the next section, the occurrence of an extremum in the family parameter may prevent requirement (ii) from being satisfied. In either case, the linear predictor has to be used as a starting procedure.

The parameter  $u$  introduced in Equations (4.37) has been taken to be arbitrary; it is usual (although not necessary) to identify  $u$  with one of the initial conditions ( $s_{0K}$ , where  $K = 1, 5$  or  $i$ ) or the integration interval  $t$ . In Section 4.5 a criterion is described for selecting the family parameter on a "local" basis.

The construction of linear and quadratic predictor algorithms applicable to the elliptic case of the restricted problem follows the analogy employed in Section 4.3. The orbital period  $T$  has a fixed value along a family of periodic orbits in the elliptic problem, and instead we consider the eccentricity  $e$  of the primaries to vary, the mass parameter  $\mu$  being held fixed. The linear and quadratic predictors of the elliptic restricted

problem are therefore obtained by replacing  $(\Delta t, f_2, f_4, f_j)$  in the predictor equations of the circular problem by  $(\Delta e, v_{2e}, v_{4e}, v_{je})$ .

#### 4.5 Selection of Family Parameter

In the previous two sections, the importance of the family parameter in the numerical determination of a family of symmetric periodic orbits of the restricted problem was discussed. We recall that for a fixed value of the mass parameter, families of periodic orbits in the circular problem are monoparametric, and that in the elliptic problem it is possible to speak of monoparametric families of periodic orbits if the primary eccentricity is considered to vary along such families. In principle, an arbitrary parametrisation may be adopted, but it is often convenient, and in some circumstances necessary, to choose as family parameter one of the non-zero initial conditions of the orbits, denoted by  $s_{OK}$  in the variable subscript notation, where  $K$  is equal to 1, 5 or  $i$ ; this particular component of  $s_0$  is then incremented by some previously-specified amount between successive orbits along the family being traced out, and fixed in value when the corrector is applied. Difficulties arise, however, when an extremum in the chosen family parameter is encountered: the systems of predictor and corrector equations become near-singular, so that the predictor may "overshoot", and the corrector may converge slowly or not at all. Since it is often the case that each of the three non-zero initial conditions possesses at least one extremum at some point along a family, and in any case the occurrence of an extremum is not readily foreseen, it is not generally possible to trace out an entire family using the same family parameter throughout. It would clearly be advantageous to be able to select the most suitable family parameter on a local basis at various stages in the numerical determination of a family of periodic orbits, so that breakdown of the predictor-corrector scheme does not occur.

The strategy employed in the determination of the various families presented in this thesis was to select as "local" family parameter the most rapidly-varying of  $(s_{01}, s_{05}, s_{0i})$  at each newly-computed orbit belonging to the family being traced out. We saw in Section 4.4 that in the circular restricted problem, the derivatives  $s'_{01}$ ,  $s'_{05}$  and  $s'_{0i}$  with respect to the parameter  $u$ , components of the tangent vector to the

family characteristic, satisfy the system of equations (in matrix form)

$$\begin{pmatrix} v_{21} & v_{25} & v_{2i} & f_2 \\ v_{41} & v_{45} & v_{4i} & f_4 \\ v_{j1} & v_{j5} & v_{ji} & f_j \end{pmatrix} \begin{pmatrix} s'_{01} \\ s'_{05} \\ s'_{0i} \\ t' \end{pmatrix} = \begin{pmatrix} 0 \\ 0 \\ 0 \\ 0 \end{pmatrix} \quad (4.47)$$

Defining the following determinants involving the elements of the matrix appearing in this equation:

$$D_1 = \begin{vmatrix} v_{2i} & v_{25} & f_2 \\ v_{4i} & v_{45} & f_4 \\ v_{ji} & v_{j5} & f_j \end{vmatrix} \quad (4.48)$$

$$D_5 = \begin{vmatrix} v_{21} & v_{2i} & f_2 \\ v_{41} & v_{4i} & f_4 \\ v_{j1} & v_{ji} & f_j \end{vmatrix} \quad (4.49)$$

$$D_i = \begin{vmatrix} v_{25} & v_{21} & f_2 \\ v_{45} & v_{41} & f_4 \\ v_{j5} & v_{j1} & f_j \end{vmatrix} \quad (4.50)$$

$$D = \begin{vmatrix} v_{21} & v_{25} & v_{2i} \\ v_{41} & v_{45} & v_{4i} \\ v_{j1} & v_{j5} & v_{ji} \end{vmatrix} \quad (4.51)$$

we have, by Kramers' rule

$$s'_{01} : s'_{05} : s'_{0i} : t' = D_1 : D_5 : D_i : D \quad (4.52)$$

The four determinants  $D_1$ ,  $D_5$ ,  $D_i$  and  $D$  can be evaluated from the variational matrix and derivative of the state vector at the final epoch ( $\theta = t$ ) of a periodic orbit; Equation (4.52) then shows that the most rapidly-varying of  $s_{01}$ ,  $s_{05}$  and  $s_{0i}$  along the family is that associated with the determinant  $D_1$ ,  $D_5$  or  $D_i$  having the largest absolute value. If the subscript  $K$  is chosen accordingly and the initial condition  $s_{0K}$  incremented

by some fixed amount  $\Delta s_{OK}$ , the corresponding solutions of Equations (4.36) are

$$\begin{aligned}\Delta s_{OL} &= \Delta s_{OK} D_L / D_K \\ \Delta s_{OM} &= \Delta s_{OK} D_M / D_K \\ \Delta t &= \Delta s_{OK} D / D_K .\end{aligned}\tag{4.53}$$

These values can then be used to predict either linearly or quadratically the parameters  $(s_{01}, s_{05}, s_{0i}, t)$  of the next orbit of the family. These predicted values are refined by iterative application of the corrector, with  $s_{OK}$  kept fixed; once the periodicity criterion is satisfied, the determinants  $D_1, D_5, D_i$  and  $D$  are re-computed from the new variational matrix and derivative of the state vector. If the relative values of  $|D_1|$ ,  $|D_5|$  and  $|D_i|$  are now such that a change of family parameter is necessary, the subscript  $K$  in the predictor-corrector scheme is redefined. The whole procedure is repeated as each new orbit is obtained, with changes of family parameter occurring as often as necessary to ensure that the orbits are in a geometrical sense more or less evenly-spaced along the family characteristic, and avoiding entirely the difficulties associated with extrema in the initial conditions.

The increment applied to the local family parameter for the prediction of a new orbit is most conveniently taken to be some "round" number, such as 0.001 or 0.005. If this value is retained when the family parameter is changed, it will not in general be equal to the interval in this parameter between the previous two orbits. This means that the quadratic predictor cannot be used immediately following a change of family parameter; the linear predictor must be used instead, for just one step, and thereafter the quadratic predictor may be used until another change of family parameter becomes necessary to take account of variations in the relative rates of change of the initial conditions along the family.

The criterion for the selection of the family parameter described above is readily implemented in a computer program for the determination of families of periodic orbits. The criterion has been described in the context of the circular restricted problem, with the integration interval  $t$  (equal to half or quarter of the period, depending on the symmetry) varying along the family. In the elliptic problem, as we have

seen,  $t$  is replaced by  $e$ , and the derivatives  $f_2, f_4, f_j$  by  $v_{2e}, v_{4e}, v_{je}$ , respectively; with this substitution, the criterion is applicable in the elliptic case as well as in the circular case of the restricted problem. It has been found that this automatic selection criterion, together with integration to a specified epoch (the predicted value of  $t$ ) rather than to a given crossing of the  $(x,z)$ -plane, to avoid difficulties associated with multiplicity changes along a family, can result in an entire family of periodic orbits being obtained, without interruption, in a single run of the computer program.

#### 4.6 Numerical Determination of Vertical Branches

The computational techniques described up to now in this chapter are of general application in the numerical determination of symmetric periodic orbits of the restricted three-body problem. In this section we confine our attention to the problem of determining the "vertical branches" of a family of planar periodic orbits, that is, the families of three-dimensional periodic orbits which originate through vertical bifurcation from a member of a planar family; and in particular, we consider how suitable starting orbits may be found for the various types of vertical branches. As in previous sections, we deal first with the circular case of the restricted problem, and then indicate the differences that arise in the elliptic case.

Suppose that the symmetric planar periodic orbit with initial conditions  $(s_{01}, 0, 0, 0, s_{05}, 0)$  and period  $T_0$  has vertical stability index  $a_v$  satisfying the self-resonance condition

$$a_v = \cos\left(\frac{2\pi n}{m}\right), \quad (4.54)$$

for some integers  $m$  and  $n$  (mutually prime, with  $m \geq 1, 0 < n \leq m$ ). In the cases  $a_v = \pm 1$  (vertical-critical), as we saw in Chapter 3, there is in general only one vertical branch, consisting of orbits of simple symmetry for  $m=1$  and of double symmetry for  $m=2$ , the exact symmetry class depending on which of the elements of  $V_v(T_0/2)$  is zero. Let us consider the more general case of an  $m$ -tuple vertical bifurcation with  $m > 2$ , where there are two vertical branches.

If  $m$  is odd ( $m = 3, 5, 7, \dots$ ), one of the two vertical branches consists

of axisymmetric orbits and the other of plane symmetric orbits. The expressions "axisymmetric family", "plane symmetric family" or "doubly-symmetric family" will be used in the sequel to mean "a family consisting of axisymmetric (plane symmetric, doubly-symmetric) periodic orbits". In the linear approximation, the initial conditions of the orbits of the plane symmetric family in the neighbourhood of the bifurcation are given by

$$\underline{s}_0 = (s_{01}, 0, \delta s_{03}, 0, s_{05}, 0), \quad (4.55)$$

and for the axisymmetric family,

$$\underline{s}_0 = (s_{01}, 0, 0, 0, s_{05}, \delta s_{06}), \quad (4.56)$$

where  $\delta s_{03}$ ,  $\delta s_{06}$  are small. Because of the decoupling of the horizontal and vertical parts of the variational equation, the components  $s_{01}$  and  $s_{05}$  of the state vector, to first order in  $\delta s_{0i}$ , do not vary along the family. For the same reason, for small values of  $\delta s_{03}$  and  $\delta s_{06}$ , the orbits of both families have period

$$T = m T_0. \quad (4.57)$$

Numerical determination of the two branches commences with estimated initial conditions and period given by Equations (4.55) or (4.56) with a suitable value of  $\delta s_{0i}$ , and (4.57). In the predictor-corrector scheme, it is essential to choose  $s_{0i}$  as the local family parameter at the beginning of each family ( $i = 3$  for the plane symmetric and  $i = 6$  for the axisymmetric family), in order to ensure that the process does not revert to an orbit (described  $m$  times) of the planar family to which the vertical self-resonant orbit belongs; the value  $\delta s_{0i}$  is fixed in the corrector, so that a genuinely three-dimensional periodic orbit will be obtained, and subsequent orbits of the vertical branch are computed with  $s_{0i}$  increased by some fixed amount. The selection criterion described in the previous section will automatically choose  $s_{0i}$  as family parameter, because to first order in  $\delta s_{0i}$ , the tangent to the family characteristic in the vicinity of the bifurcation is in the "vertical" direction, that is, parallel to the  $s_{0i}$ -axis.

For  $m$ -tuple bifurcations with  $m$  even ( $m = 4, 6, 8, \dots$ ), there are two doubly-symmetric branches. In order to obtain the initial conditions of suitable starting orbits for the two branches, it is necessary to consider separately the cases distinguished in Table 3.2:

$$\begin{aligned} \text{(a)} \quad m &= 4r & (\quad &= 4, 8, 12, \dots), \\ \text{(b)} \quad m &= 2(2r + 1) & (\quad &= 6, 10, 14, \dots), \end{aligned} \tag{4.58}$$

corresponding to  $\gamma_r = 0$  and  $\alpha_r = 0$ , respectively. The period of a three-dimensional orbit in the neighbourhood of the bifurcation is given by Equation (4.57), and the interval  $t$  between successive mirror configurations is  $t = T/4$ ; in case (a) above

$$t = r T_0, \tag{4.59}$$

while in case (b)

$$t = (2r+1) T_0 / 2. \tag{4.60}$$

Let the two distinct mirror configurations of the planar bifurcation orbit be denoted  $C_0$  and  $C_1$ . A doubly-symmetric three-dimensional periodic orbit belonging to one of the vertical branches can be generated from initial conditions satisfying either Equation (4.55) (type (P) mirror configuration) or Equation (4.56) (type (A) mirror configuration), the horizontal components  $s_{01}$  and  $s_{05}$  of the state vector corresponding to either  $C_0$  or  $C_1$ ; the four possibilities may be denoted by  $C_0(P)$ ,  $C_0(A)$ ,  $C_1(P)$  and  $C_1(A)$ . Two of these four cases correspond to the initial and final conditions of the same orbit, according to the value of  $m$ , as shown in the following table.

Table 4.1

Case	$m$	Initial Mirror Configuration	Final Mirror Configuration
(a)	$4r$	$C_0(A)$	$C_0(P)$
		$C_1(A)$	$C_1(P)$
(b)	$2(2r + 1)$	$C_0(A)$	$C_1(P)$
		$C_1(A)$	$C_0(P)$

In all cases, the initial and final mirror configurations are of different type, as they must be for a doubly-symmetric orbit. In case (a), Equation (4.59) shows that the interval  $t$  between successive mirror configurations of the three-dimensional orbits is an integer multiple of the period  $T_0$  of the planar orbit; thus, in the linear approximation, the horizontal components of the state vector at each three-dimensional mirror configuration are the same, and correspond to either  $C_0$  or  $C_1$ . In case (b), the interval  $t$  between successive three-dimensional mirror configurations is, by Equation (4.60), an odd multiple of the half-period of the planar orbit, so that the horizontal components of the state vector alternate between configurations  $C_0$  and  $C_1$ , at each three-dimensional mirror configuration.

There is no real distinction between the "initial" and "final" configurations of a periodic orbit, since we can always choose the starting point of the integration arbitrarily; thus, entries in the last two columns of Table 4.1 can be interchanged at will. It can be seen that in both cases (a) and (b) (that is, for all even values of  $m > 2$ ), the orbits of the two bifurcating families are distinguished in the location of the type (A) mirror configuration (or, alternatively, the type (P) mirror configuration). If we choose always to commence the integration of a doubly-symmetric periodic orbit from a type (A) (on-axis) mirror configuration, then starting orbits for the two vertical branches arising from a vertical self-resonant orbit for which  $m$  is even can be determined from initial conditions of the form (4.56), with the components  $s_{01}$  and  $s_{05}$  corresponding to each of the two distinct mirror configurations  $C_0$  and  $C_1$  of the planar orbit. The two starting orbits could equally well be found using initial conditions of type  $C_0(P)$  and  $C_1(P)$ , rather than  $C_0(A)$  and  $C_1(A)$ , but it is often advantageous to use on-axis initial conditions because the two vertical branches are more readily distinguished according to which side of one or other of the primaries their perpendicular intersections with the  $x$ -axis take place; the points of perpendicular intersection with the  $(x,z)$ -plane may migrate from one side to another as a vertical branch is traced out, whereas the points of perpendicular intersection with the axis are unable to move from one side of a primary to another, unless a collision takes place. It should be noted that in case (b) of Table 4.1, starting orbits for both branches can be obtained using only configuration  $C_0$ , giving the mirror configurations  $C_0(A)$  and  $C_0(P)$ , or alternatively using only

configuration  $C_1$ . In case (a), however, both of configurations  $C_0$  and  $C_1$  must be used to obtain the two branches.

The situation in the elliptic restricted problem is very similar to that in the circular case. First of all, the vertical branch orbits all have period given (exactly) by Equation (4.57). In the linear approximation, the value of the primary eccentricity for the three-dimensional orbits in the vicinity of the bifurcation is

$$e = e^0, \quad (4.61)$$

where  $e^0$  is the value for the planar bifurcation orbit. The initial conditions of suitable starting orbits for the numerical determination of the vertical branches are as given above for the circular restricted problem. The component  $s_{0i}$  of the initial state vector should always be taken as the family parameter at the beginning of a vertical branch, to ensure that the predictor-corrector process does not revert to planar periodic motion.

## 5. VERTICAL BRANCHES OF FAMILY $f$ IN THE SUN-JUPITER CASE OF THE CIRCULAR RESTRICTED PROBLEM

### 5.1 Introduction

In this chapter, results are presented of a numerical investigation of the vertical branches of Strömberg's family  $f$  (retrograde orbits about the less-massive primary  $m_2$ ) in the Sun-Jupiter case ( $\mu = 0.00095$ ) of the three-dimensional circular restricted problem. The object of this investigation was twofold: firstly, to verify in this particular case the predictions of the linear theory of vertical bifurcation discussed in Chapter 3, and secondly, to explore three-dimensional periodic orbits resembling the motion of Jupiter's outermost natural satellites, a project suggested by the work of Hunter (1966).

We begin by considering the orbits of family  $f$  of retrograde planar satellite orbits around the primary  $m_2$ , which for the value  $\mu = 0.00095$  of the mass parameter represents the planet Jupiter, if  $m_1$  is taken to be the Sun (the effects of the other planets are of course neglected in the model of the restricted three-body problem). The orbits of the part of family  $f$  in the vicinity of the primary  $m_2$  are simple-periodic (completing a single revolution about  $m_2$  in one orbital period) and roughly circular, centred on  $m_2$ . Each orbit crosses the  $x$ -axis perpendicularly twice in one period, one crossing corresponding to a conjunction configuration, with the massless particle located between the two primaries, and the other to an opposition configuration, with the massless particle on the far side of  $m_2$  from  $m_1$ ; these will be referred to as the "conjunction crossing" and "opposition crossing" respectively.

In order to determine the vertical bifurcation orbits of family  $f$  in the vicinity of  $m_2$ , the family was traced out, and the vertical stability index  $a_v$  of the orbits calculated, starting from small, nearly circular two-body orbits around  $m_2$  and continuing to orbits of increasing size. In Figure 5.1,  $a_v$  is plotted against  $x_1$ , the  $x$ -coordinate of the conjunction crossing, between  $x_1 \approx 0.9$  (dimensionless units: Sun-Jupiter distance = 1) and  $x_1 = 1 - \mu = 0.99905$ , the  $x$ -coordinate of the primary  $m_2$ , represented by the letter "J". We see that to the right of the minimum of the vertical stability curve, where  $a_v \approx 0.08$ ,  $x_1 \approx 0.93$ ,  $a_v$  increases monotonically with  $x_1$ ; as  $x_1$  approaches the singularity at

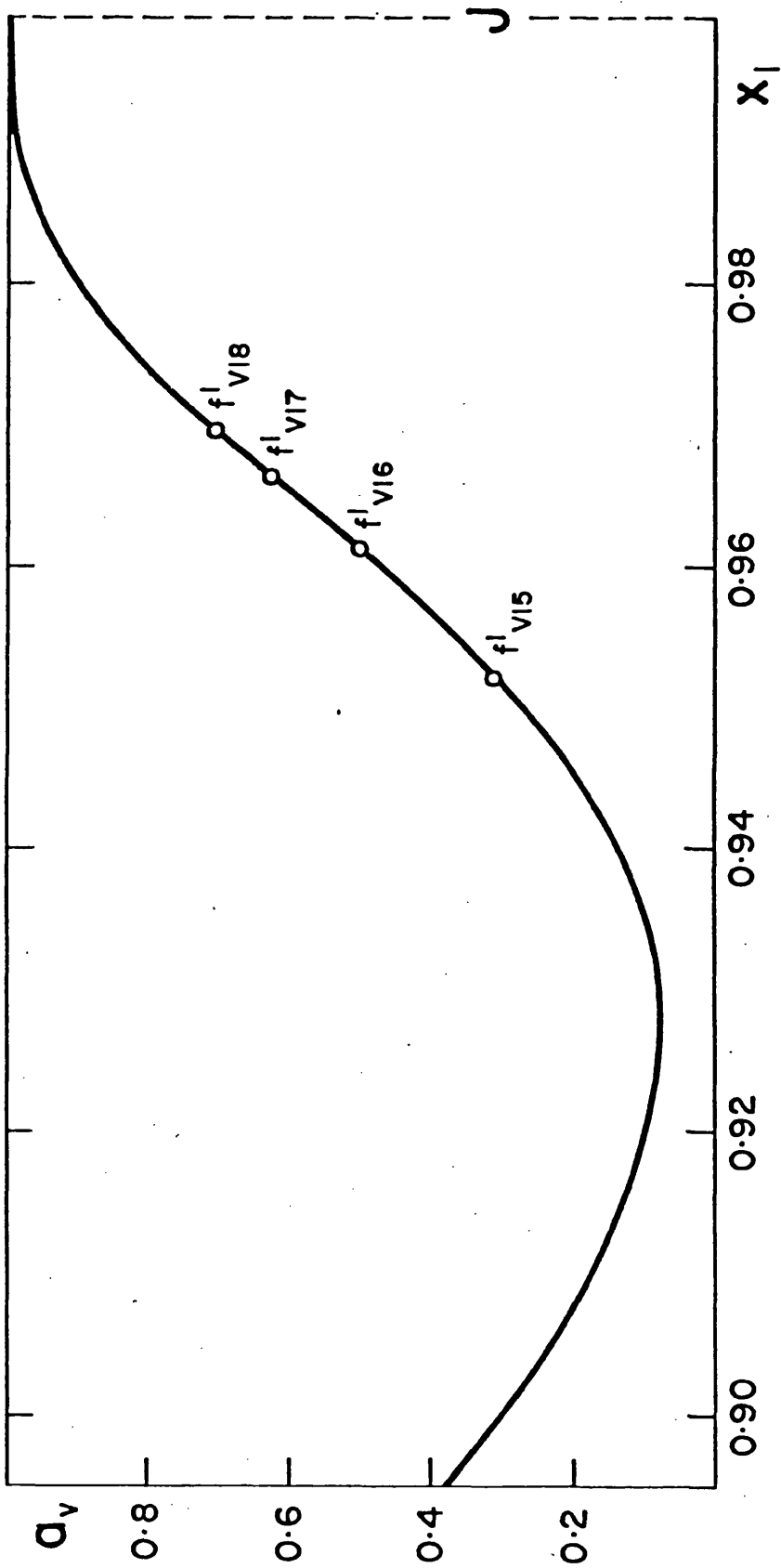


Figure 5.1 : Vertical stability curve of family f near the less massive primary  $m_2$  (Jupiter), for  $\mu = 0.00095$ .

$x = 1 - \mu$ , the orbits of family  $f$  shrink to zero size, tending towards exactly Keplerian motion; it is easily shown that in the limit, the vertical stability index has the critical value  $a_v = +1$ . Thus, the predicted vertical bifurcation orbits of the part of family  $f$  in the vicinity of  $m_2$  are those for which

$$a_v = \cos\left(\frac{2\pi n}{m}\right), \quad (5.1)$$

for some integers  $m, n$ , such that

$$0.08 \leq a_v < 1. \quad (5.2)$$

This inequality can only be satisfied for values of  $m > 4$ , and in particular, no vertical-critical orbits ( $m = 1$  or  $2$ ) are found. We shall consider the vertical bifurcation orbits corresponding to the four lowest possible values of  $m$  (5, 6, 7 and 8), with  $n = 1$ . This choice includes at least one value from each of the three possible cases listed in Equations (3.119), and therefore includes vertical branches of all possible symmetry classes.

The four vertical bifurcation orbits corresponding to the values  $n = 1$ ,  $m = 5, 6, 7$  and  $8$ , with vertical stability indices  $a_v = \cos 2\pi/5$  ( $\approx 0.30902$ ),  $a_v = \cos \pi/3$  ( $= 0.5$ ),  $a_v = \cos 2\pi/7$  ( $\approx 0.62349$ ) and  $a_v = \cos \pi/4$  ( $\approx 0.70711$ ) are represented by points marked on the vertical stability curve (Figure 5.1), and by pairs of points, corresponding to the two intersections of each orbit with the  $x$ -axis, on the projection of the family characteristic in the  $(x, C)$ -plane (Figure 5.2),  $C$  being the Jacobi constant. Each vertical self-resonant orbit is designated according to the formula  $f_{vnm}^i$ : the letter "f" indicates the generating family in Strömberg's notation, the subscript "v" is to distinguish vertical from horizontal self-resonant orbits (orbits of the planar circular restricted problem for which the horizontal stability index  $a = \cos(2\pi n/m)$ , for some  $m, n$ ), and the integers  $m$  and  $n$  are those appearing in the vertical self-resonance condition (5.1). The superscript "i" (not to be confused with the subscript  $i$  employed in previous chapters) is necessary to distinguish between vertical self-resonant orbits having the same values of  $m$  and  $n$  in Equation (5.1); it is assigned the value  $i = 1$  for the first orbit having a given value of  $a_v$  as the family evolves from its point of

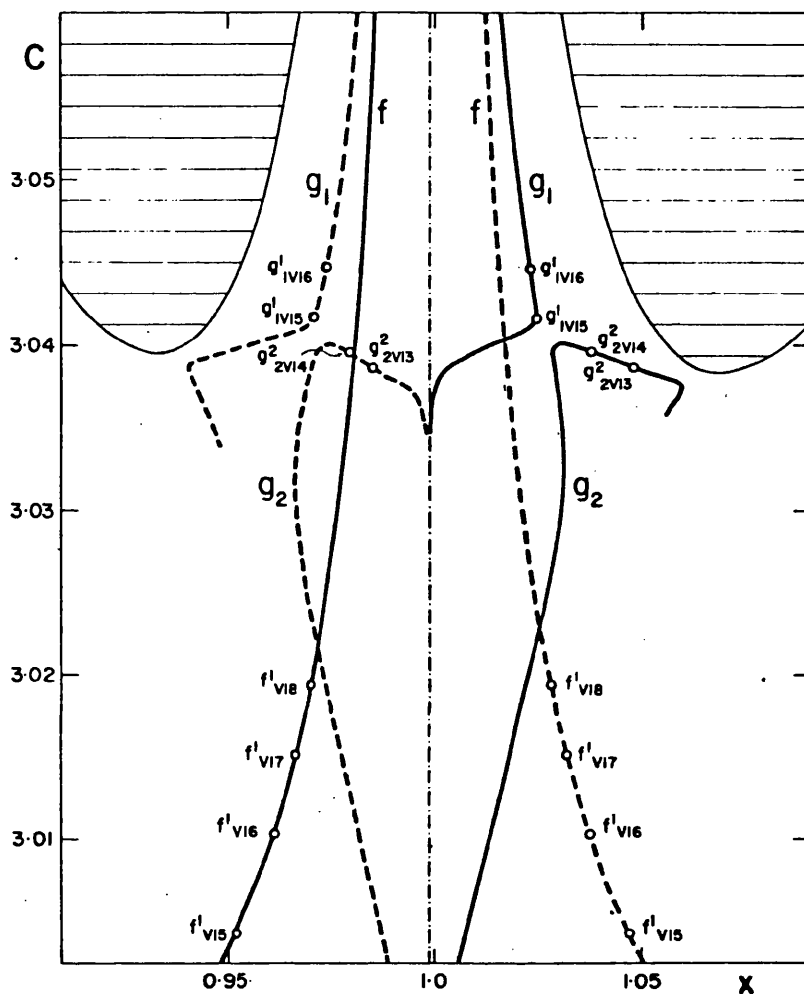


Figure 5.2 : Characteristics in the  $(x,C)$ -plane of the families  $f$ ,  $g_1$  and  $g_2$  of plane periodic orbits, in the vicinity of  $m_2$  ( $\mu = 0.00095$ ). The continuous heavy lines correspond to the positive crossings of the axis of the primaries (that is, in the positive  $y$ -direction), and the broken lines to the negative crossings. The hatched areas are the "forbidden regions" bounded by the zero-velocity curves. The points marked on the family characteristics represent the vertical self-resonant orbits at which the vertical branches of family  $f$  intersect the plane families. The line ----- indicates the position of  $m_2$  (Jupiter) at  $x = 1 - \mu = 0.99905$ .

origin, subsequent orbits having the same self-resonant value of the vertical stability index being labelled  $i = 2, 3, \dots$  etc. For the part of family  $f$  under consideration, that is, in the vicinity of  $m_2$ , and to the right of the minimum in Figure 5.1 ( $x_1 > 0.93$ ), we have the  $i = 1$  orbits.

The four pairs of vertical branches bifurcating from orbits  $f_{v15}^1, f_{v16}^1, f_{v17}^1$  and  $f_{v18}^1$  fall naturally into two groups, depending on the symmetry class of the branch orbits: for odd values of  $m$  ( $m = 5, 7$ ) the branch orbits are simply symmetric, and for even values ( $m = 6, 8$ ), doubly symmetric. Since the bifurcation orbits are simple-periodic, that is, of multiplicity 1, the branch orbits in the neighbourhood of the bifurcation have multiplicity  $m$ , and we can distinguish the two groups of vertical branches according to whether the orbital multiplicity of the branch orbits is initially odd or even. As we shall see, the property of evenness or oddness of the orbital multiplicity is not necessarily preserved along a vertical branch; however, the symmetry property of the orbits is invariant along a given branch, and is characterised by the multiplicity of the orbits at the beginning of the branch.

The notation  $f_{vnm}^i$  for the vertical self-resonant orbits can be extended to allow the vertical branches to be designated according to the formula  $F_{vnm}^i(x)$ : the Strömberg classification of the generating family is capitalised to indicate the three-dimensionality of the orbits belonging to the branch, and the superscript  $(x)$  is used to distinguish between the two branches which (for  $m > 2$ ) arise from each vertical bifurcation orbit. For example, for odd values of  $m$ , the designations  $F_{vnm}^{i(a)}$  and  $F_{vnm}^{i(p)}$  might be used to indicate the axisymmetric and plane symmetric branches, respectively; this notation will be employed for the branches bifurcating from orbits  $f_{v15}^1$  and  $f_{v17}^1$ . The two families of doubly-symmetric orbits bifurcating from each of  $f_{v16}^1$  and  $f_{v18}^1$  will be distinguished according to whether the type (A) mirror configuration of each orbit (that is, the perpendicular crossing of the  $x$ -axis) occurs at conjunction ( $x < 1 - \mu$ ) or at opposition ( $x > 1 - \mu$ ), the superscripts  $(c)$  and  $(o)$  being used to indicate this. Thus, the simply-symmetric branches are  $F_{v15}^{1(a)}$ ,  $F_{v15}^{1(p)}$ ,  $F_{v17}^{1(a)}$  and  $F_{v17}^{1(p)}$ , and the doubly-symmetric branches are  $F_{v16}^{1(c)}$ ,  $F_{v16}^{1(o)}$ ,  $F_{v18}^{1(c)}$  and  $F_{v18}^{1(o)}$ .

The existence of the four pairs of vertical branches predicted by the

linear theory was verified by the computational methods described in the previous chapter, and the results of the numerical investigation will be dealt with in Sections 5.2 and 5.3. In Section 5.4, the stability properties of the three-dimensional branch orbits are briefly discussed, and the chapter is concluded with some remarks in Section 5.5.

## 5.2 Simply-Symmetric Branches

### 5.2.1 Family $F_{v15}^{1(a)}$

This family of axisymmetric three-dimensional periodic orbits branches from family  $f$  at the vertical self-resonant orbit  $f_{v15}^1$ , for which the initial  $x$ -coordinate, corresponding to the conjunction crossing, is  $s_{01} \approx 0.952$ , the initial  $y$ -velocity  $s_{05} \approx 0.200$ , and the Jacobi constant  $C \approx 3.0044$ . The non-zero initial conditions ( $s_{01}, s_{05}, s_{06}$ ), period  $T$ , Jacobi constant  $C$  and multiplicity  $m$  (half the number of crossings of the  $(x, z)$ -plane in one orbital period) of representative orbits belonging to this branch are listed in Table 5.1. It is seen that as the family branches upward from the plane and the initial  $z$ -velocity ( $s_{06}$ ) increases, the orbits contract inwards towards the primary  $m_2$  ( $s_{01}$  increasing), and the  $y$ -velocity ( $s_{05}$ ) decreases monotonically. The initial velocity vector at the conjunction crossing, decreasing slowly in magnitude, becomes progressively more steeply inclined to the horizontal plane, and this behaviour is maintained as  $s_{05}$  decreases towards zero,  $s_{06}$  increases steadily, the period  $T$  increases, the Jacobi constant increases monotonically and the orbits continue to become smaller. Eventually, the vertical component of velocity  $s_{06}$  reaches a maximum value of about 0.173 and begins to decrease. As  $s_{05}$  passes through zero, one of the loops of the orbit disappears, and the orbital multiplicity is reduced from 5 to 4; then, after a short interval, the final  $y$ -velocity  $s_5$ , corresponding to the opposition crossing of the  $x$ -axis, also passes through zero, this time from negative to positive values, resulting in the disappearance of another loop, and a further reduction in the orbital multiplicity  $m$  from 4 to 3. As we trace the family further, the size of the orbits (indicated by the value of  $s_{01}$ ) continues to decrease, and the angle of inclination of the initial velocity vector also decreases steadily as  $s_{05}$  becomes more and more negative, while  $s_{06}$  continues to become smaller in value. The multiplicity remains unchanged at  $m = 3$  over the remainder of the family as  $s_{06}$  decreases towards zero and the orbits become flatter in character, the sense of orbital motion, originally retrograde with respect to the

Table 5.1: Family  $F_{v15}^{1(a)} / G_{2v13}^{2(a)}$

$s_{01}$	$s_{05}$	$s_{06}$	T	C	m
0.951982	0.199771	0.005	8.527992	3.004444	5
0.952009	0.199526	0.01	8.516937	3.004482	5
0.952116	0.198545	0.02	8.473496	3.004633	5
0.952528	0.194587	0.04	8.311018	3.005226	5
0.954000	0.178091	0.08	7.790756	3.007485	5
0.956194	0.146902	0.12	7.177642	3.011175	5
0.959557	0.084317	0.16	6.521408	3.017354	5
0.962546	0.013698	0.173014	6.126857	3.023174	5
0.963138	-0.001302	0.172406	6.066102	3.024294	4
0.964178	-0.026302	0.169123	5.976432	3.026075	3
0.969812	-0.086302	0.165598	5.717008	3.029878	3
0.973415	-0.116302	0.167475	5.531260	3.031697	3
0.978654	-0.176302	0.160732	5.255900	3.034653	3
0.980581	-0.206302	0.150640	5.159574	3.035809	3
0.983336	-0.261302	0.114048	5.028337	3.037521	3
0.984528	-0.291332	0.073921	4.973970	3.038283	3
0.984849	-0.300254	0.053921	4.959584	3.038491	3
0.985052	-0.306108	0.033921	4.950533	3.038623	3
0.985157	-0.309211	0.013921	4.945854	3.038691	3
0.985177	-0.309783	0.003921	4.944999	3.038704	3

rotating coordinate system, having become direct. The branch terminates back in the horizontal plane at the vertical self-resonant orbit  $g_{2v13}^2$  of family  $g_2$  (one of the two families of direct satellite orbits, denoted  $g_1$  and  $g_2$ , which exist for small values of  $\mu$ , corresponding to family  $g$  of Strömberg's classification in the Copenhagen problem,  $\mu = \frac{1}{2}$ ). This orbit, for which  $a_v = \cos 2\pi/3 = -0.5$ ,  $s_{01} \approx 0.935$ ,  $s_{05} \approx -0.310$  and  $C \approx 3.0387$ , is marked on the characteristic of family  $g_2$  in the  $(x,C)$ -plane in Figure 5.2.

From this identification of the termination orbit of the vertical branch  $F_{v15}^{1(a)}$ , we conclude that the family is also the vertical branch  $G_{2v13}^{2(a)}$  of family  $g_2$ . The choice of designation for the family is arbitrary, since there is no obvious boundary where the two branches meet; there is a kind of "no man's land" segment where a short bridge of quadruple orbits, which cannot be definitely assigned to either branch, joins together the quintuple ( $m = 5$ ) "retrograde" and triple ( $m = 3$ ) "direct" regimes. The safest course would perhaps be to classify the entire family as " $F_{v15}^{1(a)}/G_{2v13}^{2(a)}$ ".

The phenomenon of the direct linking together of two planar families (such as, in this case,  $f$  and  $g_2$ ) by a family of three-dimensional orbits which branches vertically from the two generating families, reported by Zagouras and Markellos (1977), and Zagouras and Kalogeropoulou (1978), in the case of branches arising from vertical-critical ( $a_v = \pm 1$ ) planar orbits, appears to be most common in the general case of bifurcations from vertical self-resonant orbits, and as we shall see, both families of three-dimensional orbits generated from a given vertical self-resonant orbit may terminate in the same planar orbit. All of the families given in this chapter, with a single exception, commence and terminate in the horizontal plane at intersections with planar orbits; a vertical branch may, however, effectively terminate in a three-dimensional orbit without returning to the horizontal plane, as will be seen in the next section.

Typical orbits of the family  $F_{v15}^{1(a)}$  are plotted in Figures A1 - A9, in the Appendix.

### 5.2.2 Family $F_{v15}^{1(p)}$

This is the other member of the pair of branches which bifurcate from the vertical self-resonant orbit  $f_{v15}^1$ , and consists of plane symmetric orbits. Representative orbits of the branch are given in Table 5.2. The branch exhibits generally more complicated behaviour in its development from the bifurcation than any of the other branches discussed in this chapter; the period  $T$  and Jacobi constant  $C$  do not vary monotonically along the branch, both of these parameters possessing two turning points, and the branch has no less than four different multiplicity regimes. The feature of family  $F_{v15}^{1(p)}$  which distinguishes it from the other seven branches given in this chapter, however, is that it effectively terminates in three dimensions, rather than back in the horizontal plane.

The initial condition  $s_{03}$ , which (for plane-symmetric three-dimensional orbits) confers the property of three-dimensionality on the branch orbits, increases monotonically as the branch evolves from its bifurcation with family  $f$ . At the same time,  $s_{05}$  decreases monotonically, although the  $y$ -velocity never becomes negative, so that the branch consists entirely of what might loosely be termed "synodically retrograde" orbits (insofar as the term can be applied to the complicated motion involved in the majority of cases). The initial condition  $s_{01}$  shows a general trend towards higher values, passing through first a maximum and then a minimum in the early stages of the branch. The trends in  $T$  and  $C$  are respectively towards decreased and increased values as the branch evolves, a pattern common to all eight branches under discussion.

The bulk of the orbits of the family retain the initial multiplicity of five; this drops to three, briefly increases to four, and finally decreases again to two. The reductions of two in the multiplicity (from 5 to 3 and from 4 to 2) occur when two loops of the orbit, mirror images of each other with respect to the plane of symmetry (the  $(x,z)$ -plane), migrate away from the plane so that they no longer intersect it. The increase in multiplicity from 3 to 4 occurs through the formation of a cusp in the transition orbit, with its vertex in the plane of symmetry. This cusp occurs at the final epoch when the final  $y$ -velocity  $s_5$  passes through zero from negative to positive values; consequently, at the vertex the instantaneous velocity of the massless particle with respect to the

Table 5.2: Family  $F_{v15}^{1(p)}$

$s_{01}$	$s_{03}$	$s_{05}$	T	C	m
0.952359	0.005	0.199526	8.505618	3.004521	5
0.953530	0.01	0.198536	8.427558	3.004796	5
0.958379	0.02	0.194222	8.117607	3.005996	5
0.956833	0.039158	0.169505	8.985683	3.005174	5 S
0.970833	0.044457	0.161227	8.584528	3.007524	5
0.985833	0.048168	0.150268	8.229079	3.010729	5
0.992672	0.049434	0.143539	8.120409	3.012304	5
1.002156	0.051581	0.129539	8.002749	3.014539	5
1.005978	0.052804	0.121539	7.947346	3.015475	5
1.011451	0.054889	0.107539	7.837344	3.016912	5
1.013858	0.055859	0.100539	7.774735	3.017596	5
1.017957	0.057473	0.087539	7.649209	3.018836	5
1.019708	0.058138	0.081539	7.589944	3.019390	5
1.023205	0.059455	0.068539	7.467896	3.020501	3
1.024923	0.060127	0.061539	7.409845	3.021026	3
1.027838	0.061359	0.048539	7.322457	3.021820	3
1.029281	0.062022	0.041939	7.287356	3.022143	3
1.031590	0.063145	0.029539	7.246401	3.022524	3
1.032321	0.063510	0.025539	7.237926	3.022603	4
1.034422	0.064553	0.013547	7.227158	3.022704	2

coordinate system is zero.

As the branch develops towards the effective termination point in three dimensions, along the final double-periodic ( $m = 2$ ) phase, the two perpendicular crossings of the  $(x,z)$ -plane (that is, the two mirror configurations) move more and more closely together, until they eventually coincide exactly at the termination orbit. This orbit, whose parameters are approximately those given for the last orbit of Table 5.2, is a plane symmetric simple-periodic orbit (multiplicity  $m = 1$ ) described twice, and is a member of a family of such orbits which bifurcates with the branch  $F_{v15}^{1(p)}$  in three dimensions. (The results of a further numerical investigation to identify this family of simple-periodic orbits will be discussed in a later chapter). The intersection orbit of the two families also represents a "point of reflection" of  $F_{v15}^{1(p)}$ , since as we attempt to continue the branch beyond this orbit with any choice of family parameter, we simply retrace the branch in the opposite direction - that is, back towards the starting point in the horizontal plane.

One interesting feature of the family  $F_{v15}^{1(p)}$ , a short interval over which the orbits are distinctly stable, will be described in Section 5.4. Typical orbits of the family are plotted in Figures A10 - A16, in the Appendix.

### 5.2.3 Family $F_{v17}^{1(a)}$

Family  $F_{v17}^{1(a)}$  bifurcates from its generating family  $(f)$  at the vertical self-resonant orbit  $f_{v17}^1$  for which the initial conditions at the conjunction crossing are  $s_{01} \approx 0.966$ ,  $s_{05} \approx 0.208$  and the Jacobi constant  $C \approx 3.0151$ . The general features of this family are very similar to those of the family  $F_{v15}^{1(a)}$  described above. Representative orbits are given in Table 5.3. The branch consists of axisymmetric orbits, the multiplicity being initially  $m = 7$ . As the branch develops from the bifurcation, the sizes of the orbits become smaller ( $s_{01}$  increases) and the initial velocity, decreasing gradually in magnitude, rotates around the  $x$ -axis from the  $(x,y)$ -plane towards the  $(x,z)$ -plane. The period decreases monotonically, and the Jacobi constant increases monotonically from beginning to end of the family. Shortly after the initial  $z$ -component of velocity attains the maximum value  $s_{06} \approx 0.186$ , the  $y$ -component  $s_{05}$  passes through zero from positive to negative values and the

Table 5.3: Family  $F_{v17}^{1(a)} / G_{1v15}^{1(a)}$

$s_{01}$	$s_{05}$	$s_{06}$	T	C	m
0.966244	0.207918	0.005	7.405761	3.015110	7
0.966248	0.207708	0.01	7.403231	3.015130	7
0.966267	0.206867	0.02	7.393133	3.015208	7
0.966342	0.203465	0.04	7.353133	3.015521	7
0.966659	0.189246	0.08	7.198740	3.016810	7
0.967249	0.162700	0.12	6.956258	3.019124	7
0.968262	0.114524	0.16	6.622982	3.023049	7
0.969173	0.066281	0.18	6.377806	3.026683	7
0.969630	0.039683	0.185	6.267931	3.028580	7
0.969953	0.019683	0.186245	6.194281	3.029964	7
0.970259	-0.000317	0.185372	6.127086	3.031314	6
0.970333	-0.005317	0.184819	6.111187	3.031647	5
0.970547	-0.020317	0.182336	6.065443	3.032634	5
0.971295	-0.080317	0.158320	5.906783	3.036443	5
0.971633	-0.119810	0.124564	5.817877	3.038876	5
0.971604	-0.147330	0.079564	5.757591	3.040642	5
0.971229	-0.157420	0.039564	5.728629	3.041462	5
0.971019	-0.158999	0.019564	5.720388	3.041669	5
0.970953	-0.159287	0.009564	5.718166	3.041721	5
0.970936	-0.159349	0.004564	5.717612	3.041734	5

multiplicity changes from 7 to 6 as one of the loops of the orbit disappears. At this point, the final  $y$ -velocity has a small negative value and is approaching zero; as we continue along the family,  $s_5$  also passes through zero and the multiplicity drops from 6 to 5. From here, the initial velocity vector, having passed through the  $(x,z)$ -plane, continues rotating around the  $x$ -axis towards the  $(x,y)$ -plane, but now having a negative  $y$ -component, corresponding to direct orbital motion; the final velocity vector continues rotating in the opposite direction. The orbits now become "flatter" as the branch evolves back towards the horizontal plane, the orbital multiplicity remaining at  $m = 5$ ; just before the family terminates,  $s_{01}$  reaches a maximum value of about 0.972 and starts to decrease. Termination in the horizontal plane occurs at the vertical self-resonant orbit  $g_{1v15}^1$  of family  $g_1$ , for which  $a_v = \cos 2\pi/5 \approx 0.30902$ ,  $s_{01} \approx 0.971$ ,  $s_{05} \approx -0.159$  and  $C \approx 3.0417$ . This orbit is marked on the characteristic of family  $g_1$  in the  $(x,C)$ -plane in Figure 5.2.

We see that family  $F_{v17}^{1(a)}$  acts as a three-dimensional link between the planar families  $f$  and  $g_1$ , and is identical with the vertical branch  $g_{1v15}^{1(a)}$  of family  $g_1$ . Note that branches  $F_{v15}^{1(a)}$  and  $F_{v17}^{1(a)}$  terminate on different planar families,  $g_2$  and  $g_1$  respectively. While both  $g_1$  and  $g_2$  consist of direct satellite orbits around the less massive primary  $m_2$ , they are quite distinct (Markellos et al., 1975a) for all values of the mass parameter except in Hill's case ( $\mu = 0$ ) of the restricted problem, when they intersect (Hénon, 1969).

#### 5.2.4 Family $F_{v17}^{1(p)}$

This is the plane symmetric branch which, together with  $F_{v17_1}^{1(a)}$ , bifurcates from family  $f$  at the vertical self-resonant orbit  $f_{v17}^1$ . Numerical data for the family are given in Table 5.4. As the family branches vertically out of the plane, and the initial  $z$ -coordinate  $s_{03}$  increases, the orbits become smaller ( $s_{01}$  increases) and  $s_{05}$ , the initial  $y$ -velocity, decreases. The multiplicity retains its initial value  $m = 7$  throughout the first part of the branch; the period decreases monotonically and the Jacobi constant increases monotonically over the whole family. The perpendicular crossing of the plane at the initial epoch migrates upwards and towards the primary  $m_2$  (at  $x = 0.99905$ ), and then begins to move back down towards the horizontal plane on the other side of  $m_2$ , that is, the opposition side. Shortly after the extremum in  $s_{03}$

Table 5.4: Family  $F_{v17}^{1(p)} / G_{lv15}^{1(p)}$

$s_{01}$	$s_{03}$	$s_{05}$	T	C	m
0.966260	0.001	0.207973	7.405867	3.015110	7
0.966313	0.002	0.207929	7.403649	3.015127	7
0.966525	0.004	0.207751	7.394761	3.015195	7
0.967118	0.007	0.207254	7.370149	3.015387	7
0.969377	0.013	0.205373	7.278304	3.016130	7
0.971136	0.016	0.203922	7.208931	3.016721	7
0.973431	0.019	0.202045	7.121124	3.017509	7
0.979342	0.024217	0.197311	6.908370	3.019629	7
0.985342	0.027356	0.192654	6.710559	3.021919	7
0.991342	0.029017	0.188152	6.529215	3.024351	7
0.997342	0.029439	0.183815	6.362710	3.026932	7
1.000342	0.029205	0.181714	6.284558	3.028281	7
1.003342	0.028665	0.179662	6.209571	3.029669	5
1.009342	0.026575	0.175737	6.068402	3.032569	5
1.012342	0.024933	0.173894	6.001847	3.034086	5
1.018292	0.019974	0.170676	5.876512	3.037246	5
1.022407	0.013974	0.169591	5.792046	3.039625	5
1.024434	0.007974	0.171352	5.743972	3.041039	5
1.024816	0.004974	0.173296	5.728817	3.041458	5
1.024913	0.001974	0.175150	5.719411	3.041692	5
1.024917	0.000974	0.175489	5.717933	3.041726	5

has been reached, the multiplicity drops from 7 to 5, this value being maintained as the branch evolves towards its termination back in the horizontal plane;  $s_{01}$  continues to increase, while the y-velocity  $s_{05}$  attains a minimum value of about 0.170 and then begins to increase. The branch terminates at the vertical self-resonant orbit  $g_{1v15}^1$  belonging to family  $g_1$ , which, as we have seen, is also the termination orbit of the branch  $F_{v17}^1(a)$ . Comparison of Tables 5.3 and 5.4 shows that although the initial conditions at the beginnings of both the axisymmetric and plane symmetric branches correspond to the conjunction crossing of the vertical bifurcation orbit  $f_{v17}^1$ , the initial conditions at the termination of family  $F_{v17}^1(a)$  correspond to the conjunction crossing of  $g_{1v15}^1$ , while at the termination of family  $F_{v17}^1(p)$  the initial conditions correspond to the opposition crossing of that orbit. This is because the type (A) mirror configurations of the axisymmetric family, constrained to move only along the x-axis, do not pass through the singularity at  $m_2$ , while the type (P) mirror configurations of the plane symmetric family, with two degrees of freedom in the (x,z)-plane, are able to avoid the singularity.

### 5.3 Doubly-Symmetric Branches

#### 5.3.1 Family $F_{v16}^1(c)$

This family is one of the pair of doubly-symmetric branches which bifurcate from family  $f$  at the vertical self-resonant orbit  $f_{v16}^1$ , for which  $a_v = \cos \pi/3 = 0.5$  and the Jacobi constant  $C \approx 3.0103$ . The two mirror configurations of this orbit are given by

$$\begin{aligned} s_{01} &\approx 0.961, & s_{05} &\approx 0.203 & (\text{conjunction crossing}) \\ s_{01} &\approx 1.038, & s_{05} &\approx -0.202 & (\text{opposition crossing}). \end{aligned}$$

The orbits of family  $F_{v16}^1(c)$  are those which have their type (A) (on-axis) mirror configuration at conjunction, and the other member of the pair,  $F_{v16}^1(o)$ , comprises those orbits which have their axis-crossings at opposition. The initial conditions of representative orbits of family  $F_{v16}^1(c)$  given (together with the other parameters) in Table 5.5, are those for the type (A) mirror configurations of the orbits.

The behaviour of the initial conditions ( $s_{01}, s_{05}, s_{06}$ ) as the family evolves from the bifurcation is very similar to that exhibited by the initial conditions of the branches  $F_{v15}^1(a)$  and  $F_{v17}^1(a)$ . As the initial

Table 5.5: Family  $F_{v16}^{1(c)} / G_{2v14}^{2(c)}$

$s_{01}$	$s_{05}$	$s_{06}$	T	C	m
0.960903	0.202786	0.005	7.768097	3.010288	6
0.960912	0.202563	0.01	7.763612	3.010314	6
0.960949	0.201669	0.02	7.745780	3.010414	6
0.961095	0.198055	0.04	7.676075	3.010816	6
0.961705	0.182945	0.08	7.419880	3.012447	6
0.962793	0.154532	0.12	7.051156	3.015313	6
0.964290	0.110066	0.155	6.652516	3.019381	6
0.965770	0.057581	0.175	6.334946	3.023697	6
0.966509	0.027342	0.178983	6.196464	3.026002	6
0.966890	0.010568	0.179040	6.129494	3.027233	6
0.967344	-0.010570	0.176928	6.053228	3.028740	4
0.967729	-0.029511	0.172892	5.991444	3.030054	4
0.968179	-0.052960	0.164851	5.922218	3.031634	4
0.968547	-0.073149	0.154851	5.868134	3.032958	4 S
0.969324	-0.117005	0.119851	5.765421	3.035716	4 S
0.976955	-0.198339	0.082300	5.553752	3.038516	4 S
0.978980	-0.228014	0.04	5.470898	3.039450	4 S
0.979326	-0.233753	0.02	5.456139	3.039621	4 S
0.979408	-0.235142	0.01	5.452629	3.039662	4 S
0.979431	-0.235528	0.004	5.451658	3.039673	4 S

z-velocity  $s_{06}$  increases to a maximum value of about 0.179,  $s_{01}$  increases steadily, with the result that the overall sizes of the orbits become smaller, and  $s_{05}$  decreases monotonically, passing through zero after the maximum in  $s_{06}$ , and assuming negative values. Associated with the change of sign of the initial y-velocity, there is a drop in the orbital multiplicity from 6 to 4, through the simultaneous disappearance of two loops cutting the (x,z)-plane, which, because of the double symmetry of the orbits, are mirror images of one another in that plane. The orbital symmetry remains  $m = 4$  as the branch evolves back towards the horizontal plane,  $s_{01}$  continuing to increase and  $s_{05}$  becoming more negative. As usual, the period is monotonic decreasing, and the Jacobi constant monotonic increasing. The branch terminates in the horizontal plane at the vertical self-resonant orbit  $g_{2v14}^2$  of family  $g_2$ , for which  $a_v = 0$ ,  $s_{01} \approx 0.979$ ,  $s_{05} \approx -0.236$  and  $C \approx 3.0310$ ; we therefore conclude that the vertical branches  $F_{v16}^1(c)$  and  $G_{2v14}^2(c)$  are identical. The termination orbit  $g_{2v14}^2$  is marked on the characteristic of family  $g_2$  in the (x,C)-plane in Figure 5.2.

Typical orbits of family  $F_{v16}^1(c)$  are plotted in Figures A17 - A22, in the Appendix.

### 5.3.2 Family $F_{v16}^1(o)$

This is the other member of the pair of branches of doubly-symmetric orbits bifurcating from family  $f$  at  $f_{v16}^1$ . The initial conditions corresponding to the perpendicular crossing of the x-axis (occurring at opposition throughout the branch) and other parameters of representative orbits are given in Table 5.6. The orbital multiplicity, initially  $m = 6$ , drops to  $m = 4$  as the initial y-velocity  $s_{05}$  passes through zero from negative to positive values. The maximum value of  $s_{06}$ , approximately 0.178, is very nearly the same as that for family  $F_{v16}^1(c)$ , and is attained just before the multiplicity change. The multiplicity remains quadruple as  $s_{06}$  decreases;  $s_{01}$  reaches a minimum value of about 1.030 and starts to increase, and the branch eventually terminates back in the (x,y)-plane at the vertical self-resonant orbit  $g_{2v14}^2$ , the initial conditions corresponding to the opposition crossing of the x-axis.

We conclude that the pair of branches  $F_{v16}^1(c)$  and  $F_{v16}^1(o)$  not only

Table 5.6: Family  $F_{v16}^{1(o)} / G_{2v14}^{2(o)}$

$s_{01}$	$s_{05}$	$s_{06}$	T	C	m
1.037500	-0.201469	0.003632	7.768784	3.010285	6
1.037478	-0.201174	0.010909	7.762293	3.010321	6
1.037404	-0.200162	0.021919	7.740325	3.010445	6
1.037168	-0.196806	0.040779	7.670487	3.010849	6
1.036220	-0.181203	0.082771	7.394357	3.012624	6
1.035071	-0.156718	0.118252	7.069467	3.015152	6
1.033255	-0.100918	0.160394	6.583780	3.020217	6
1.032780	-0.081762	0.168295	6.463212	3.021809	6
1.032321	-0.061049	0.174096	6.349708	3.023468	6
1.031877	-0.038705	0.177471	6.242791	3.025197	6
1.031447	-0.014654	0.177948	6.142026	3.026998	6
1.031030	0.011181	0.174840	6.047014	3.028871	4
1.030724	0.031774	0.169549	5.979317	3.030325	4
1.030425	0.053441	0.161001	5.914524	3.031821	4
1.029780	0.108779	0.120015	5.772498	3.035518	4
1.033248	0.111504	0.080294	5.670506	3.037257	4
1.036641	0.105860	0.040743	5.513805	3.038963	4
1.037492	0.104951	0.019207	5.465535	3.039512	4
1.037667	0.104783	0.010102	5.455374	3.039630	4
1.037713	0.104740	0.005605	5.452675	3.039662	4

originate from the same vertical bifurcation orbit of family  $f$ , but also terminate at the same orbit of family  $\mathcal{E}_2$ ; we can also identify  $F_{v16}^{1(o)}$  with the branch  $G_{2v14}^{2(o)}$ . As usual, the period is a monotonic decreasing function and the Jacobi constant monotonic increasing along the branch, in the direction from  $f$  to  $\mathcal{E}_2$ .

Typical orbits of family  $F_{v16}^{1(o)}$  are plotted in Figures A23 and A24, in the Appendix.

### 5.3.3 Family $F_{v18}^{1(c)}$

This family has many characteristics in common with  $F_{v16}^{1(c)}$ . It is one of the pair of doubly-symmetric branches bifurcating from family  $f$  at  $f_{v18}^1$ , for which  $a_v = \cos \pi/4 \approx 0.70711$  and  $C \approx 3.0194$ , the perpendicular crossings of the x-axis being given by

$$\begin{aligned} s_{01} &\approx 0.970, & s_{05} &\approx 0.214 & (\text{conjunction}), \\ s_{01} &\approx 1.028, & s_{05} &\approx -0.213 & (\text{opposition}). \end{aligned}$$

As indicated by the superscript (c), the branch with which we are concerned here is the one whose orbits all intersect the x-axis at conjunction; numerical data for the family are given in Table 5.7. The usual pattern of behaviour of the initial conditions is found in the development of the family:  $s_{05}$  decreases monotonically from positive to negative values, a drop in the multiplicity from 8 to 6 occurring as the sign of the y-velocity changes;  $s_{06}$  rises to a maximum of 0.194 just before this happens, and then decreases towards zero. The resulting rotation of the initial velocity vector through half a revolution about the x-axis from beginning to end of the family changes the sense of motion from synodically retrograde to direct (although these terms can be applied meaningfully only to orbits at either end of the branch, where the motion is more nearly confined to a common plane). The initial condition  $s_{01}$  increases to a maximum value of about 0.974 just before the branch terminates, and then decreases slightly. The familiar monotonic behaviour of the period and Jacobi constant is apparent. The branch terminates at the vertical self-resonant orbit  $\mathcal{E}_{1v16}^1$  of family  $\mathcal{E}_1$ , for which  $a_v = \cos \pi/3 = 0.5$ , the Jacobi constant  $C \approx 3.0447$ , and the conjunction crossing is given by  $s_{01} \approx 0.974$ ,  $s_{05} \approx -0.173$ . Family  $F_{v18}^{1(c)}$  is therefore identical to the vertical branch  $G_{1v16}^{1(c)}$  of  $\mathcal{E}_1$ . The termination orbit  $\mathcal{E}_{1v16}^1$  is marked on the characteristic of family  $\mathcal{E}_1$  in Figure 5.2.

Table 5.7: Family  $F_{v18}^{1(c)} / G_{1v16}^{1(c)}$

$s_{01}$	$s_{05}$	$s_{06}$	T	C	m
0.969965	0.213616	0.005	7.188209	3.019407	8
0.969968	0.213416	0.01	7.186556	3.019423	8
0.969979	0.212616	0.02	7.179954	3.019487	8
0.970025	0.209384	0.04	7.153648	3.019745	8
0.970218	0.195906	0.08	7.049825	3.020811	8
0.970580	0.170971	0.12	6.879715	3.022734	8
0.971207	0.127298	0.16	6.635554	3.025953	8
0.971727	0.089138	0.18	6.463596	3.028622	8
0.972165	0.054864	0.19	6.333291	3.030919	8
0.972689	0.010452	0.193566	6.190106	3.033770	8
0.972914	-0.010152	0.191774	6.131537	3.035051	6
0.973024	-0.020647	0.19	6.103327	3.035694	6
0.973355	-0.054550	0.18	6.018741	3.037734	6
0.973671	-0.091943	0.16	5.935203	3.039927	6
0.973932	-0.134017	0.12	5.850409	3.042355	6
0.973991	-0.157386	0.08	5.805840	3.043716	6
0.973970	-0.169632	0.04	5.782423	3.044451	6
0.973957	-0.172506	0.02	5.776826	3.044629	6
0.973952	-0.173213	0.01	5.775439	3.044673	6
0.973951	-0.173389	0.005	5.775093	3.044684	6

### 5.3.4 Family $F_{v18}^{1(o)}$

This the family of doubly-symmetric orbits starting from the x-axis at opposition, and together with  $F_{v18}^{1(c)}$  forms the pair of branches bifurcating from family  $f$  at the vertical self-resonant orbit  $f_{v18}^1$ . Representative orbits are listed in Table 5.8. Owing to the fact that both branches consist of relatively small orbits about  $m_2$ , they are almost mirror images of one another with respect to the plane passing through  $m_2$ , parallel to the (y,z)-plane, and this is apparent in the comparison of the various orbital parameters listed in Tables 5.7 and 5.8. It can be seen from Figure 5.1 that as the branch multiplicity  $m$  increases and  $a_v$  approaches unity, the vertical bifurcation orbits become smaller and, as a result, more nearly symmetrical with respect to the axis passing through  $m_2$ , parallel to the y-axis. This special kind of symmetry is characteristic of Hill's problem, which is a fairly good approximation in the case of small orbits about  $m_2$ , for small values of the mass parameter  $\mu$  (see, e.g. Hénon, 1969, 1970). We would therefore expect that the two members of a pair of doubly-symmetric branches be more nearly symmetrical to one another as the multiplicity  $m$  increases.

The initial z-velocity  $s_{06}$  for family  $F_{v18}^{1(o)}$  has a maximum value of about 0.193 (compared with 0.194 for  $F_{v18}^{1(c)}$ ); after this value is attained,  $s_{05}$  passes through zero, and the multiplicity is reduced from 8 to 6. Throughout the branch,  $s_{01}$ ,  $T$  and  $C$  all vary monotonically. The branch terminates at the same orbit,  $g_{1v16}^1$ , as its "twin"  $F_{v18}^{1(c)}$ ; thus the three pairs of branches of family  $f$  of initial multiplicities 6, 7 and 8 form twofold connections between three vertical self-resonant orbits of family  $f$  ( $f_{v16}^1, f_{v17}^1, f_{v18}^1$ ) and the three vertical self-resonant orbits  $g_{2v14}^2, g_{1v15}^1, g_{1v16}^1$  belonging to families  $g_2$  and  $g_1$ .

### 5.4 Stability of Branch Orbits

In this section we deal briefly with the stability of the three-dimensional orbits belonging to the eight vertical branches of family  $f$  given in Sections 5.2 and 5.3. For each orbit, the stability indices  $p$  and  $q$  defined in Section 3.4 were calculated from the equations

$$p = \frac{1}{2} (\alpha + \sqrt{\Delta}) \quad ; \quad q = \frac{1}{2} (\alpha - \sqrt{\Delta}) \quad , \quad (5.3)$$

Table 5.8: Family  $F_{v18}^{1(o)} / G_{1v16}^{1(o)}$

$s_{01}$	$s_{05}$	$s_{06}$	T	C	m
1.028278	-0.212692	0.005	7.188201	3.019407	8
1.028273	-0.212500	0.01	7.186528	3.019423	8
1.028254	-0.211730	0.02	7.179844	3.019488	8
1.028180	-0.208619	0.04	7.153270	3.019749	8
1.027891	-0.195597	0.08	7.049182	3.020818	8
1.027424	-0.171335	0.12	6.880437	3.022726	8
1.026854	-0.135225	0.155135	6.673746	3.025409	8
1.026348	-0.096225	0.177582	6.492206	3.028151	8
1.025908	-0.056225	0.189787	6.337656	3.030838	8
1.025709	-0.036225	0.192514	6.269615	3.032141	8
1.025520	-0.016225	0.193155	6.206672	3.033421	8
1.024340	0.003775	0.191739	6.148217	3.034679	6
1.024996	0.043775	0.182521	6.042852	3.037135	6
1.024610	0.088775	0.160395	5.939737	3.039803	6
1.024190	0.132711	0.121170	5.852337	3.042298	6
1.023876	0.158774	0.081170	5.806242	3.043704	6
1.023658	0.173219	0.041170	5.782597	3.044446	6
1.023598	0.176794	0.021170	5.776967	3.044624	6
1.023581	0.177715	0.011170	5.775530	3.044670	6
1.023577	0.177962	0.006170	5.775146	3.044682	6

where

$$\begin{aligned} \Delta &= \alpha^2 - 4(\beta - 2) \\ \alpha &= 2 - \text{Tr}(M) \\ \beta &= \frac{1}{2} (\alpha^2 + 2 - \text{Tr}(M^2)) \end{aligned} \quad (5.4)$$

and  $M$  is the monodromy matrix of the variational matrix  $V$ , that is,  $M = V(T)$  (e.g. Bray and Goudas, 1967). The relations given in Section 4.2 were used to compute  $V(T)$  in terms of  $V(T/2)$  (for the simply-symmetric orbits) or  $V(T/4)$  (for the doubly-symmetric branches).

The results of the stability calculations indicated that the vertical branch orbits are mostly unstable, although there exist intervals where the stability criterion

$$\left. \begin{aligned} \Delta &\geq 0 \\ |p| &\leq 2 \\ |q| &\leq 2 \end{aligned} \right\} \quad (5.5)$$

is marginally satisfied: that is, both stability parameters are real ( $\Delta \geq 0$ ), one being distinctly within the stable zone between the values -2 and +2, while the other is very close to either limit of this zone. Since no numerical checks were made on the accuracy of calculation of the stability indices, such cases of marginal stability are somewhat uncertain, and in Tables 5.1 - 5.8 only those orbits which appear to be definitely stable have been marked with the letter "S". The absence of the letter S from a given entry should not, therefore, be taken to imply that the corresponding orbit is necessarily unstable, although any stable orbits not so marked would possess marginal (very nearly critical) stability. Orbits of all eight branches involving significant departures from the horizontal plane, indicated by large values of  $s_{03}$  or of  $s_{06}$ , were found to be definitely unstable, the degree of instability (as indicated by the values of the stability indices) tending to increase with increasing orbital inclination to the horizontal plane.

The only two of the eight branches containing definitely stable orbits, as indicated in the tables, are  $F_{v15}^{1(p)}$  and  $F_{v16}^{1(c)}$  (Tables 5.2 and 5.5). In the latter case, the stability is still somewhat marginal:  $q$  is never further from the critical value of -2 than -1.995. In the

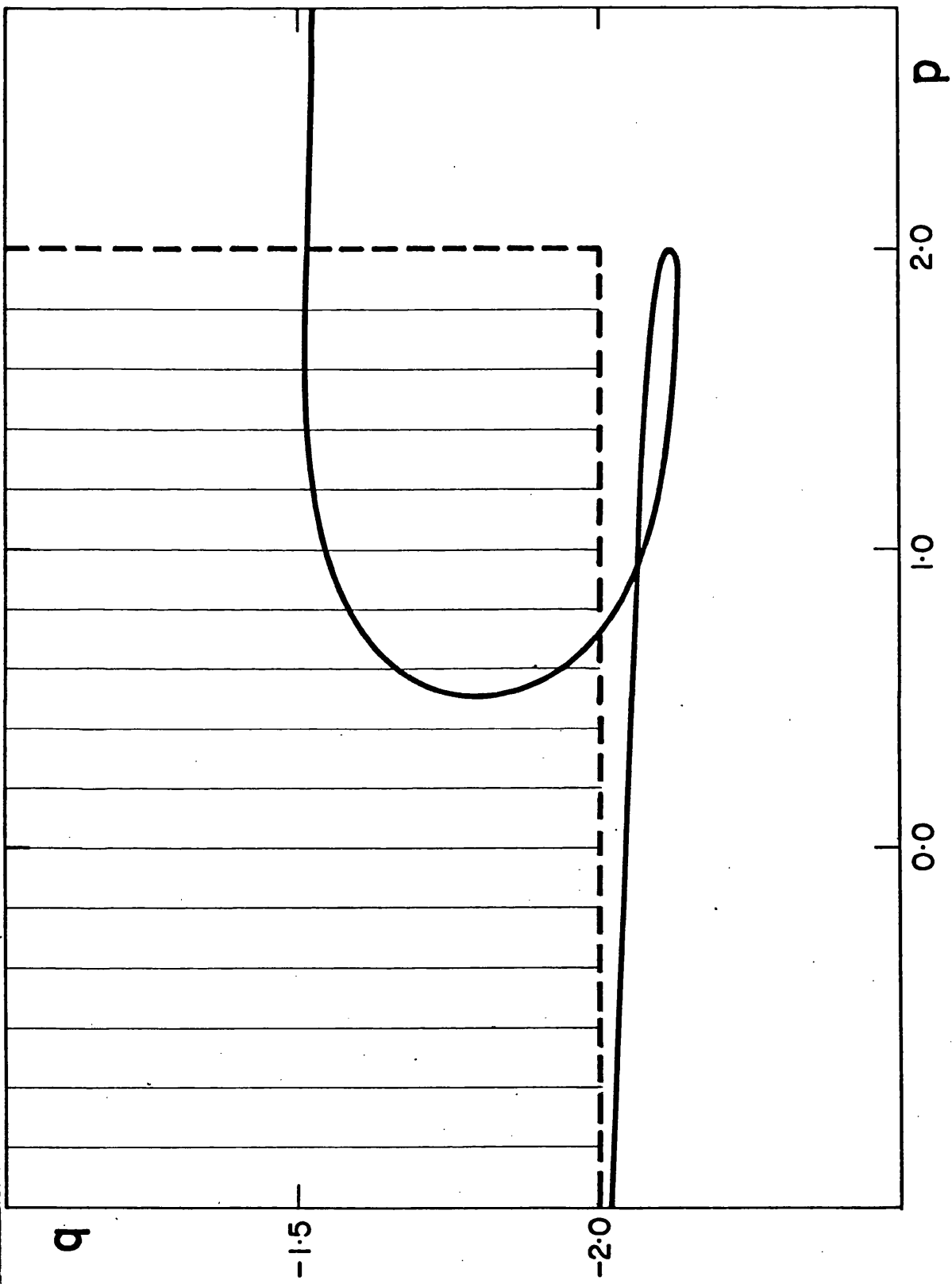


Figure 5.3 : Stability curve in the  $(p,q)$ -plane of part of the vertical branch  $F_{v15}^1(p)$  containing distinctly stable orbits. The hatching marks part of the stable region defined by  $|p| < 2$ ,  $|q| < 2$ .

former case, the short segment of definitely stable orbits, represented by a single orbit in Table 5.2, has been surveyed in greater detail, and a plot of  $q$  against  $p$  for a part of family  $F_{v15}^1(p)$  including the stable segment is given in Figure 5.3. In this figure, the hatching indicates the part of the  $(p,q)$ -plane in which the stability criterion (5.5) is satisfied.

In conclusion, it would appear that the vertical branches of family  $f$  are, for the most part, unstable, although the instability is often mild, particularly near the beginning and end of a branch where the orbits are moderately inclined to the horizontal, and cases of nearly-critical values of either  $p$  or  $q$  (or both) are very common. The general trend towards greater instability as the orbits become more inclined to the horizontal plane is in agreement with previous work, such as that of Halioulis et al. (1976).

### 5.5 Remarks

(1) The following table lists the vertical self-resonant orbits of families  $f$ ,  $g_1$  and  $g_2$  at which the vertical branches of family  $f$  discussed in this chapter commence and terminate:

Table 5.9

Branch	Starting Orbit	Termination Orbit
$F_{v15}^1(a)$	$f_{v15}^1$	$g_{2v13}^2$
$F_{v16}^1(c), F_{v16}^1(o)$	$f_{v16}^1$	$g_{2v14}^2$
$F_{v17}^1(a), F_{v17}^1(p)$	$f_{v17}^1$	$g_{1v15}^1$
$F_{v18}^1(c), F_{v18}^1(o)$	$f_{v18}^1$	$g_{1v16}^1$

Recalling that the vertical branch orbits in the neighbourhood of a simple-periodic vertical bifurcation orbit  $f_{vnm}^1$  have multiplicity  $m$ , we see from this table (and from Tables 5.1 - 5.8) that the multiplicity of the termination orbit of family  $g_1$  or  $g_2$  is two less than that of the starting orbit of family  $f$ . This pattern has been found to apply also to higher-multiplicity branches of family  $f$  not discussed in this chapter,

and appears to be a general feature of the three-dimensional branches which connect the retrograde family  $f$  with the direct families  $\mathcal{E}_1$  and  $\mathcal{E}_2$ .

(2) As can also be seen from Table 5.9, the multiplicity 5 and 6 branches of family  $f$  (with the exception of  $F_{v15}^1(p)$  terminate on  $\mathcal{E}_2$ , while those of multiplicity 7 and 8 terminate on  $\mathcal{E}_1$ . Figure 5.2 shows that this sequence of termination orbits occurs in the sense of increasing values of the Jacobi constant  $C$ , the jump between families  $\mathcal{E}_2$  and  $\mathcal{E}_1$  taking place in the vicinity of the narrow "neck" where the two family characteristics in the  $(x, C)$ -plane approach most closely (and where the two curves actually intersect in Hill's case,  $\mu = 0$ ). There seems to be a general trend in the termination points of vertical branches of  $f$  in the vicinity of the primary  $m_2$ , indicated by the four multiplicity cases given here, whereby those (higher-multiplicity) branches starting from the neighbourhood of  $f_{v15}^1$  and  $f_{v16}^1$  connect with  $\mathcal{E}_2$ , while those beyond  $f_{v17}^1$  end up on  $\mathcal{E}_1$ .

(3) As many authors have pointed out, the circular restricted problem may not be an adequate model for studies of certain astronomical systems, such as the Earth-Moon or outer Jovian satellite systems, in which the non-zero eccentricity of the orbit of the primaries may have important dynamical consequences, particularly with regard to capture and escape mechanisms. It may therefore be desirable to investigate such systems in the framework of the elliptic restricted problem. The determination of vertical branches in the circular problem is a useful starting point for finding symmetric periodic orbits in the three-dimensional elliptic problem, for these branches contain infinite numbers of isolated orbits whose periods are commensurable with the period of the primaries, and can therefore be continued into the elliptic problem, with either the mass parameter  $\mu$  or eccentricity  $e$  of the primaries as family parameter. This possibility will be discussed in Chapter 6, and results obtained by this method, using commensurable orbits of the vertical branches of family  $f$  will be presented.

(4) It should be emphasised that the generation of families of three-dimensional periodic orbits from the vertical-critical ( $a_v = 1$ ) orbits of simple-periodic planar families is a special case providing the simpler form of three-dimensional periodic orbits, namely the cases of multiplicity 1 or 2, and these forms occur in a finite and relatively

small number of instances. In this thesis we have described the mechanism of generation of three-dimensional periodic orbits in the general case where the generating planar orbit is vertical self-resonant and the multiplicity of the resulting orbits can be any integer  $m > 2$ . The work presented in this chapter exemplifies the behaviour of the great abundance of the three-dimensional periodic orbits of the circular restricted problem; for, even if we confine ourselves to the vertically stable segments of simple-periodic (one-revolution) planar families, there are many infinities of families of three-dimensional periodic orbits of arbitrary multiplicity that can be found to arise as a result of vertical bifurcation, in the way described, by taking sufficiently large values of the integers  $m$  and  $n$  in Equation (5.1).

(5) Because the equations of motion of the restricted three-body problem are symmetrical with respect to the horizontal plane, any solution  $(x(\theta), y(\theta), z(\theta))$  always has a mirror image  $(x(\theta), y(\theta), -z(\theta))$  in that plane. In particular, any vertical branch always has a "mirror image" consisting of orbits which are the images under reflection in the  $(x,y)$ -plane of the orbits belonging to the first branch. The existence of pairs of vertical branches resulting from this symmetry of the problem is quite different to the occurrence of pairs of branches arising from vertical self-resonant orbits due to the vanishing of pairs of elements of the matrix  $V_v$ ; thus we should really speak of pairs of branches generated from vertical-critical orbits, and sets of four branches arising in the more general type of vertical bifurcation orbit. The expression "termination orbit" has been employed in this chapter to mean the planar orbit at which a three-dimensional family generated from a vertical bifurcation again intersects a planar family, although this is not strictly a termination of the family in the sense that it is possible to continue beyond it; the orbits thus obtained belong to the "mirror image" branch.

(6) The linking together of distinct families of planar periodic orbits via bifurcating families of three-dimensional orbits appears to be a rather common feature; examples of this behaviour of vertical branches have been given by Zagouras and Markellos (1977) and by Zagouras and Kalogeropoulou (1978), in the case of the planar families  $\ell$  and  $m$ . The results of Sections 5.2 and 5.3 establish a "three-dimensional" link between families of retrograde and direct orbits in the plane, in addition to the "planar" link (involving periodic orbits of Poincaré's second kind) established by Schmidt (1972).

## 6. CONTINUATION OF PERIODIC ORBITS FROM THE CIRCULAR INTO THE ELLIPTIC RESTRICTED PROBLEM

### 6.1 Introduction

In previous chapters, we have considered the continuation of periodic orbits of the planar restricted problem into the more general three-dimensional case, through the phenomenon of vertical bifurcation. In this chapter, we shall examine the continuation, for fixed values of the mass parameter  $\mu$ , of periodic orbits of the circular case of the restricted problem into the elliptic case, the eccentricity of the primaries being increased from zero to non-zero values. The possibility of these two types of continuation is of key importance in the structure of symmetric periodic orbits of the restricted problem; both methods of continuation allow the extensive results of explorations of periodic motion in the planar circular restricted problem to be generalised, resulting in an improved correspondence with actual physical problems.

It was shown in Chapter 2 that every member of a family of periodic orbits of the elliptic restricted problem (an "elliptic family") has the same period,  $T$  say, which must satisfy

$$T = 2k\pi \quad (6.1)$$

for some positive integer  $k$ . In the case of a family parametrised by the eccentricity  $e$  of the primaries, the orbit corresponding to the value  $e = 0$  (if such an orbit exists) is a periodic orbit of the circular restricted problem, with period equal to an integer multiple of the period of the primaries. In general, the  $e = 0$  orbit of the elliptic family may be equivalent to an  $n$ -fold description of an orbit of the circular problem (of basic period  $T_0$ , say) where  $n$  is again a positive integer; thus,  $T = nT_0$ , and from Equation (6.1) we have the "commensurability condition"

$$T_0 = 2\pi k/n \quad (6.2)$$

for the continuation of a periodic orbit of the circular problem into the elliptic problem. In order to ensure that  $T$  is the basic period of the starting orbit of the elliptic family and not an integer multiple thereof,

we require that the integers  $k$  and  $n$  be mutually prime; the value of  $T_0$  given by Equation (6.2) will be referred to as the  $k/n$  commensurability. Equation (6.2) can be regarded as a bifurcation condition, in the sense that those orbits of the circular problem with periods satisfying the commensurability condition may be continued into the elliptic problem, periodicity being preserved as  $e$  is increased from zero to non-zero values. Thus, a commensurable orbit of the circular problem is the intersection of a family of periodic orbits of the circular problem with a family of the elliptic case, just as a vertical self-resonant orbit is the intersection of a family of planar orbits with a family of three-dimensional orbits. (In fact, as we shall see, just as a vertical self-resonant orbit gives rise to a pair of vertical branches, two families of periodic orbits of the elliptic problem can always be generated by continuation from a commensurable orbit of the circular problem).

The continuation of a commensurable periodic orbit can be effected in the particular case of symmetric orbits by means of the linear predictor algorithm, described in Chapter 4, for the determination of families of periodic orbits of the elliptic problem. The  $e = 0$  orbit of the elliptic family has non-zero initial conditions ( $s_{01}, s_{05}, s_{0i}$ ) identical to those for the commensurable orbit of the circular case, and the changes ( $\Delta s_{01}, \Delta s_{05}, \Delta s_{0i}$ ) in these quantities corresponding to an increment  $\Delta e$  in the primary eccentricity are given, to first order in  $e$ , by the matrix equation

$$\begin{pmatrix} v_{21} & v_{25} & v_{2i} \\ v_{41} & v_{45} & v_{4i} \\ v_{j1} & v_{j5} & v_{ji} \end{pmatrix} \begin{pmatrix} \Delta s_{01} \\ \Delta s_{05} \\ \Delta s_{0i} \end{pmatrix} = -\Delta e \begin{pmatrix} v_{2e} \\ v_{4e} \\ v_{je} \end{pmatrix}. \quad (6.3)$$

The values of the subscripts  $i$  and  $j$  depend on the types of mirror configurations occurring at the initial ( $\theta = \theta_0$ ) and final ( $\theta = \theta_1$ ) epochs, as in Table 3.1. The  $v$ 's appearing on both sides of Equation (6.3) are evaluated at  $\theta = \theta_1$  on the  $e = 0$  orbit, where  $\theta_1 = \theta_0 + T/2$  in the case of an orbit of simple symmetry, and  $\theta_1 = \theta_0 + T/4$  for a doubly-symmetric orbit. (The question of symmetry properties will be considered in more detail in a later section). As long as the matrix appearing on the left-hand side of Equation (6.3) is non-singular, the system of equations can be solved and continuation to non-zero values of  $e$  is therefore possible.

The simplest type of commensurability is that for which  $n = 1$ , so that  $T_0 = 2k\pi$  for some positive integer  $k$ , and the  $e = 0$  orbit of the elliptic family is identical to the commensurable orbit of the circular case, described once. In this special case, the elements of the matrix on the left-hand side of Equation (6.3) have the same values as in Equation (4.35); this shows that the matrix is singular only at an extremum in the orbital period along the family of periodic orbits of the circular restricted problem ("circular family") to which the commensurable orbit belongs. The numerical continuation of commensurable periodic orbits of the circular problem in the case  $n = 1$  has been investigated by Broucke (1968,1969) (planar periodic orbits) and by Katsiaris (1973) (three-dimensional periodic orbits).

The most general type of commensurability is that for which  $n$  may have any positive integer value, and the  $e = 0$  orbit of the elliptic family is equivalent to the commensurable orbit of the circular family described  $n$  times. The argument stated above for the case  $n = 1$  is easily generalised to values of  $n$  greater than unity, since an orbit of basic period  $T^*$ , say, also has period  $nT^*$ ; thus the condition for the continuation of a commensurable periodic orbit of the circular restricted problem is that its period does not correspond to a maximum or minimum value along the family to which it belongs. Shelus and Kumar (1970) and Shelus (1972) have done some preliminary work on the continuation of commensurable periodic orbits into the planar elliptic restricted problem, both in the case  $n = 1$  and for  $n > 1$ , starting with circular orbits of the restricted two-body problem ( $\mu = 0$ ), and increasing the mass parameter, as well as the eccentricity of the primaries, from zero to non-zero values. Markellos (1975) has given some examples of the continuation of periodic orbits of the second generation into the planar elliptic problem.

It is our object in the remainder of this chapter to consider the continuation of commensurable symmetric periodic orbits of both the planar and three-dimensional cases of the restricted problem, for commensurabilities  $k/n$  where  $k$  and  $n$  are arbitrary positive integers; we shall deal particularly with symmetry properties and the classification of families of periodic orbits obtained by numerical continuation into the elliptic problem. The case of planar orbits is discussed in Section 6.2, and three-dimensional orbits in Section 6.3. Numerical results to illustrate the discussion are given in Section 6.4, with an

example of the continuation into the elliptic problem of each category of commensurable, symmetric periodic orbits. A number of concluding remarks are presented in Section 6.5.

## 6.2 Planar Orbits

In this section, we shall consider the continuation into the elliptic restricted problem of symmetric, planar periodic orbits of the circular restricted problem, commensurable in period with the period of the primaries; that is, with period  $T_0$  satisfying Equation (6.2). As already stated, the integer  $n$  in the commensurability condition may have any positive value. It is assumed throughout this chapter that the mass parameter  $\mu$  is kept fixed, the commensurable orbit being continued into the elliptic case ( $e > 0$ ), resulting in a family of periodic orbits parametrised by the eccentricity of the primaries; however, as we shall see in Chapter 7, the same conclusions with regard to symmetry and classification are arrived at if the mass parameter is allowed to vary and another orbital parameter (the vertical stability index  $a_v$ ) is fixed in value instead.

Let us as usual denote the two distinct mirror configurations of a planar periodic orbit of the circular problem by  $C_0$  and  $C_1$ ; the interval between successive mirror configurations is equal to half the (basic) orbital period  $T_0$ . Now if the period  $T_0$  is commensurable, satisfying Equation (6.2), this orbit, as we have already seen, if described  $n$  times, is a symmetric periodic orbit of the planar elliptic restricted problem for zero eccentricity of the primaries. Successive mirror configurations in this orbit of the elliptic problem occur at intervals of

$$nT_0/2 = k\pi. \quad (6.4)$$

This form of Equation (6.2) shows that the massless particle makes perpendicular crossings of the  $x$ -axis at the instants when the primaries are at one or other apse in their elliptic orbit, as required by the "strong periodicity criterion".

In order to continue the  $e = 0$  orbit to some small non-zero value of the eccentricity of the primaries, either of the two perpendicular intersections of the orbit with the  $x$ -axis can be chosen as the starting point of the massless particle, while the primaries may be initially at either periapsis ( $\theta_0 = 0$ ) or at apoapsis ( $\theta_0 = \pi$ ). The initial state of the

system is therefore one of four possible mirror configurations, which we denote by  $C_0^\pi$ ,  $C_0^\alpha$ ,  $C_1^\pi$  and  $C_1^\alpha$ , the " $\pi$ " and " $\alpha$ " superscripts indicating that the primaries are at periapsis and apoapsis, respectively. The next mirror configuration occurs when the true anomaly of the primaries is

$$\theta = \theta_0 + k\pi = \theta_0 + nT_0/2; \quad (6.5)$$

at this final epoch, the primaries will have performed  $k/2$  revolutions in their elliptic orbit, while the massless particle will have followed an orbit which (for sufficiently small  $e$ ) is essentially  $n/2$  descriptions of the commensurable orbit of the circular problem. The final mirror configuration must also be one of the four possible kinds listed above; the relationship between the initial and final types of mirror configuration depends solely on the values of  $k$  and  $n$ , and in particular on their evenness or oddness, as shown in Table 6.1.

Table 6.1

Case	k	n	Mirror Configuration Occurring at:		
			Initial Epoch	Final Epoch	
1	even	odd	(a)	$C_0^\pi$	$C_1^\pi$
			(b)	$C_0^\alpha$	$C_1^\alpha$
2	odd	odd	(a)	$C_0^\pi$	$C_1^\alpha$
			(b)	$C_0^\alpha$	$C_1^\pi$
3	odd	even	(a)	$C_0^\pi$	$C_0^\alpha$
			(b)	$C_1^\pi$	$C_1^\alpha$

The last two columns of Table 6.1 are interchangeable, since the two distinct mirror configurations defining a symmetric planar periodic orbit occur alternately and either may be taken to be the initial state of the system. In each of the three cases listed in the table, there are two and only two different ways of continuing a commensurable orbit of the planar circular problem into the elliptic problem, resulting in exactly two distinct families of periodic orbits as  $e$  is increased from zero to non-zero values.

In his paper on the stability of periodic orbits in the (planar) elliptic restricted three-body problem, Broucke (1969) stated that "for every symmetric periodic orbit with  $e = 0$ , there are two ways of prolongating it to the elliptic problem". Broucke distinguished between the two resulting families of periodic orbits of the elliptic problem ("elliptic families") according to whether the initial states of the orbits correspond to periapsis ( $\theta_0 = 0$ ) or apoapsis ( $\theta_0 = \pi$ ) of the primaries, and referred to "periapsis orbits" and "apoapsis orbits". Examination of Table 6.1 shows that Broucke's classification is applicable in Cases 1 and 2 (that is, for odd values of  $n$ ) since it is possible to distinguish between the different types of orbits according to the state of the primaries at the initial epoch, if the massless particle is started at either  $C_0$  or  $C_1$ , as appropriate; the numerical results given by Broucke (1968, 1969) are for commensurabilities  $k/n$  with  $n = 1$ , which belong to Cases 1 and 2 of the table. In Case 3, however (that is, for even values of  $n$ ), the periapsis/apoapsis classification is not applicable: having chosen either  $C_0$  or  $C_1$  as the starting point of the massless particle, the same family of periodic orbits will be obtained whether the primaries are initially taken to be at periapsis or apoapsis, and in order to determine both families in this case, both of the configurations  $C_0$  and  $C_1$  of the commensurable orbit have to be used, the initial state of the primaries being unimportant.

When Broucke's classification is applied to the two families of periodic orbits arising from a commensurability corresponding to Case 2 of Table 6.1, it is important to specify which of the configurations  $C_0$  or  $C_1$  is adopted as the starting point of the massless particle, in order to avoid ambiguity. Only in Case 1 is there a clear, unambiguous distinction between the "periapsis" and "apoapsis" orbits, as the former have mirror configurations only at periapsis, and the latter only at apoapsis. The most obvious way to classify the two families of periodic orbits arising from a Case 3 commensurability would be in terms of the perpendicular axis-crossings of the commensurable orbit from which the orbits of the massless particle are commenced in each case (either  $C_0$  or  $C_1$ ). For example, for simple-periodic orbits of Strömberg's classes  $f$  or  $g$  (retrograde or direct satellite orbits), the points  $C_0$  and  $C_1$  correspond to conjunction and opposition with respect to the primaries.

### 6.3 Three-Dimensional Orbits

Many features of the continuation of symmetric planar periodic orbits from the circular into the elliptic restricted problem, discussed in the previous section, are applicable to the continuation of three-dimensional periodic orbits; the main difference is that there is only one kind of orbital symmetry in the planar restricted problem, while as we saw in Section 2.4, symmetric periodic orbits of the three-dimensional problem can be classified into those of simple and those of double symmetry. The importance of the symmetry classification is that there exist doubly-symmetric periodic orbits of arbitrary period in the circular restricted problem, while in the elliptic problem the period must be an even multiple of  $2\pi$ , the period of the primaries; thus, when a doubly-symmetric periodic orbit is continued into the elliptic problem, the property of double symmetry (symmetry with respect to both the x-axis and the (x,z)-plane) is preserved only if the commensurability  $k/n$  is such that  $k$  is an even number, while if  $k$  is odd there must be a loss of one of the symmetries. This question of symmetry and classification is the main theme of the present section.

Any commensurable, symmetric periodic orbit of the three-dimensional circular restricted problem can be placed in one of the following three categories, according to the symmetry class and the commensurability relation:

- (i) simply-symmetric
- (ii) doubly-symmetric ( $k$  odd)
- (iii) doubly-symmetric ( $k$  even).

It is convenient to deal with each of these three categories in turn.

#### (i) Simply-symmetric

This category of commensurable three-dimensional periodic orbits can be treated in much the same way as the symmetric planar periodic orbits discussed in the previous section. It is clear that the symmetry type of the commensurable orbit (axisymmetric or plane symmetric) will be carried over into the orbits of the elliptic problem generated by continuation to non-zero values of the parameter  $e$ , since only one type of mirror configuration, either type (A) or type (P), can take place at both the initial and final epochs. The classification of the different types of commensurability  $k/n$  given in Table 6.1 is applicable, except that the two

distinct mirror configurations  $C_0$  and  $C_1$  of the commensurable orbit are no longer simply perpendicular crossings of the x-axis, but are true "three-dimensional" mirror configurations; in particular, in each of the three cases listed in the table, there are always exactly two ways in which the commensurable orbit may be continued, with the result that there are two, and only two, families of periodic orbits of the elliptic problem arising from a commensurable periodic orbit of simple symmetry. The orbits belonging to both of these families must, of course, have the same type of symmetry.

(ii) Doubly-symmetric (k odd)

Mirror configurations of alternate type take place at intervals of a quarter of the basic period of a doubly-symmetric orbit of the circular restricted problem. If the period is commensurable, satisfying Equation (6.2), such that k is an odd number ( $k = 1, 3, 5, \dots$ ), then the  $n^{\text{th}}$  mirror configuration of the commensurable orbit will occur at

$$\theta = \theta_0 + nT_0/4 = \theta_0 + k\pi/2. \quad (6.6)$$

Since  $\theta_0$  must be equal to an integer multiple of  $\pi$ , and k is odd, this value of the true anomaly does not correspond to either of the apses of the primary orbit, and so the strong periodicity criterion is not satisfied. The next true mirror configuration, satisfying the requirement that the primaries be located at either periapsis or apoapsis, does not occur until

$$\theta = \theta_0 + nT_0/2 = \theta_0 + k\pi, \quad (6.7)$$

and since the interval between successive mirror configurations is a multiple of the half-period ( $T_0/2$ ), rather than the quarter-period ( $T_0/4$ ), these mirror configurations must both be of the same type. Thus, a doubly-symmetric periodic orbit of the circular restricted problem satisfying the commensurability  $k/n$ , such that k is odd, may be regarded as either an axisymmetric or a plane symmetric orbit of the elliptic restricted problem for  $e = 0$ , according to the choice of starting point on the orbit. For zero eccentricity of the primaries, these two orbits are essentially identical, but as the eccentricity is increased to non-zero values, distinct orbits of different symmetry classes will be obtained.

It is easily shown that, once again, there are two and only two ways in

which a commensurable periodic orbit of this category can be continued into the elliptic problem, one family of simply-symmetric orbits arising from each of the "axisymmetric" and "plane symmetric" forms of the commensurable orbit. The reason for this is that as we saw in Section 2.4, the two mirror configurations separated by half of the period in a doubly-symmetric orbit are mirror images of one another in the  $(x,y)$ -plane. The configurations  $C_0$  and  $C_1$  are therefore essentially identical (apart from a reflection in the horizontal plane) and the pairs of families corresponding to the various combinations of mirror configurations in Cases 2 and 3 of Table 6.1 are images of one another in the  $(x,y)$ -plane: this is the universal property of three-dimensional periodic orbits mentioned earlier.

(iii) Doubly-symmetric ( $k$  even)

For even values of  $k$  ( $k = 2,4,6,\dots$ ), the value of the true anomaly  $\theta$  given by Equation (6.6) is an integer multiple of  $\pi$ , and therefore corresponds to one or other of the apses of the primary orbit when the eccentricity  $e$  is increased to non-zero values. Moreover, since the integers  $k$  and  $n$  in the commensurability condition (6.2) must be mutually prime,  $n$  is necessarily odd for this category of commensurable orbits: this means that successive mirror configurations of the  $e = 0$  orbit of the elliptic problem must be of opposite type, and the orbital symmetry is therefore double. The two families of doubly-symmetric periodic orbits of the elliptic restricted problem arising from this category of commensurable orbit can be classified as consisting of "periapsis orbits" and "apoapsis orbits", according to the location of the primaries at a given mirror configuration (the type (A) configuration, say).

Few results have been published on the numerical continuation of three-dimensional symmetric periodic orbits into the elliptic restricted problem. Katsiaris (1973) offers some results on the continuation of simply-symmetric orbits, while the case of doubly-symmetric periodic orbits has been explored by Macris et al. (1975). In the next section, numerical examples are given for each of the three categories of symmetric commensurable orbits listed above.

#### 6.4 Numerical Examples

In this section, numerical results are presented to illustrate the

continuation of three-dimensional periodic orbits of the circular restricted problem into the elliptic case: firstly, categories (i) and (ii) of commensurable, symmetric periodic orbits, both of which give rise to simply-symmetric orbits of the elliptic restricted problem, and secondly, category (iii), giving rise to doubly-symmetric orbits.

Examination of Tables 5.1 - 5.8 shows that, with the exception of family  $F_{v15}^{1(p)}$ , each of the vertical branches of family  $f$  given in the previous chapter contains an orbit of period  $T = 2\pi$  ( $\approx 6.283$ ): that is, in the commensurability  $1/1$  with the period of the primaries. We take the  $T = 2\pi$  orbits of the families  $F_{v15}^{1(a)}$  and  $F_{v16}^{1(c)}$  as starting points for numerical continuation into the three-dimensional elliptic restricted problem, to exemplify the two possible ways in which families of simply-symmetric periodic orbits, parametrised by the eccentricity of the primaries, may be established. The orbit of period  $T = 12\pi/5$  belonging to the family  $F_{v16}^{1(c)}$  is used as an example of a category (iii) commensurability, from which two families of doubly-symmetric periodic orbits of the elliptic restricted problem can be established.

(i) Continuation of the  $1/1$  Commensurable Orbit of Family  $F_{v15}^{1(a)}$

Family  $F_{v15}^{1(a)}$  consists of axisymmetric periodic orbits, and so those orbits of this family with commensurable periods belong to category (i) (simply-symmetric) of commensurable, symmetric periodic orbits, and can be classified into Cases 1, 2 and 3 of Table 6.1 according to the commensurability  $k/n$ . The  $1/1$  commensurability, in particular, comes under Case 2: the two families of axisymmetric periodic orbits which are obtained by continuation of this orbit into the elliptic problem are distinguishable according to the location of the massless particle at periapsis of the primaries. This is perhaps the most convenient classification, since the mirror configurations of all of the orbits established by numerical continuation are of type (A) (on-axis), and the two perpendicular axis crossings occur at conjunction and at opposition relative to the primaries. We therefore have a "conjunction" family and an "opposition" family: the former results from taking the massless particle to be at the conjunction axis-crossing at periapsis, and the latter from taking the particle to be at the opposition crossing when the primaries are at periapsis. (The alternative classification, that of Broucke, would be to specify whether the primaries are at periapsis or at apoapsis

**Table 6.2** : Conjunction Family Generated from the 1/1 Commensurability of Family  $F_{v15}^{1(a)}$  ( $\mu = 0.00095$ )

e	$s_{01}$	$s_{05}$	$s_{06}$	m
0	0.961227	0.046428	0.170391	5
0.005	0.961156	0.046575	0.170053	5
0.01	0.961088	0.046713	0.169730	5
0.05	0.960679	0.047552	0.167685	5
0.1	0.960482	0.048074	0.166252	5
0.2	0.960949	0.047675	0.165938	5
0.3	0.962306	0.045368	0.167965	5
0.4	0.964360	0.042674	0.171657	4
0.5	0.966764	0.043908	0.175895	4
0.6	0.969095	0.053580	0.178901	4
0.7	0.971096	0.075153	0.177527	4
0.8	0.972519	0.114708	0.162577	4
0.9	0.972653	0.189644	0.077942	4

**Table 6.3** : Opposition Family Generated from the 1/1 Commensurability of Family  $F_{v15}^{1(a)}$  ( $\mu = 0.00095$ )

e	$s_{01}$	$s_{05}$	$s_{06}$	m
0	1.036944	-0.048406	0.168970	5
0.005	1.037017	-0.048474	0.168645	5
0.01	1.037086	-0.048533	0.168339	5
0.05	1.037488	-0.048692	0.166508	5
0.1	1.037618	-0.048232	0.165561	5
0.2	1.036807	-0.045621	0.166797	5
0.3	1.034930	-0.041379	0.170721	5
0.4	1.032385	-0.038369	0.176126	4
0.5	1.029809	-0.042788	0.180966	4
0.6	1.027689	-0.057885	0.182663	4
0.7	1.026180	-0.084616	0.177447	4
0.8	1.025573	-0.126738	0.155008	4
0.89	1.026493	-0.187517	0.075217	4

at the instant the massless particle was at, say, conjunction).

Numerical data for the conjunction family generated from the 1/1 commensurability of family  $F_{v15}^{1(a)}$  are given in Table 6.2, and for the opposition family in Table 6.3. The on-axis initial conditions ( $s_{01}$ ,  $s_{05}$ ,  $s_{06}$ ) for the  $e = 0$  members of the two families are, naturally, those for the conjunction and opposition axis-crossings of the commensurable orbit. The initial conditions given for each orbit of both families correspond to periapsis of the primaries ( $\theta_0 = 0$ ), and the period of each orbit is, of course,  $T = 2\pi$ . Since the  $e = 0$  orbit is equivalent to a single description of the commensurable orbit of the circular problem ( $n = 1$ ), the multiplicity  $m$  is initially equal to that of the commensurable orbit, that is,  $m = 5$ ; this falls to  $m = 4$  at about  $e = 0.36$  for the conjunction family, and  $e = 0.34$  for the opposition family. The orbits of both families remain distinctly three-dimensional in character throughout, the initial  $z$ -component of velocity  $s_{06}$  retaining a non-zero value, and showing little variation except at values of the parameter  $e$  above about 0.8. Numerical continuation of the orbits beyond  $e \approx 0.9$  was found to be increasingly difficult because of numerical difficulties associated with high orbital instability. Indeed, calculation of the indices  $k_1$ ,  $k_2$  and  $k_3$  by the methods described in Chapters 3 and 4 indicated that the orbits of both families are entirely unstable, the instability increasing with the eccentricity  $e$  of the primaries.

Typical orbits of both the conjunction and opposition families are plotted in Figures A25 - A36, in the Appendix.

(ii) Continuation of the 1/1 Commensurable Orbit of Family  $F_{v16}^{1(c)}$

The orbit of period  $T = 2\pi$  (the 1/1 commensurability) belonging to family  $F_{v16}^{1(c)}$  of doubly-symmetric orbits is an example of category (ii) (doubly-symmetric,  $k$  odd) of commensurable symmetric periodic orbits of the circular restricted problem. This orbit can therefore be continued into the elliptic problem to produce two families of simply-symmetric periodic orbits, one consisting of axisymmetric orbits and the other of plane symmetric orbits. Numerical data for these two families are given in Tables 6.4 and 6.5.

The initial conditions given in each of the tables correspond to

**Table 6.4** : Axisymmetric Family Generated from the 1/1 Commensurability  
of Family  $F_{v16}^{1(c)}$  ( $\mu = 0.00095$ )

e	$s_{01}$	$s_{05}$	$s_{06}$	m
0	0.966039	0.046917	0.176984	6
0.005	0.965892	0.047043	0.176269	6
0.01	0.965746	0.047165	0.175568	6
0.05	0.964612	0.048029	0.170478	6
0.1	0.963368	0.048779	0.165578	6
0.2	0.961870	0.048837	0.160690	6
0.3	0.961859	0.046073	0.160905	6
0.4	0.963215	0.039465	0.164738	6
0.5	0.965776	0.030820	0.171315	5
0.6	0.968776	0.030328	0.178633	5
0.7	0.971196	0.047742	0.182769	5
0.8	0.972722	0.086331	0.175945	5
0.9	0.972503	0.160158	0.121971	5

**Table 6.5** : Plane-Symmetric Family Generated from the 1/1 Commensurability  
of Family  $F_{v16}^{1(c)}$  ( $\mu = 0.00095$ )

e	$s_{01}$	$s_{03}$	$s_{05}$	m
0	0.997095	0.032160	-0.174842	6
0.005	0.997077	0.032283	-0.174148	6
0.01	0.997057	0.032405	-0.173461	6
0.05	0.996855	0.033419	-0.168086	6
0.1	0.996452	0.034853	-0.161261	6
0.2	0.994896	0.039218	-0.144135	6
0.3	0.993624	0.047659	-0.121075	6
0.4	0.995270	0.057763	-0.104231	6
0.5	0.997441	0.068109	-0.092587	6
0.6	0.998367	0.079869	-0.081706	6
0.7	0.997325	0.094350	-0.069553	6
0.8	0.995343	0.113703	-0.057558	6
0.9	0.997193	0.141005	-0.054317	6
0.98	0.998515	0.187258	-0.052248	6

periapsis of the primaries ( $\theta_0 = 0$ ), and the orbital period is once again in every case  $T = 2\pi$ . The orbital multiplicity  $m$ , initially equal to that of the commensurable orbit ( $m = 6$ ), drops to  $m = 5$  for the axisymmetric family at about  $e = 0.40$ , but retains its initial value throughout the plane symmetric family. The orbits are again distinctly three-dimensional, the initial  $z$ -velocity  $s_{06}$  for the axisymmetric family and the initial  $z$ -component  $s_{03}$  for the plane symmetric family remaining non-zero throughout. The orbits of both families were found to be entirely unstable, the plane symmetric orbit for a given value of the primary eccentricity being somewhat less unstable than the corresponding axisymmetric orbit. For this reason, it was possible to trace the plane symmetric family to a higher value of the eccentricity, before numerical difficulties associated with highly unstable orbits made further progress impractical.

Typical orbits of both the axisymmetric and plane symmetric families are plotted in Figures A37 - A48, in the Appendix.

(iii) Continuation of the 6/5 Commensurable Orbit of Family  $F_{vl6}^{1(c)}$

Two families of doubly-symmetric periodic orbits of the elliptic restricted problem are now presented to illustrate the continuation of a commensurable orbit of category (iii) (doubly-symmetric,  $k$  even) as the eccentricity of the primaries is increased from zero to non-zero values. The doubly-symmetric orbit chosen for this purpose was the  $T = 12\pi/5$  ( $\approx 7.540$ ) member of family  $F_{vl6}^{1(c)}$ , corresponding to the 6/5 commensurability; this in fact is the lowest-order commensurability with an even value of  $k$  of any of the four doubly-symmetric vertical branches given in Chapter 5. Since the commensurable orbit of the circular family has multiplicity six, and the  $e = 0$  orbit of the elliptic family is equivalent to a five-fold description of this orbit, the orbits of the elliptic families are of multiplicity  $m = 30$ .

As was shown in Section 6.3, the two families of periodic orbits arising from a commensurability of category (iii) can be classified as the "periapsis" and "apoapsis" families. In the numerical determination of both families generated from the 6/5 commensurability of family  $F_{vl6}^{1(c)}$ , the same starting point was chosen for the massless particle, namely, the type (A) mirror configuration, corresponding to conjunction with the primaries; the periapsis and apoapsis families were established by taking the primaries

Table 6.6 : Periapsis Family Generated from the 6/5 Commensurability  
of Family  $F_{v16}^{1(c)}$  ( $\mu = 0.00095$ )

e	$s_{01}$	$s_{05}$	$s_{06}$	m
0	0.961406	0.190405	0.063836	30
0.005	0.961216	0.189915	0.063524	30
0.01	0.961023	0.189423	0.063233	30
0.05	0.959406	0.185423	0.061648	30
0.1	0.957178	0.180388	0.061281	30
0.2	0.952063	0.170975	0.064230	30
0.3	0.946458	0.163439	0.070107	30
0.4	0.941078	0.157554	0.078320	30
0.5	0.936537	0.151298	0.090172	30
0.6	0.931126	0.147843	0.102295	30

Table 6.7 : Apoapsis Family Generated from the 6/5 Commensurability  
of Family  $F_{v16}^{1(c)}$  ( $\mu = 0.00095$ )

e	$s_{01}$	$s_{05}$	$s_{06}$	m
0	0.961406	0.190405	0.063836	30
0.005	0.961593	0.190893	0.064171	30
0.01	0.961779	0.191377	0.064528	30
0.05	0.963186	0.195128	0.068203	30
0.1	0.964758	0.199398	0.074876	30
0.2	0.967408	0.206203	0.094807	30
0.3	0.969738	0.211083	0.123109	30
0.4	0.971969	0.214877	0.159830	30
0.5	0.974049	0.218839	0.205257	30
0.6	0.975956	0.229213	0.260065	30

to be initially at periapsis ( $\theta_0 = 0$ ) and apoapsis ( $\theta_0 = \pi$ ), respectively. Numerical data for the two families of doubly-symmetric orbits are given in Tables 6.6 and 6.7.

The common period of the orbits of the periapsis and apoapsis families is  $T = 12\pi$ ; the orbital multiplicity retains the initial value  $m = 30$  for all of the orbits which have been determined. The orbits of both families become generally more inclined to the horizontal plane with increasing eccentricity of the primaries, the initial z-velocity  $s_{06}$  showing a trend towards increased values. Calculation of the stability indices indicates that the orbits are without exception unstable, the degree of instability becoming extremely high at values of the eccentricity of about 0.3 or 0.4 (the magnitude of one of the stability indices for the final orbit of Table 6.6 is of order  $10^8$ ); because of this, the orbits could not be continued to such large eccentricities as those of the previous section. A smooth transition is evident in the initial conditions  $(s_{01}, s_{05}, s_{06})$  between the periapsis and apoapsis families across the  $e = 0$  orbit, which is common to both families; this behaviour will be discussed further in the next section.

### 6.5 Remarks

(1) An important feature of the continuation of symmetric periodic orbits into the elliptic problem, discussed in Sections 6.2 and 6.3, is that there are exactly two ways in which any commensurable periodic orbit of the circular restricted problem can be continued, so that each such orbit always gives rise to two (and only two) families of periodic orbits of the elliptic restricted problem, parametrised by the eccentricity of the primary orbit. As we saw in Chapter 3, this is also a characteristic feature of the continuation of vertical self-resonant (not vertical-critical) orbits of the planar into the three-dimensional case of the restricted problem. Indeed, an analogy can be drawn between the continuation of a vertical self-resonant orbit of the planar restricted problem into the three-dimensional restricted problem, and the continuation of a commensurable orbit of the planar circular restricted problem into the elliptic problem, involving the classifications of the pairs of families generated in each case, as we now show.

Families of symmetric periodic orbits can be classified in terms of the

types of mirror configurations defining each member orbit. The pair of vertical branches arising from each type of vertical bifurcation orbit can be classified, according to the value of the integer  $m$  in the self-resonance condition (4.54), as follows (see Table 4.1):

Table 6.8

Case	$m$	$m/2$		Initial Mirror Configuration	Final Mirror Configuration
1	odd	-	(a)	$C_0(P)$	$C_1(P)$
			(b)	$C_0(A)$	$C_1(A)$
2	even	odd	(a)	$C_0(P)$	$C_1(A)$
			(b)	$C_0(A)$	$C_1(P)$
3	even	even	(a)	$C_0(P)$	$C_0(A)$
			(b)	$C_1(P)$	$C_1(A)$

The corresponding classification for the pairs of families of periodic orbits generated from a commensurable orbit of the planar circular problem has already been given in Table 6.1 (Section 6.2). Comparison of Tables 6.1 and 6.8 shows a direct one-to-one correspondence between the types of mirror configuration characterising each family in the various categories of vertical self-resonant and commensurable orbits. (It is important to remember, however, that in Table 6.8 the mirror configurations are "three-dimensional", while in Table 6.1 the mirror configurations are confined to the horizontal plane and are distinguished according to the state of the primaries at the epoch).

(2) As Broucke (1969) found in the case of planar periodic orbits of the elliptic problem, the periapsis and apoapsis families originating from the same commensurable orbit of the planar circular problem connect together smoothly and continuously at the common  $e = 0$  orbit. A further illustration of this property in the case of three-dimensional orbits is given in Figure 6.1, which shows the continuous variation of the initial conditions ( $s_{01}, s_{05}, s_{06}$ ) between the periapsis and apoapsis families given in Tables 6.6 and 6.7.

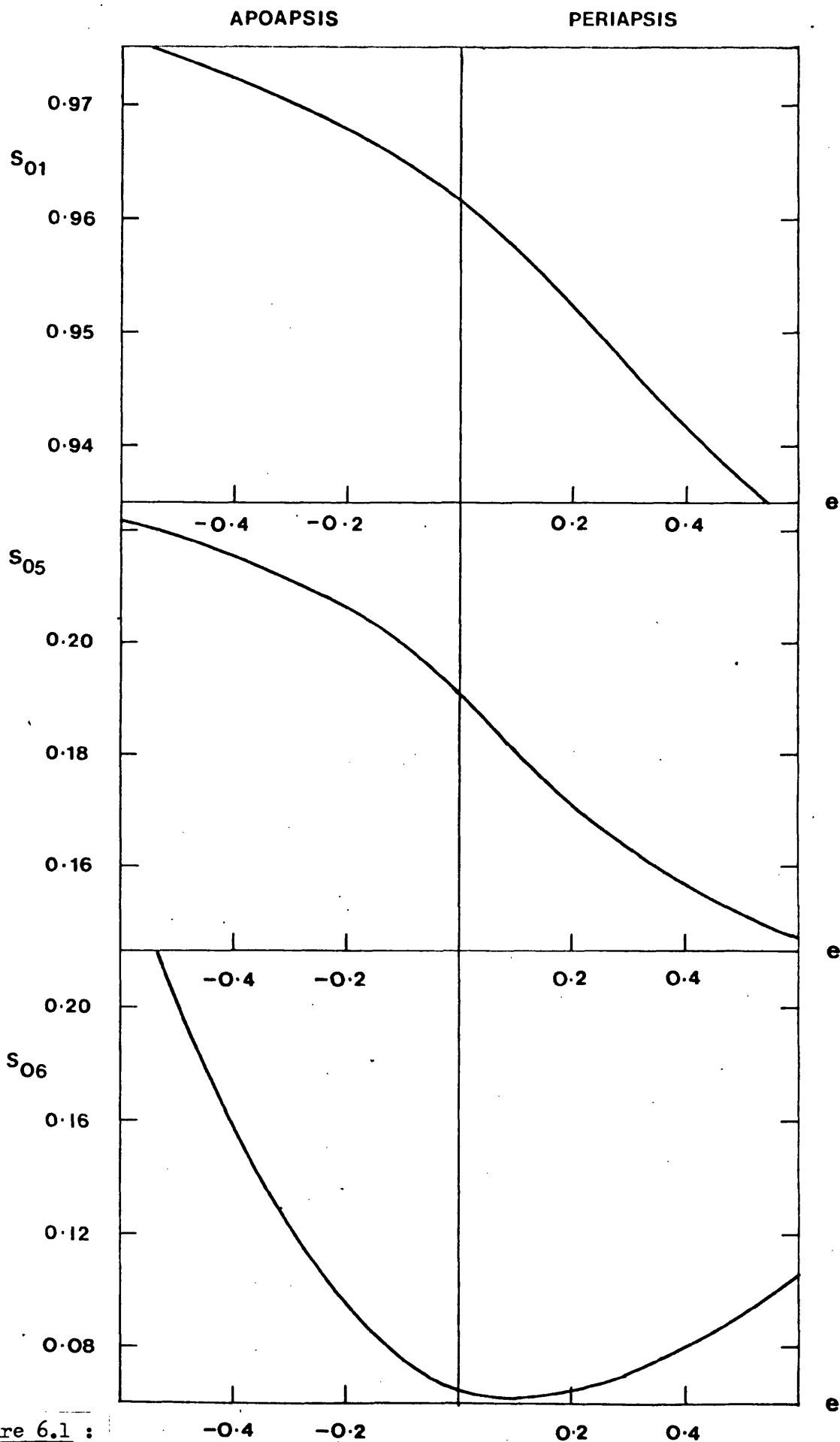


Figure 6.1 : Characteristics of the periapsis and apoapsis families generated from the 6/5 commensurability of family  $F_{v16}^{1(c)}$ .

The reason for this lies in the fact that the equations of motion of the elliptic restricted problem with respect to the rotating-pulsating coordinate system and with the true anomaly  $\theta$  as the independent variable (Equations (1.38)), contain the eccentricity  $e$  and true anomaly  $\theta$  of the primaries only in the form of a multiplying factor

$$E(\theta) = (1 + e \cos \theta)^{-1}, \quad (6.8)$$

which is invariant under the transformation

$$\begin{aligned} e' &= -e \\ \theta' &= \theta - \pi. \end{aligned} \quad (6.9)$$

The equations of motion are formally identical whether expressed in terms of  $(\theta, e)$  or  $(\theta', e')$ , and an orbit starting at apoapsis ( $\theta_0 = \pi$ ) of the primaries for some given value of  $e$  can equivalently be integrated with a change of independent variable from  $\theta$  to  $\theta'$  (since  $d\theta' = d\theta$ ), starting at  $\theta'_0 = 0$ , and with the primary eccentricity having the new value  $e'$ . The periapsis and apoapsis families can therefore be regarded as the two segments of a single family, corresponding to  $e > 0$  and  $e < 0$  respectively,  $\theta_0$  being kept fixed at zero. As the two segments are connected at  $e = 0$  and the eccentricity varies continuously from one orbit to the next, the periapsis and apoapsis families must connect in a continuous fashion, through the continuity properties of the solutions of the differential equations of motion. This is evidently a general property of those pairs of families (or series) of symmetric periodic orbits of the elliptic restricted problem (planar and three-dimensional) which have a common  $e = 0$  member; further examples of this will be given in the next chapter.

(3) In the previous section, attention was drawn to the fact that the orbits of all six families obtained by numerical continuation from three-dimensional periodic orbits of the circular restricted problem remain distinctly three-dimensional in character as the eccentricity of the primaries is increased, and there is no indication that any of these families is directly connected with a family (or families) of planar periodic orbits of the elliptic problem through a vertical bifurcation orbit (this also appears to be the case with the family given in Table I of Katsiaris, 1973). It seems likely that families of three-dimensional symmetric periodic orbits generated by the two methods described in this

thesis, namely (a) by continuation of commensurable periodic orbits of the three-dimensional circular problem into the elliptic case, and (b) by continuation of vertical self-resonant orbits of the planar elliptic problem into three dimensions (Chapter 7), may be unconnected, at least for a fixed value of the mass parameter. This would imply that the supposition that all families of three-dimensional periodic orbits can be generated from vertical self-resonant orbits of the planar restricted problem (e.g. Zagouras and Kalogeropoulou, 1978) cannot be extended from the circular to the elliptic restricted problem. (A possible exception to this rule in the circular problem will be discussed in Chapter 8).

## 7. VERTICAL BIFURCATION SERIES

### 7.1 Introduction

In previous chapters, the important class of periodic orbits known as vertical bifurcation orbits has been discussed, with particular reference to the continuation of such orbits from the planar restricted problem into three dimensions. The discussion has been based on the assumption that the mass parameter  $\mu$  is fixed, and vertical bifurcation orbits have been identified as discrete members of the various families of planar periodic orbits satisfying the vertical self-resonance condition (Equation (4-54))

$$a_v = \cos(2\pi n/m) \quad (7.1)$$

for some integers  $m$  and  $n$ . In this chapter, we examine the possibility of determining a continuous series of vertical bifurcation orbits over a range of values of the mass parameter: in other words, a special kind of family of planar periodic orbits for which the vertical stability index  $a_v$ , rather than the mass parameter  $\mu$ , is a constant. This will be referred to as a "vertical bifurcation series". (The numerical determination of vertical bifurcation series consisting of asymmetric vertical-critical orbits has been discussed by Markellos (1977b)).

The practical usefulness of vertical bifurcation series, and the importance of their role in the structure of symmetric periodic orbits of the restricted problem (over the range of all possible values of  $\mu$ ) is evident, since every orbit belonging to such a series is the intersection of a family of planar periodic orbits with either one or two families of three-dimensional orbits. As well as providing an infinite number of starting orbits for continuation into three dimensions, a vertical bifurcation series also yields information on the stability properties of the three-dimensional orbits, at least in the neighbourhood of the bifurcation. Series of vertical self-resonant orbits, and particularly vertical-critical orbits, are also useful for distinguishing the vertically stable from the vertically unstable segments of a family of planar periodic orbits (for fixed  $\mu$ ), as has been shown by Hénon (1973a).

A vertical bifurcation series of the planar circular restricted problem

consists of orbits whose initial conditions  $(x_0, y_0, x'_0, y'_0)$  satisfy the conditions of periodicity and vertical self-resonance. Since we are concerned only with symmetric periodic orbits, the periodicity conditions have the form (2.15), the initial conditions  $y_0$  and  $x'_0$  being equal to zero. The periodicity conditions may therefore be written as

$$\begin{aligned} y(x_0, y'_0; T/2; \mu) &= 0 \\ x'(x_0, y'_0; T/2; \mu) &= 0, \end{aligned} \tag{7.2}$$

where  $T$  is the orbital period, and the dependence on the mass parameter  $\mu$  is indicated explicitly; the values of the true anomaly  $\theta$  at the initial and final epochs are  $\theta_0 = 0$  and  $\theta_1 = T/2$ , respectively.

We saw in Chapter 3 that the vertical stability index  $a_v$  of a symmetric periodic orbit is related to the elements  $(A_v, B_v, C_v, D_v)$  of the vertical variational matrix  $V_v$  evaluated at the half-period ( $\theta = T/2$ ) by (Equation (3.87))

$$a_v = A_v D_v + B_v C_v. \tag{7.3}$$

Since  $V_v(T/2)$  depends only on the initial conditions and period, we may write

$$a_v = a_v(x_0, y'_0; T/2; \mu), \tag{7.4}$$

where once again the mass parameter appears explicitly; this is necessary because we wish to vary the value of  $\mu$ . The vertical self-resonance condition can therefore be expressed in the form

$$a_v(x_0, y'_0; T/2; \mu) = a_{v0}, \tag{7.5}$$

where

$$a_{v0} = \cos(2\pi n/m). \tag{7.6}$$

Together, Equations (7.2) and (7.5) form a system of three simultaneous equations in the four unknowns  $(x_0, y'_0, T, \mu)$ ; this system is underdetermined, with one degree of freedom, and so solutions occur in continuous monoparametric sets. The situation in the planar elliptic problem is very similar: the periodicity conditions (7.2) become

$$\begin{aligned} y(x_0, y_0'; \mu; e) &= 0 \\ x'(x_0, y_0'; \mu; e) &= 0, \end{aligned} \tag{7.7}$$

where  $e$  is the eccentricity of the orbit of the primaries, and the vertical self-resonance condition (7.5) becomes

$$a_v(x_0, y_0'; \mu; e) = a_{v0}, \tag{7.8}$$

with  $a_{v0}$  given by Equation (7.6), as before. The primary eccentricity  $e$  replaces the orbital period  $T$  as a variable parameter along the series, and once again we have a continuous monoparametric set of solutions. Notice that both of the parameters  $\mu$  and  $e$  vary along a vertical bifurcation series of the elliptic restricted problem.

In Section 7.2, predictor-corrector algorithms for the numerical determination of vertical bifurcation series of both the circular and elliptic problems are developed, and numerical examples are given in Sections 7.3 (circular problem) and 7.4 (elliptic problem). The chapter is concluded with a number of remarks in Section 7.5.

## 7.2 Numerical Determination

### 7.2.1 Circular Restricted Problem

The system of three simultaneous equations defining a vertical bifurcation orbit (Equations (7.2) and (7.5)) in the circular restricted problem is formally very similar to the system of equations (4.19), the periodicity conditions for a three-dimensional symmetric periodic orbit of the circular restricted problem; the methods described in Chapter 4 for the numerical determination of families of three-dimensional periodic orbits can easily be modified for the numerical determination of vertical bifurcation series, as we now show. (The determination of vertical bifurcation series of the elliptic restricted problem will be dealt with later). For convenience, the state vector notation ( $s_1 = x$ ,  $s_2 = y$ , etc.) will be used.

Suppose that approximate values  $s_{01}^*$ ,  $s_{05}^*$ ,  $t^*$  of the initial conditions and half-period ( $T/2$ ) of a vertical self-resonant orbit of the circular restricted problem, corresponding to the value  $\mu = \mu^*$  of the mass parameter,

are known. In order to improve the accuracy of these estimated values, a differential corrector algorithm is required; this is constructed in much the same way as that described in Section 4.3. If the "errors"  $\delta s_{01}$ ,  $\delta s_{05}$ ,  $\delta t$  and  $\delta \mu$ , that is, the differences between the estimated and exact solutions of Equations (7.2) and (7.5), are sufficiently small for second and higher orders in the Taylor series expansion to be neglected, we may write

$$\begin{aligned} \frac{\partial s_2}{\partial s_{01}} \delta s_{01} + \frac{\partial s_2}{\partial s_{05}} \delta s_{05} + \frac{ds_2}{dt} \delta t + \frac{ds_2}{d\mu} \delta \mu &= -s_2^* \\ \frac{\partial s_4}{\partial s_{01}} \delta s_{01} + \frac{\partial s_4}{\partial s_{05}} \delta s_{05} + \frac{ds_4}{dt} \delta t + \frac{ds_4}{d\mu} \delta \mu &= -s_4^* \\ \frac{\partial a_v}{\partial s_{01}} \delta s_{01} + \frac{\partial a_v}{\partial s_{05}} \delta s_{05} + \frac{da_v}{dt} \delta t + \frac{da_v}{d\mu} \delta \mu &= a_{v0} - a_v^* \end{aligned} \quad (7.9)$$

where  $(s_2^*, s_4^*, a_v^*)$  are the final conditions and vertical stability index evaluated at  $\theta = t^*$  on the orbit with initial conditions  $(s_{01}^*, s_{05}^*)$ , and with the value  $\mu^*$  of the mass parameter. This is the basic form of the differential corrector equations for a vertical bifurcation series of the circular restricted problem ("circular series"). The quantities on the right-hand sides of Equations (7.9) are calculated by trial integration; to allow the system of corrector equations to be solved, the various coefficients appearing on the left-hand sides must also be evaluated. The coefficients on the left-hand sides of the first two of Equations (7.9) are already known: these are the elements  $v_{21}$ ,  $v_{25}$ ,  $v_{41}$  and  $v_{45}$  of the variational matrix  $V$ , the components  $f_2$  and  $f_4$  of the vector function  $f$ , and the components  $v_{2\mu}$  and  $v_{4\mu}$  of the vector  $v_\mu$ , all of which have been defined in Chapter 3. It remains only to obtain expressions for the four coefficients  $\partial a_v / \partial s_{01}$ ,  $\partial a_v / \partial s_{05}$ ,  $da_v / dt$  and  $da_v / d\mu$  appearing in the third of Equations (7.9), in a form suitable for numerical integration.

We recall that the vertical stability index  $a_v$  of a symmetric periodic orbit is given by

$$a_v = A_v D_v + B_v C_v, \quad (7.10)$$

where  $A_v$ ,  $B_v$ ,  $C_v$ ,  $D_v$  are the elements of the vertical variational matrix  $V_v$

evaluated at the half-period ( $\theta = t$ ). We may therefore write

$$\frac{\partial a_v}{\partial s_{01}} = \frac{\partial A_v}{\partial s_{01}} D_v + A_v \frac{\partial D_v}{\partial s_{01}} + \frac{\partial B_v}{\partial s_{01}} C_v + B_v \frac{\partial C_v}{\partial s_{01}}, \quad (7.11)$$

with similar expressions for  $\partial a_v / \partial s_{05}$ ,  $da_v/dt$  and  $da_v/d\mu$ . The values of  $A_v$ ,  $B_v$ ,  $C_v$  and  $D_v$  are known from the numerical integration, and we require to evaluate their derivatives with respect to  $s_{01}$ ,  $s_{05}$ ,  $t$  and  $\mu$ . Differentiating Equation (3.46) with respect to  $s_{01}$ , we obtain

$$\left( \frac{\partial V_v}{\partial s_{01}} \right)' = \frac{\partial F_v}{\partial s_{01}} V_v + F_v \frac{\partial V_v}{\partial s_{01}}, \quad (7.12)$$

with similar expressions for the derivatives of matrix  $V_v$  with respect to the parameters  $s_{05}$ ,  $\mu$ ; the derivative with respect to  $t$  is given directly by Equation (3.46). For a planar periodic orbit of the circular restricted problem, the matrix  $F_v$  is given by

$$F_v = \begin{pmatrix} 0 & 1 \\ A-1 & 0 \end{pmatrix}, \quad (7.13)$$

where  $A$  is a function only of the coordinates ( $s_1, s_2$ ) and the mass parameter  $\mu$ , given by Equation (1.44). In order to numerically integrate Equation (7.12), and the corresponding equations for  $\partial V_v / \partial s_{05}$  and  $dV_v/d\mu$ , expressions for the derivatives of the function  $A$  with respect to the initial conditions ( $s_{01}, s_{05}$ ) and the mass parameter  $\mu$  must be found. The required expressions are

$$\begin{aligned} \frac{\partial A}{\partial s_{01}} &= \frac{\partial A}{\partial s_1} \frac{\partial s_1}{\partial s_{01}} + \frac{\partial A}{\partial s_2} \frac{\partial s_2}{\partial s_{01}} \\ &= A_1 v_{11} + A_2 v_{21}, \end{aligned} \quad (7.14)$$

$$\begin{aligned} \frac{\partial A}{\partial s_{05}} &= \frac{\partial A}{\partial s_1} \frac{\partial s_1}{\partial s_{05}} + \frac{\partial A}{\partial s_2} \frac{\partial s_2}{\partial s_{05}} \\ &= A_1 v_{15} + A_2 v_{25}, \end{aligned} \quad (7.15)$$

$$\begin{aligned} \frac{dA}{d\mu} &= \frac{\partial A}{\partial s_1} \frac{ds_1}{d\mu} + \frac{\partial A}{\partial s_2} \frac{ds_2}{d\mu} + \frac{\partial A}{\partial \mu} \\ &= A_1 v_{1\mu} + A_2 v_{2\mu} + A_\mu, \end{aligned} \quad (7.16)$$

where

$$\left. \begin{aligned} A_1 &= \frac{3(1-\mu)(s_1+\mu)}{\sigma_1^5} + \frac{3\mu(s_1-1+\mu)}{\sigma_2^5} \\ A_2 &= 3 \left( \frac{1-\mu}{\sigma_1^5} + \frac{\mu}{\sigma_2^5} \right) s_2 \\ A_\mu &= \frac{3(1-\mu)(s_1+\mu)}{\sigma_1^5} + \frac{3\mu(s_1-1+\mu)}{\sigma_2^5} + \frac{1}{\sigma_1^3} - \frac{1}{\sigma_2^3} \end{aligned} \right\} \quad (7.17)$$

The matrix equation (7.12) can be written in component form

$$\begin{aligned} \left( \frac{\partial v_{33}}{\partial s_{01}} \right)' &= \frac{\partial v_{63}}{\partial s_{01}} \\ \left( \frac{\partial v_{36}}{\partial s_{01}} \right)' &= \frac{\partial v_{66}}{\partial s_{01}} \\ \left( \frac{\partial v_{63}}{\partial s_{01}} \right)' &= \frac{\partial A}{\partial s_{01}} v_{33} + (A-1) \frac{\partial v_{33}}{\partial s_{01}} \\ \left( \frac{\partial v_{66}}{\partial s_{01}} \right)' &= \frac{\partial A}{\partial s_{01}} v_{36} + (A-1) \frac{\partial v_{36}}{\partial s_{01}}. \end{aligned} \quad (7.18)$$

This system of four simultaneous ordinary differential equations can be integrated numerically along with the equations of motion and the equations for the variational matrix. The initial conditions for these equations are

$$\left( \frac{\partial v_{33}}{\partial s_{01}} \right)_0 = \left( \frac{\partial v_{36}}{\partial s_{01}} \right)_0 = \left( \frac{\partial v_{63}}{\partial s_{01}} \right)_0 = \left( \frac{\partial v_{66}}{\partial s_{01}} \right)_0 = 0. \quad (7.19)$$

Two similar systems of equations can be written down for the elements of  $\partial V_v / \partial s_{05}$  and  $dV_v/d\mu$ , the initial values of each element being zero. Numerical integration of a trial solution starting from the estimated initial conditions  $(s_{01}^*, s_{05}^*)$  up to the estimated half-period  $\theta = t^*$  yields the quantities needed in the corrector equations (7.9), which can then be solved by setting one of the quantities  $\delta s_{01}$ ,  $\delta s_{05}$ ,  $\delta t$  or  $\delta \mu$  to zero, according to the choice of series parameter.

Corresponding to the system (7.9) of corrector equations, we may write down the (linear) predictor equations

$$\frac{\partial s_2}{\partial s_{01}} \Delta s_{01} + \frac{\partial s_2}{\partial s_{05}} \Delta s_{05} + \frac{ds_2}{dt} \Delta t + \frac{ds_2}{d\mu} \Delta \mu = 0$$

$$\frac{\partial s_4}{\partial s_{01}} \Delta s_{01} + \frac{\partial s_4}{\partial s_{05}} \Delta s_{05} + \frac{ds_4}{dt} \Delta t + \frac{ds_4}{d\mu} \Delta \mu = 0 \quad (7.20)$$

$$\frac{\partial a_v}{\partial s_{01}} \Delta s_{01} + \frac{\partial a_v}{\partial s_{05}} \Delta s_{05} + \frac{da_v}{dt} \Delta t + \frac{da_v}{d\mu} \Delta \mu = 0 .$$

The predictor is applied by assigning a fixed (small) increment to the series parameter ( $\mu$ , say) and solving for the corresponding increments in the other three quantities. The methods described in Chapter 4 for quadratic prediction and, if desired, selection of the "local" series parameter, can easily be adopted to suit the present problem.

The predictor and corrector algorithms are used together to trace out a series of vertical bifurcation orbits parametrised by (say)  $\mu$ , the mass parameter of the primaries, in an analogous way to the determination of a vertical branch of a planar family. In order to start the procedure, approximate values of the initial conditions and period of a vertical self-resonant orbit, with vertical stability index  $a_{v0}$  given by Equation (7.6) for given  $m$  and  $n$ , corresponding to a particular value of  $\mu$ , must be known.

### 7.2.2 Elliptic Restricted Problem

The main difference between a vertical bifurcation series of the

elliptic restricted problem ("elliptic series") and a circular series is that the eccentricity of the primary orbit replaces the orbital period of the massless particle in the periodicity and self-resonance conditions. The system of equations (7.7) and (7.8) is formally very similar to the system (4.27) of periodicity conditions for a three-dimensional periodic orbit of the elliptic problem, and the analogous corrector equations can immediately be written as

$$\begin{aligned} \frac{\partial s_2}{\partial s_{01}} \delta s_{01} + \frac{\partial s_2}{\partial s_{05}} \delta s_{05} + \frac{ds_2}{d\mu} \delta \mu + \frac{ds_2}{de} \delta e &= -s_2^* \\ \frac{\partial s_4}{\partial s_{01}} \delta s_{01} + \frac{\partial s_4}{\partial s_{05}} \delta s_{05} + \frac{ds_4}{d\mu} \delta \mu + \frac{ds_4}{de} \delta e &= -s_4^* \\ \frac{\partial a_v}{\partial s_{01}} \delta s_{01} + \frac{\partial a_v}{\partial s_{05}} \delta s_{05} + \frac{da_v}{d\mu} \delta \mu + \frac{da_v}{de} \delta e &= a_{v0} - a_v^* \end{aligned} \quad (7.21)$$

where the starred quantities are those computed at the half-period on the orbit with initial conditions  $(s_{01}^*, s_{05}^*)$  approximately satisfying the periodicity and vertical self-resonance conditions for values  $\mu^*$  and  $e^*$  of the mass parameter and eccentricity of the primaries. The orbital period is, of course, constant along any series, and must be equal to an integer multiple of the period of the primaries.

With the exception of the quantity  $da_v/de$ , all of the coefficients on the left-hand sides of Equations (7.21) are known: these include the components  $v_{2e}$  and  $v_{4e}$  of the vector  $\underline{v}_e$  defined in Section 3.3, and the derivatives of  $a_v$  with respect to  $s_{01}$ ,  $s_{05}$  and  $\mu$ , for which expressions have already been obtained in this section†. The coefficient  $da_v/de$  can be calculated from

$$\frac{da_v}{de} = \frac{dA_v}{de} D_v + A_v \frac{dD_v}{de} + \frac{dB_v}{de} C_v + B_v \frac{dC_v}{de}, \quad (7.22)$$

where the derivatives on the right-hand side of Equation (7.22) are the solutions of the differential equations

†since E is no longer equal to unity, however, the quantity A in these expressions must be replaced by the product AE.

$$\begin{aligned} \left(\frac{dv_{33}}{de}\right)' &= \frac{dv_{63}}{de} \\ \left(\frac{dv_{36}}{de}\right)' &= \frac{dv_{66}}{de} \\ \left(\frac{dv_{63}}{de}\right)' &= \frac{d}{de}(AE)v_{33} + (AE-1)\frac{dv_{33}}{de} \\ \left(\frac{dv_{66}}{de}\right)' &= \frac{d}{de}(AE)v_{63} + (AE-1)\frac{dv_{36}}{de} \end{aligned} \tag{7.23}$$

evaluated at the half-period, starting from initial conditions

$$\left(\frac{dv_{33}}{de}\right)_0 = \left(\frac{dv_{36}}{de}\right)_0 = \left(\frac{dv_{63}}{de}\right)_0 = \left(\frac{dv_{66}}{de}\right)_0 = 0. \tag{7.24}$$

Note the appearance of the function  $E$  in Equation (7.23): for  $e > 0$ ,  $E(e, \theta)$  is no longer equal to unity, as in the circular problem. From Equations (1.44), we have

$$\begin{aligned} \frac{d}{de}(AE) &= E \left( \frac{\partial A}{\partial s_1} \frac{ds_1}{de} + \frac{\partial A}{\partial s_2} \frac{ds_2}{de} \right) + A \frac{dE}{de} \\ &= E \left( A_1 v_{1e} + A_2 v_{2e} - AE \cos \theta \right). \end{aligned} \tag{7.25}$$

Once again, the system (7.23) of four simultaneous differential equations can be integrated numerically, and the values obtained at the half-period substituted into Equation (7.22), together with the values of the elements of  $V_v$  at the same epoch, to give  $da_v/de$ . In the corrector equations (7.21), the chosen series parameter ( $\mu$  or  $e$ , say) is kept fixed and the corrections in the remaining three quantities computed; the corrector is applied iteratively, until the periodicity and self-resonance errors satisfy some appropriate criterion.

The predictor equations for the elliptic case are the same as for the circular restricted problem (Equations (7.20)), except that the eccentricity  $e$  replaces the half-period  $t$ .

Suitable starting orbits for the determination of vertical bifurcation

series can be found in a number of different ways, such as

- (i) by tracing out a family of planar periodic orbits of the elliptic problem ( $\mu$  fixed,  $e$  varying), and identifying those orbits which satisfy the vertical self-resonance condition for some integers  $m, n$ ;
- (ii) by establishing a vertical bifurcation series of the circular restricted problem, and identifying those orbits which have commensurable periods, and can therefore be continued into the elliptic problem.

Numerical examples of vertical bifurcation series started from commensurable, vertical self-resonant orbits of the circular restricted problem (method (ii)) are presented in Section 7.4.

### 7.3 Results: Circular Restricted Problem

In this section, numerical results are presented to illustrate the foregoing discussion of vertical bifurcation series of the planar circular restricted problem. Four series have been determined over all possible values  $0 < \mu < 1$  of the mass parameter; for  $\mu < \frac{1}{2}$  the orbits of these series belong to Strömberg's class  $f$  (retrograde satellite orbits), and for  $\mu > \frac{1}{2}$  to class  $h$  (retrograde planetary orbits). These distinctions are, of course, somewhat arbitrary, and the two designations will be used interchangeably.

The four series comprise simple-periodic, vertical self-resonant orbits having values of the vertical stability index  $a_v = \cos 2\pi/5$  ( $\approx 0.30902$ ),  $a_v = \cos \pi/3$  ( $= 0.5$ ),  $a_v = \cos 2\pi/7$  ( $\approx 0.62349$ ) and  $a_v = \cos \pi/4$  ( $\approx 0.70711$ ), respectively. Each series was started from the known orbit corresponding to the Sun-Jupiter value  $\mu = 0.00095$  of the mass parameter; these orbits were used in Chapter 5 in the determination of the vertical branches of family  $f$ , and designated  $f_{v15}^1$ ,  $f_{v16}^1$ ,  $f_{v17}^1$  and  $f_{v18}^1$ . The designation of each of these four starting orbits will be applied to the entire series to which it belongs: thus, we refer to the series  $f_{v15}^1$ , a particular orbit of that series being designated, for example, the  $\mu = 0.1$  orbit of series  $f_{v15}^1$ .

Numerical data for the four vertical bifurcation series are given in

Tables 7.1 - 7.4, and the characteristics of each series are projected in the  $(\mu, x)$ -plane in Figure 7.1. The limiting orbit of each series, corresponding to the value  $\mu = 1$  of the mass parameter, is a retrograde circular Keplerian orbit; it can be shown that the limiting orbit of series  $f_{vnm}^1$  has radius

$$\rho = \left( \frac{m}{n} - 1 \right)^{-2/3} \quad (7.26)$$

(e.g. Hénon and Guyot, 1970 and Hénon, 1974).

Figure 7.1 shows that the sizes of the orbits decrease very slowly with  $\mu$ , until the mass parameter reaches a value of about 0.025, when a rapid contraction of the orbits becomes apparent with decreasing  $\mu$ . As  $\mu \rightarrow 0$ , the orbits tend towards vertical self-resonant orbits of Hill's problem.

In addition to the vertical stability index  $a_v$  of the orbits belonging to the four series, the horizontal stability index  $a$  was calculated; it was found that all four series consist entirely of stable orbits. It is therefore possible that the vertical branches which bifurcate from planar orbits belonging to these series consist at least partly of stable three-dimensional periodic orbits (although for the value  $\mu = 0.00095$  of the mass parameter, numerical results indicate that the three-dimensional orbits are mainly unstable, as we saw in Chapter 5).

For the limiting value  $\mu = 1$  of the mass parameter, the synodic orbital periods (that is, with respect to the rotating coordinate system) corresponding to the radii  $\rho$  given by Equation (7.26) for each series are

$$T = 2\pi n/m, \quad (7.27)$$

where  $n = 1$ , and  $m = 5, 6, 7$  or  $8$ , respectively. Examination of Tables 7.1 - 7.4 shows that as  $\mu$  decreases along each series, the orbital period increases from this  $n/m$  commensurability, and it is found that for non-zero masses of the two primaries ( $0 < \mu < 1$ ), the lowest-order commensurability occurring in series  $f_{v1m}^1$  is

$$T = 2\pi / (m-1). \quad (7.28)$$

The commensurabilities  $1/(m-1)$  belong to either Case 2 or Case 3 of

Table 7.1: Series  $f_{v15}^4$

$\mu$	$s_{01}$	$s_{05}$	T
0.001	0.951115	0.203315	1.706373
0.002	0.937742	0.256463	1.706849
0.005	0.913402	0.348768	1.707213
0.01	0.887460	0.440244	1.706527
0.02	0.851337	0.555872	1.703339
0.05	0.777173	0.756677	1.688785
0.1	0.685609	0.954894	1.659508
0.2	0.537331	1.202704	1.598875
0.3	0.406570	1.373969	1.542060
0.4	0.283836	1.507955	1.490374
0.5	0.165668	1.618813	1.443455
0.6	0.050381	1.713359	1.400612
0.7	-0.062987	1.795369	1.361138
0.8	-0.175049	1.867072	1.324381
0.9	-0.286229	1.929796	1.289740
1.0	-0.396850	1.984251	1.256637

Table 7.2: Series  $f_{v16}^1$

---

$\mu$	$s_{01}$	$s_{05}$	T
0.001	0.960195	0.206371	1.294937
0.002	0.949158	0.260235	1.294965
0.005	0.928835	0.353715	1.294727
0.01	0.906812	0.446285	1.293939
0.02	0.875517	0.563250	1.291822
0.05	0.809217	0.766511	1.283996
0.1	0.724403	0.967827	1.269461
0.2	0.582603	1.221396	1.239593
0.3	0.454943	1.398365	1.210675
0.4	0.333956	1.538030	1.183288
0.5	0.216900	1.654570	1.157484
0.6	0.102420	1.754872	1.133158
0.7	-0.010273	1.842804	1.110149
0.8	-0.121685	1.920729	1.088277
0.9	-0.232171	1.990139	1.067357
1.0	-0.341995	2.051971	1.047198

---

Table 7.3: Series  $f_{v17}^4$

---

$\mu$	$s_{01}$	$s_{05}$	T
0.001	0.965628	0.211584	1.058086
0.002	0.955989	0.266763	1.058047
0.005	0.938069	0.362482	1.057785
0.01	0.918392	0.457227	1.057173
0.02	0.890004	0.576895	1.055708
0.05	0.828543	0.784827	1.050660
0.1	0.748137	0.990912	1.041590
0.2	0.611145	1.251090	1.023095
0.3	0.486278	1.433362	1.005021
0.4	0.367175	1.577809	0.987650
0.5	0.251513	1.698894	0.971033
0.6	0.138140	1.803657	0.955145
0.7	0.026387	1.896081	0.939930
0.8	-0.084177	1.978630	0.925319
0.9	-0.193850	2.052907	0.911235
1.0	-0.302853	2.119974	0.879598

---

Table 7.4: Series  $f_{v18}^1$

---

$\mu$	$s_{01}$	$s_{05}$	T
0.001	0.969414	0.217375	0.898593
0.002	0.960749	0.274032	0.898544
0.005	0.944507	0.372284	0.898318
0.01	0.926472	0.469505	0.897849
0.02	0.900124	0.592262	0.896780
0.05	0.842088	0.805505	0.893228
0.1	0.764875	1.016876	0.886959
0.2	0.631525	1.283972	0.874239
0.3	0.508907	1.471443	0.861753
0.4	0.391411	1.620353	0.849660
0.5	0.276988	1.745524	0.837993
0.6	0.164629	1.854177	0.826748
0.7	0.053746	1.950417	0.815900
0.8	-0.056037	2.036801	0.805418
0.9	-0.164981	2.115014	0.795264
1.0	-0.273276	2.186207	0.785398

---

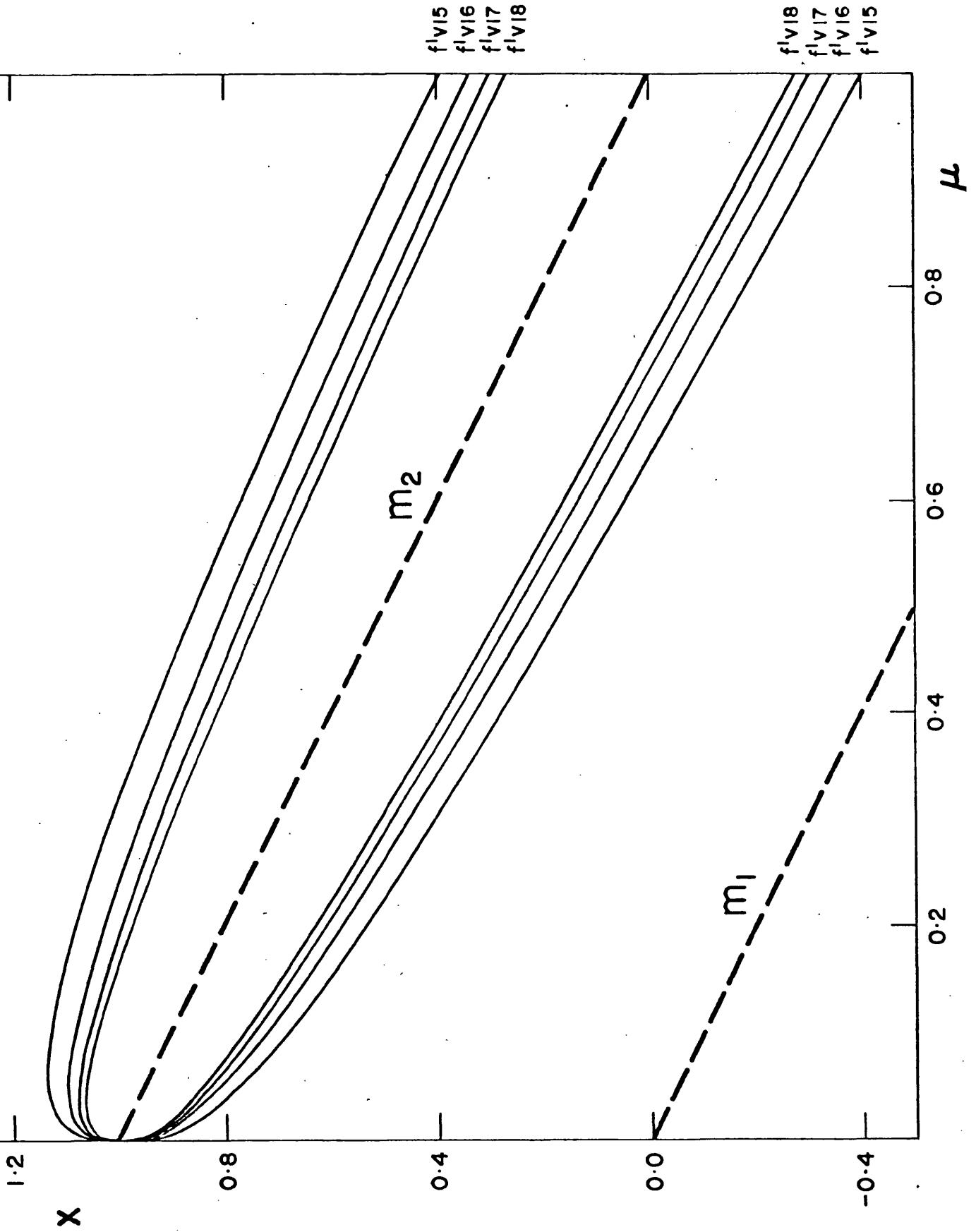


Figure 7.1 : Characteristics of the circular series  $f_{v15}^1$ ,  $f_{v16}^1$ ,  $f_{v17}^1$  and  $f_{v18}^1$  projected in the  $(\mu, x)$ -plane. Each series is represented by two curves, corresponding to the two perpendicular crossings of the x-axis. The broken lines indicate the positions of the primaries  $m_1$  ( $x = -\mu$ ) and  $m_2$  ( $x = 1-\mu$ ).

Table 6.1, depending on the value of  $m$ : for series  $f_{v15}^1$  and  $f_{v17}^1$  the lowest-order commensurabilities are  $1/4$  and  $1/6$ , respectively (Case 3), and for series  $f_{v16}^1$  and  $f_{v18}^1$  the lowest-order commensurabilities are respectively  $1/5$  and  $1/7$  (corresponding to Case 2). These four commensurable, vertical self-resonant orbits (one from each of the four circular series) were used as starting-points in the determination of vertical bifurcation series of the elliptic restricted problem; the results of this procedure are discussed in the next section.

#### 7.4 Results: Elliptic Restricted Problem

The results given in this section illustrate the technique of establishing vertical bifurcation series in the elliptic restricted problem by continuation of commensurable, vertical self-resonant orbits of the circular restricted problem to non-zero values of the eccentricity of the primaries. The starting orbits chosen for this purpose were the four lowest-order commensurabilities from each of the four circular series given in the previous section: as we have just seen, this is the  $1/(m-1)$  commensurability of series  $f_{v1m}^1$ , where  $m = 5, 6, 7$  and  $8$ . Since the orbits of the four circular series are all simple-periodic, that is, crossing the  $x$ -axis twice in each orbital period, the corresponding orbits of the elliptic problem for zero eccentricity of the primaries have multiplicity equal to  $m-1$ , and period  $2\pi$ .

The vertical stability index for the orbits of series  $f_{v1m}^1$  is given by

$$a_v = \cos(2\pi/m); \quad (7.29)$$

thus the value of  $a_v$  for the  $e = 0$  orbit equivalent to an  $(m-1)$ -fold description of the commensurability  $1/(m-1)$  orbit is

$$a_v = \cos \frac{2\pi(m-1)}{m} = \cos\left(\frac{2\pi}{m}\right). \quad (7.30)$$

The orbits of the elliptic series obtained by continuation from the  $e = 0$  orbits therefore have, in this particular case, the same value of the vertical stability index as the orbits of the circular series from which they originate. (This is not the case in general for elliptic series generated from other commensurabilities).

It was shown in Chapter 6 that there are always two distinct ways of

continuing a commensurable orbit of the planar circular case of the restricted problem into the elliptic case, giving rise to two families of periodic orbits. It is found that this is still the case when instead of fixing the mass parameter  $\mu$ , we allow  $\mu$  to vary and keep the vertical stability index  $a_v$  constant, as confirmed by the results of numerical continuation. The two series of vertical self-resonant orbits of the elliptic problem generated from each of the four commensurable orbits already mentioned can be classified as consisting of "conjunction" and "opposition" orbits, according to whether the massless particle is at the conjunction or opposition axis-crossing at periapsis of the primaries.

Representative orbits of the eight elliptic series are given in Tables 7.5 - 7.12. Those marked with the letter "S" satisfy the stability criteria in terms of the (horizontal) stability indices  $p$  and  $q$ , as defined in Chapter 3 (the orbits are, of course, automatically vertically stable since they are vertical self-resonant). The characteristics of the eight series are projected, in four pairs, in the  $(\mu, e)$ -plane in Figures 7.2 - 7.5; it is seen that in each of the four projections, the two curves representing the two series originating from the same commensurable orbit are distinct, and only intersect at the starting point on the  $\mu$ -axis. Of the eight series investigated, one (the opposition series arising from the  $1/4$  commensurability of series  $f_{v15}^1$ ) has been determined in its entirety, starting and finishing at  $e = 0$  in commensurable orbits of the circular restricted problem. The termination orbit of this series, corresponding to the last entry of Table 7.6, has been identified as a vertical self-resonant quadruple-periodic orbit, of period  $2\pi$ , belonging to the horizontal branch  $h_{14}$  of family  $h$ , for  $\mu = 0.798528$ . This orbit is in the commensurability  $1/1$ , and so corresponds to Case 2 of Table 6.1; by contrast, the starting orbit of the series is in the commensurability  $1/4$  and so comes under Case 3. From the considerations of Section 6.2, the termination orbit of the opposition series generated from the  $1/4$  commensurability of series  $f_{v15}^1$  must also be the termination of another vertical bifurcation series of the elliptic restricted problem: it can be predicted that the orbits of this second series will be quadruple-periodic (that is, of multiplicity four), of period  $2\pi$ , and have vertical stability index  $a_v = \cos(2\pi \cdot 4/5) = \cos 2\pi/5$ .

The remaining seven of the eight vertical bifurcation series have not

Table 7.5: Conjunction series generated from 1/4 commensurability  
of series  $f_{v15}^1$

$\mu$	e	$s_{01}$	$s_{05}$	
0.248314	0	0.472798	1.291561	S
0.248534	0.01	0.472271	1.290604	S
0.253802	0.05	0.464037	1.294139	S
0.270107	0.1	0.440868	1.314740	S
0.331498	0.2	0.361349	1.398568	S
0.421149	0.3	0.260280	1.517923	S
0.535145	0.4	0.161182	1.688813	
0.7	0.489840	0.115764	2.293181	
0.8	0.496910	0.146384	4.436017	
0.831	0.479279	0.147331	7.167914	

Table 7.6: Opposition series generated from 1/4 commensurability  
of series  $f_{v15}^1$

$\mu$	e	$s_{01}$	$s_{05}$	
0.248314	0	1.047901	-1.230261	
0.248533	0.01	1.053509	-1.220206	
0.253362	0.05	1.074192	-1.191696	
0.266002	0.1	1.096202	-1.178297	
0.309967	0.2	1.133414	-1.202482	
0.456048	0.4	1.221498	-1.374554	
0.689678	0.6	0.974782	-1.577432	
0.894119	0.7034	0.668962	-1.751216	
0.925561	0.6	0.481090	-1.904443	
0.890170	0.4	0.397658	-2.151547	
0.835776	0.2	0.368427	-2.536875	
0.811982	0.1	0.347668	-2.913524	
0.803765	0.05	0.330110	-3.232135	
0.799349	0.01	0.311161	-3.621237	
0.798528	0	0.305617	-3.750011	

Table 7.7: Conjunction series generated from 1/5 commensurability of series  $f_{v16}^1$

$\mu$	e	$s_{01}$	$s_{05}$	
0.142845	0	0.660935	1.091047	S
0.143088	0.01	0.660367	1.090470	S
0.148663	0.05	0.650949	1.098563	S
0.164358	0.1	0.625321	1.125512	S
0.219340	0.2	0.540274	1.215449	S
0.302355	0.3	0.425504	1.338987	S
0.411266	0.4	0.299819	1.495404	S
0.6	0.512910	0.174536	1.922996	
0.6504	0.523302	0.173432	2.218021	

Table 7.8: Opposition series generated from 1/5 commensurability of series  $f_{v16}^1$

$\mu$	e	$s_{01}$	$s_{05}$	
0.142845	0	1.061117	-1.056091	
0.143088	0.01	1.064847	-1.045897	
0.148591	0.05	1.078101	-1.019868	
0.163173	0.1	1.091611	-1.013090	
0.210321	0.2	1.113007	-1.049783	
0.381515	0.4	1.158275	-1.244332	
0.586859	0.6	1.253105	-1.523084	
0.92	0.775348	0.656820	-1.757868	
0.922962	0.6	0.416882	-1.984365	
0.868000	0.4	0.357462	-2.324362	
0.809649	0.2	0.317321	-3.127789	

Table 7.9: Conjunction series generated from 1/6 commensurability of series  $f_{v17}^1$

$\mu$	e	$s_{01}$	$s_{05}$	
0.069361	0	0.795600	0.876150	S
0.069578	0.01	0.794735	0.874771	S
0.074683	0.05	0.784126	0.886270	S
0.089797	0.1	0.756446	0.929417	S
0.144050	0.2	0.665299	1.057728	S
0.225641	0.3	0.540810	1.202762	S
0.331432	0.4	0.398821	1.360044	S
0.466610	0.5	0.257891	1.568840	
0.63	0.561323	0.192168	2.142006	

Table 7.10: Opposition series generated from 1/6 commensurability of series  $f_{v17}^1$

$\mu$	e	$s_{01}$	$s_{05}$	
0.069361	0	1.069040	-0.857718	
0.069578	0.01	1.071215	-0.850049	
0.074680	0.05	1.079156	-0.837612	
0.089654	0.1	1.087714	-0.852733	
0.141306	0.2	1.100785	-0.928530	
0.321767	0.4	1.120038	-1.150328	
0.566843	0.6	1.218315	-1.455623	
0.935	0.822902	0.668607	-1.760727	
0.918617	0.6	0.373237	-2.069433	
0.854023	0.4	0.320618	-2.572262	
0.801126	0.2	0.266733	-4.287916	

Table 7.11: Conjunction series generated from 1/7 commensurability of series  $f_{v18}^1$

$\mu$	e	$s_{01}$	$s_{05}$	
0.012455	0	0.919231	0.505337	S
0.012682	0.01	0.918101	0.505891	S
0.017989	0.05	0.902066	0.558251	S
0.033579	0.1	0.864799	0.674571	S
0.089559	0.2	0.760036	0.905602	S
0.172819	0.3	0.626392	1.096608	S
0.279054	0.4	0.472538	1.266789	S
0.407365	0.5	0.315317	1.450562	S
0.6	0.593254	0.191352	1.928257	

Table 7.12: Opposition series generated from 1/7 commensurability of series  $f_{v18}^1$

$\mu$	e	$s_{01}$	$s_{05}$	
0.012455	0	1.056653	-0.500214	
0.012682	0.01	1.057739	-0.498882	
0.017989	0.05	1.065536	-0.541214	
0.033572	0.1	1.077258	-0.637357	
0.089010	0.2	1.091487	-0.813790	
0.276286	0.4	1.095355	-1.082563	
0.544082	0.6	1.160130	-1.386880	
0.95	0.855548	0.666145	-1.771335	

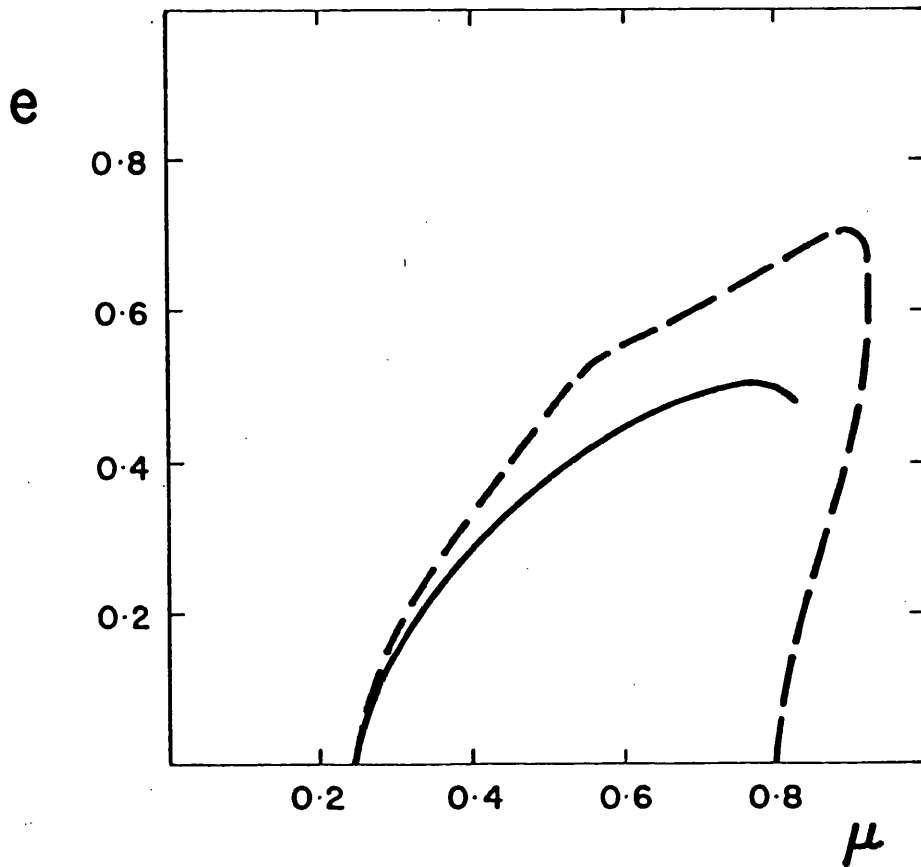


Figure 7.2 : Characteristics of the conjunction (—) and opposition (----) series generated from the 1/4 commensurability of series  $f_{v15}^1$ .

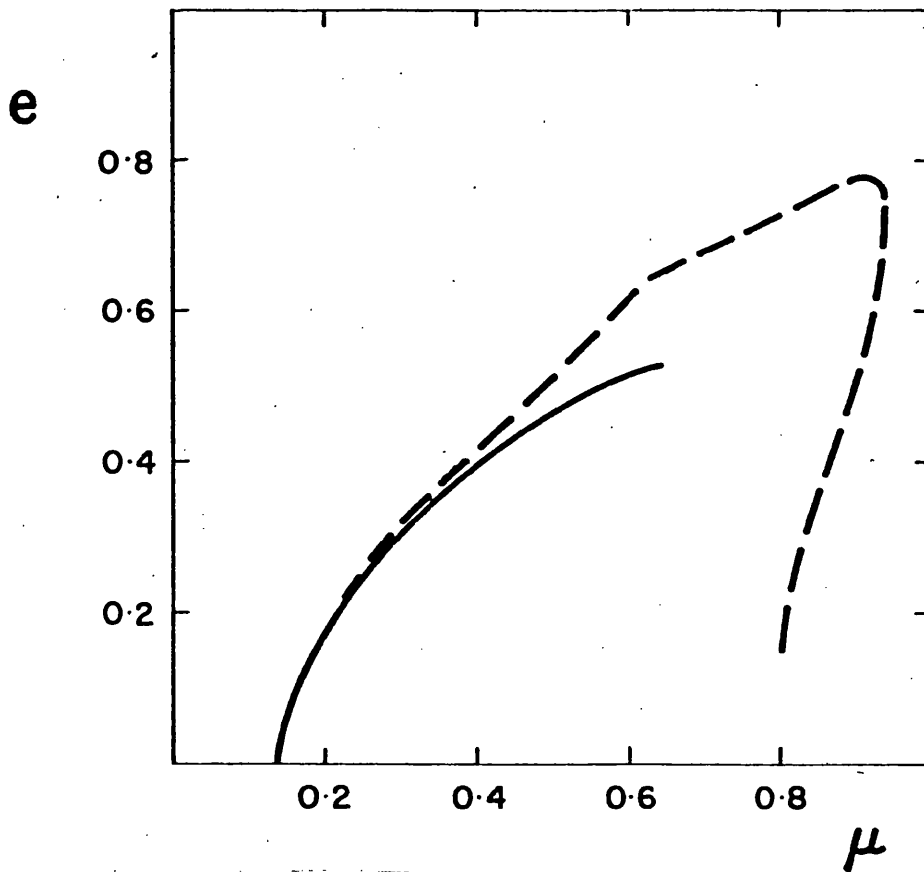


Figure 7.3 : Characteristics of the conjunction (—) and opposition (----) series generated from the 1/5 commensurability of series  $f_{v16}^1$ .

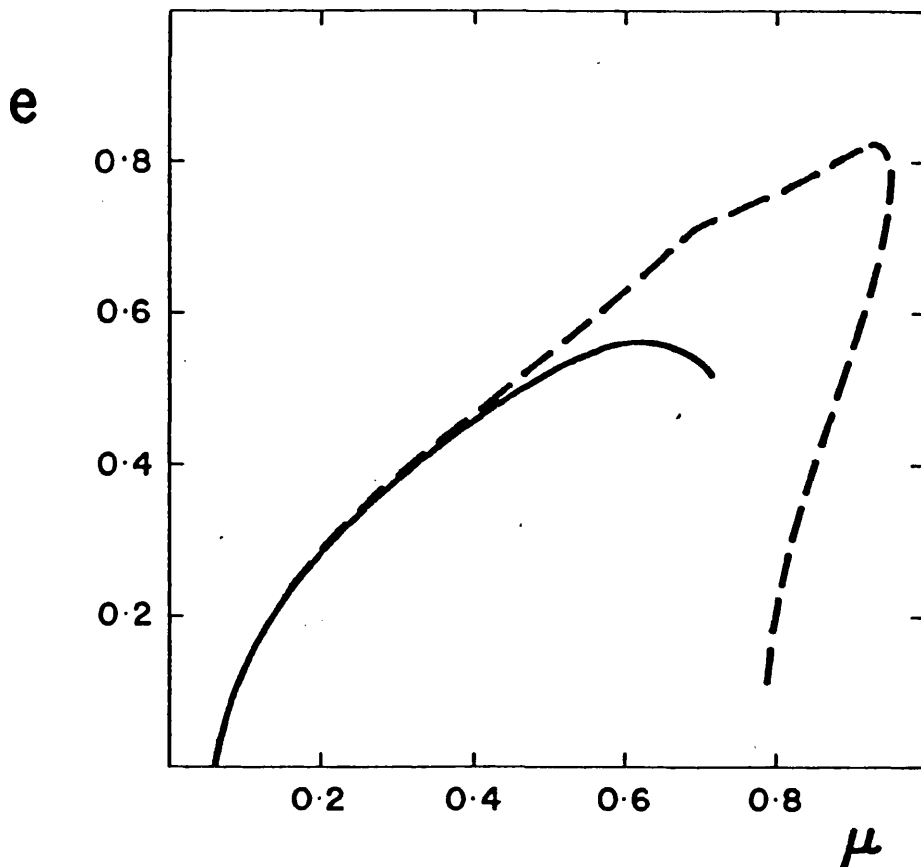


Figure 7.4 : Characteristics of the conjunction (—) and opposition (----) series generated from the 1/6 commensurability of series  $f_{v17}^1$ .

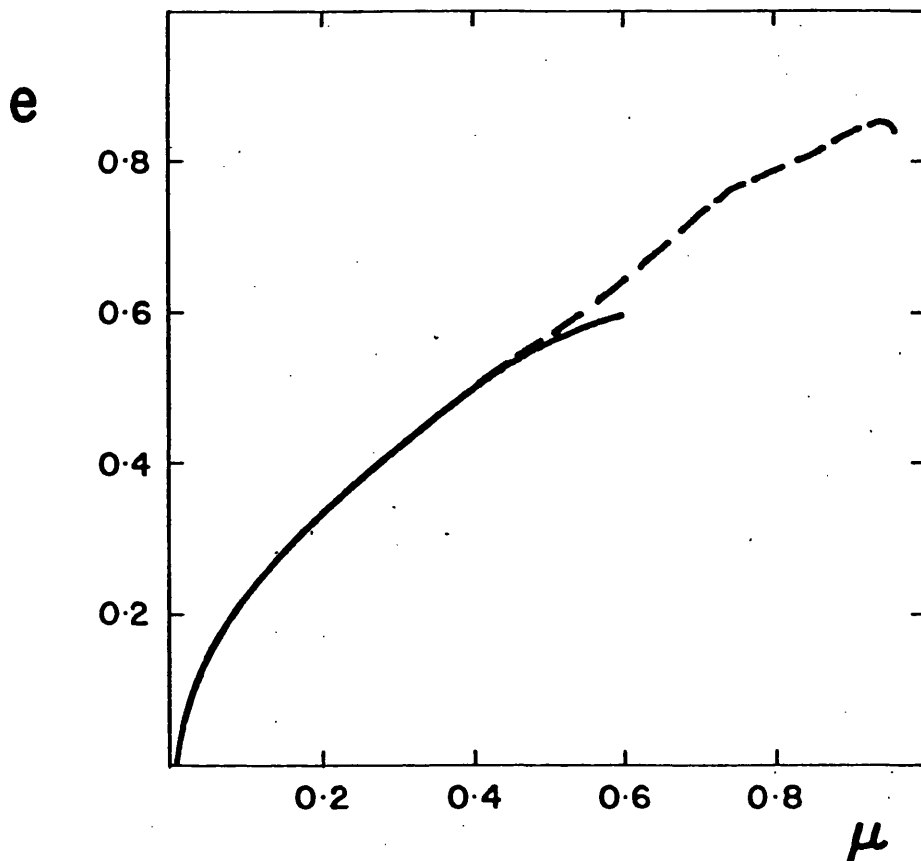


Figure 7.5 : Characteristics of the conjunction (—) and opposition (----) series generated from the 1/7 commensurability of series  $f_{v18}^1$ .

been completely determined, because of numerical difficulties resulting from close approaches of the orbits to the primary  $m_2$ . It is thought likely that the "opposition" series terminate at  $e = 0$  without passing through collision orbits, although very close approaches to the primary  $m_2$  may occur. By contrast, all four of the "conjunction" series appear to terminate at non-zero values of the eccentricity in collision orbits with  $m_2$ ; continuation of these series through the collision would require regularisation of the equations of motion and the vertical stability equations.

Representative orbits of the conjunction and opposition series generated from the  $1/4$  commensurability of series  $f_{v15}^1$  are plotted in Figures A49 - A56, in the Appendix.

### 7.5 Further Results

The elliptic series discussed in Section 7.4 were obtained by continuing commensurable, vertical self-resonant orbits of the circular restricted problem into the elliptic problem, starting from  $e = 0$  and progressing to non-zero values of the eccentricity of the primaries. This technique has the limitation that it can only be used to establish elliptic series which have members corresponding to  $e = 0$ ; we now offer an example of a vertical bifurcation series of the elliptic restricted problem which has no  $e = 0$  orbit, and is therefore not directly accessible from the circular restricted problem. The starting orbit of this series, corresponding to the value  $\mu = 0.5$  of the mass parameter, and  $e \approx 0.43$ , was computed by Dr. V. Markellos as a result of his work in the general three-body problem. The series is designated  $\ell_{3v}$  because it is uniquely linked with the vertical-critical orbit  $\ell_{3v}$  of the planar circular problem for  $\mu = 0.5$  (Henon, 1973b) via the vertical bifurcation series  $\ell_{3v}$  of the general three-body problem (Markellos, 1980).

The series comprises orbits of Strömberg's class  $\ell$ , that is, orbits around both primaries, the sense of motion being retrograde with respect to the rotating frame and direct with respect to the inertial frame; numerical data are given in Table 7.13. The orbits are simple-periodic and have period  $T = 4\pi$ , corresponding to the  $2/1$  commensurability with the period of the primaries, and since the mirror configurations always occur at periapsis of the primaries ( $\theta_0 = 0$ ), this is a "periapsis" series.

Table 7.13:      The vertical bifurcation series  $\ell_{3v}$   
( $a_v = +1$ ) of the elliptic restricted problem

$\mu$	$e$	$s_{01}$	$s_{05}$
0.0005	0.474482	-3.676451	3.296529
0.001	0.474381	-3.675084	3.295131
0.005	0.473651	-3.664845	3.284699
0.01	0.472755	-3.652185	3.271796
0.02	0.470998	-3.627222	3.246337
0.05	0.466000	-3.554960	3.172487
0.1	0.458544	-3.442727	3.057261
0.15	0.452104	-3.339674	2.950737
0.2	0.446620	-3.244768	2.851826
0.25	0.442044	-3.157139	2.759597
0.3	0.438341	-3.076047	2.673245
0.35	0.435485	-3.000858	2.592067
0.4	0.433457	-2.931017	2.515438
0.45	0.432245	-2.866038	2.442796
0.5	0.431842	-2.805485	2.373630

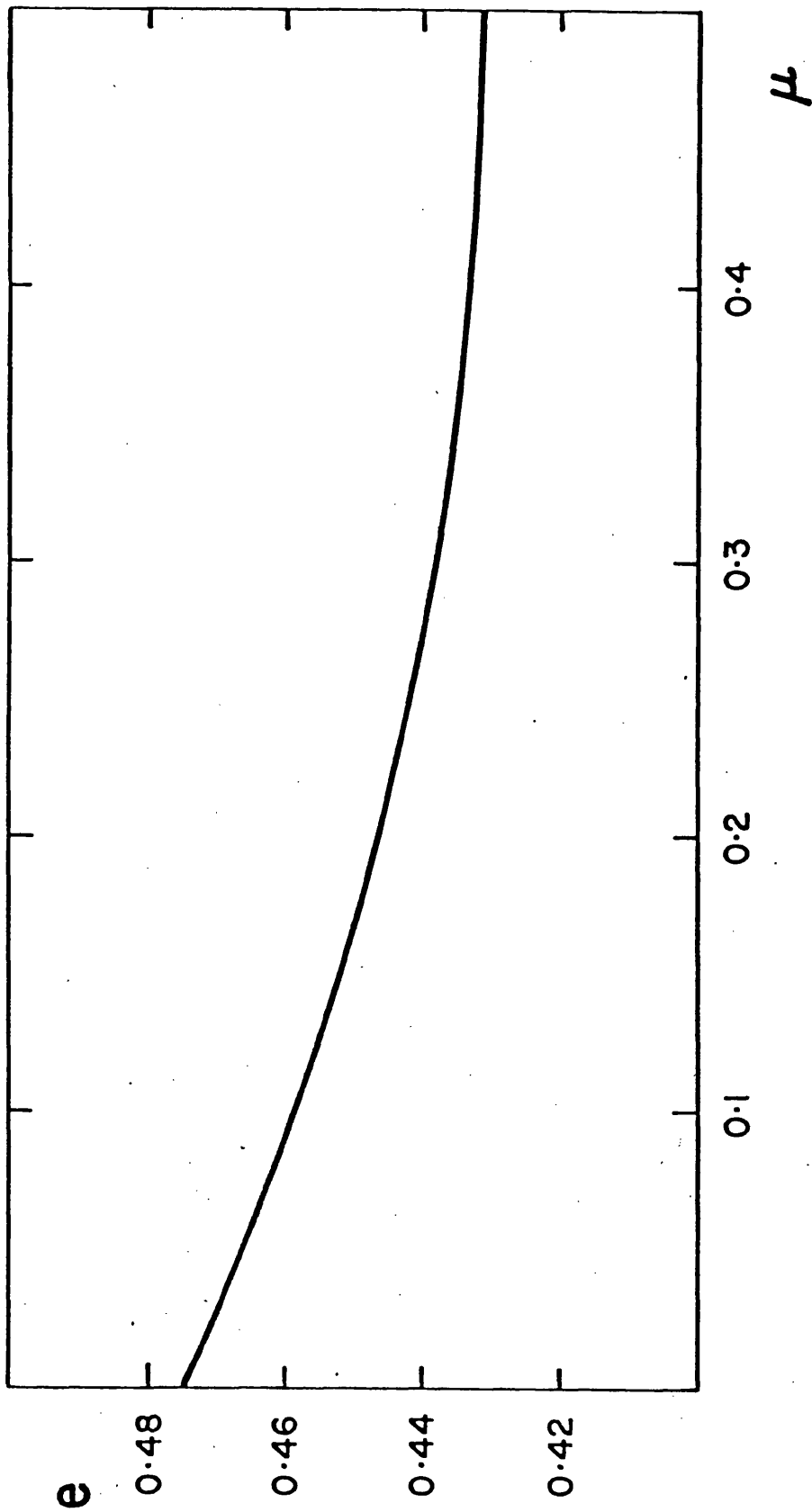


Figure 7.6 : Characteristic of vertical bifurcation series  $e_{3v}$  of the elliptic restricted problem projected in the  $(\mu, e)$ -plane.

The vertical stability index has the constant value  $a_v = +1$  along the series, and the parameter  $B_v$  is zero; thus, a single family of axisymmetric periodic orbits of the three-dimensional elliptic restricted problem branches from each orbit of the series (see Section 3.6).

It can be seen from Table 7.13 that over the entire range of values of the mass parameter from almost zero to  $\mu = \frac{1}{2}$ , the eccentricity  $e$  of the primaries varies only slightly between about 0.43 and 0.47 (see also Figure 7.6); in particular, as already emphasised, since  $e$  never reaches zero, the series does not connect directly with the circular problem via a commensurable, vertical-critical orbit. The special symmetry property of the orbits of Strömberg's class  $\mathcal{L}$  in the planar circular problem, whereby the orbits for  $\mu > \frac{1}{2}$  are identical (apart from a  $180^\circ$  rotation about the origin) to those for  $\mu < \frac{1}{2}$  (Hénon and Guyot, 1970), applies also in the elliptic restricted problem, and the  $\mu = \frac{1}{2}$  orbit of the series is symmetrical with respect to both coordinate axes.

The termination orbit of the series  $\mathcal{L}_{3v}$ , corresponding to  $\mu = 0$ , is an elliptical orbit of the two-body problem, of period  $4\pi$ ; we conclude that the series comprises orbits of Poincaré's second kind. Calculation of the stability indices showed that the series consists entirely of horizontally unstable orbits.

The determination of a series of vertical self-resonant orbits in either the circular or elliptic cases of the restricted problem allows an infinite number of families of symmetric three-dimensional periodic orbits to be found, since a vertical branch can be started from any member orbit of the series. This can be done by keeping the mass parameter fixed along a given branch and allowing the orbital period or eccentricity of the primaries to vary, using the numerical techniques described in Chapter 4.

In the determination of three-dimensional periodic orbits of the elliptic restricted problem, the continuation of vertical bifurcation orbits into three dimensions is an alternative approach to that described in Chapter 6, in which commensurable three-dimensional orbits of the circular problem are continued into the elliptic problem by increasing the eccentricity  $e$  from zero to non-zero values. In order to illustrate the continuation of periodic orbits of the planar elliptic problem into three dimensions, two orbits belonging to the series  $\mathcal{L}_{3v}$  were selected and the initial

Table 7.14: The family of three-dimensional periodic orbits of the elliptic restricted problem branching from series  $\ell_{3v}$  for  $\mu = 0.01$ .

e	$s_{01}$	$s_{05}$	$s_{06}$
0.472753	-3.652176	3.271788	0.001
0.472750	-3.652151	3.271765	0.002
0.472736	-3.652050	3.271672	0.004
0.472714	-3.651881	3.271517	0.006
0.472682	-3.651646	3.271301	0.008
0.472641	-3.651343	3.271023	0.010

Table 7.15: The family of three-dimensional periodic orbits of the elliptic restricted problem branching from series  $\ell_{3v}$  for  $\mu = 0.4$ .

e	$s_{01}$	$s_{05}$	$s_{06}$
0.433456	-2.931013	2.515435	0.001
0.433454	-2.931000	2.515425	0.002
0.433444	-2.930951	2.515384	0.004
0.433428	-2.930869	2.515316	0.006
0.433405	-2.930754	2.515220	0.008
0.433376	-2.930606	2.515098	0.010

segment of the vertical branch arising from each orbit was determined. The two orbits used were those corresponding to the values  $\mu = 0.01$  and  $\mu = 0.4$  of the mass parameter (see Table 7.13); numerical data for the two branches are presented in Tables 7.14 and 7.15.

Since the vertical stability index of the orbits of series  $\ell_{3v}$  is  $a_v = +1$ , we have a "simple bifurcation": the three-dimensional orbits are of the same multiplicity as the planar orbits, and are therefore simple-periodic. The orbital period is also the same as that of the vertical-critical orbits, equal to  $4\pi$ . The branch orbits have their perpendicular crossings of the x-axis (type (A) mirror configurations) when the primaries are at periapsis, as is the case for the planar orbits. Both of the vertical branches were traced out of the horizontal plane by using the initial z-velocity  $s_{06}$  as the family parameter, to ensure that genuinely three-dimensional orbits were obtained. Stability calculations for the three-dimensional orbits indicated that these are all unstable, as would be expected from the fact that the bifurcation orbits are unstable.

## 8. BIFURCATION IN THREE DIMENSIONS

### 8.1 Introduction

The major part of the work presented in this thesis is concerned with the phenomenon of vertical bifurcation: that is, the bifurcation of planar with three-dimensional periodic orbits of the restricted problem. Analytical and numerical study of vertical bifurcation is greatly facilitated by the special property of separability of the variational matrix into "horizontal" and "vertical" parts and the corresponding decoupling of the variational equations. This particular type of bifurcation is also important because it leads to the generalisation into three dimensions of existing numerical results in the planar restricted problem, and allows genealogical relationships to be established between families of three-dimensional periodic orbits and the planar families from which they may be generated. A study of the structure of periodic solutions of the restricted problem would be incomplete, however, without some mention being made of the more general type of bifurcation of families of symmetric periodic orbits, that is, bifurcation in three dimensions. In this chapter we present some preliminary numerical results illustrating the occurrence of this type of bifurcation.

The two examples of three-dimensional bifurcation discussed in the next section were discovered as a result of numerical investigations of the family  $F_{v15}^{1(p)}$ , one of the vertical branches of family  $f$  discussed in Chapter 5. This family has the peculiar property of turning back on itself at a certain point in three dimensions, rather than returning to the horizontal plane and connecting with a family of planar orbits, as do the other branches described in Chapter 5. The effective termination orbit of the branch was found to be a twofold description of a plane symmetric, simple-periodic orbit, belonging to an unknown family of such orbits bifurcating with the family  $F_{v15}^{1(p)}$  in three dimensions. It was decided to investigate this family numerically with a view to its identification; the results of this investigation are presented in the next section.

The general condition for the occurrence of a bifurcation of two families of periodic orbits was given in Section 3.5 as (Equation (3.69))

$$k = -2 \cos (2\pi n/m), \quad (8.1)$$

where  $k$  is one of the linear stability indices, and  $m, n$  are integers. In the present case, we have a double bifurcation: the termination orbit of  $F_{v15}^{1(p)}$  has double the multiplicity and twice the period of the bifurcation orbit. This corresponds to the values  $m = 2, n = 1$  in Equation (8.1), giving  $k = +2$ ; direct calculation of the stability indices of the simple-periodic bifurcation orbit gave a value of one of the indices in agreement with this prediction. (One of the stability indices of the termination orbit of the vertical branch  $F_{v15}^{1(p)}$  was found to be equal to  $-2$ , as would be expected from Equation (3.67), with  $m = 2$ ). The use of Equation (8.1) in identifying probable three-dimensional bifurcation orbits will be discussed further in Section 8.3.

## 8.2 Numerical Results

The three-dimensional bifurcation orbit corresponding to the termination of the vertical branch  $F_{v15}^{1(p)}$  was continued numerically in order to trace out the family of plane symmetric orbits to which it belongs. Since this orbit is somewhere in the "middle" of the family, it was necessary to continue it in two opposite directions so that the two "ends" of the family could be found. Numerical data for the family are given in Table 8.1; the bifurcation orbit with family  $F_{v15}^{1(p)}$ , corresponding approximately to the entry marked with an asterisk, is plotted in Figure A60 in the Appendix (see also Figure 8.1).

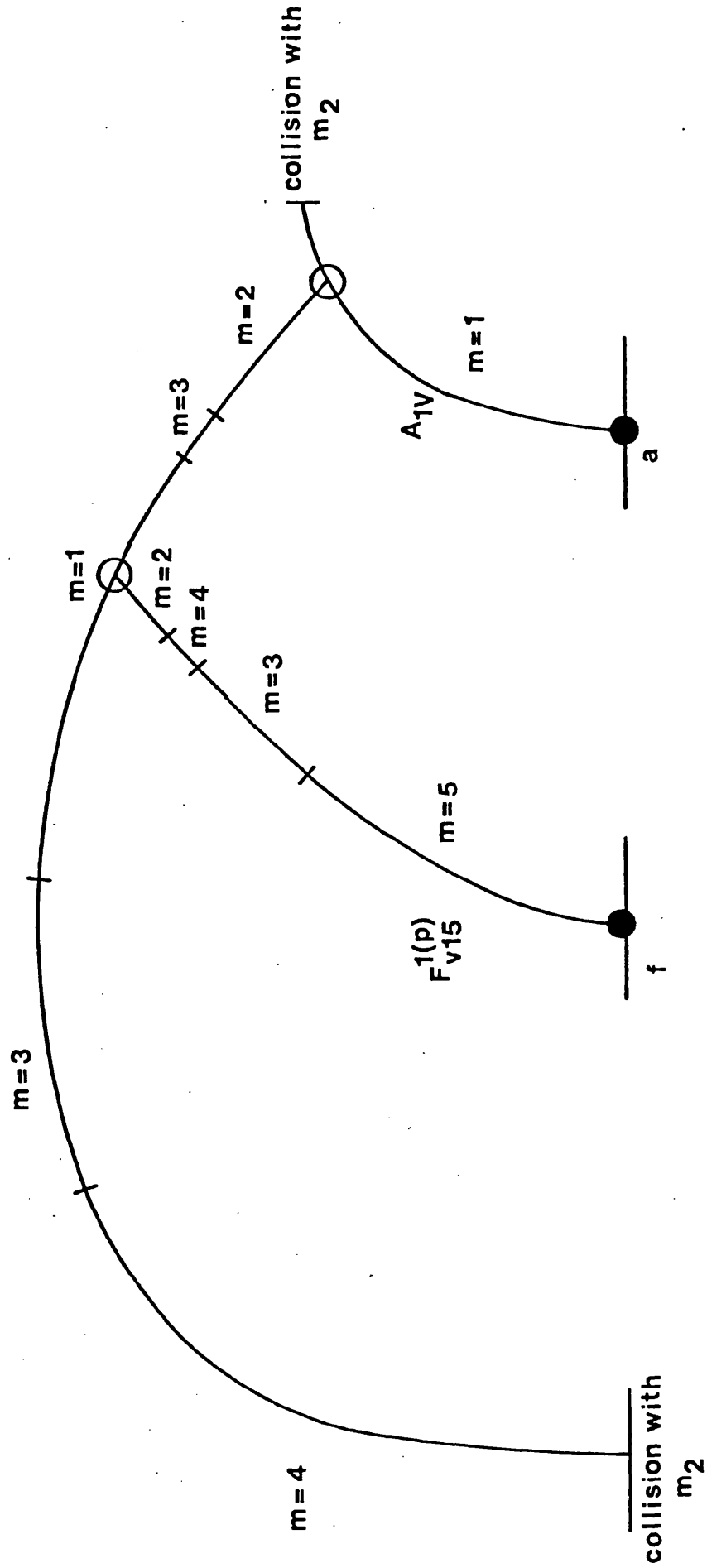
It was found that continuation along the family from the bifurcation towards lower values of the orbital period  $T$  results firstly in an increase in the multiplicity from 1 to 3, and shortly after in a drop in multiplicity from 3 to 2. Continuing in this direction, a "reflection" orbit is encountered: that is, the family begins to turn back on itself, the turning point or "reflection" occurring when the two type (P) mirror configurations defining the orbits become exactly coincident. As in the case of family  $F_{v15}^{1(p)}$  (Section 5.2), this indicates a bifurcation with another family of three-dimensional periodic orbits. The termination orbit at this bifurcation, corresponding approximately to the first entry of Table 8.1, is a twofold description of a simple-periodic, plane symmetric orbit. Investigation showed that this orbit belongs

Table 8.1 Family of Plane Symmetric Periodic Orbits Bifurcating with Family  $F_{v15}^{1(p)}$  in Three Dimensions ( $\mu = 0.00095$ )

$s_{01}$	$s_{03}$	$s_{05}$	T	C	m
1.005886	0.074370	-0.021505	2.635984	3.016876	2
1.019954	0.073142	-0.019252	2.740713	3.018044	2
1.032667	0.066788	0.000597	3.276811	3.021852	3
1.034431	0.064560	0.013472	3.613052	3.022704	1 *
1.022965	0.066370	0.063599	4.847426	3.017639	1
1.012989	0.068787	0.084693	5.417080	3.013106	3
0.959727	0.111152	0.136418	10.002877	2.985634	3
0.903315	0.376199	0.145344	12.304728	2.840827	4
0.860711	0.470564	0.181885	12.416191	2.747747	4
0.723696	0.666794	0.310978	12.511294	2.459661	4
0.292082	0.942179	0.735518	12.555049	1.571928	4
0.008672	0.986447	1.017379	12.561477	0.992779	4
-0.440717	0.880630	1.466559	12.566355	0.075419	4
-0.802063	0.560049	1.832139	12.571112	-0.667305	4
-0.626735	0.764444	1.648865	14.291673	-0.301416	4

**Figure 8.1 :** Schematic representation of families of plane symmetric periodic orbits connected with family  $F_{v15}^1(p)$  through bifurcations in three dimensions. Each family is divided into segments of various multiplicities  $m$ .

● vertical bifurcation  
○ three-dimensional bifurcation



to a vertical branch of the planar family  $a$  (periodic orbits around the Lagrange collinear equilibrium point  $L_1$ ). The vertical bifurcation orbit of family  $a$  from which this branch is generated was found to be the vertical-critical orbit  $a_{1v}$  (in the notation of Hénon, 1973b), that is, the first vertical-critical orbit of family  $a$  to be encountered as the family evolves from infinitesimal orbits around  $L_1$ ; the vertical branch was therefore designated  $A_{1v}$ , following the notation of Zagouras and Markellos (1977).

Numerical data for the family  $A_{1v}$  are given in Table 8.2; the letter "S" indicates orbital stability, and the entry marked with an asterisk corresponds approximately to the bifurcation orbit, which once again has a stability index equal to +2 (double bifurcation). The bifurcation orbit is plotted in Figure A57 in the Appendix. The family  $A_{1v}$  appears to terminate in a collision orbit with the primary  $m_2$  shortly after this bifurcation; it is interesting to note that the highly-inclined, highly-eccentric orbits of the final segment of family  $A_{1v}$  are linearly stable, despite the close approach to the primary  $m_2$ .

On continuing the first (as yet unidentified) family in the other direction from its bifurcation with the vertical branch  $F_{v15}^{1(p)}$  towards increased values of the orbital period, two further multiplicity regimes (multiplicity 3 and 4) are encountered. There is a radical change in the characteristics of the orbits along the family, as illustrated by the series of orbit plots at intervals along the family given in Figures A58 - A69 in the Appendix; this can also be seen from the entries of Table 8.1. Beginning with essentially satellite orbits around the less massive primary  $m_2$  (Jupiter), these eventually become orbits of the planetary type about the more massive primary  $m_1$  (Sun); the motion in these later orbits is very nearly circular Keplerian motion except for a short interval of each orbit in which the massless particle has a close encounter with the primary  $m_2$  and experiences a significant perturbation. As the family evolves towards termination, the orbits develop two distinct parts, one very nearly planar and the other three-dimensional (see Figure A69). The massless particle, initially in an almost planar orbit, has a close approach above the primary  $m_2$ , which sends it into a highly-inclined orbit about  $m_1$  (rather reminiscent of an out-of-ecliptic mission orbit). The three-dimensional part of the orbit comprises three loops, one above and two below the horizontal plane, connecting together close

Table 8.2 Family  $A_{1V}$  of Plane Symmetric Orbits ( $\mu = 0.00095$ )

$s_{01}$	$s_{03}$	$s_{05}$	T	C	m
1.077821	0.002685	-0.063143	3.223310	3.034961	1
1.077724	0.007685	-0.064083	3.221611	3.034687	1
1.075305	0.032685	-0.077965	3.186339	3.029728	1
1.060668	0.071685	-0.099939	2.925641	3.013929	1
1.038612	0.084742	-0.086509	2.220504	3.008201	1 S
1.015666	0.080156	-0.045509	1.551854	3.013027	1
1.005699	0.074365	-0.021443	1.317964	3.016876	1 *
1.003954	0.072271	-0.016831	1.263272	3.018046	1 S
1.000240	0.060880	-0.006112	1.007276	3.024640	1 S
0.999723	0.055880	-0.004299	0.898827	3.028026	1 S

Table 8.3 Family of Plane Symmetric Periodic Orbits Generated from a Quadruple Bifurcation with Family  $A_{1V}$  ( $\mu = 0.00095$ )

$s_{01}$	$s_{03}$	$s_{05}$	T	C	m
1.000115	0.059951	-0.005711	3.948288	3.025239	4
1.000215	0.059952	-0.005688	3.948255	3.025239	4
1.000415	0.059955	-0.005643	3.948314	3.025239	4
1.000823	0.059958	-0.005549	3.948429	3.025241	4
1.001619	0.059956	-0.005362	3.948926	3.025247	4

to the primary  $m_2$ . Eventually, the massless particle has another close encounter with  $m_2$  which renders the motion once again very nearly planar. It seems likely that the family terminates in a planar collision orbit with  $m_2$ ; the termination orbit has not been identified.

Calculation of the stability indices of the orbits of this unidentified family indicated that they are all unstable, the degree of instability becoming very high towards the termination orbit.

### 8.3 Remarks

(1) The numerical results given in the previous section illustrate the importance of three-dimensional bifurcation in the structure of periodic orbits. We saw in Chapter 5 that the planar families  $f$ ,  $g_1$  and  $g_2$  are connected through vertical bifurcation with families of three-dimensional periodic orbits; the link between families  $f$  and  $a$  discussed in the previous section, however, involves both vertical and three-dimensional bifurcations. The unidentified family which bifurcates with the vertical branches  $A_{1v}$  and  $F_{v15}^1(p)$  cannot be established from a vertical self-resonant orbit, and it seems likely that this is merely one example of a whole class of such families generated from bifurcations in three dimensions. There is clearly a great deal of scope for further investigation in this area.

(2) The families mentioned in Section 8.2 all consist of plane symmetric orbits. It is easy to see that in a bifurcation of two families of three-dimensional symmetric periodic orbits, the symmetry properties of the orbits of both families must be the same, since the type of mirror configuration cannot alter. Thus, a family of plane symmetric orbits can only bifurcate with another plane symmetric family, and an axisymmetric family with another axisymmetric family; one of the families, however, may have additional symmetry, and bifurcations of simply-symmetric with doubly-symmetric families would appear to be possible.

(3) The first-order treatment of bifurcation outlined in Section 3.5 predicts the occurrence of infinite numbers of bifurcations along those segments of families of three-dimensional periodic orbits for which one of the stability indices satisfies the stability criterion. Note that this does not require actual stability of the orbits, since the other

indices need not satisfy the stability criterion (for example, in the special case of vertical bifurcations, a family of three-dimensional orbits can arise from a horizontally unstable planar orbit). The denseness of bifurcations of periodic orbits, related to Poincaré's famous conjecture (Vol. I of "Méthodes Nouvelles"), has been discussed by Katsiaris and Goudas (1973).

(4) The results presented in this chapter are of a preliminary nature, providing numerical evidence for the occurrence of families of symmetric periodic orbits in three dimensions. Clearly, an analytical theory of three-dimensional bifurcation is required, and there is a large amount of scope for numerical investigation of the phenomenon. The general bifurcation condition (Equation (8.1)) can be used to identify probable bifurcation orbits, and indicates the order of the bifurcation (that is, the value of the integer  $m$ ); the bifurcation condition is not specific to symmetric periodic orbits, however, and an analysis similar to that of Section 3.6, exploiting the property of orbital symmetry, would allow detailed predictions about the mechanism of bifurcation in the case of symmetric orbits.

The possibility of the occurrence of bifurcation of higher order than the second, that is, bifurcation from a self-resonant, non-critical orbit with one stability index satisfying Equation (8.1) for  $m \geq 2$ , was investigated numerically. An orbit belonging to the family  $A_{1v}$  (Table 8.2) with one stability index equal to zero ( $m = 4$ ,  $n = 1$  in Equation (8.1)) was chosen for this purpose. This orbit belongs to the stable final segment of the family, and falls between the last two entries of Table 8.2. Attempts to establish numerically a family of quadruple-periodic plane symmetric orbits in the neighbourhood of the predicted bifurcation yielded the results given in Table 8.3, which contains orbits belonging to the initial segment of the family in the neighbourhood of the bifurcation. In order to check that this family does in fact originate from a bifurcation in three dimensions, the family was traced back towards the starting orbit. The characteristic "reflection" phenomenon was once again encountered, the parameters of the reflection orbit corresponding closely to those of the bifurcation orbit of family  $A_{1v}$ ; this was considered to be a satisfactory confirmation of the occurrence of the bifurcation.

The final orbit of Table 8.3 is plotted in Figure A70, in the Appendix.

## 9. SUGGESTIONS FOR FURTHER WORK

(1) As has already been pointed out, the planar case of the restricted problem has been explored much more extensively than the three-dimensional case. A great deal of work remains to be done in the generalisation of existing numerical information on the periodic orbits of the planar circular problem into three dimensions, by tracing the vertical branches of families of planar orbits.

There is a similar paucity of numerical results on the periodic orbits of the elliptic restricted problem, particularly in the three-dimensional case, and it is clear from the discussion of Chapters 6 and 7 that there is an abundance of suitable starting orbits for continuation from the circular into the elliptic problem, and from the planar to the three-dimensional elliptic problem. A major computational effort is required to map out the families of periodic orbits obtainable by these methods, and to survey the stability and other properties of the orbits.

(2) The possibility of establishing series of periodic orbits parametrised by the mass parameter  $\mu$  has been dealt with in Chapters 3 and 7, but has not been discussed in detail. Hénon and Guyot (1970) have presented a survey of the (horizontal) stability of planar periodic orbits of the circular restricted problem for all possible values of the mass parameter  $0 \leq \mu \leq 1$ , and other authors (e.g. Benest, 1976, 1977; Broucke, 1968, 1969; Shelus, 1972; Hénon, 1973a; Katsiaris, 1972; Markellos et al., 1974, 1975a, b) have considered the effect of varying the mass parameter on the structure and stability of periodic orbits. This is another important area for numerical exploration; the significance of the mass parameter in the overall structure of the solutions of the restricted problem is underlined by the existence of certain critical values of  $\mu$  at which changes in the topology of the solution space take place (see, e.g. Markellos et al., 1974).

(3) Markellos (1974a, b, 1975), Markellos and Zagouras (1977) and Benest (1976, 1977) have investigated the relationship between linearly stable regions of families of periodic orbits and the stability properties (in a more general sense) of semi-periodic motion close to the periodic orbits. Further work (numerical and/or analytical) would be of great value in the application of results on the stability of periodic orbits

to real astronomical problems, such as the stability of the outer Jovian satellite system. An outstanding question worthy of some attention concerns the results reported by Hunter (1967) on the anomalous relationship between stability and inclination of retrograde satellites of Jupiter.

(4) The numerical computations presented in this thesis were performed using non-regularised equations, with the result that it was not possible to continue certain families and series of periodic orbits as far as or beyond collision with one of the primaries. In most cases, this is not a serious disadvantage, since a collision orbit represents a natural termination of a family of periodic orbits, and from the practical point of view, collision or near-collision orbits are of limited interest. From the mathematical point of view, however, it is important to establish connections between various families (or different phases of the same family) via collision orbits, and this necessitates the use of regularised equations. There is a substantial literature on the subject of regularisation; a detailed discussion of various methods, including regularisation techniques for the variational equations, has been given by Taylor (1979).

(5) The identification of the  $\mu = 0$  termination orbit of the vertical bifurcation series  $\mathcal{L}_{3v}$  of the elliptic restricted problem, described in Section 7.5, with an elliptic orbit of the two-body problem having a period commensurable with that of the primaries, and an eccentricity of about 0.47, raises the question of the continuation of elliptic Keplerian orbits into the restricted three-body problem, the mass parameter being increased from zero to non-zero values, in order to generate a series of vertical bifurcation orbits. The case of circular orbits has been considered by Hénon and Guyot (1970) and Hénon (1974); the four vertical bifurcation series of the circular problem given in Section 7.3 were found, in the limit  $\mu \rightarrow 1$ , to be vertical self-resonant circular orbits of the two-body problem. Commensurable elliptic two-body orbits, giving rise to periodic orbits of Poincaré's second kind, are known to be of critical stability and would therefore result in series of vertical-critical orbits upon continuation into the restricted problem. Further study of this type of analytical continuation would be an interesting and worthwhile exercise, leading to the possibility of establishing a connection between elliptic two-body orbits and three-dimensional periodic orbits of the elliptic restricted problem.

(6) The preliminary results of Chapter 8 indicate that three-dimensional bifurcations of families of periodic orbits are of great importance in the structure of symmetric periodic solutions of the restricted problem. Numerical and analytical work in this area would almost certainly lead to an improved understanding of the structure of periodic orbits (see the discussion of Section 8.3).

(7) A growing body of literature on the periodic orbits of the general three-body problem has appeared in recent years. One of the ways of determining such periodic orbits is by numerical continuation from the restricted problem, the mass of the third body of the system being increased from zero to non-zero values; results obtained by this method have been given by, for example, Hadjidemetriou and Christides (1975). This technique can be regarded as a further generalisation of the periodic orbits of the planar and three-dimensional cases of the restricted problem, in both the circular and elliptic cases, and there is again plenty of scope for further work.

## 10. REFERENCES

- Benest, D.: 1976, *Astron. Astrophys.* 53, 231  
1977, *Astron. Astrophys.* 54, 563
- Bray, T.A. and Goudas, C.L.: 1967, *Adv. Astron. Astrophys.* 5, 71
- Broucke, R.A.: 1968, J.P.L. Technical Report 32 - 1360  
1969, *A.I.A.A. Journal* 7, 1003
- Goudas, C.L.: 1961, *Bull. Soc. Math. Grèce, Nouv. Serie* 2, 1
- Hadjidemetriou, J.D. and Christides, T.: 1975, *Celest. Mech.* 12, 175
- Halioulias, A., Katsiaris, G.A. and Markellos, V.V.: 1976, *Astrophys. Space Sci.* 41, 417
- Hénon, M.: 1965a, *Ann. Astrophys.* 28, 499  
1965b, *Ann. Astrophys.* 28, 992  
1969, *Astron. Astrophys.* 1, 223  
1970, *Astron. Astrophys.* 9, 24  
1973a, *Celest. Mech.* 8, 269  
1973b, *Astron. Astrophys.* 28, 415  
1974, *Astron. Astrophys.* 30, 317
- Hénon, M. and Guyot, M.: 1970, in "Periodic Orbits, Stability and Resonances",  
p. 349, ed. G.E.O. Giacaglia, D. Reidel, Dordrecht
- Hindmarsh, A.C. and Byrne, G.D.: 1975, Report VCID-30112 of the Lawrence  
Livermore Laboratory, University of California
- Hunter, R.B.: 1966, Ph.D. Thesis, University of Glasgow  
1967, *Mon. Not. R. Astr. Soc.* 136, 245
- Katsiaris, G.: 1973, in "Recent Advances in Dynamical Astronomy", p. 118,  
ed. B.D. Tapley and V. Szebehely, D. Reidel, Dordrecht
- Katsiaris, G. and Goudas, C.L.: 1973, *ibid.*, p. 109
- Kopal, Z. and Lyttleton, R.A.: 1963, *Icarus* 1, 455
- Macris, G., Katsiaris, G.A. and Goudas, C.L.: 1975, *Astrophys. Space Sci.*  
33, 333

- Markellos, V.V.: 1974a, *Celest. Mech.* 2, 365  
1974b, *Celest. Mech.* 10, 87  
1975, *Celest. Mech.* 12, 215  
1977a, *Astron. Astrophys.* 61, 195  
1977b, *Mon. Not. R. Astr. Soc.* 180, 103  
1978, in "Dynamics of Planets and Satellites and Theories of their Motion", p. 315, ed. V. Szebehely, D. Reidel, Dordrecht  
1980, unpublished results
- Markellos, V.V., Black, W. and Moran, P.E.: 1974, *Celest. Mech.* 2, 507
- Markellos, V.V., Moran, P.E. and Black, W.: 1975a, *Astrophys. Space Sci.* 33, 385  
1975b, *Astrophys. Space Sci.* 33, 129
- Markellos, V.V. and Kazantsis, P.G.: 1977, *Celest. Mech.* 15, 35
- Markellos, V.V. and Zagouras, C.G.: 1977, *Celest. Mech.* 16, 123
- Markellos, V.V., Kazantsis, P.G. and Zagouras, C.G.: 1978, *Astrophys. Space Sci.* 54, 379
- Message, P.J.: 1970, in "Periodic Orbits, Stability and Resonances", p. 19, ed. G.E.O. Giacaglia, D. Reidel, Dordrecht
- Message, P.J. and Taylor, D.B.: 1978, in "Dynamics of Planets and Satellites and Theories of their Motion", p. 319, ed. V. Szebehely, D. Reidel, Dordrecht
- Minorsky, N.: 1962, "Nonlinear Oscillations", Van Nostrand, Princeton
- Pars, L.A.: 1965, "A Treatise on Analytical Dynamics", Heinemann, London
- Poincaré, H.: 1899, "Les Méthodes Nouvelles de la Mécanique Céleste" (Vols. I-III), Gauthier-Villars, Paris
- Roy, A.E. and Ovenden, M.W.: 1955, *Mon. Not. R. Astr. Soc.* 115, 296
- Schmidt, D.S.: 1972, *S.I.A.M. Journal Appl. Math.* 22, 27
- Schwarzschild, K.: 1898, *Astron. Nachr.* 147, 17, 289
- Shelus, P.J.: 1972, *Celest. Mech.* 5, 72
- Shelus, P.J. and Kumar, S.S.: 1970, *Astron. J.* 75, 315

Siegel, C.L. and Moser, J.K.: 1971, "Lectures on Celestial Mechanics",

Springer-Verlag, Berlin

Strömngren, E.: 1933, Bull. Astron. (2) 2, 87

Szebehely, V.: 1967, "Theory of Orbits", Academic Press, New York

Taylor, D.B.: 1979, Ph.D. Thesis, University of Glasgow

Whittaker, E.T.: 1904, "Analytical Dynamics", Cambridge University Press

Wintner, A.: 1946, "Analytical Foundations of Celestial Mechanics",

Princeton University Press

Zagouras, C. and Markellos, V.V.: 1977, Astron. Astrophys. 59, 79

Zagouras, C.G. and Kalogeropoulou, M.: 1978, Astron. Astrophys. Suppl.

11. APPENDIX: ORBIT PLOTS

This Appendix contains computer plots of representative periodic orbits belonging to the new families and series given in Chapters 5 - 8; reference should be made to the relevant text in each case. The figures are numbered A1, A2, A3 ..., and are arranged by chapter into four groups as follows.

Group (a) : Figures A1 - A24 (Chapter 5)

Group (b) : Figures A25 - A48 (Chapter 6)

Group (c) : Figures A49 - A56 (Chapter 7)

Group (d) : Figures A57 - A70 (Chapter 8)

The figure captions are given at the beginning of each group of figures.

Group (a): Figures A1 - A24

In Figures A1 - A24, orbits representing various parts of the vertical branches of family f described in Chapter 5 are plotted with respect to coordinates (X,Y,Z) (not to be confused with the inertial coordinate system used in Chapter 1) defined by

$$\begin{aligned} X &= x - (1-\mu) = x - 0.99905 \\ Y &= y \\ Z &= z, \end{aligned}$$

where (x,y,z) are the usual barycentric coordinates rotating with the primaries, with unit of length equal to the distance between the primaries ("rotating-pulsating" coordinates). Thus, the origin of the plot coordinates is located at the primary  $m_2$  (Jupiter) ( $x = 1-\mu$ ). The scale of the plots is such that the length of the positive half of each axis is 0.1, in units of the Sun-Jupiter distance. The orbits are projected orthogonally on the (X,Y), (X,Z) and (Y,Z) planes. Figure A16 is an isometric projection, that is, an orthogonal projection on a plane perpendicular to the vector (1,1,1); the positive half of the Z-axis in this case has length 0.1, while the positive X and Y half-axes are longer by a factor  $2/\sqrt{3}$ .

Figures A1 - A9: Typical orbits of family  $F_{v15}^{1(a)}$ . Figures A1 - A3 are projections, in the (X,Y), (X,Z) and (Y,Z) planes, of an orbit belonging to the  $m = 5$  segment of the family; Figures A4 - A6 are the three projections of a representative quadruple ( $m = 4$ ) member, and Figures A7 - A9 the projections of a representative triple-periodic ( $m = 3$ ) member.

Figures A10 - A16: Typical orbits of family  $F_{v15}^{1(p)}$ . Figures A10 - A12 are the (X,Y), (X,Z) and (Y,Z) projections of an orbit belonging to the  $m = 5$  segment, and Figures A13 - A15 are the projections of a representative orbit of the  $m = 3$  segment. Figure A16 is a "three-dimensional" isometric projection of a double-periodic orbit near the termination of the family.

Figures A17 - A22: Typical orbits of family  $F_{v16}^{1(c)}$ . Figures A17 - A19 and A20 - A22 are the three plane projections of orbits representing the  $m = 6$  and  $m = 4$  segments of the family, respectively.

Figures A23, A24: A typical orbit of the  $m = 6$  segment of family  $F_{v16}^{1(o)}$ , in (X,Y) and (X,Z) projections. This orbit is almost the mirror image in the (Y,Z) plane of the orbit belonging to  $F_{v16}^{1(c)}$  plotted in Figures A17 - A19. The orbits of the quadruple segment of  $F_{v16}^{1(o)}$ , not plotted here, are similarly almost mirror images of those belonging to the corresponding part of  $F_{v16}^{1(c)}$ .

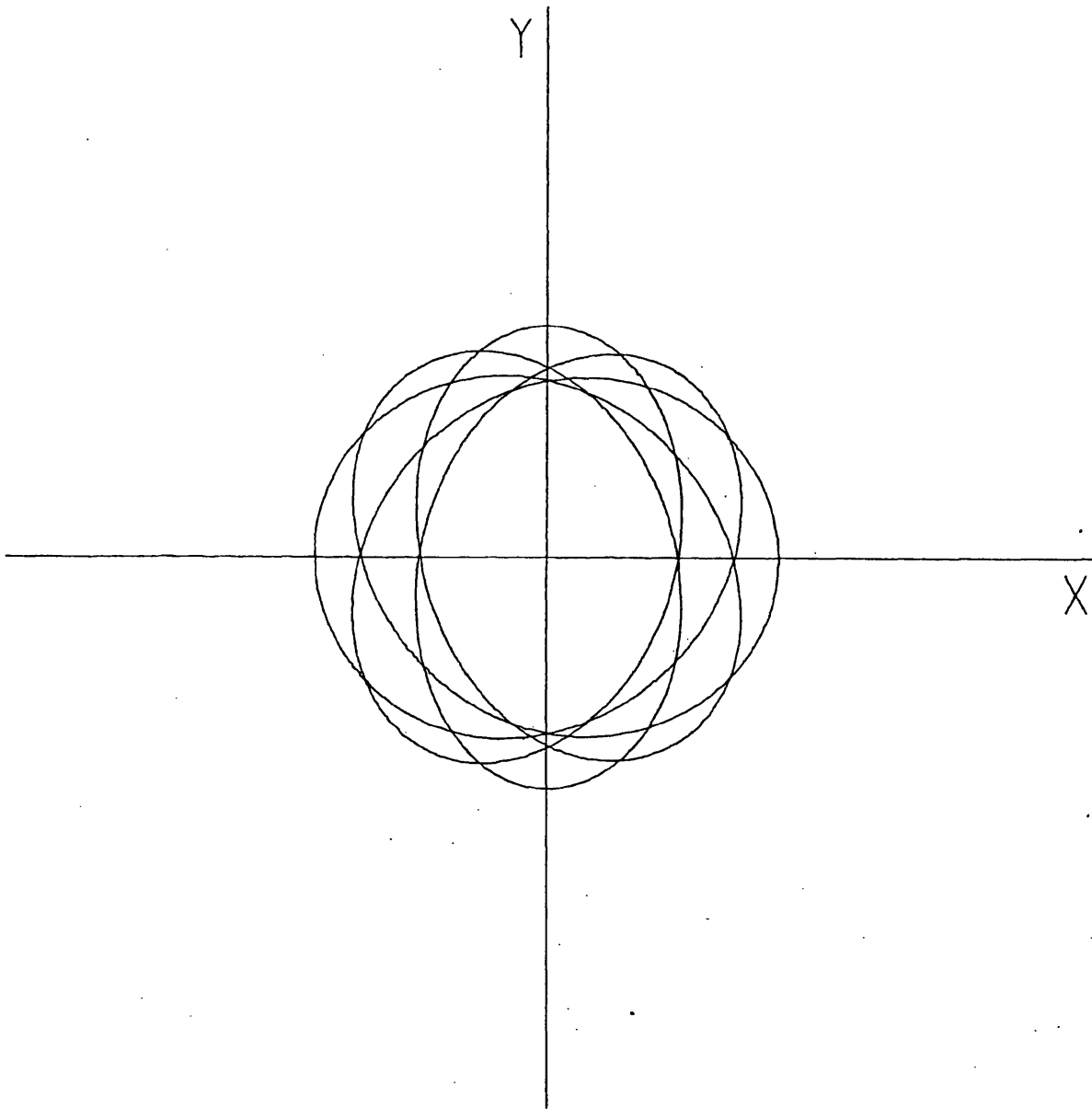


Figure A1

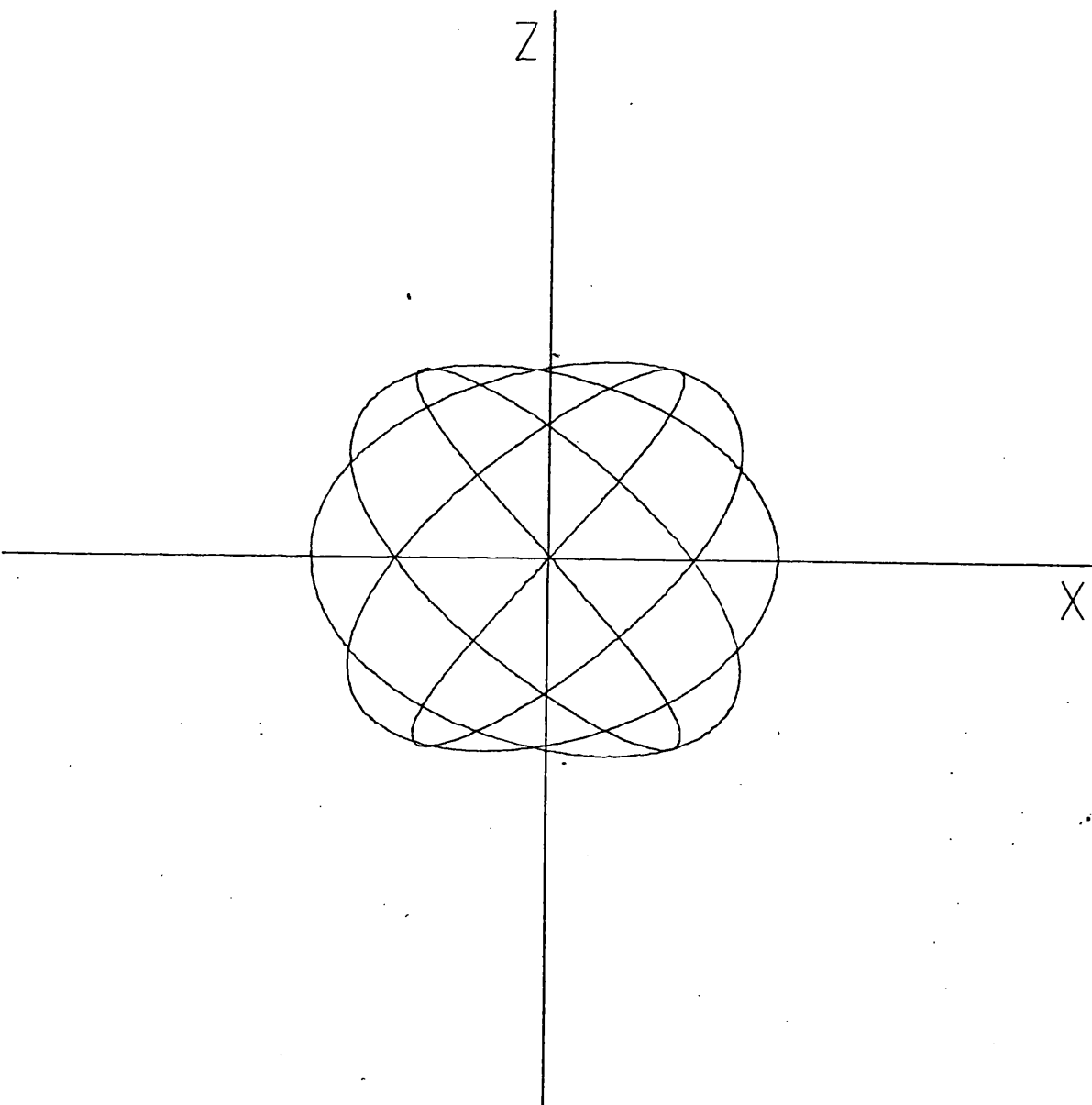


Figure A2

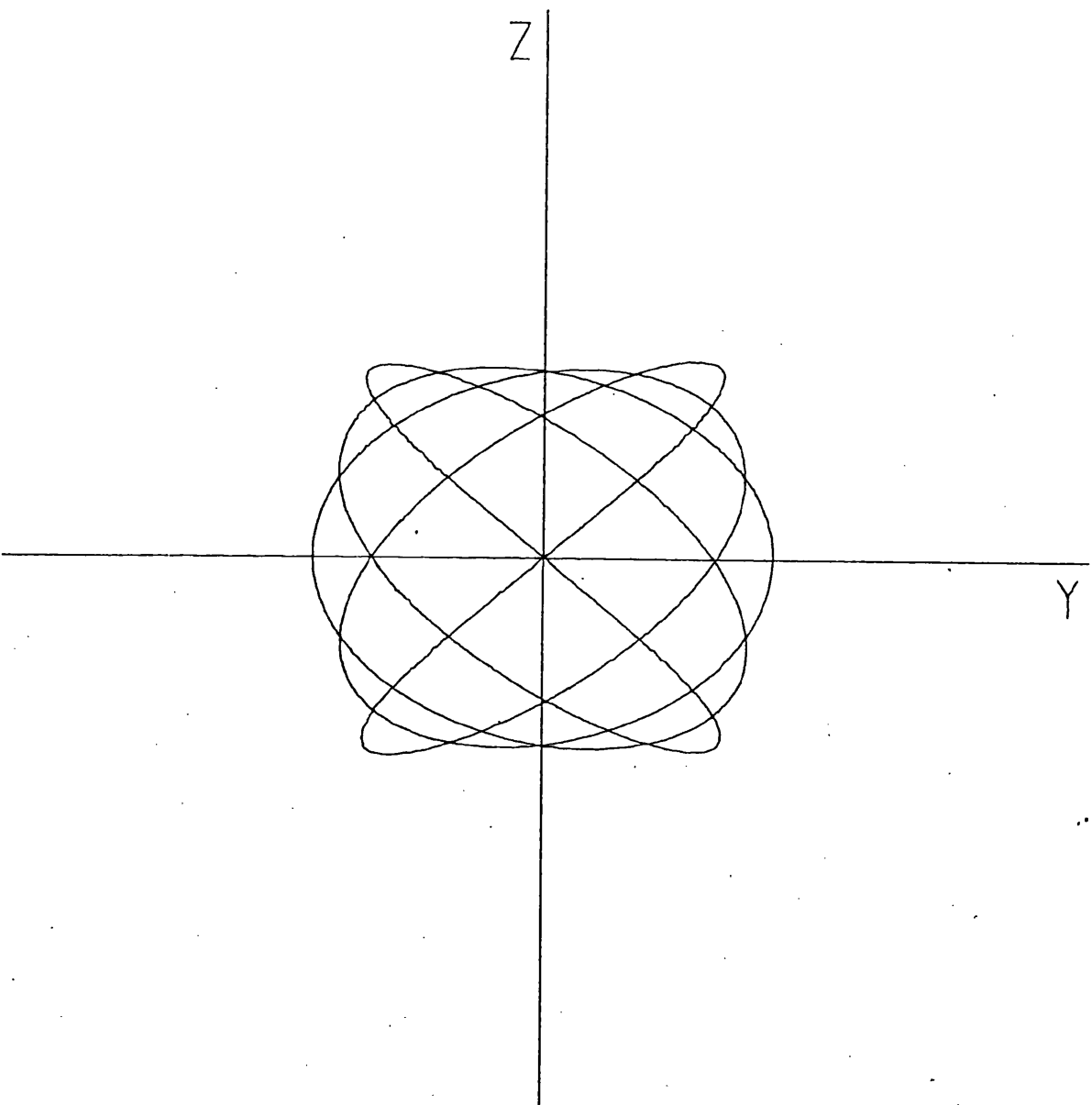


Figure A3

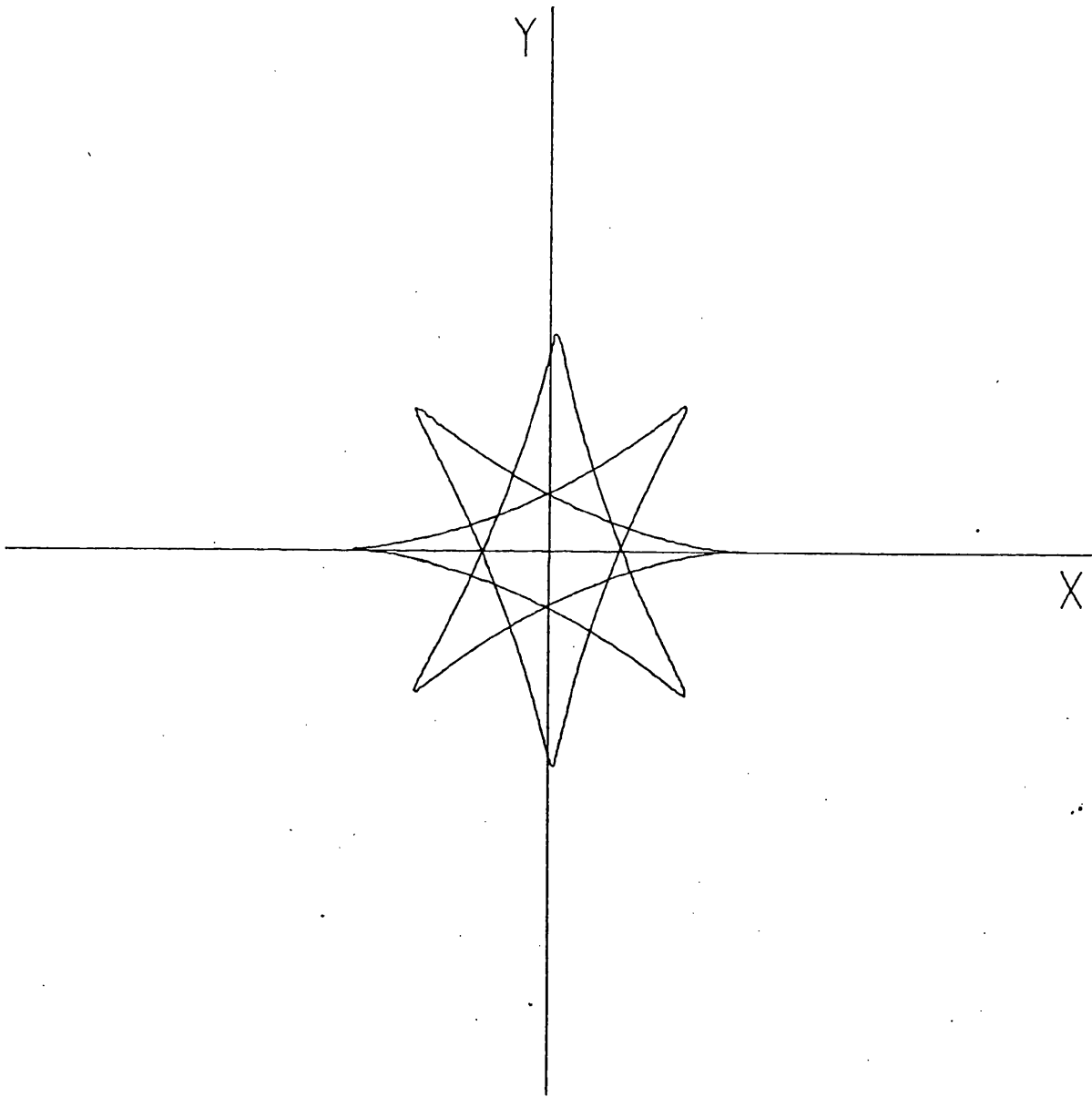


Figure A4

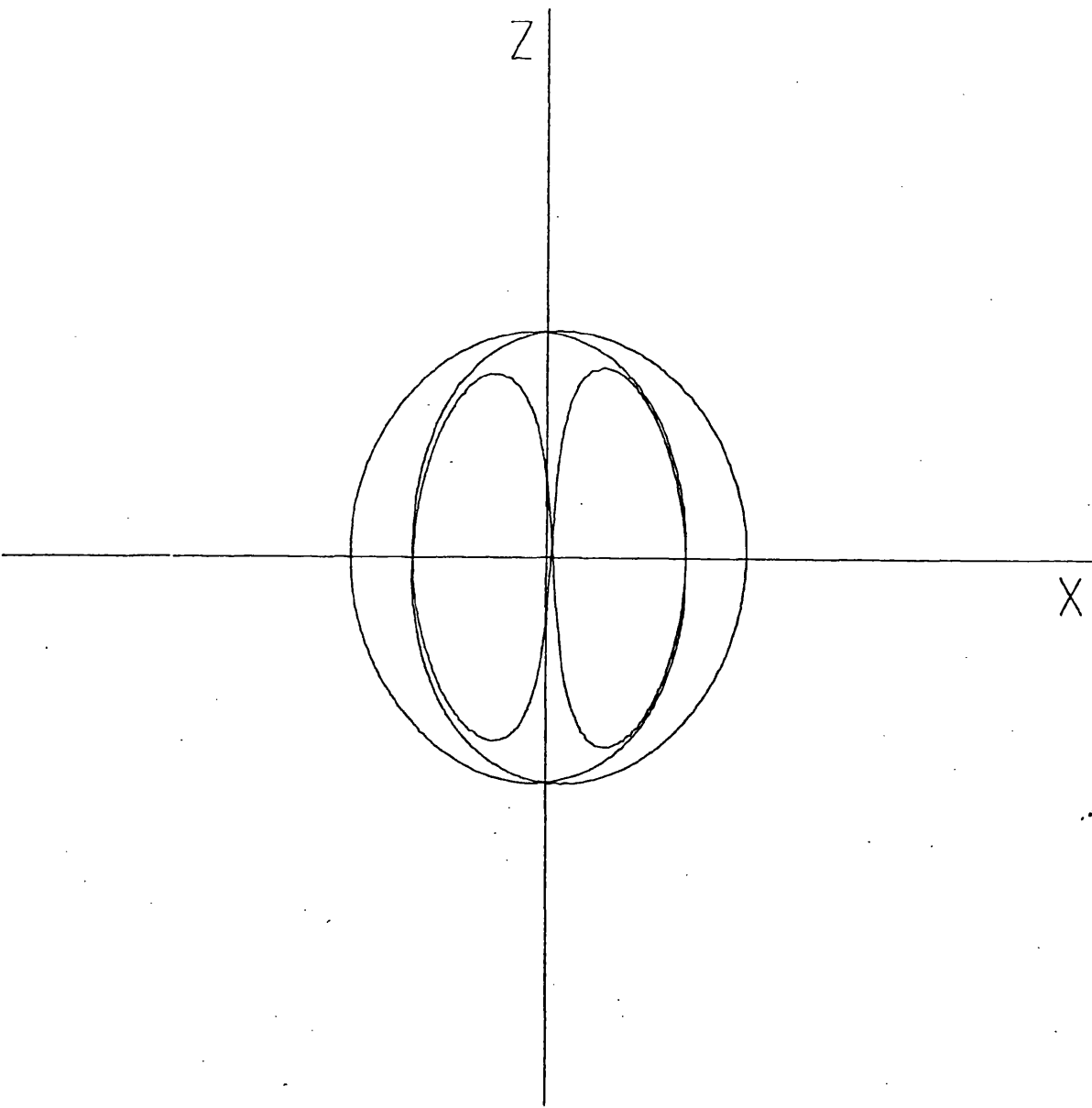


Figure A5

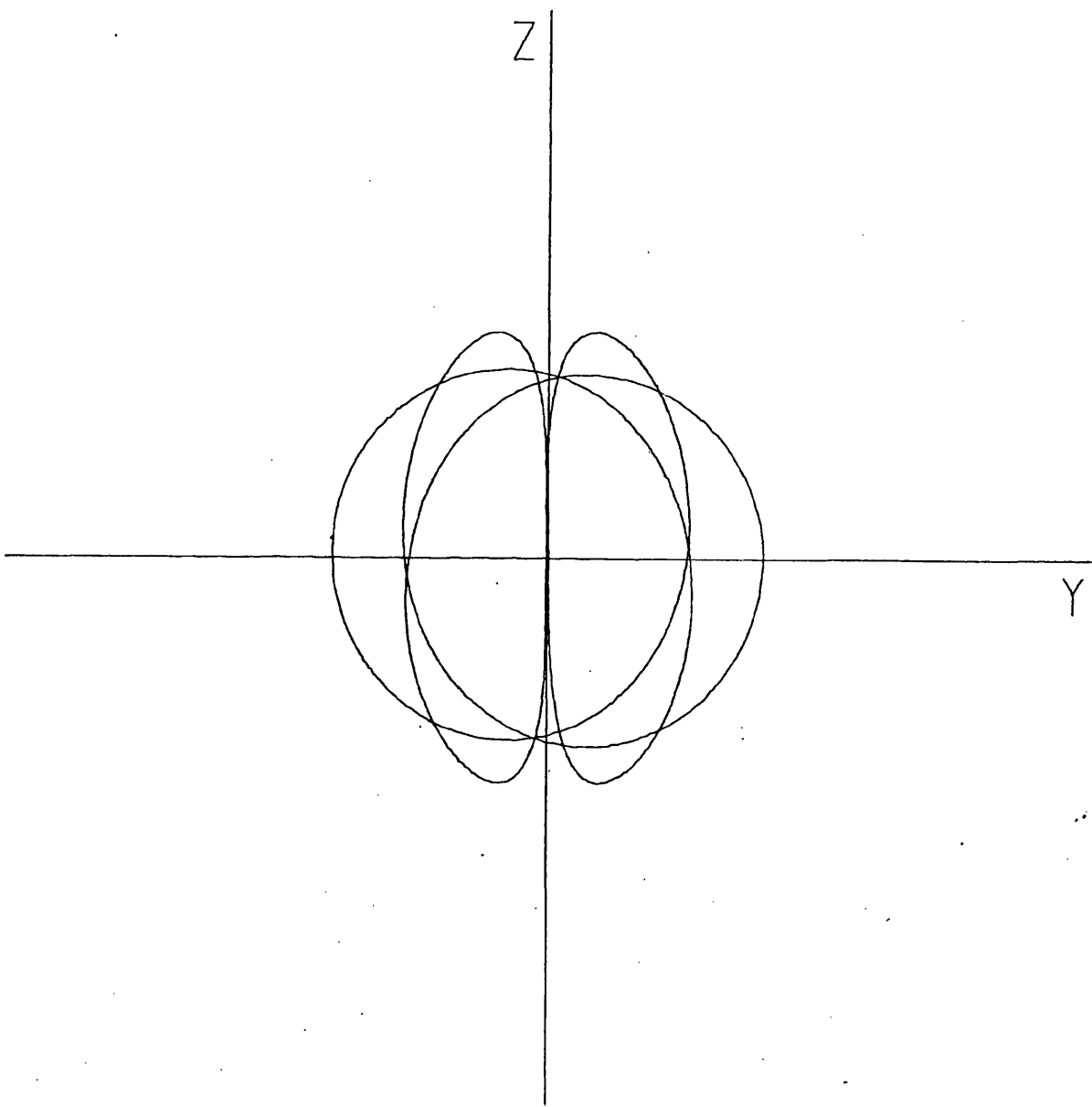


Figure A6

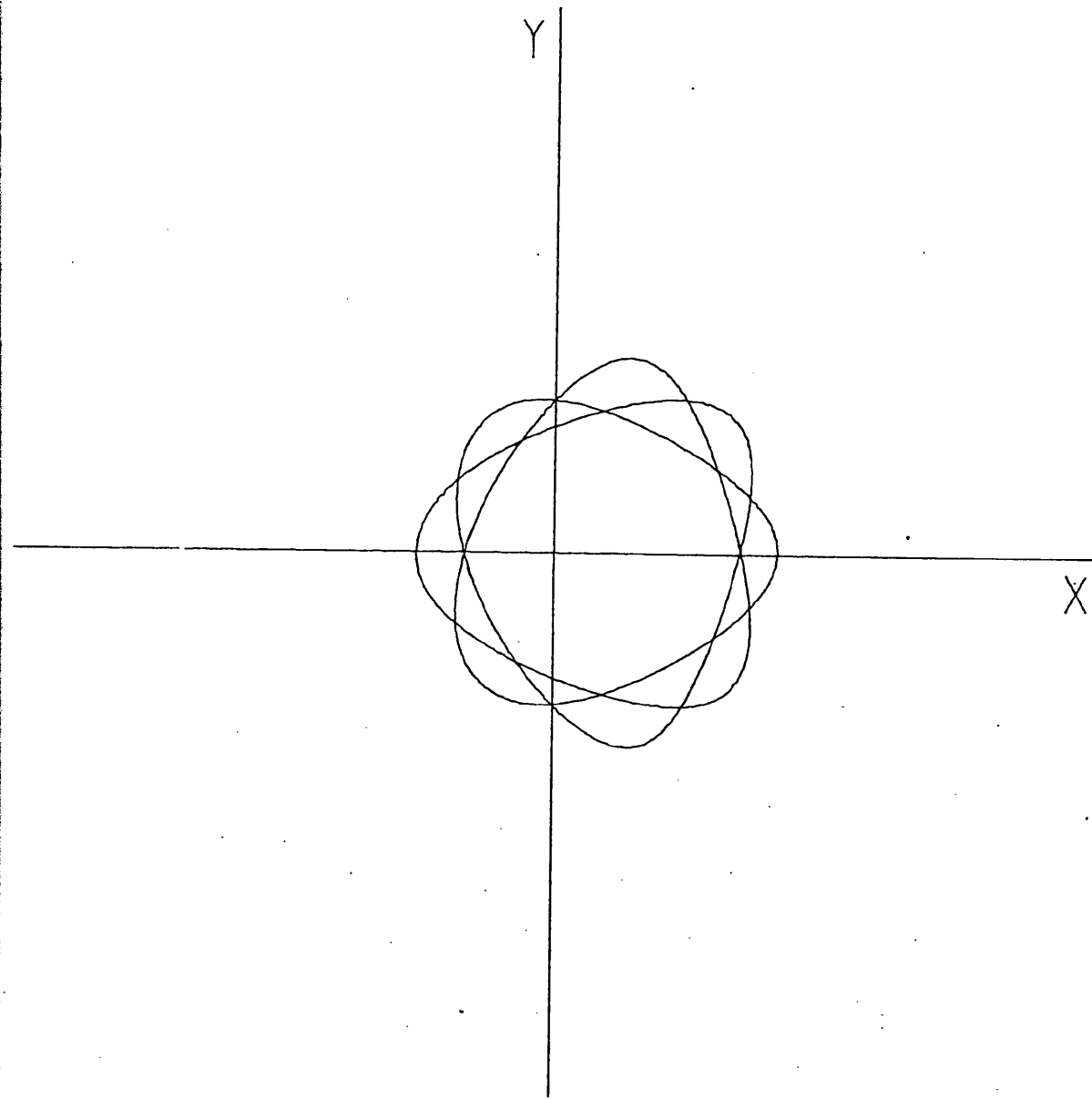


Figure A7

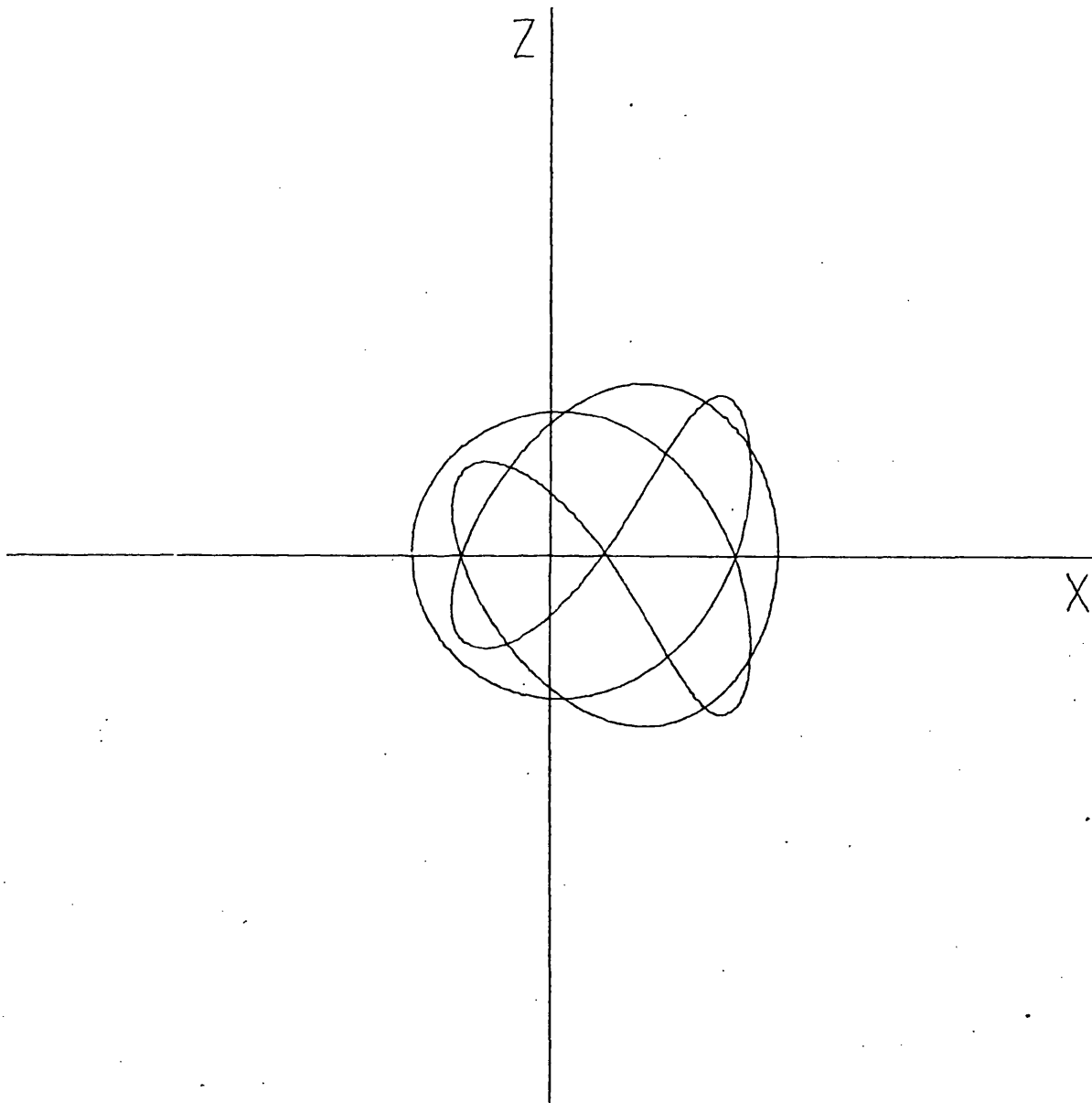


Figure A8

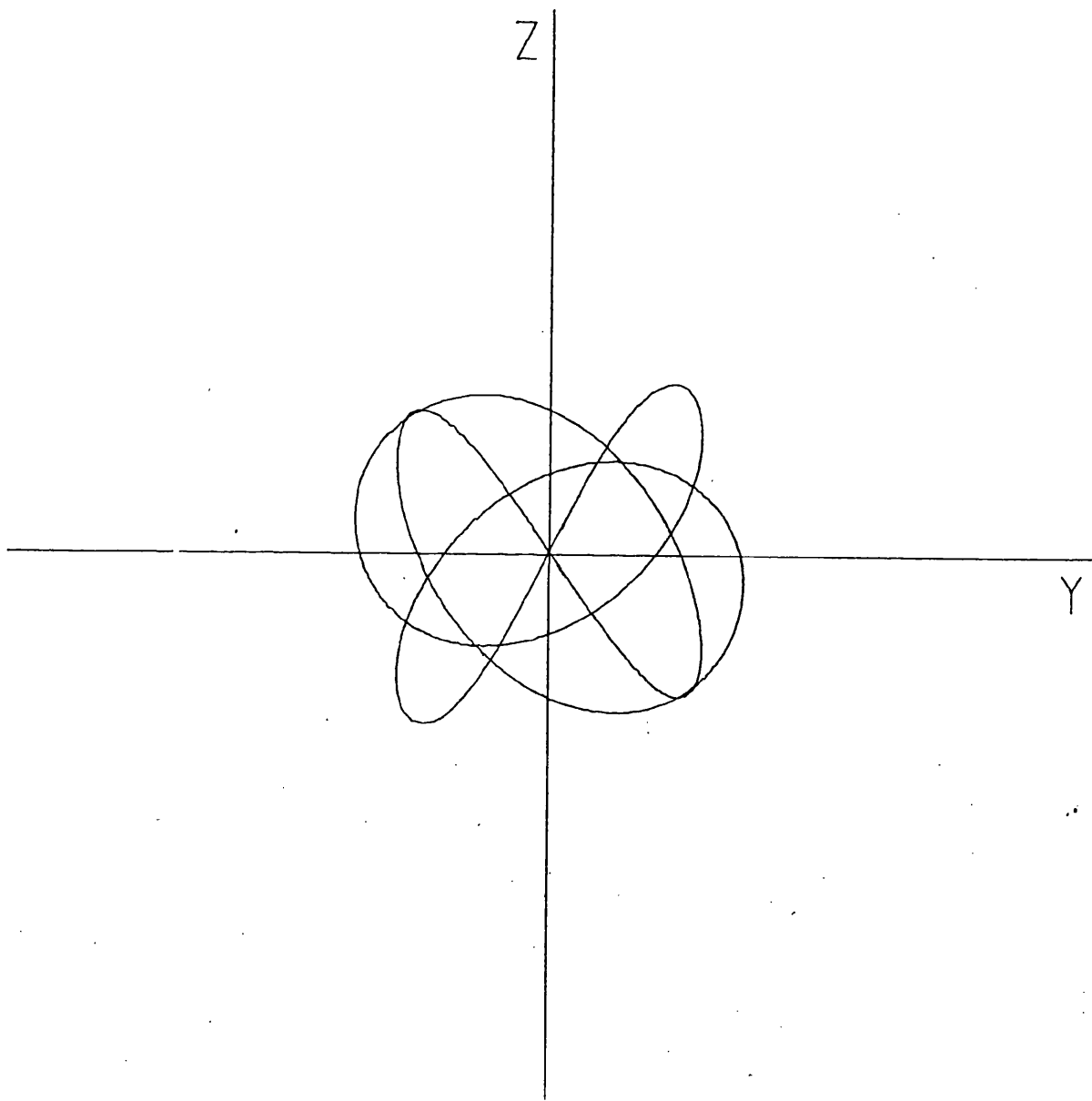


Figure A9

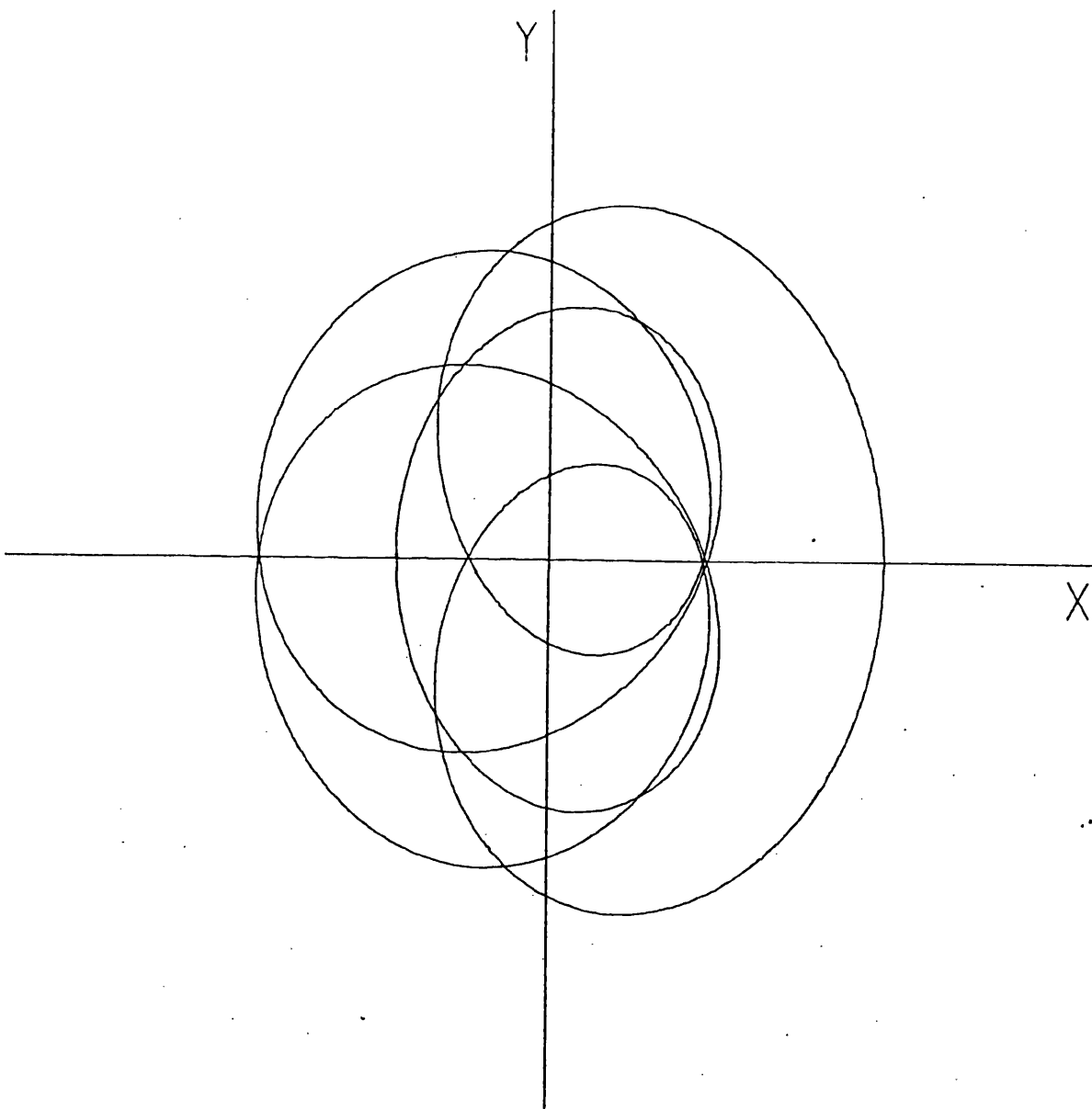


Figure A10

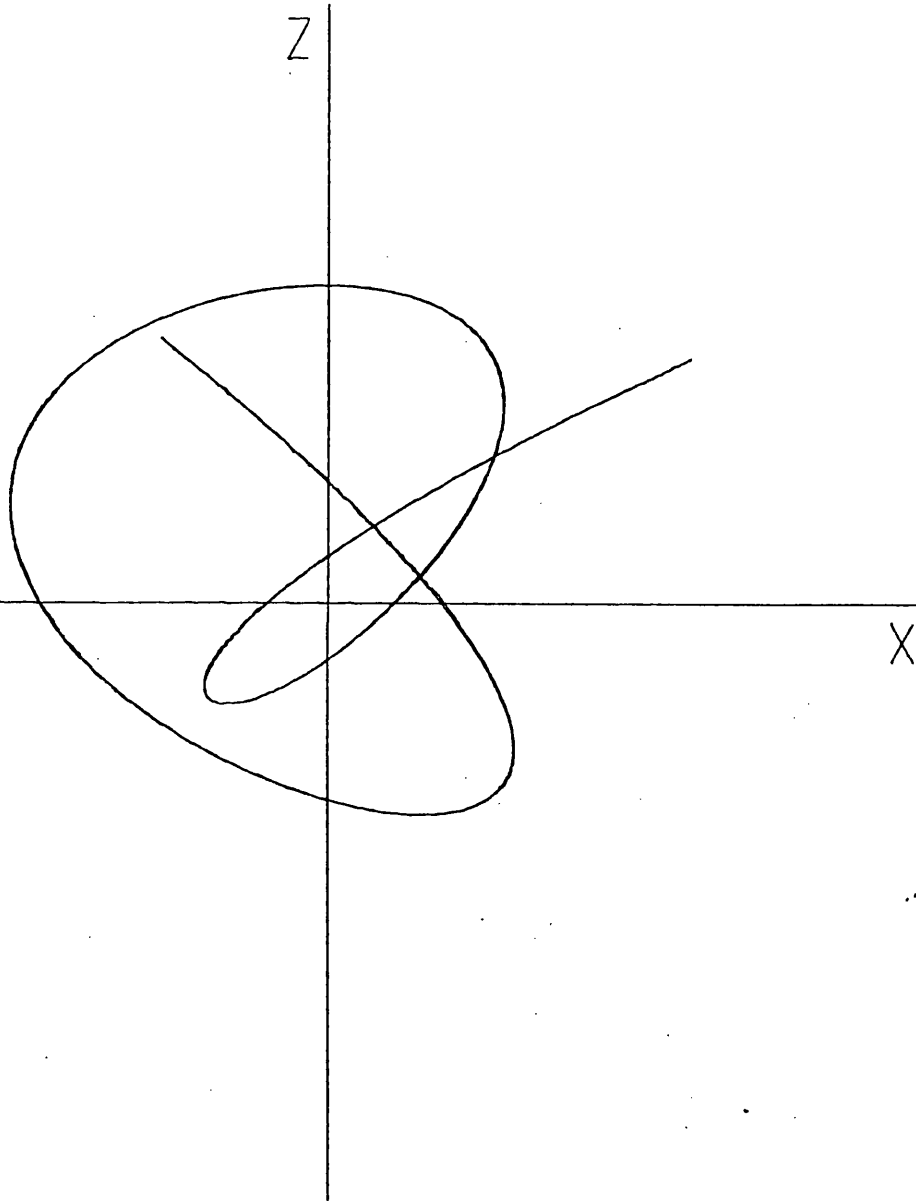


Figure A11

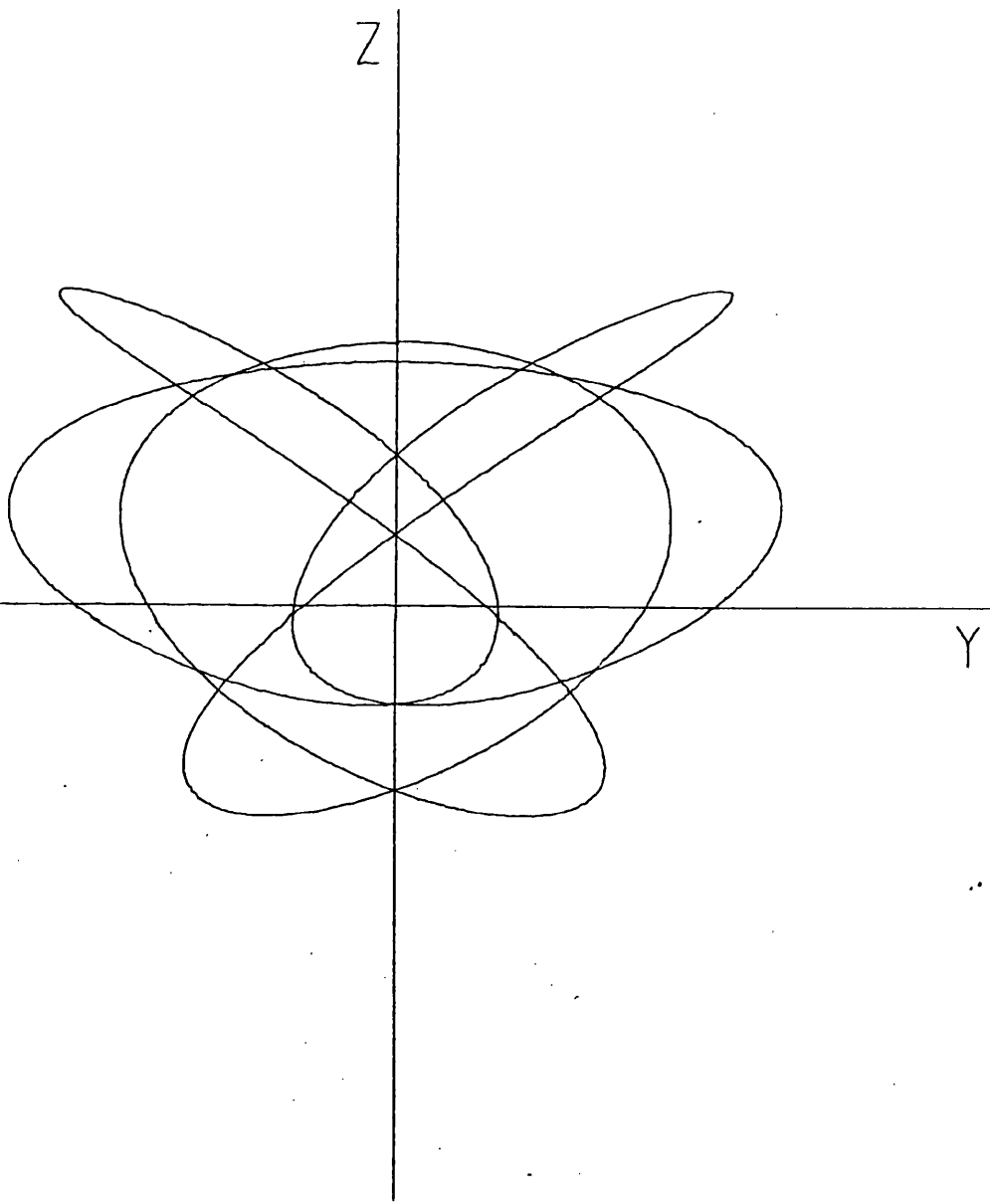


Figure A12

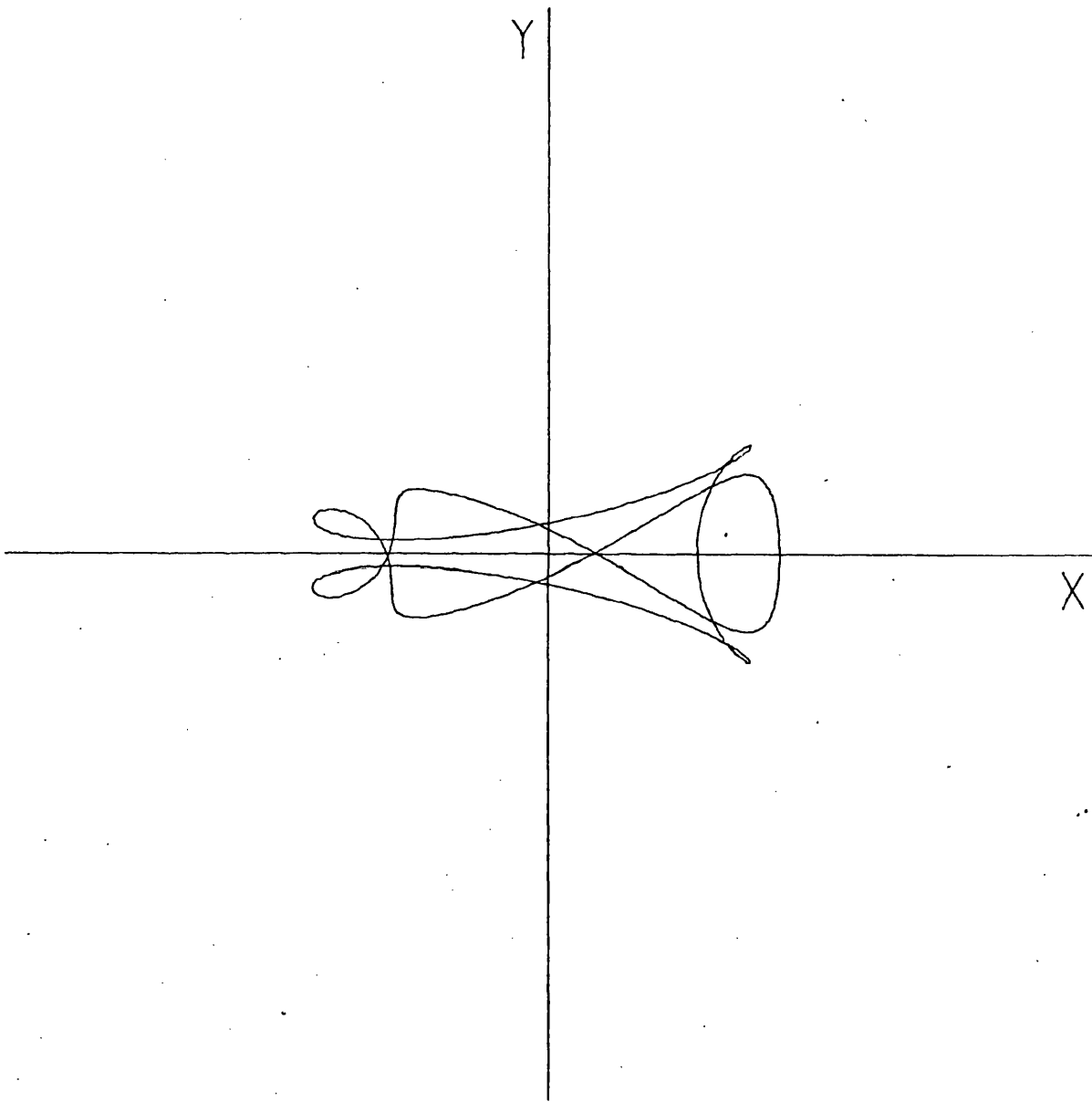


Figure A13

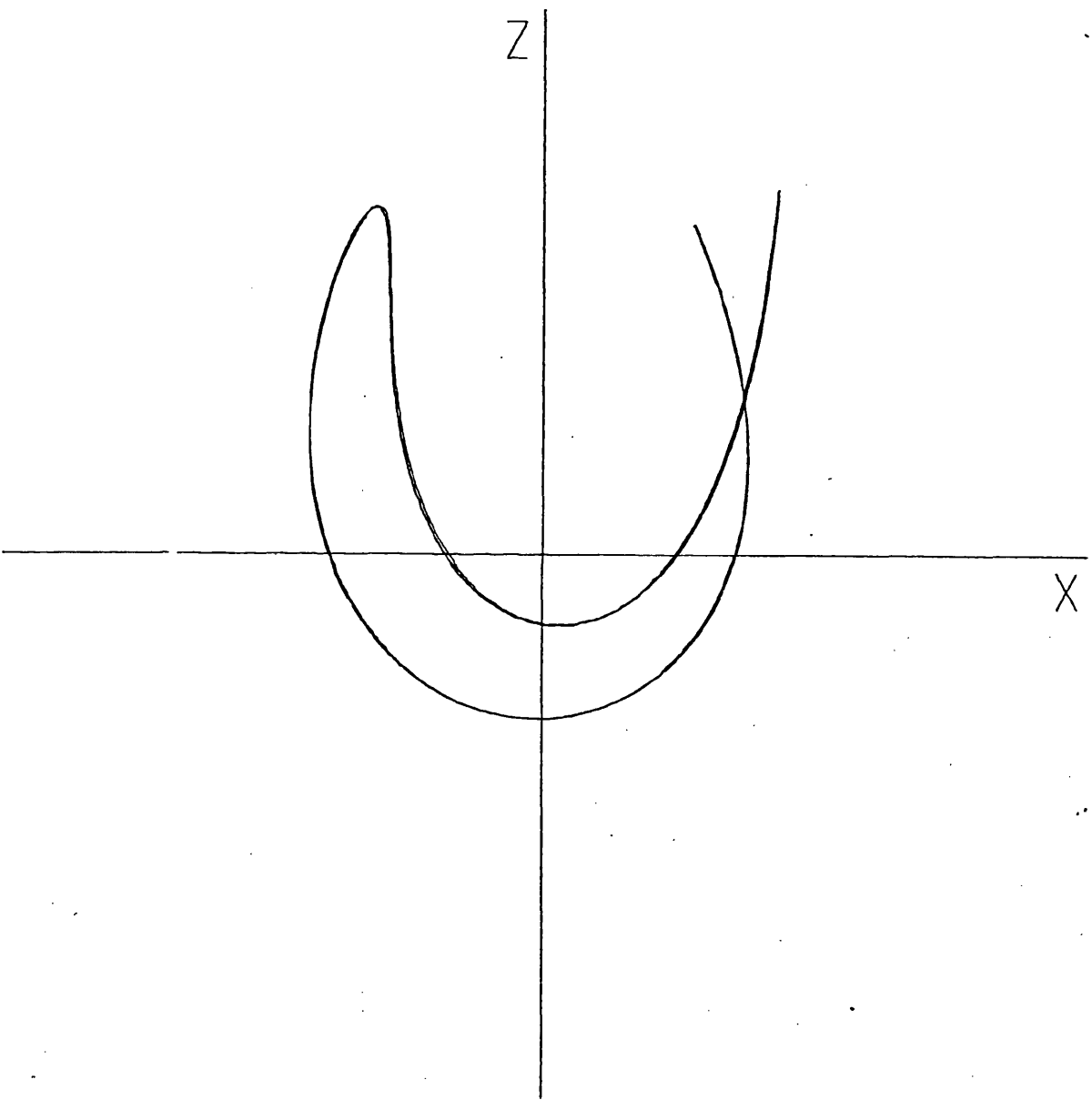


Figure A14

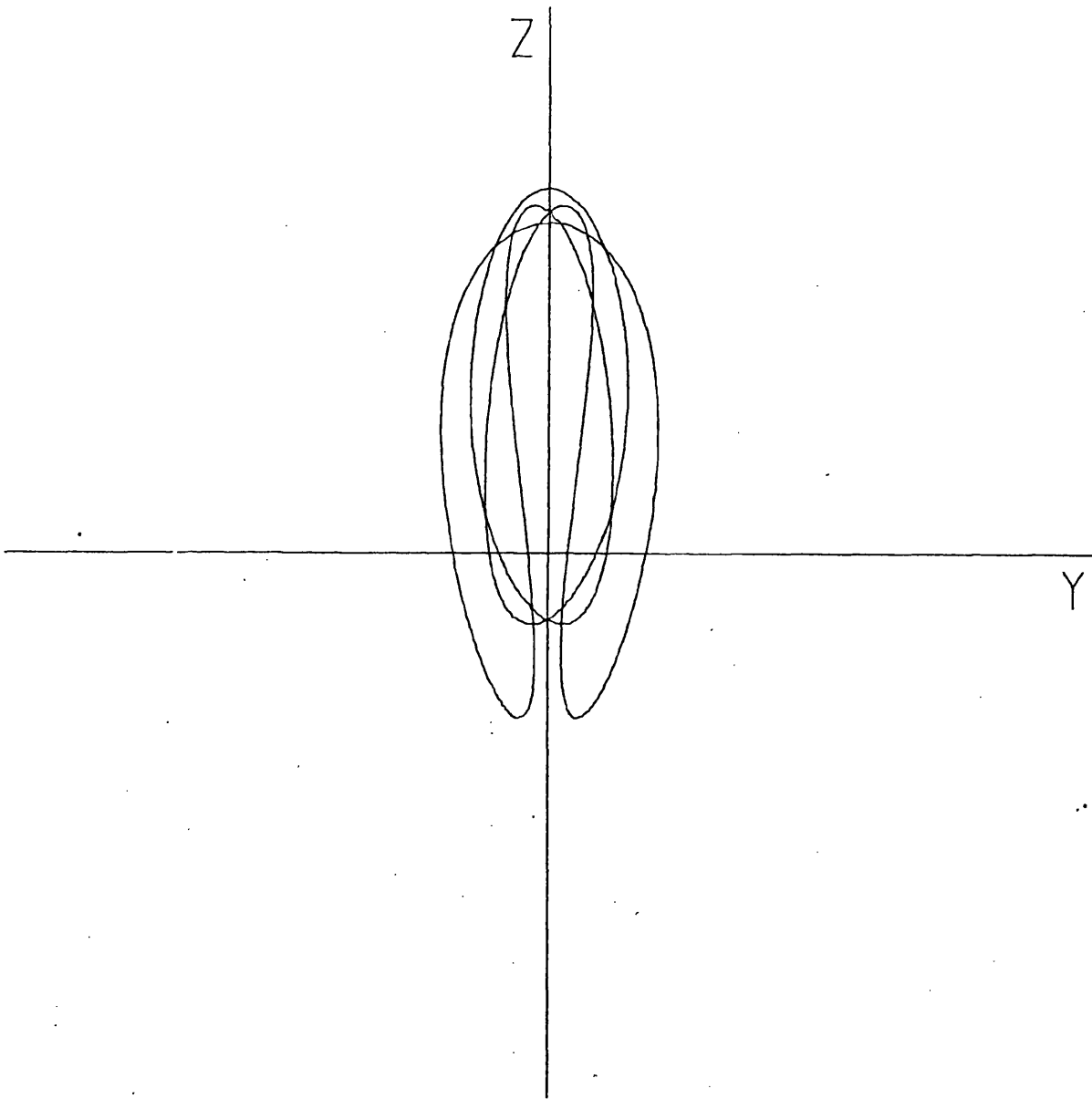


Figure A15

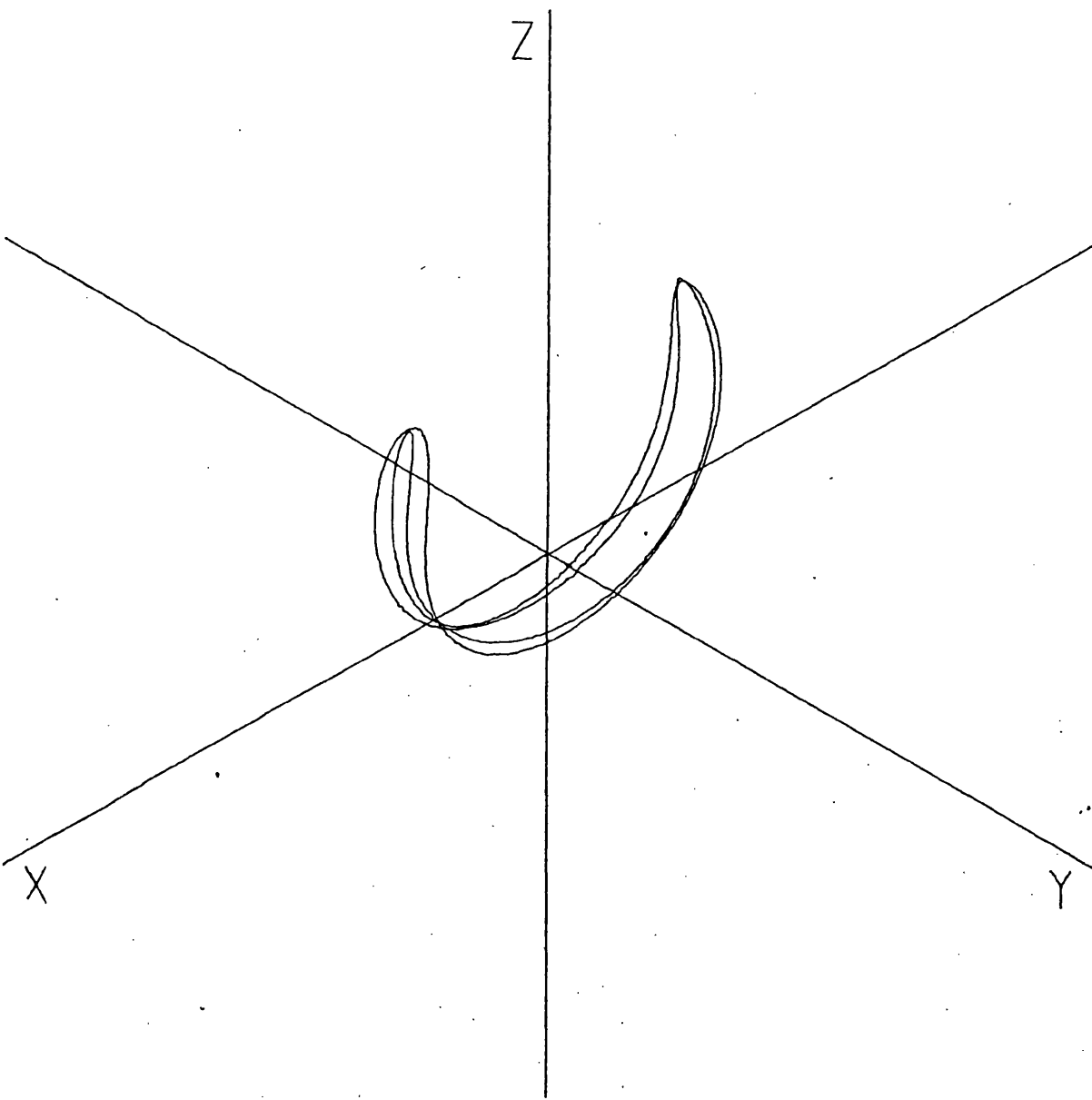


Figure A16

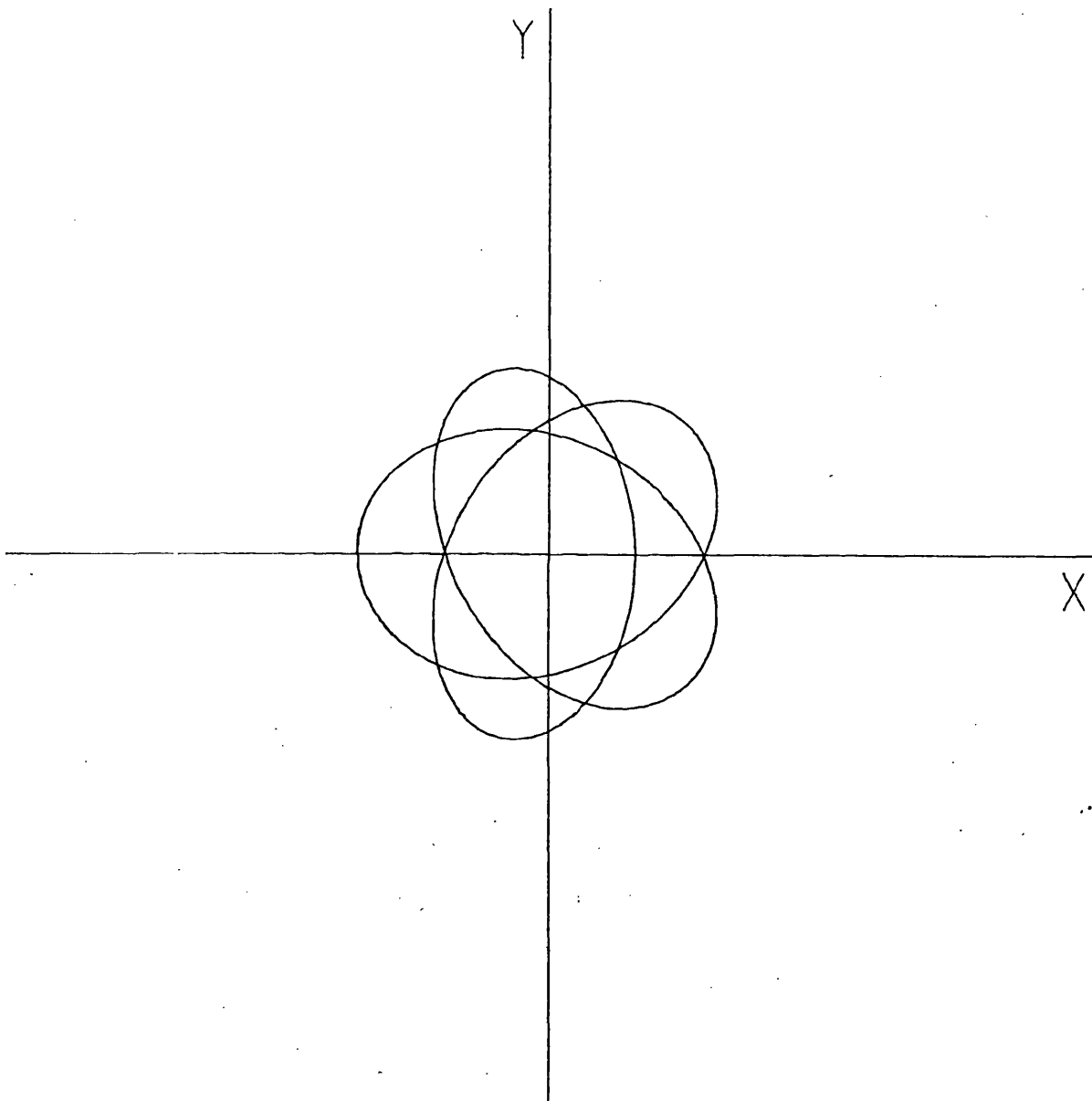


Figure A17

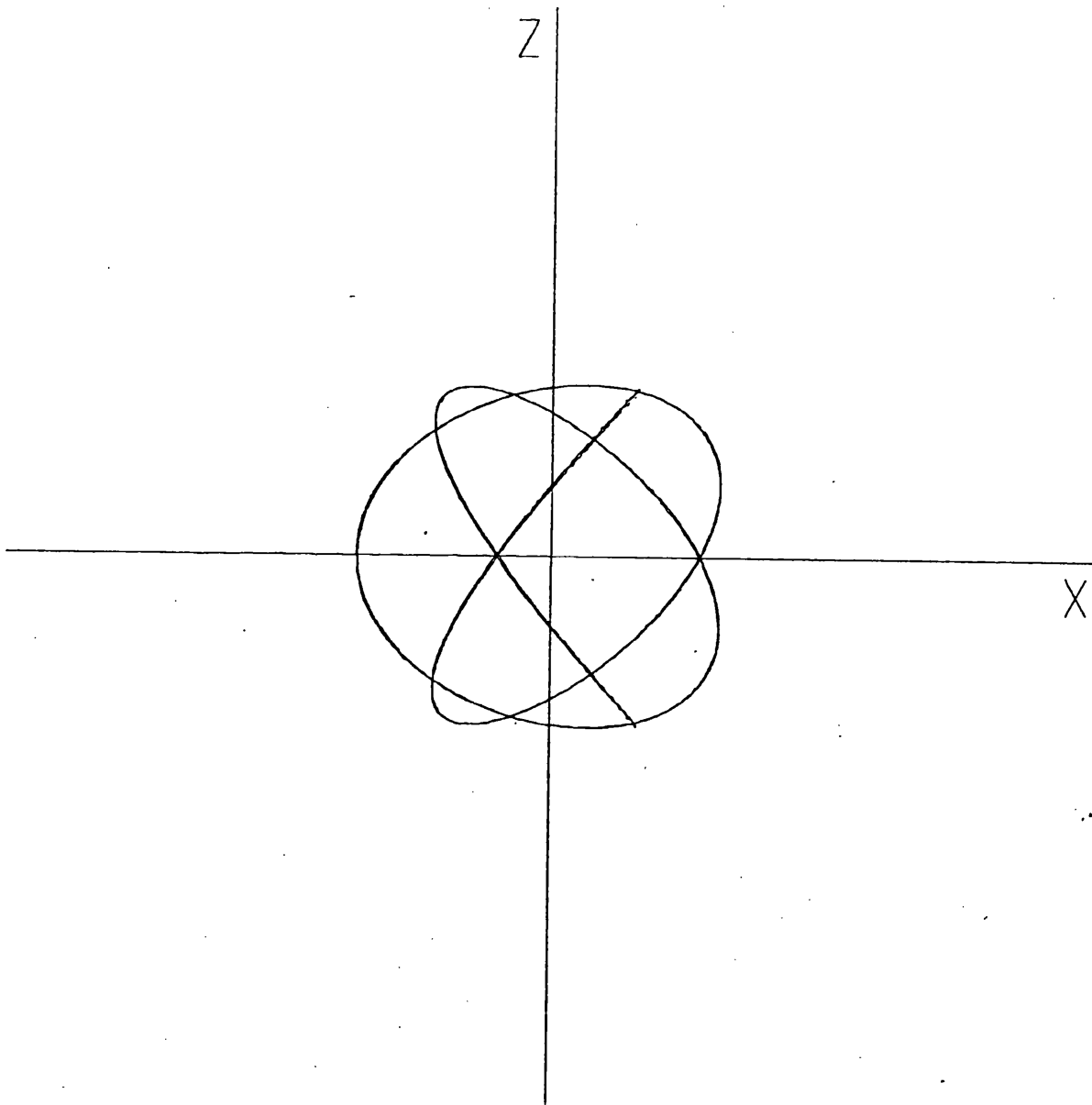


Figure A18

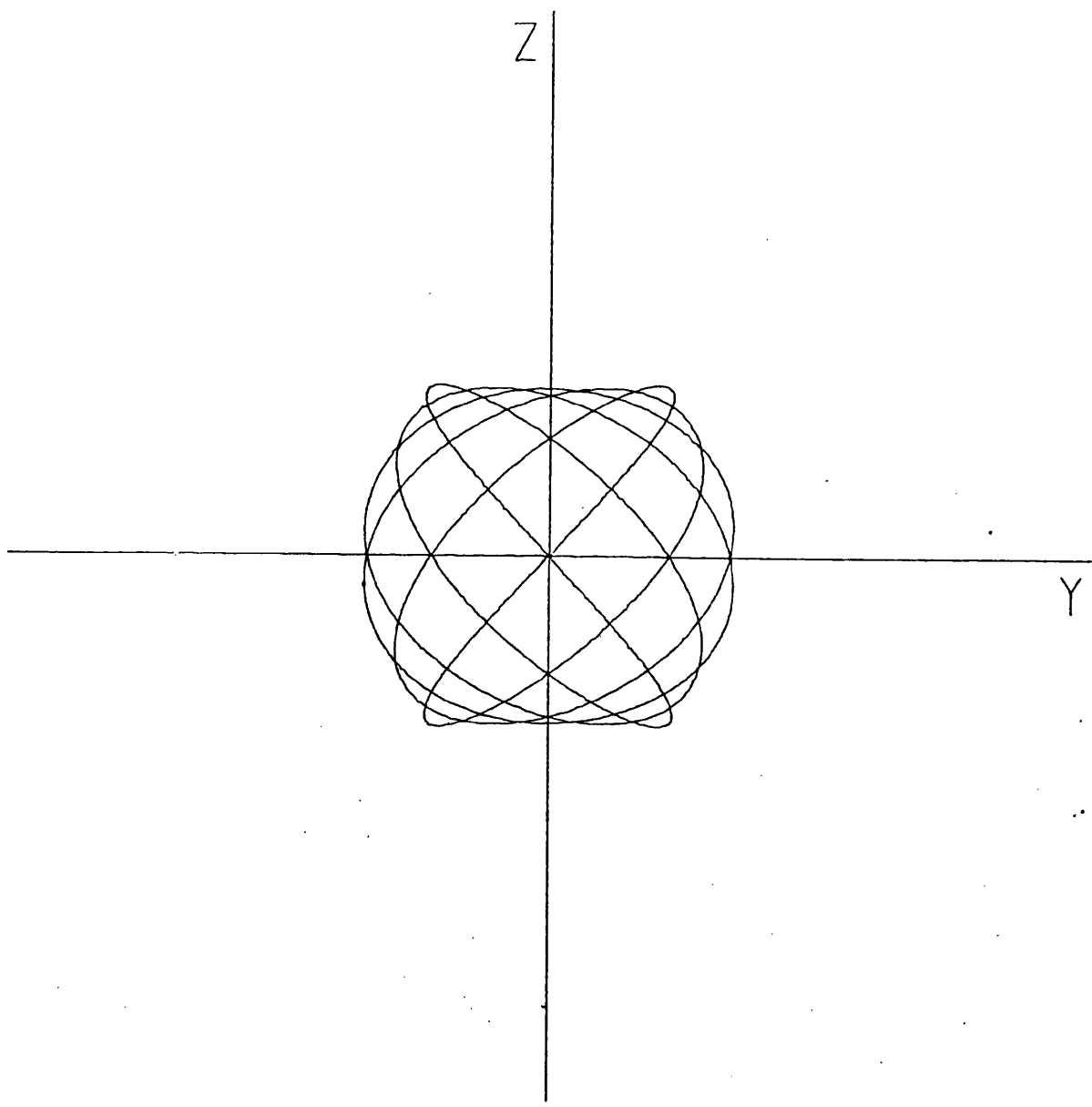


Figure A19

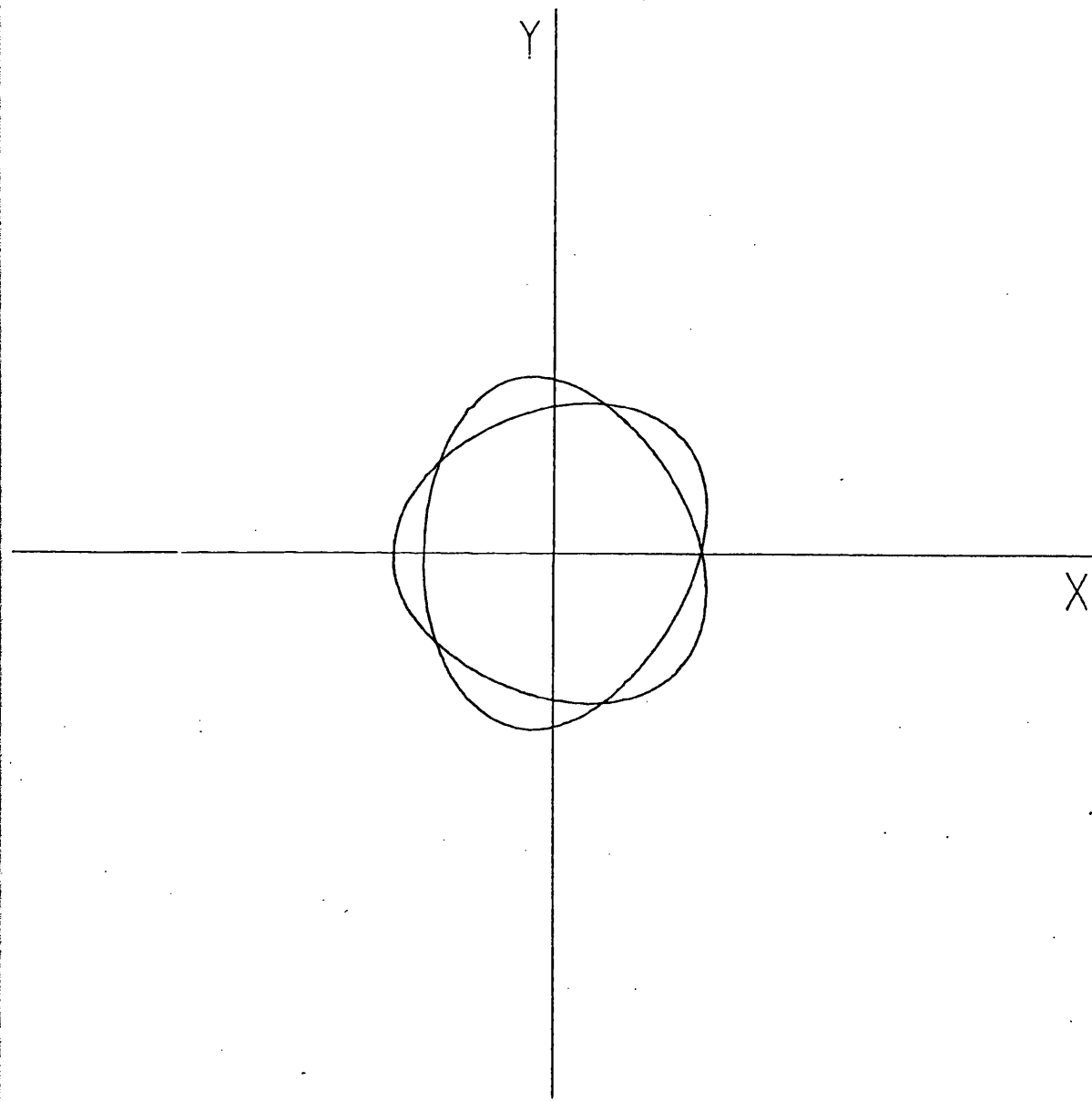


Figure A20

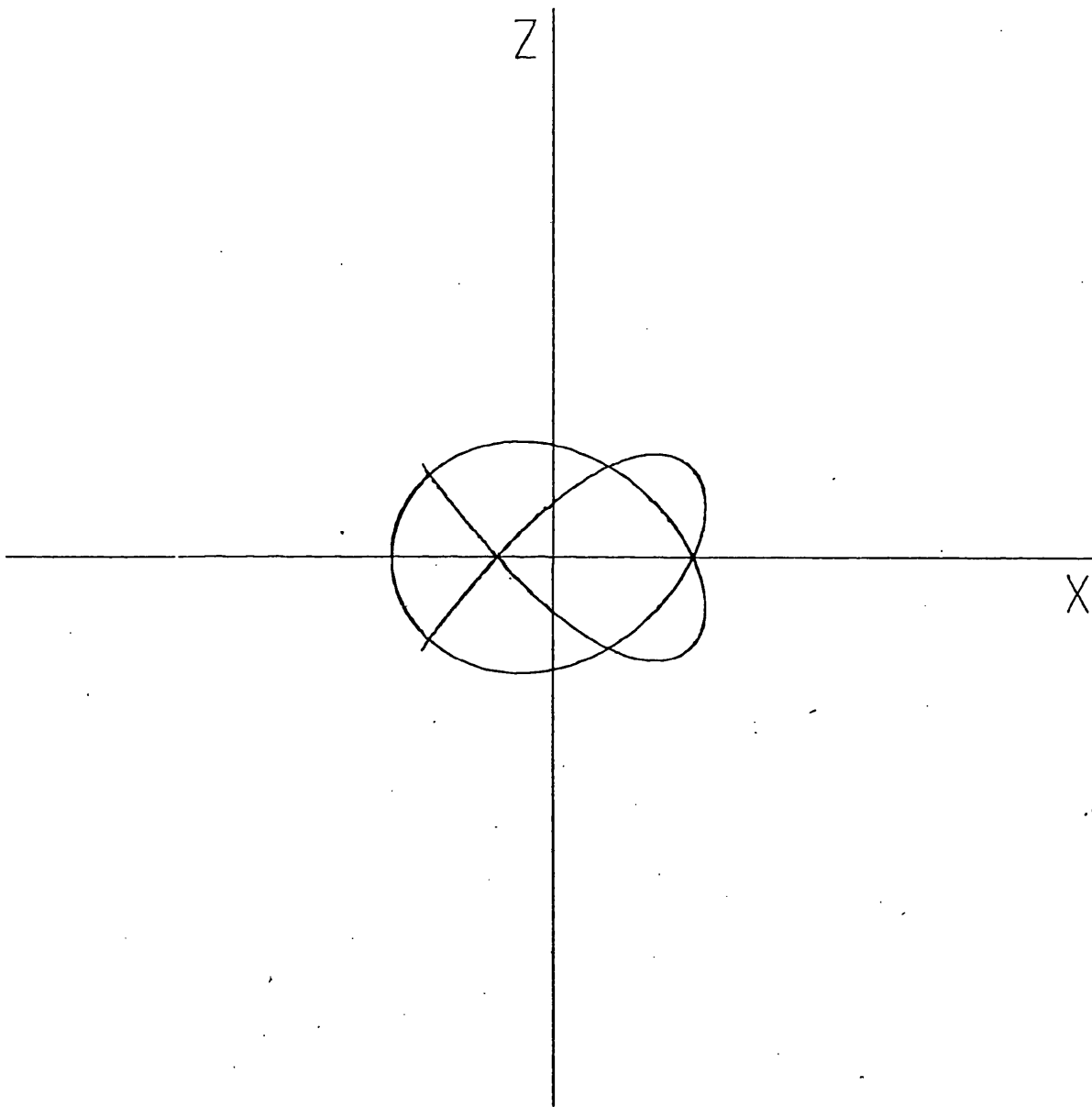


Figure A21

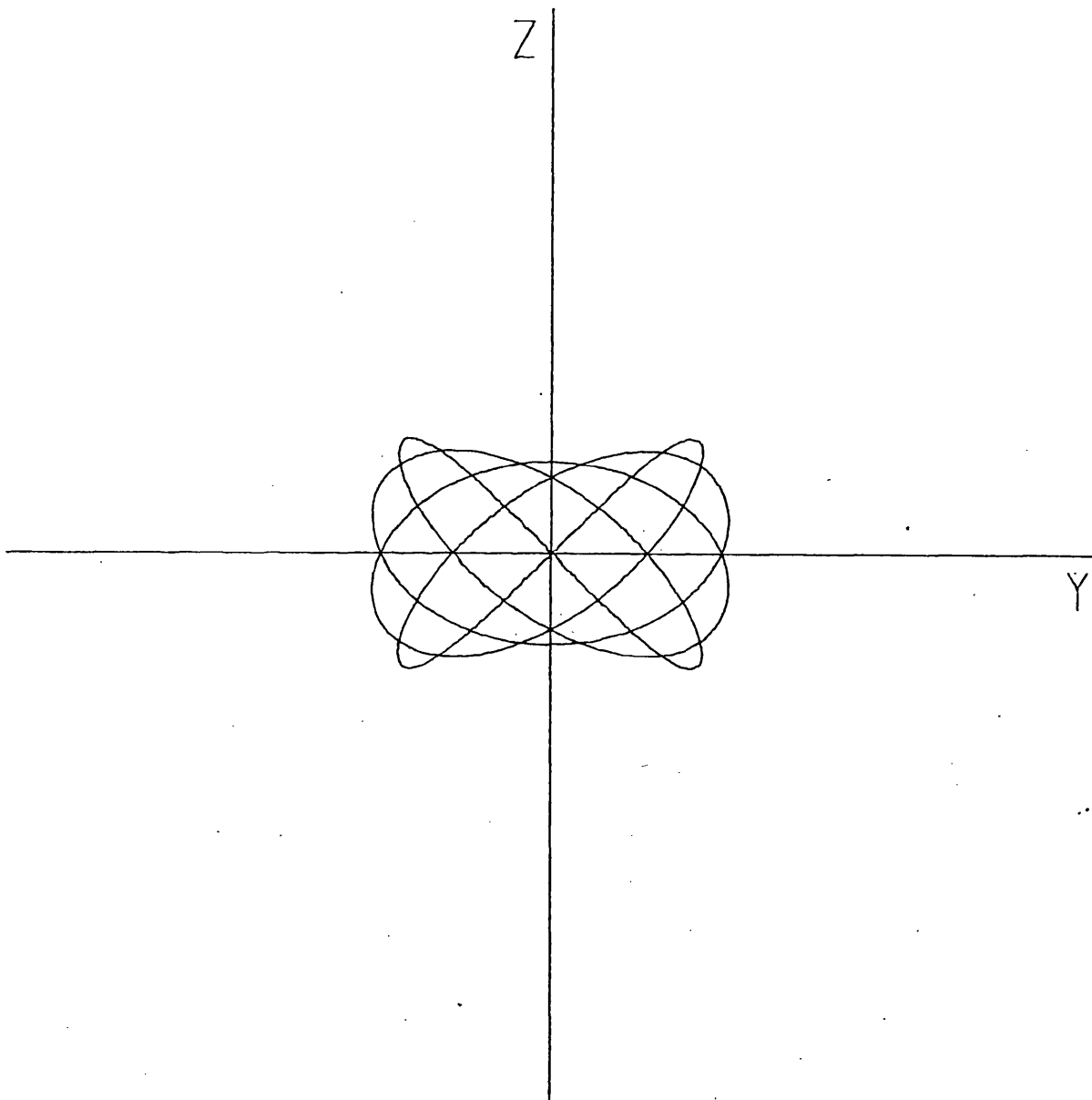


Figure A22

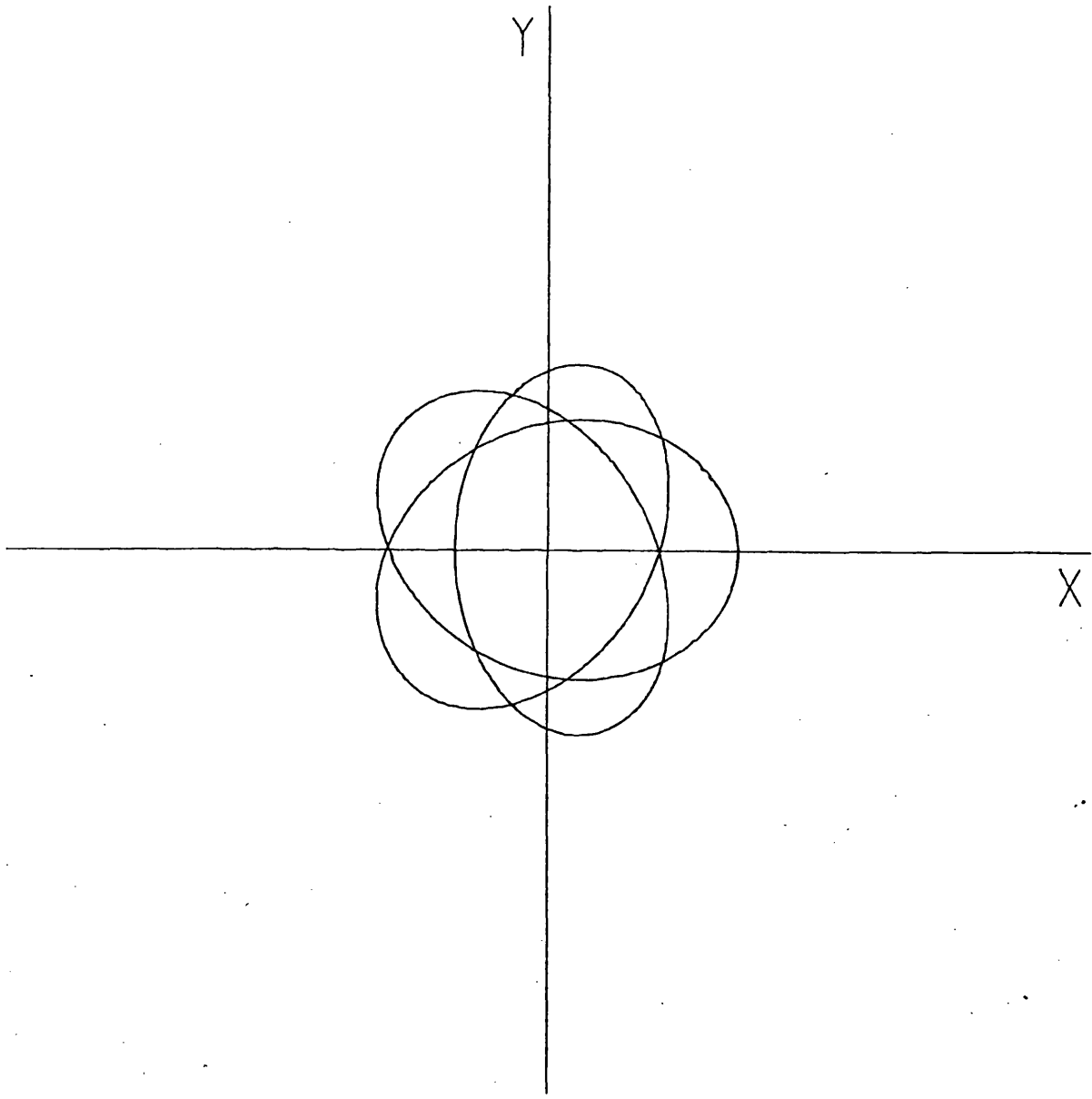


Figure A23

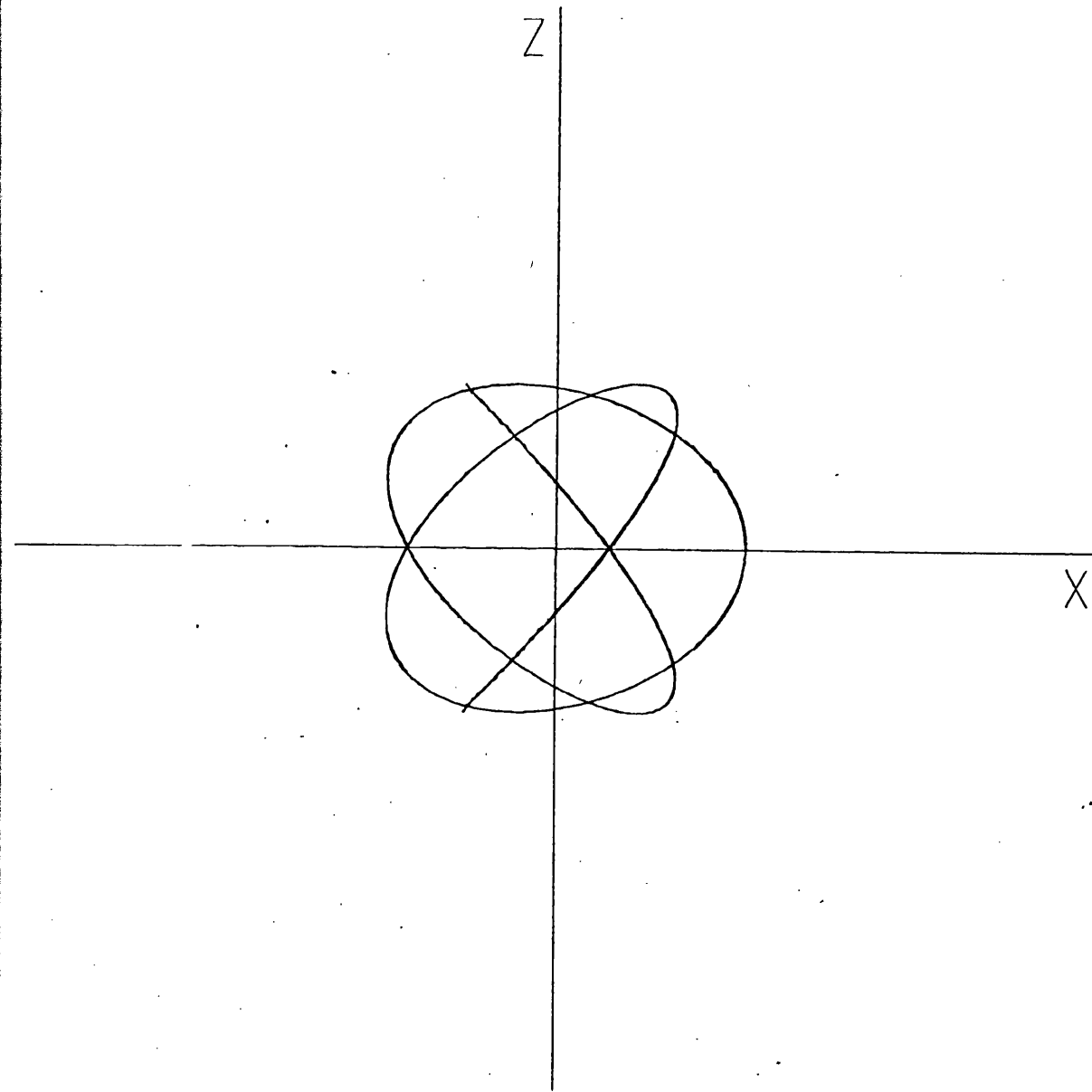


Figure A24

Group (b): Figures A25 - A48

Computer plots of representative periodic orbits of the three-dimensional elliptic restricted problem obtained by continuation of commensurable orbits of the circular problem to non-zero values of the primary eccentricity  $e$ . Each orbit is plotted in  $(X,Y)$ ,  $(X,Z)$  and  $(Y,Z)$  projections. The plot coordinates  $(X,Y,Z)$  are the same as those for the previous group of plots: that is, with origin at  $m_2$  (Jupiter) and rotating with the primaries. The plotted orbits can be identified from the following table:

Figures	Table	Primary Eccentricity
A25 - A27	6.2	0.1
A28 - A30	6.2	0.7
A31 - A33	6.3	0.1
A34 - A36	6.3	0.7
A37 - A39	6.4	0.1
A40 - A42	6.4	0.7
A43 - A45	6.5	0.1
A46 - A48	6.5	0.7

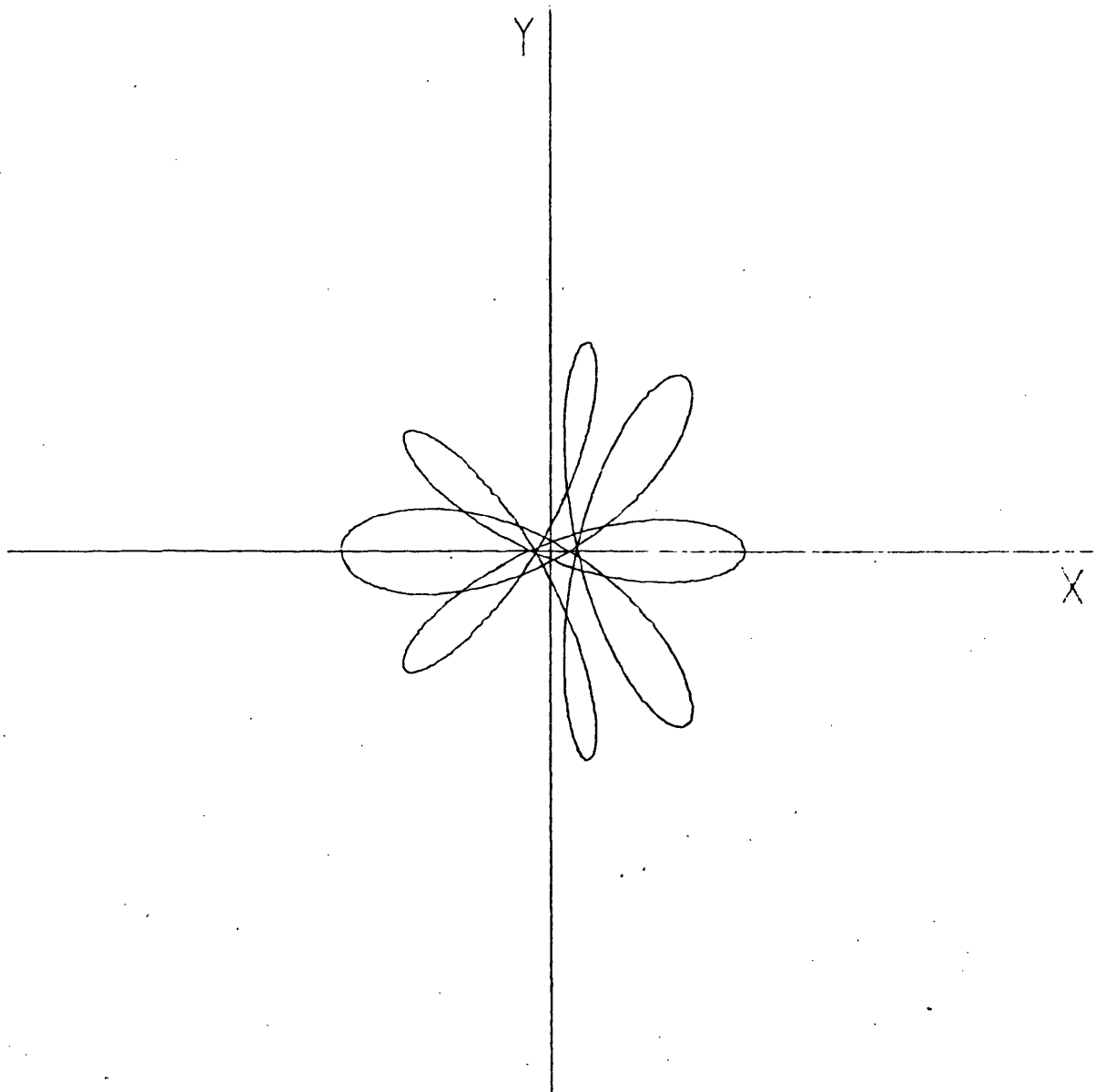


Figure A25

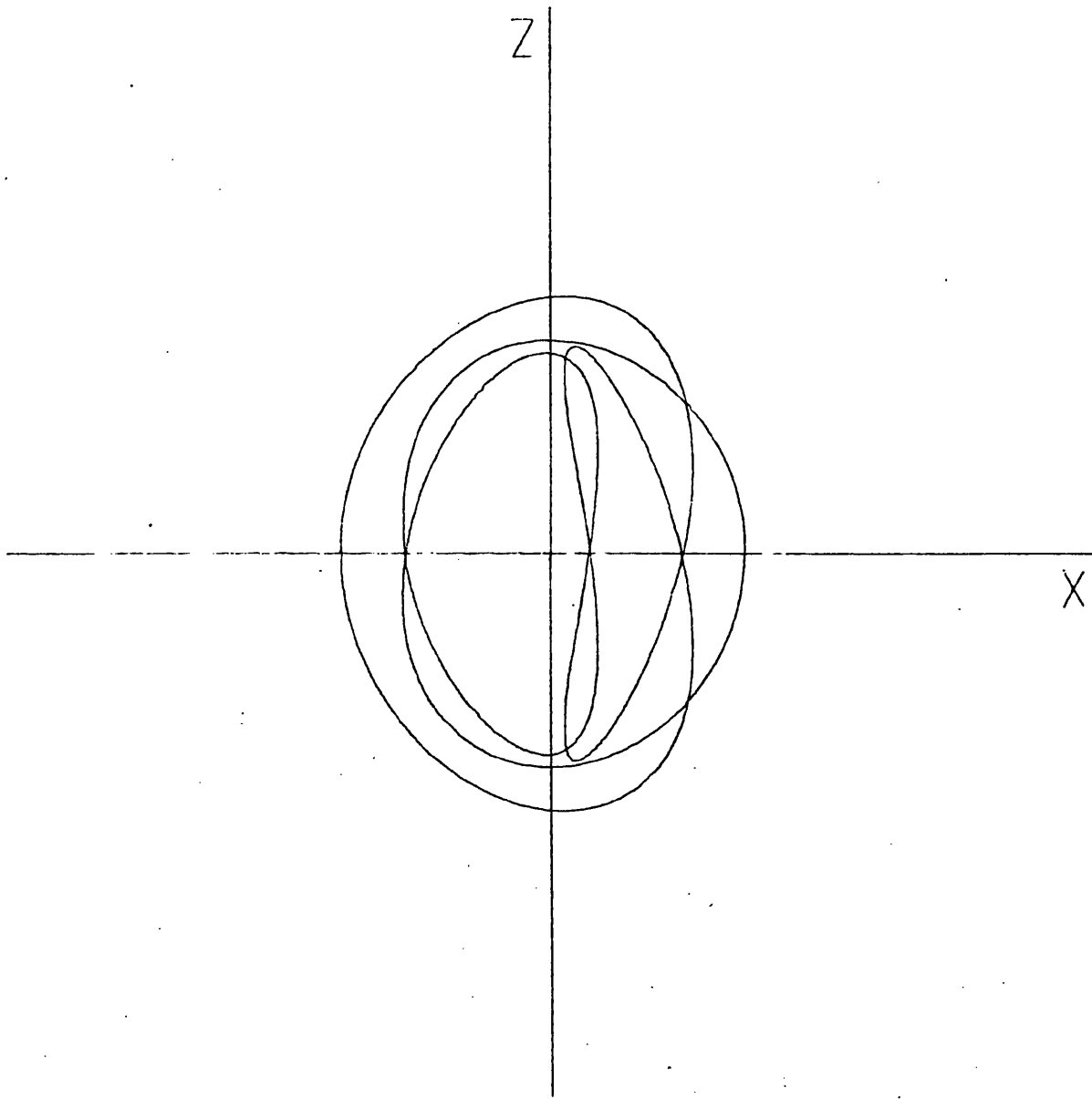


Figure A26

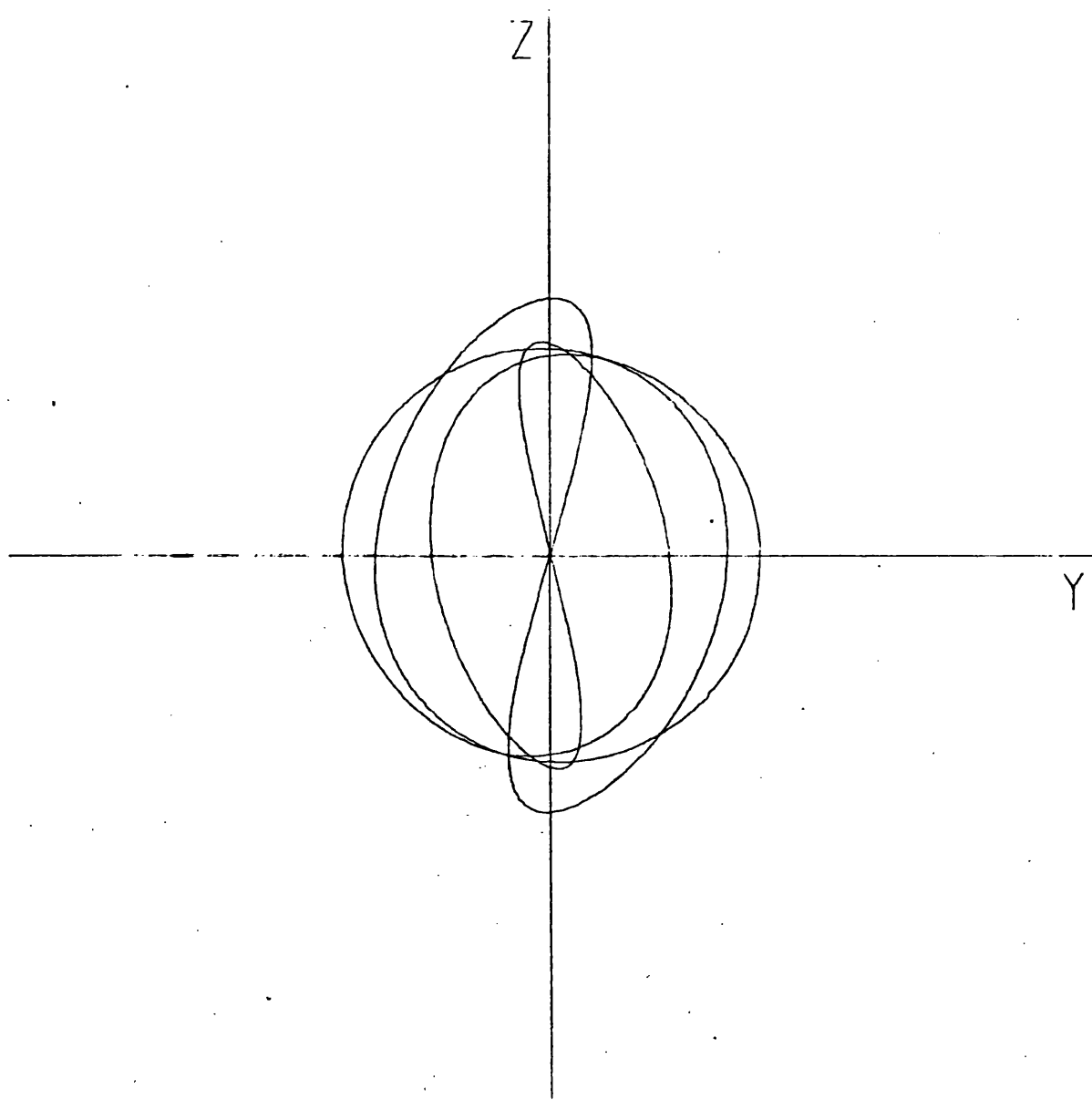


Figure A27

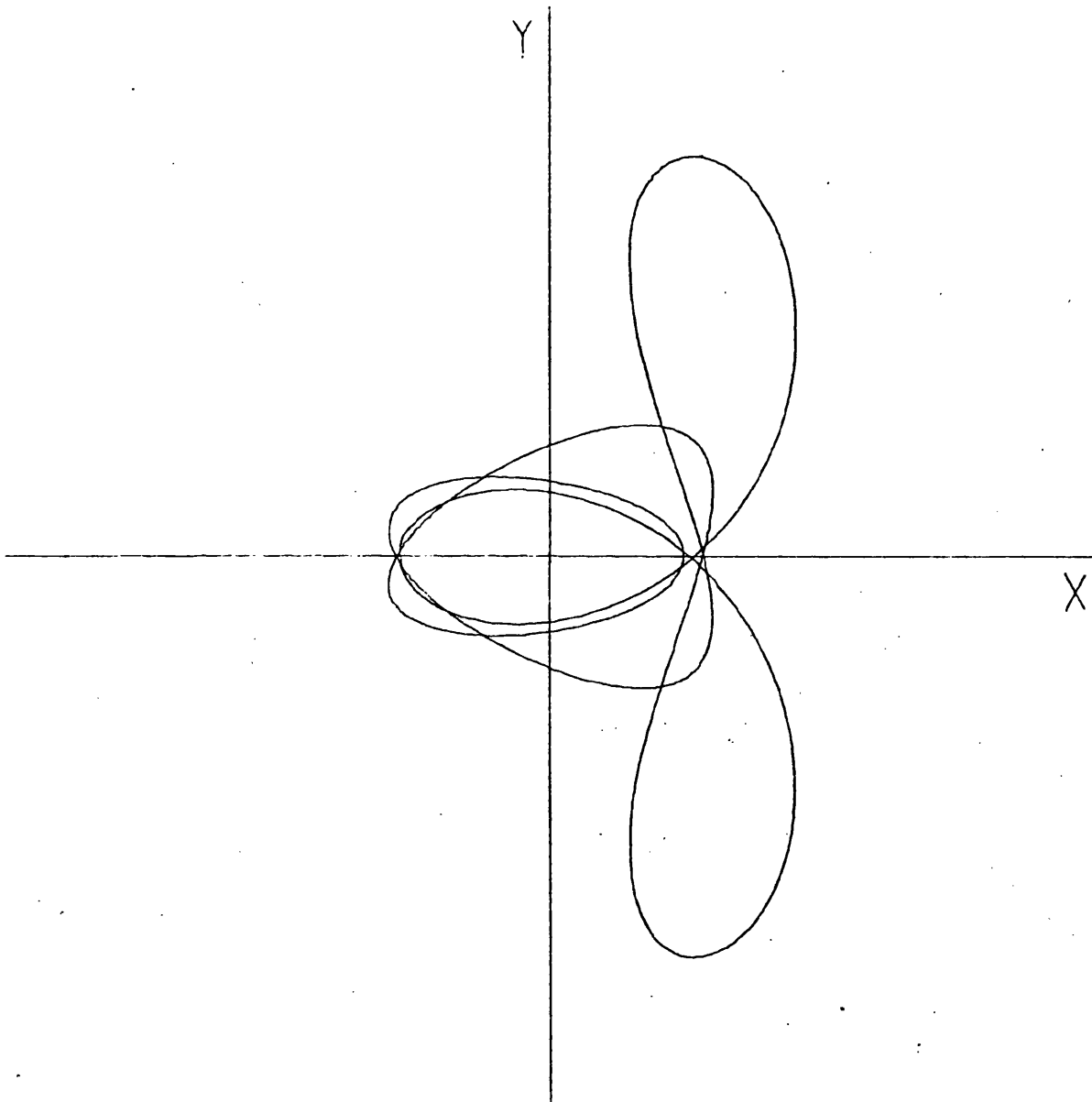


Figure A28

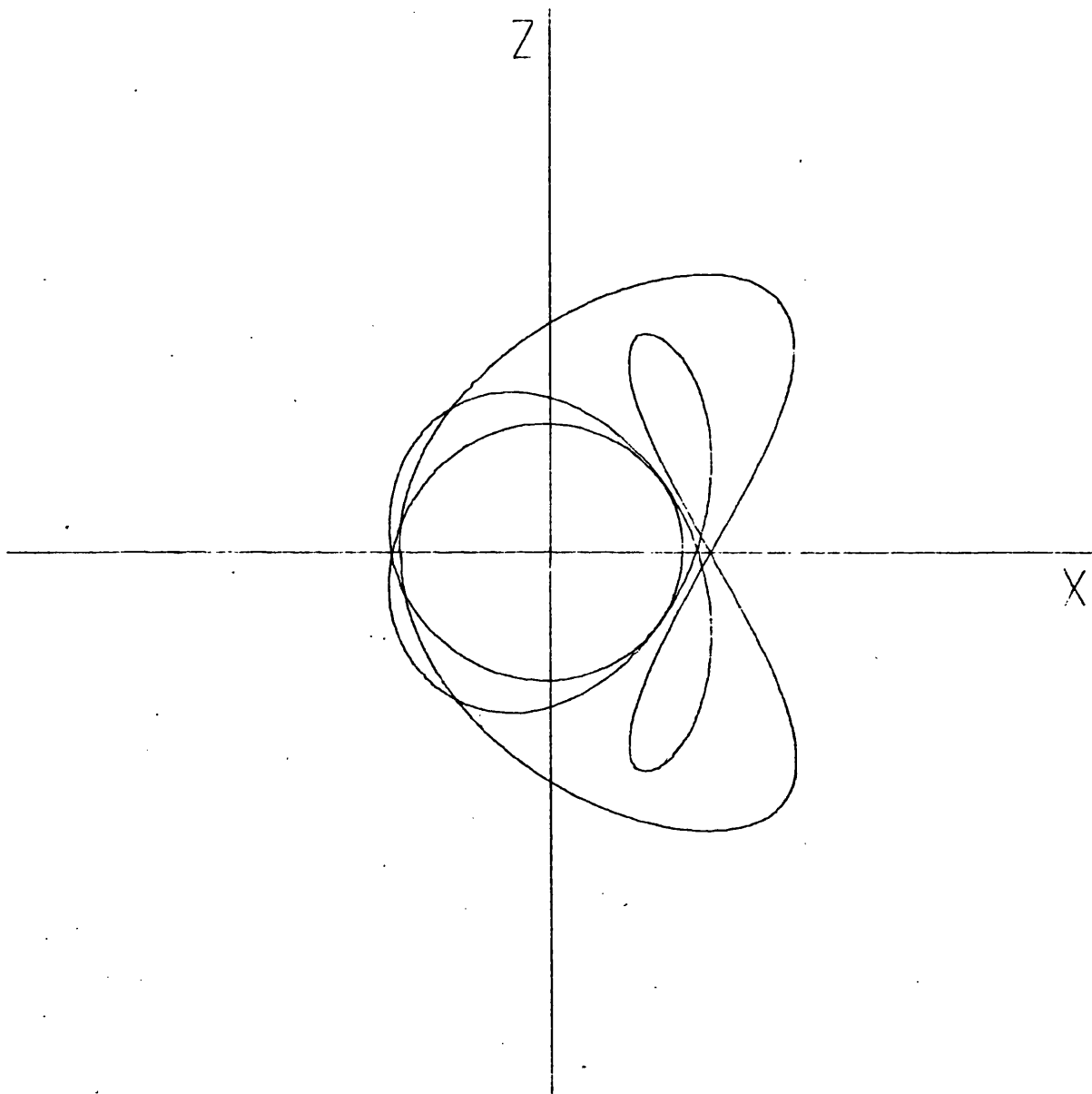


Figure A29

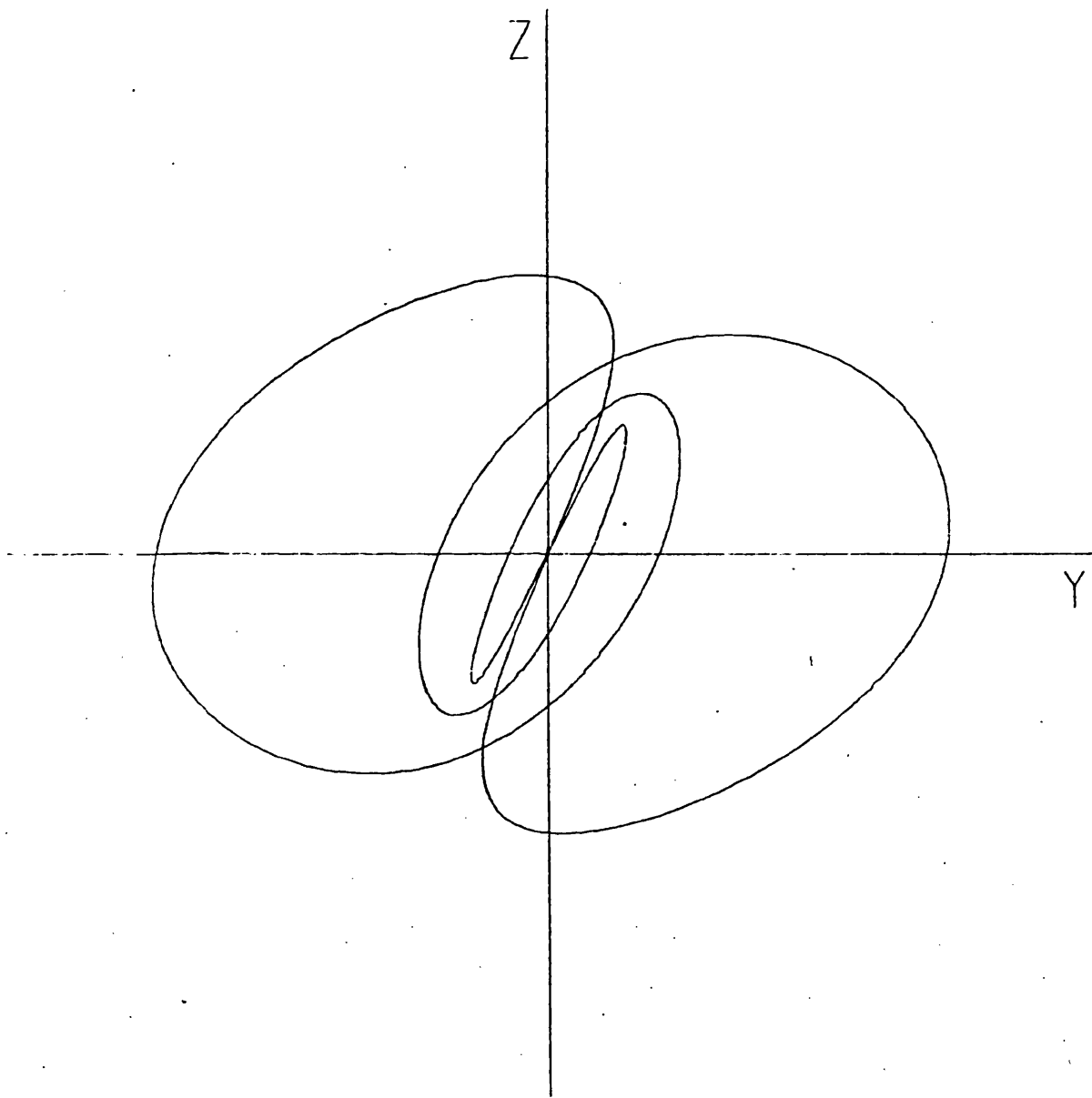


Figure A30

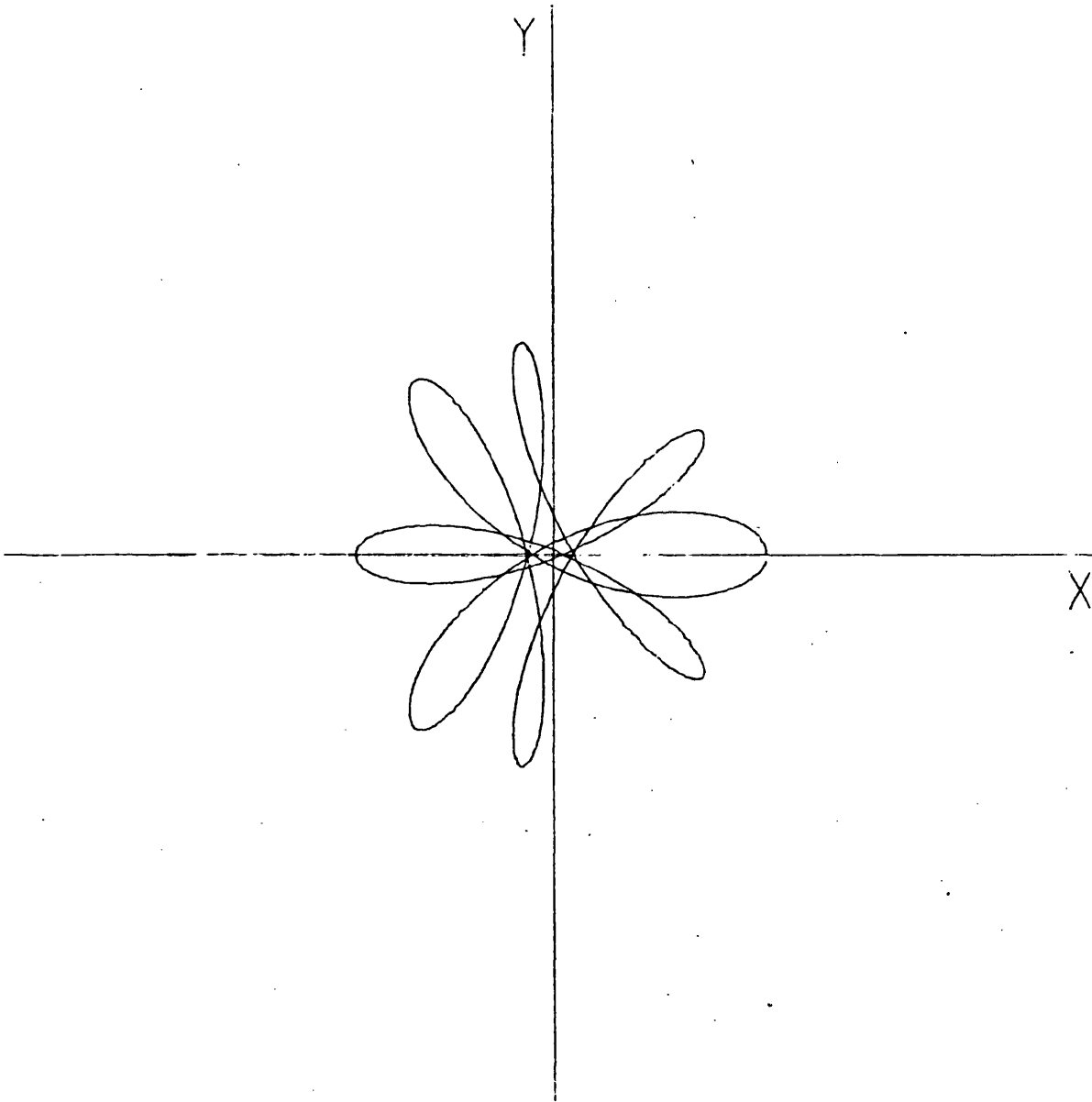


Figure A31

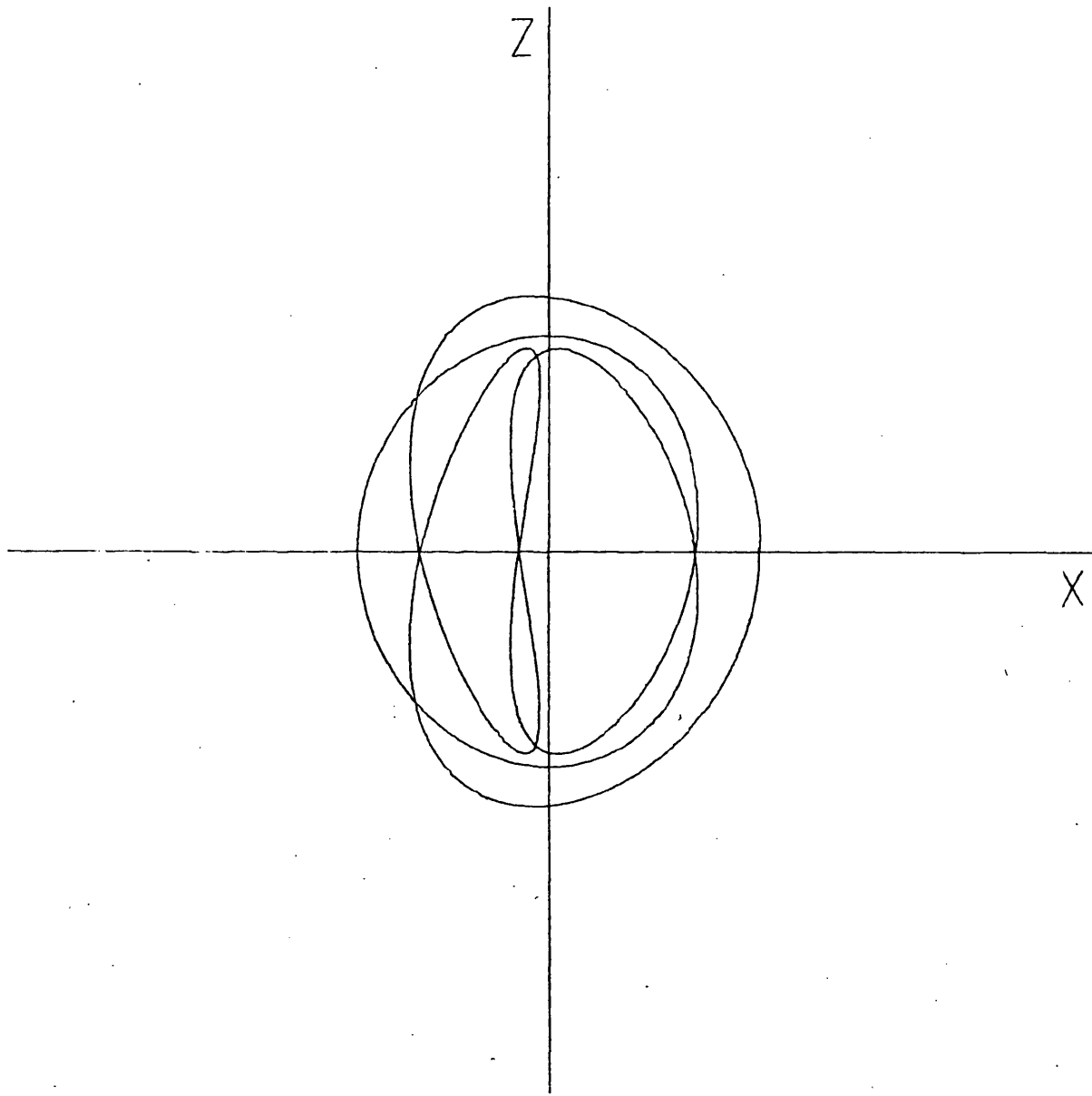


Figure A32

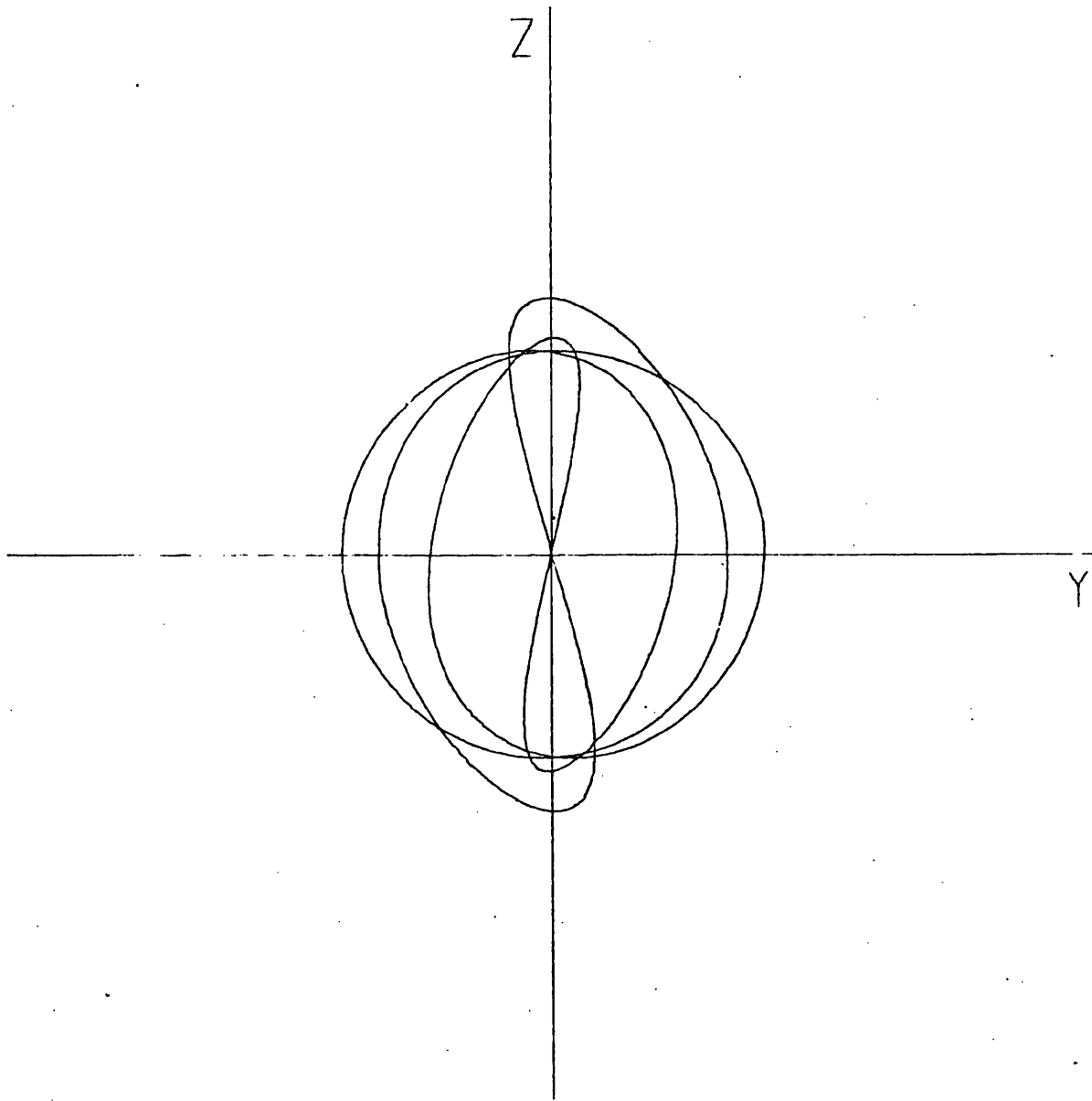


Figure A33

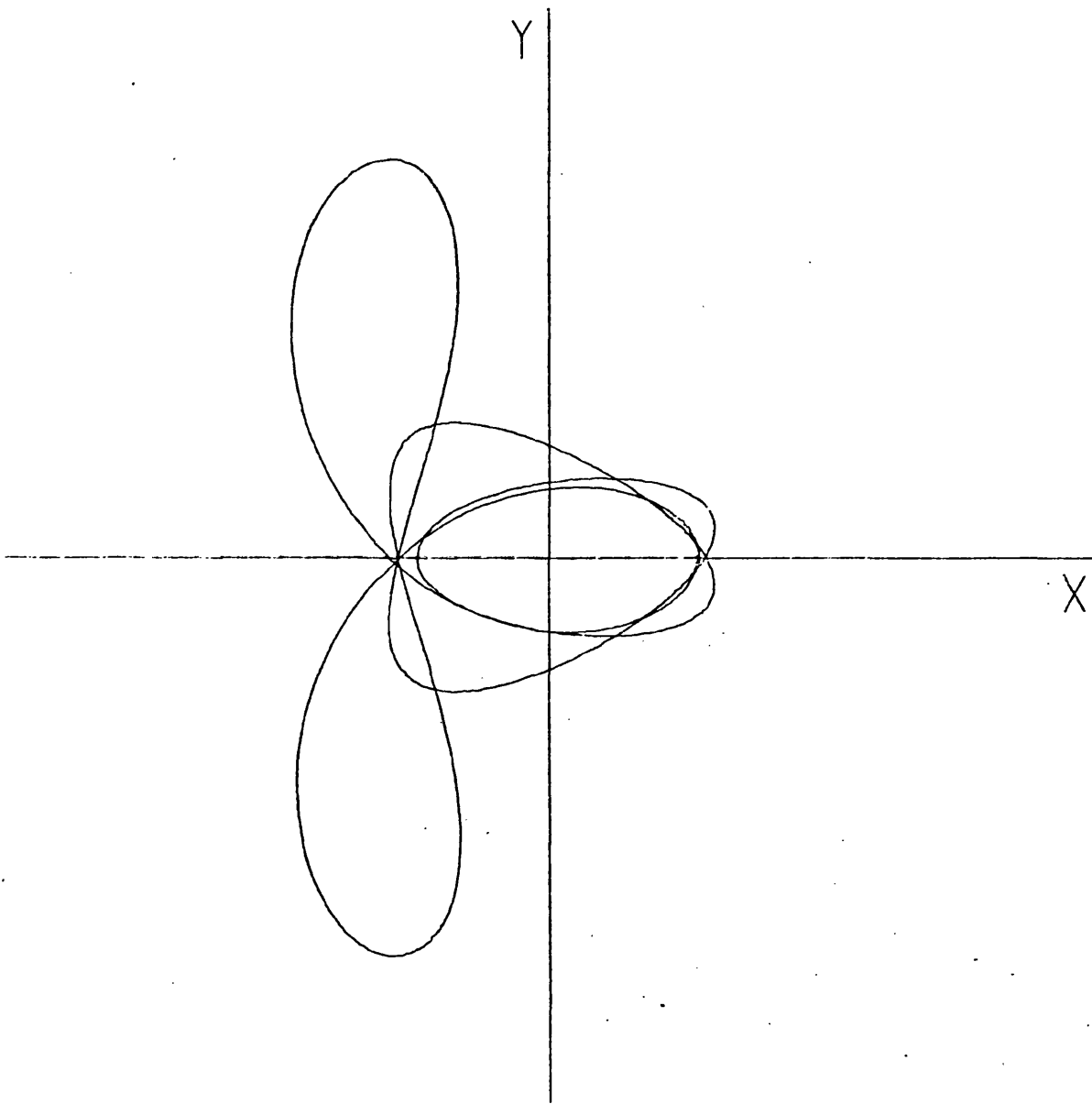


Figure A34

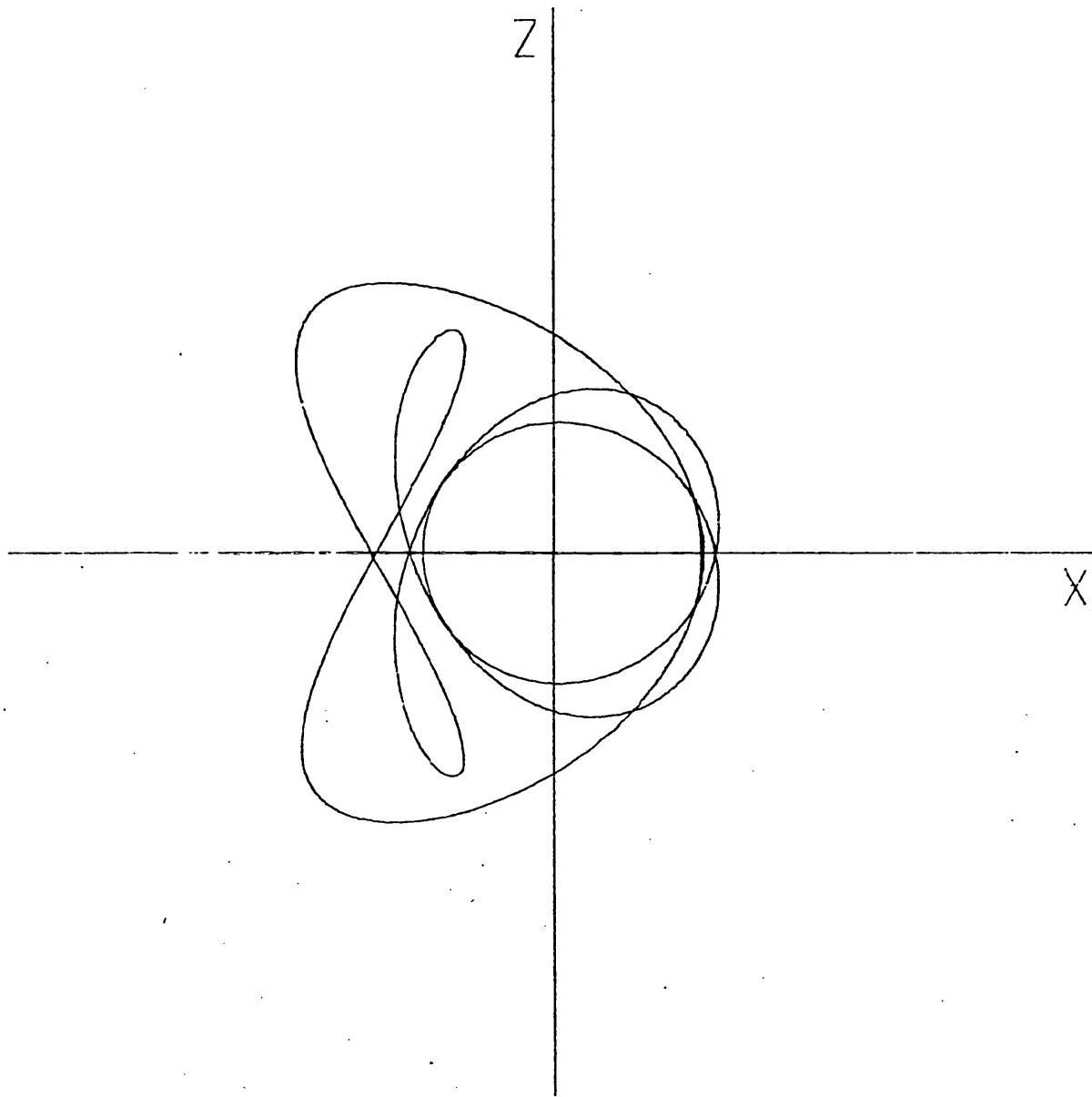


Figure A35

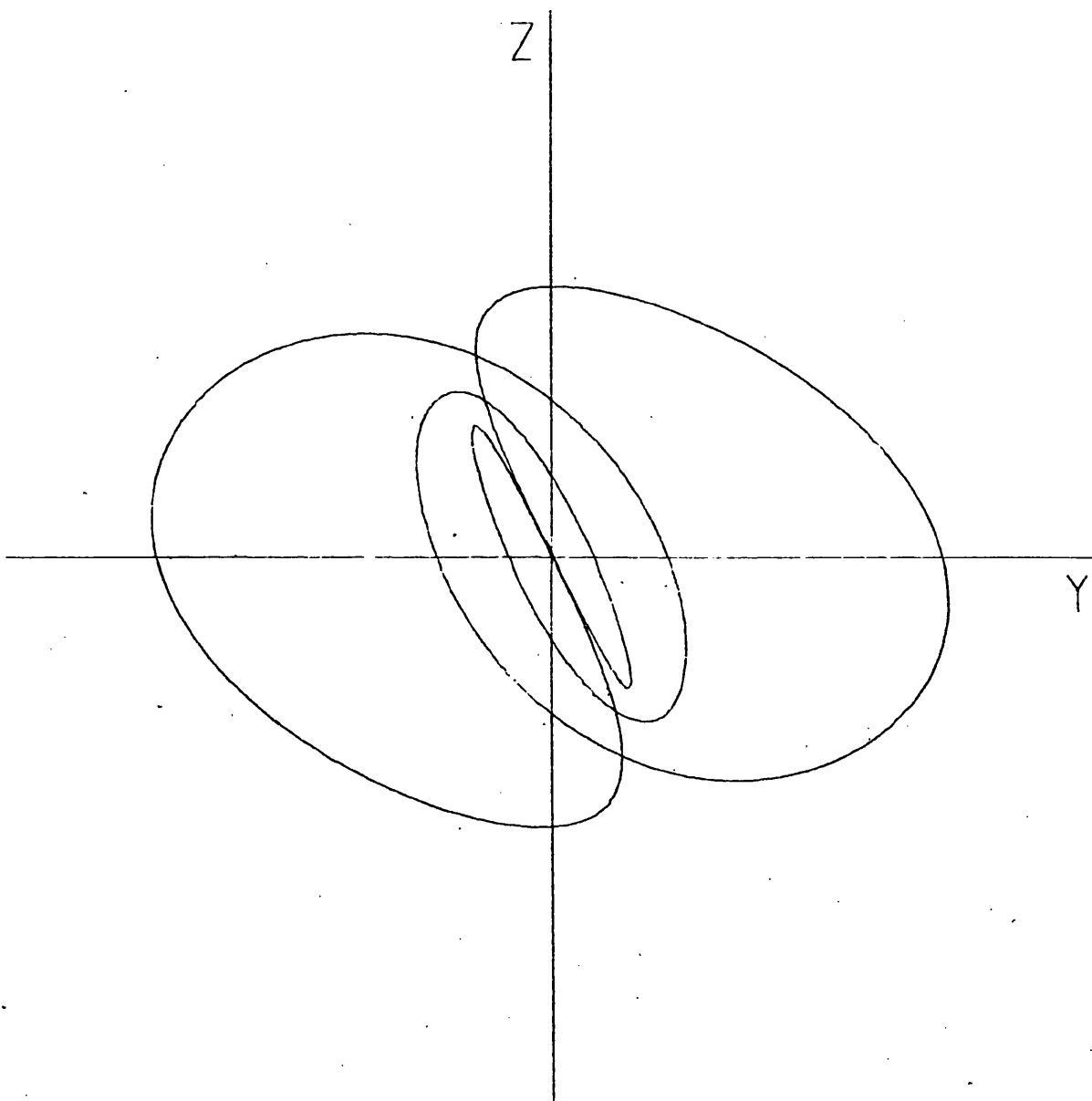


Figure A36

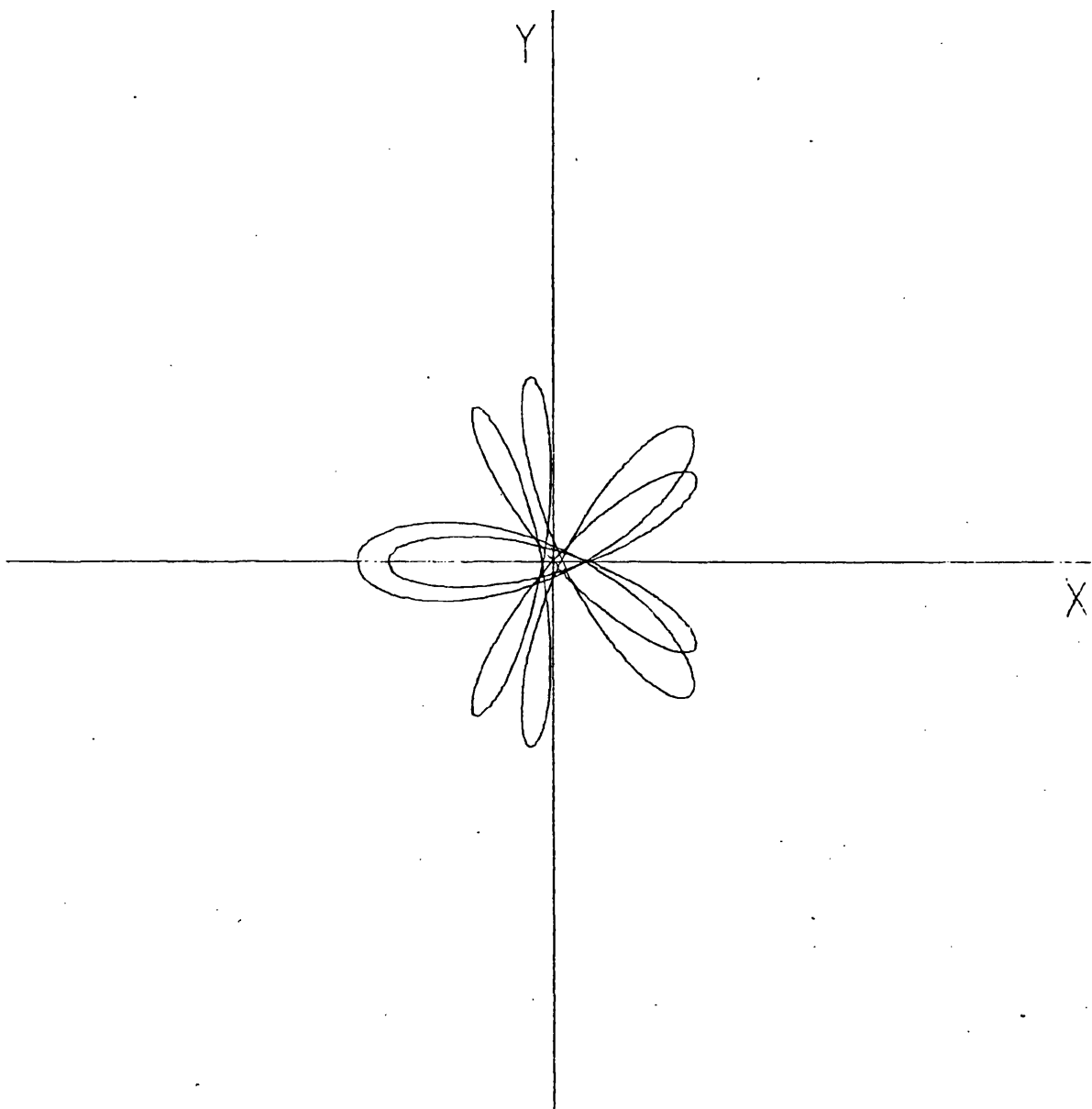


Figure A37

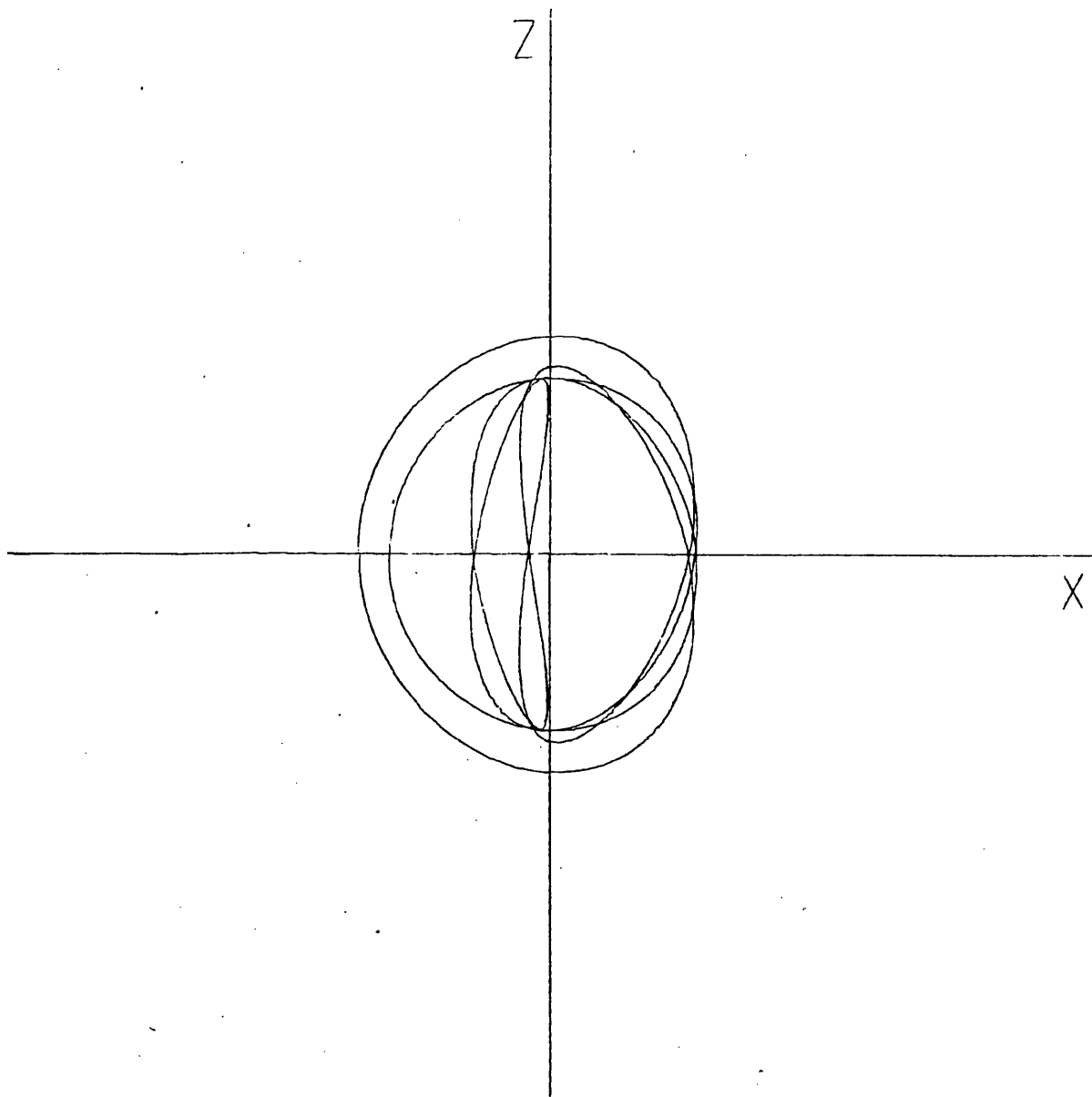


Figure A38

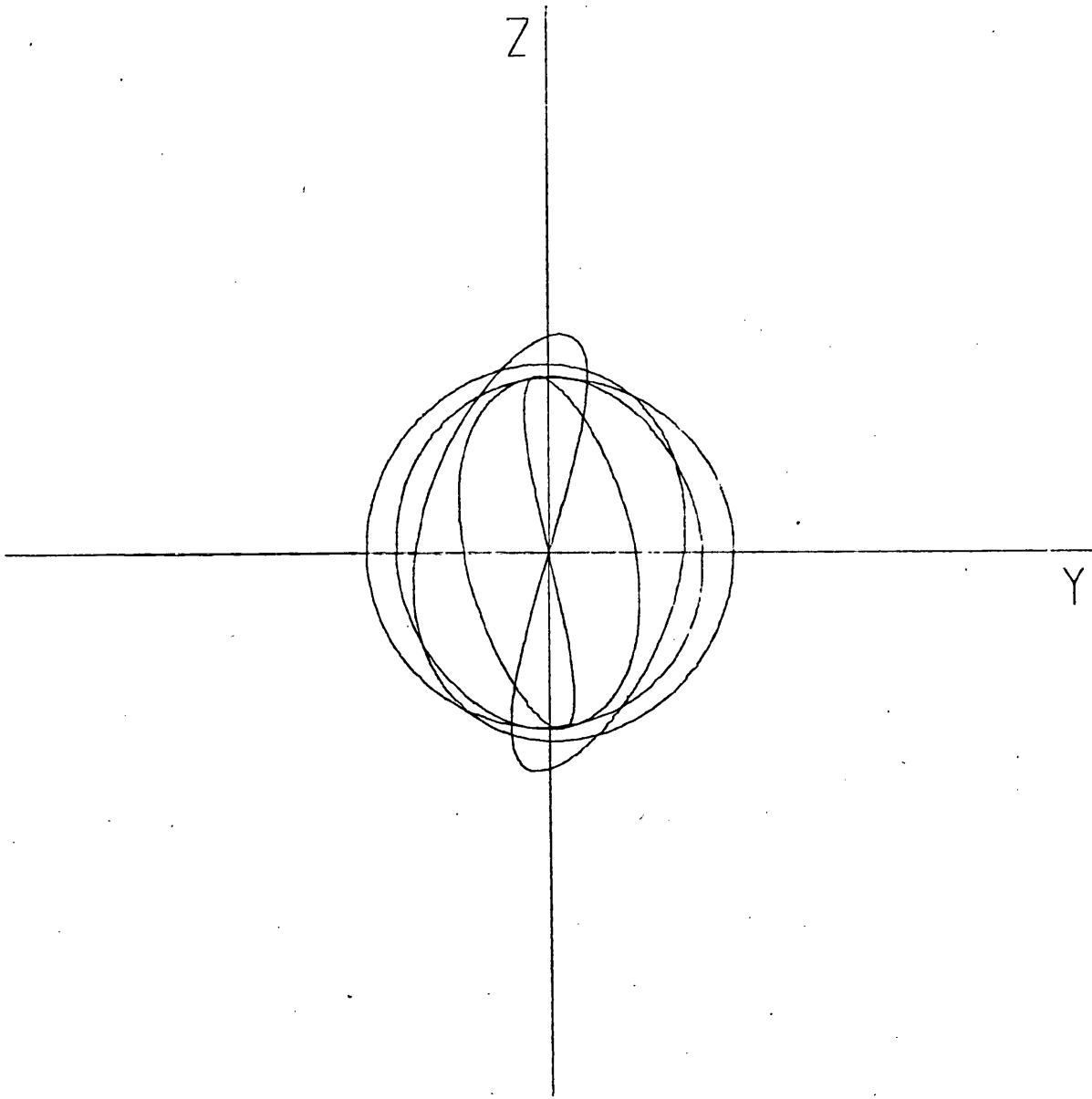


Figure A39

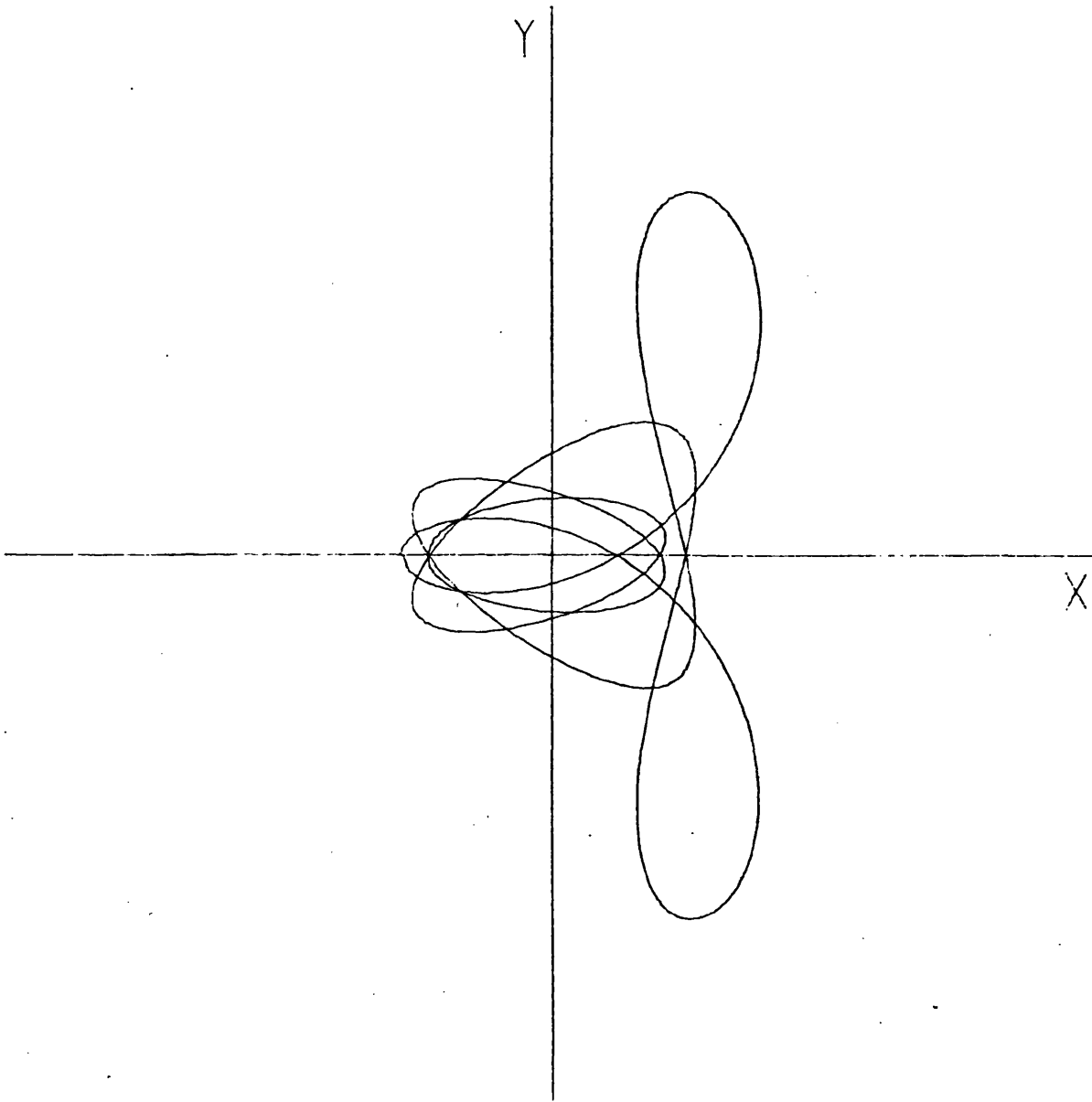


Figure A40

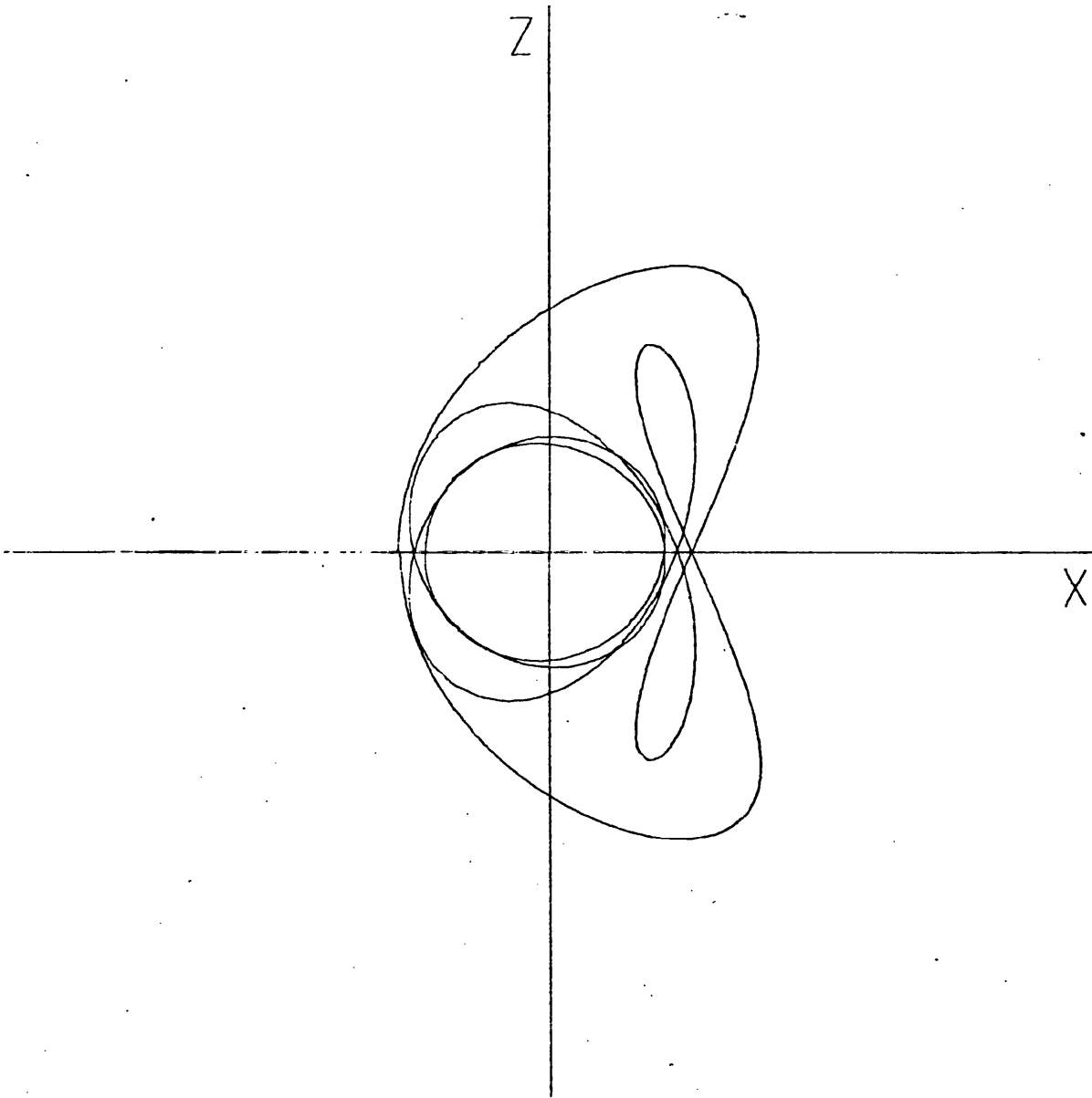


Figure A41

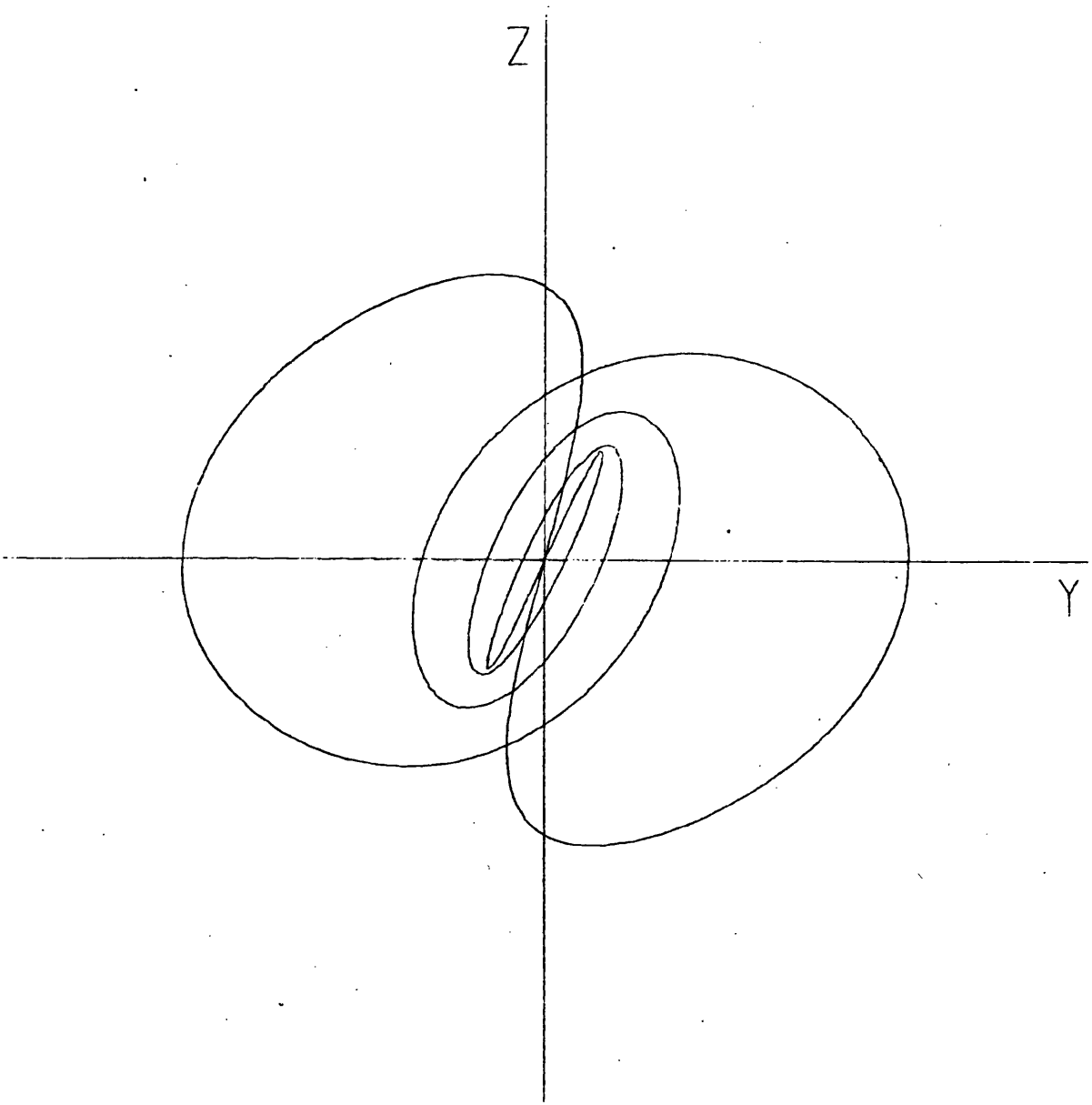


Figure A42

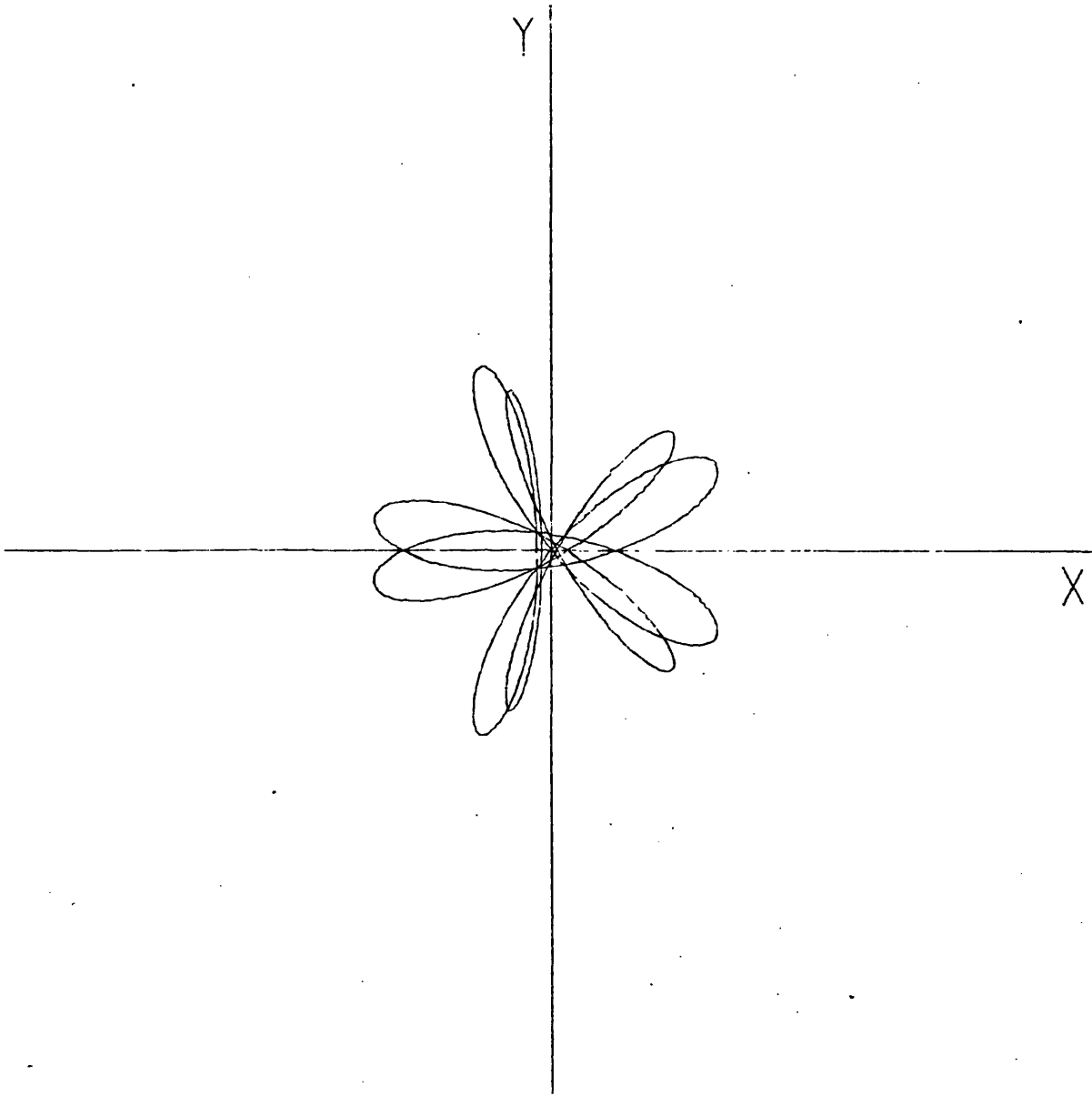


Figure A43

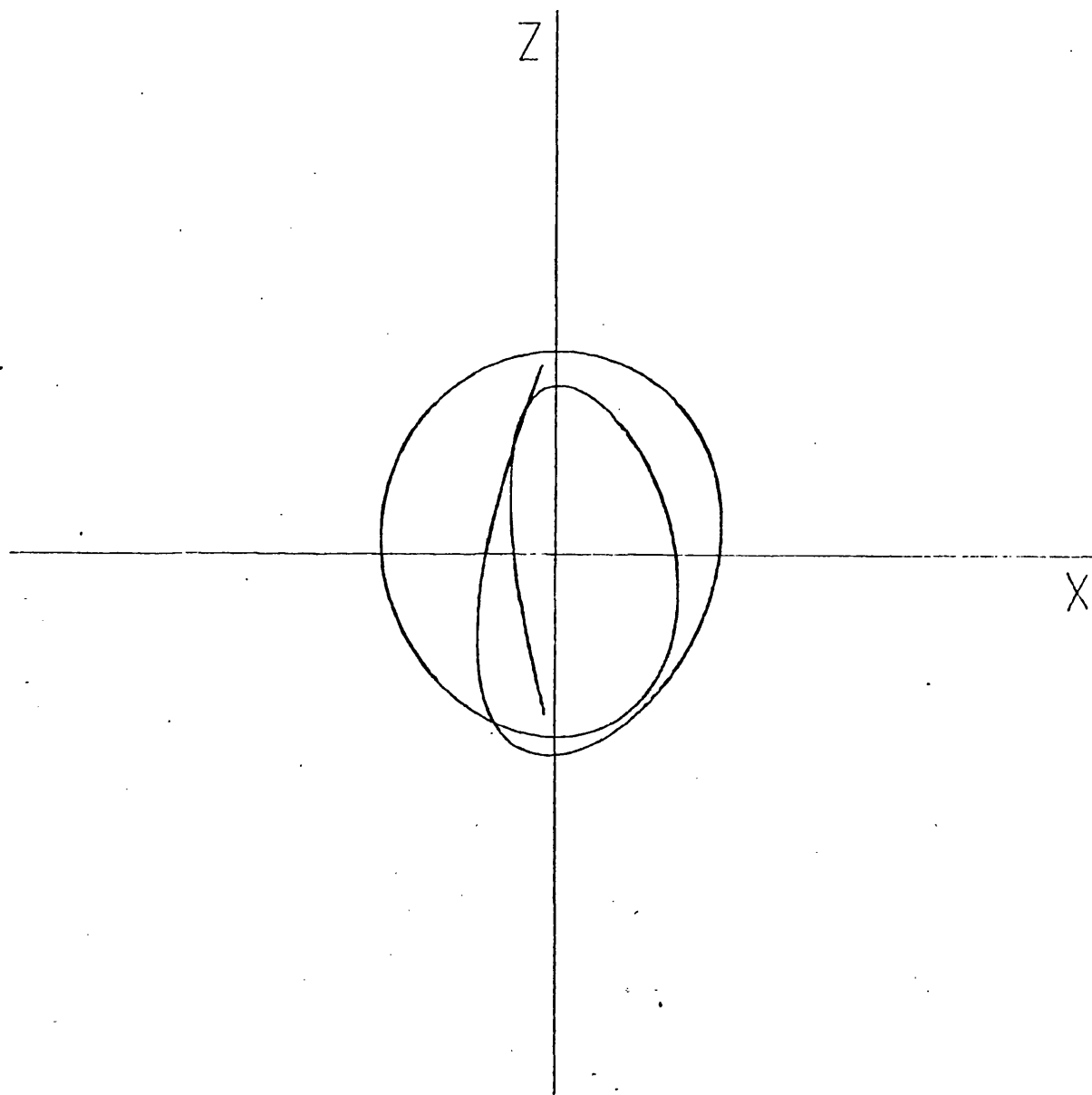


Figure A44

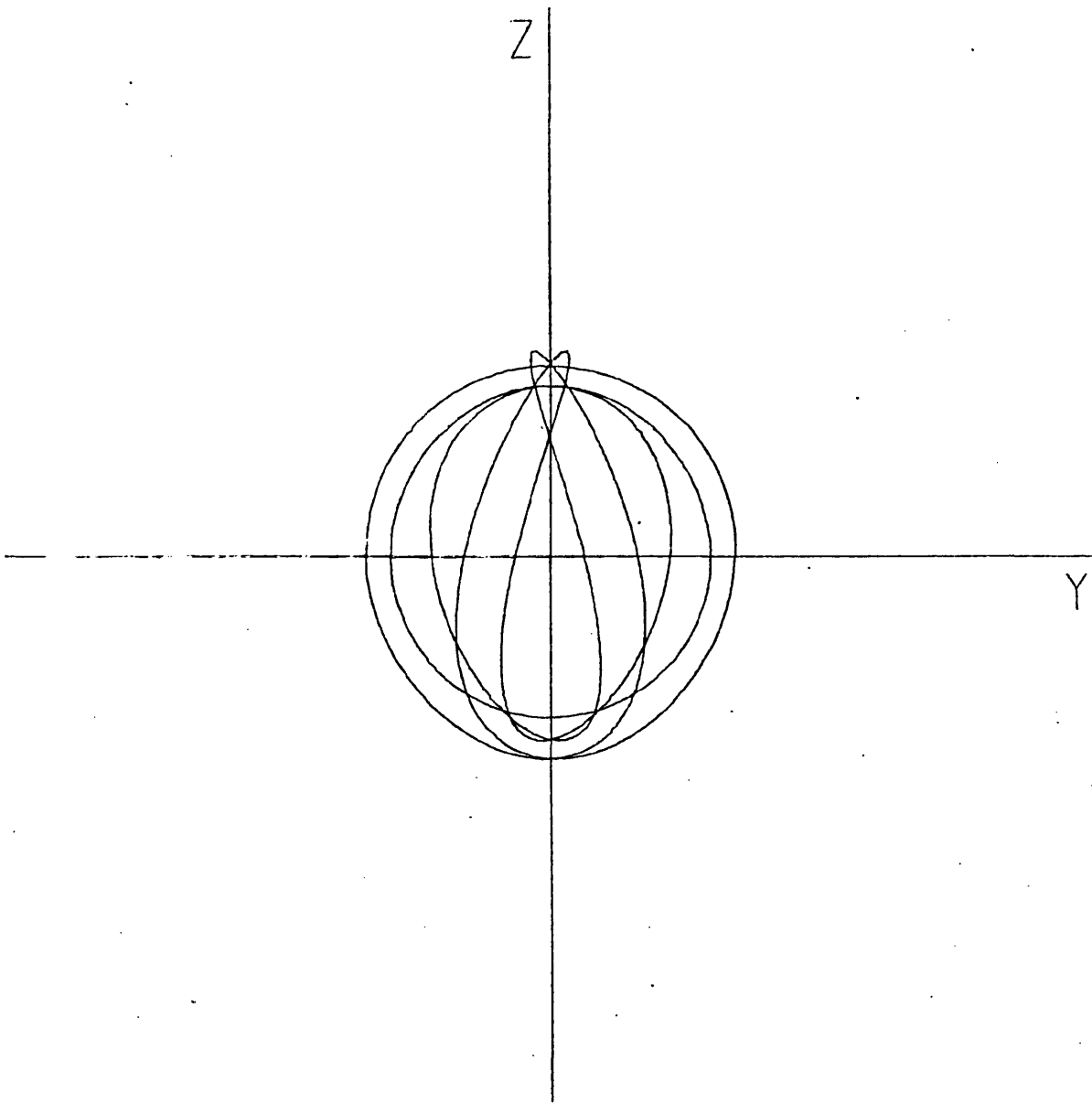


Figure A45

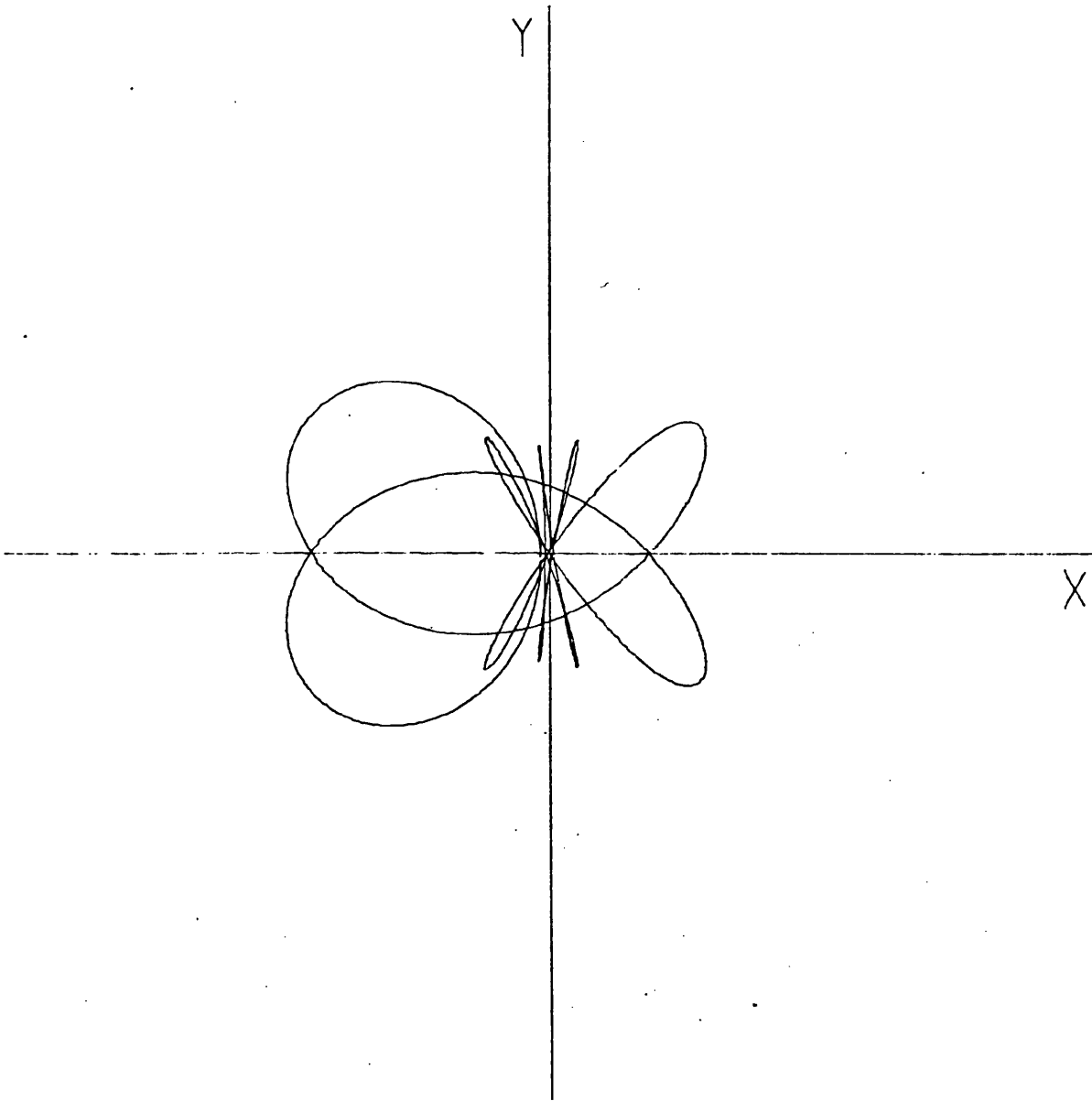


Figure A46

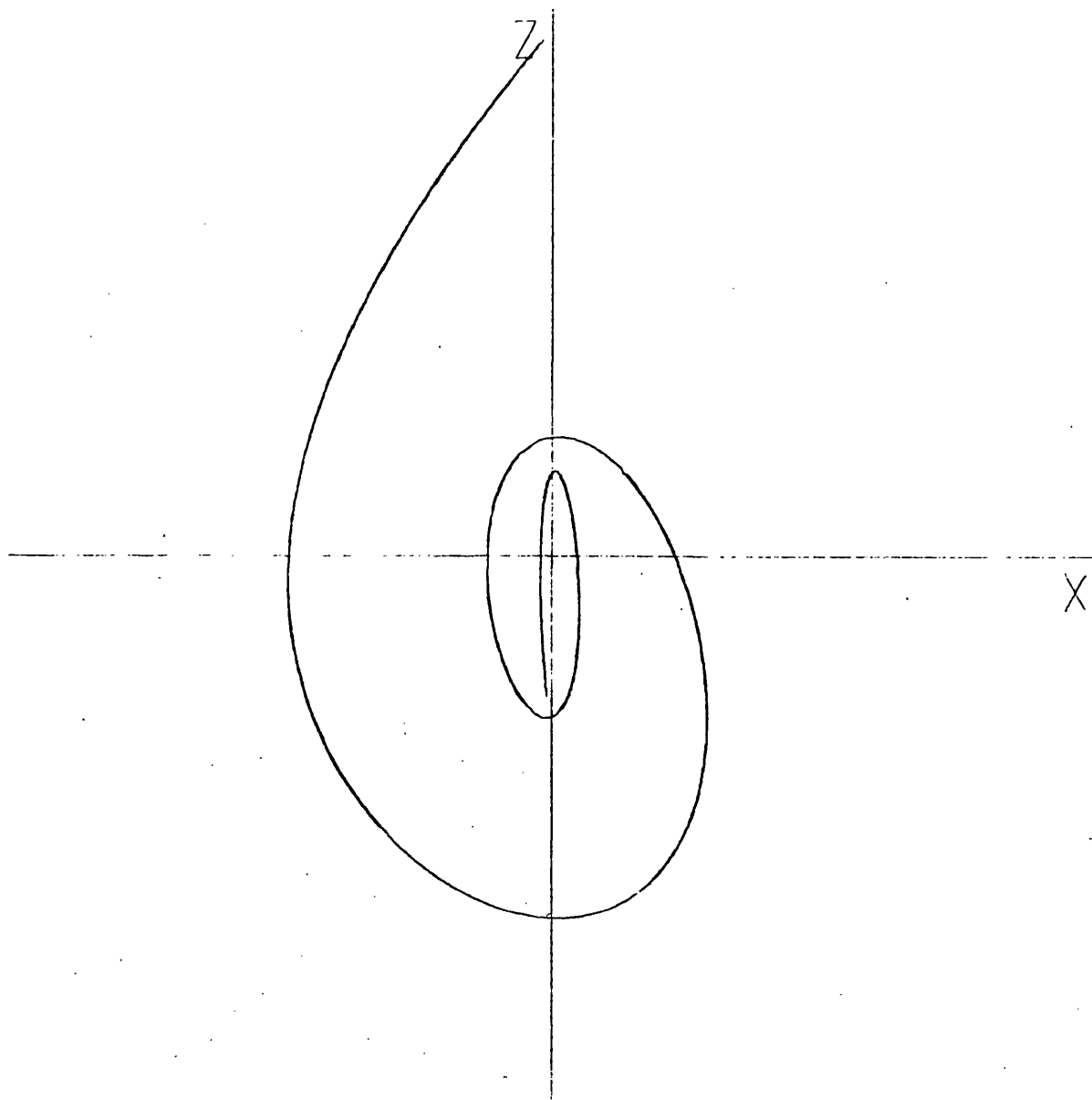


Figure A47

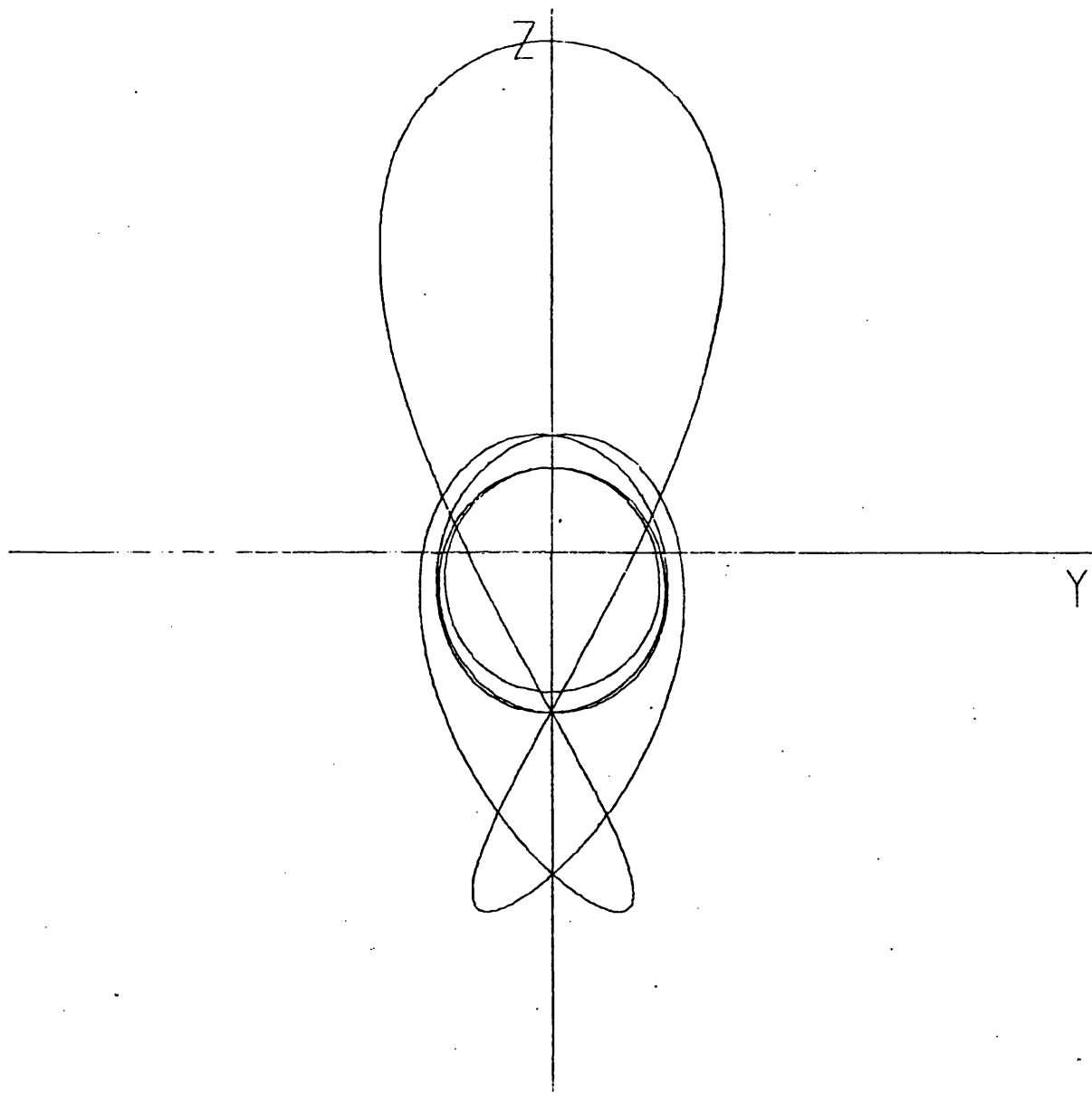


Figure A48

Group (c): Figures A49 - A56

Representative vertical self-resonant orbits of the planar elliptic problem, belonging to the conjunction and opposition series generated from the  $1/4$  commensurability of series  $f_{v15}^1$  (Section 7.4). The plot coordinates  $(X,Y)$  are identical to the coordinates  $(x,y)$  of the rotating-pulsating system, with origin at the centre of mass of the primaries. The ticks on the X-axis indicate the positions of the primaries  $m_1$  (on the left,  $X = -\mu$ ) and  $m_2$  (on the right,  $X = 1-\mu$ ).

Figure A49 : Starting orbit for both series, the  $1/4$  commensurability of circular series  $f_{v15}^1$ .

Figures A50 - A52: Evolution along the conjunction series.

Figures A53 - A55: Evolution along the opposition series.

Figure A56 : Termination orbit ( $e = 0$ ) of the opposition series.

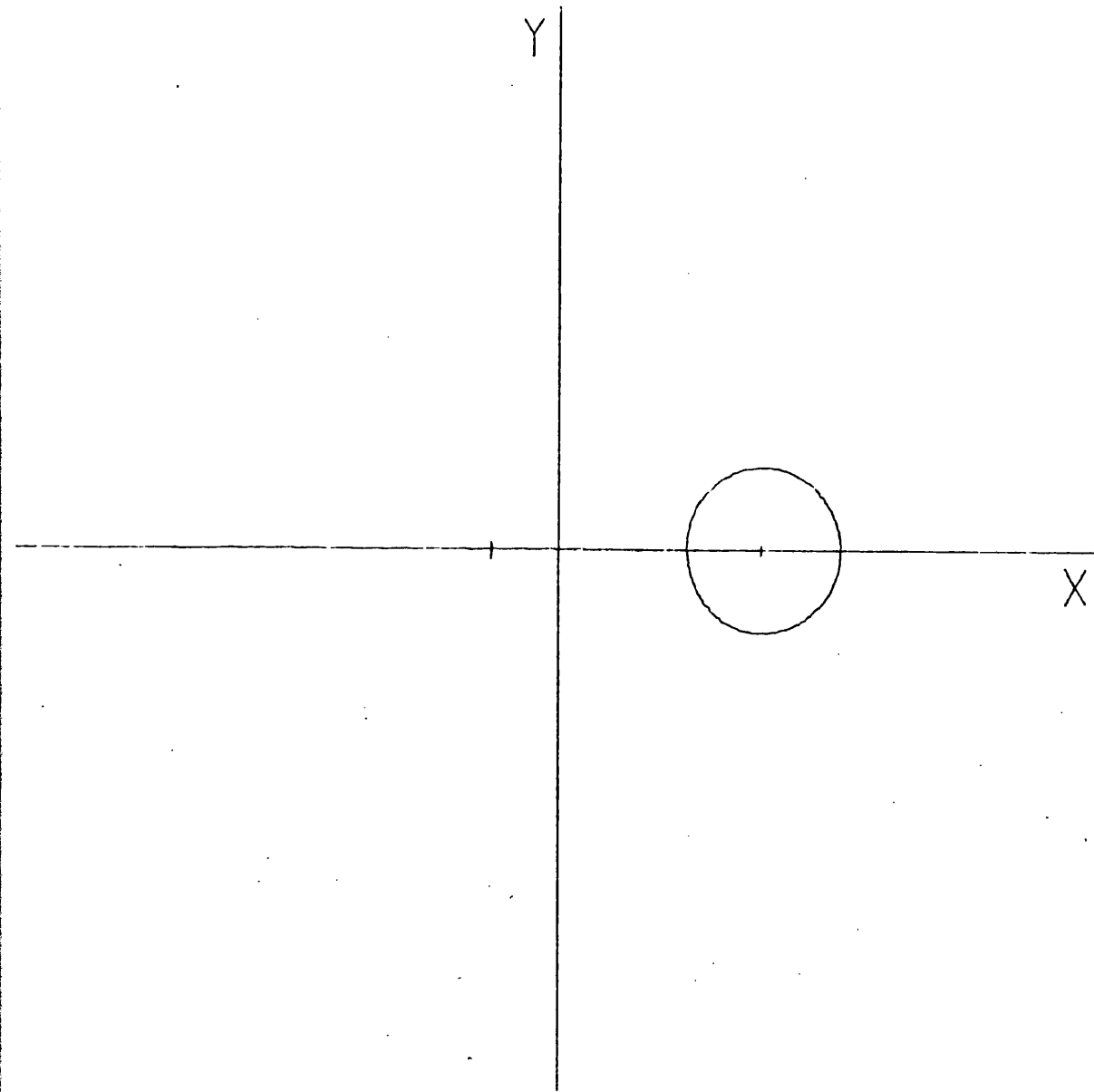


Figure A49

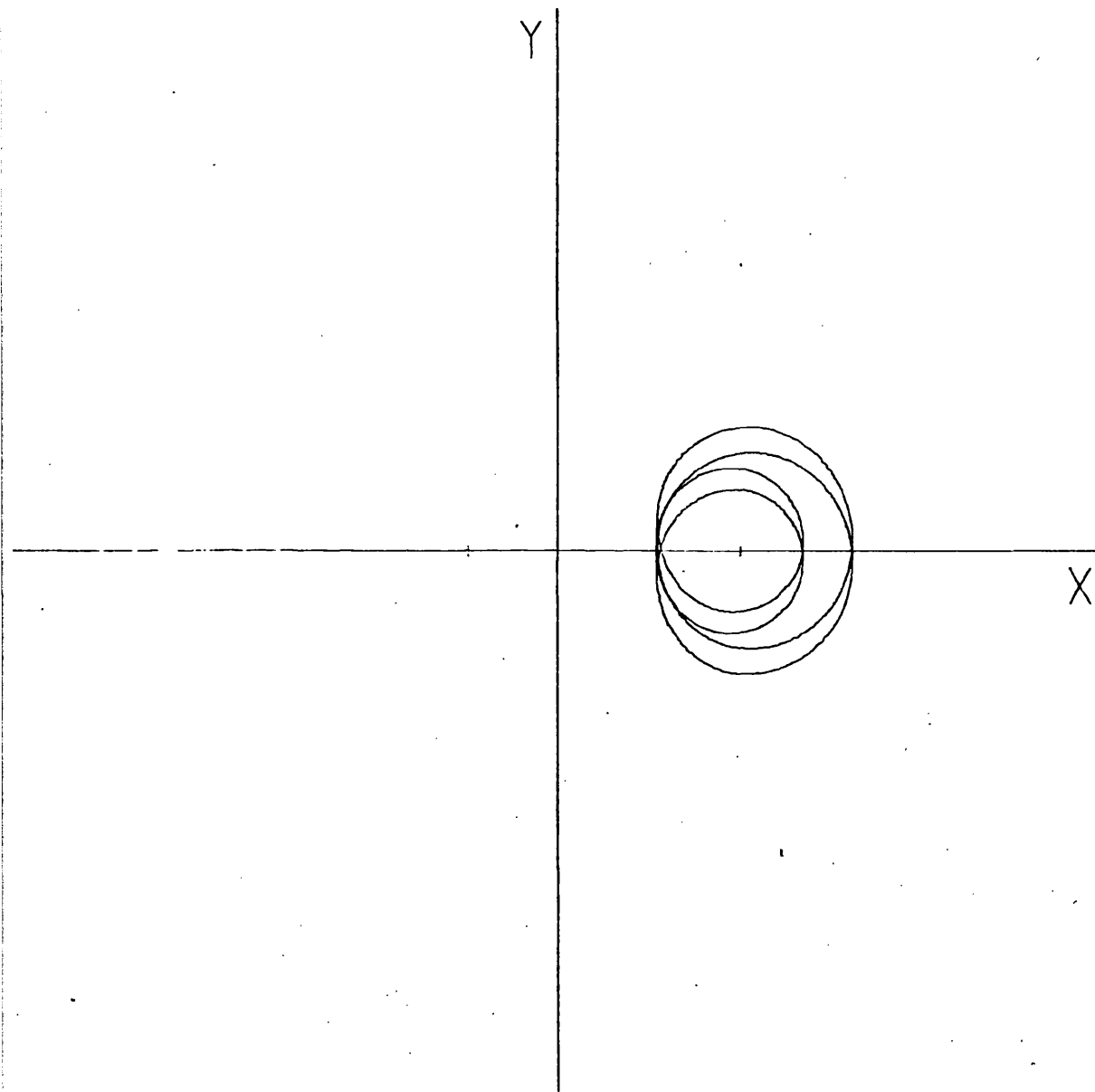


Figure A50

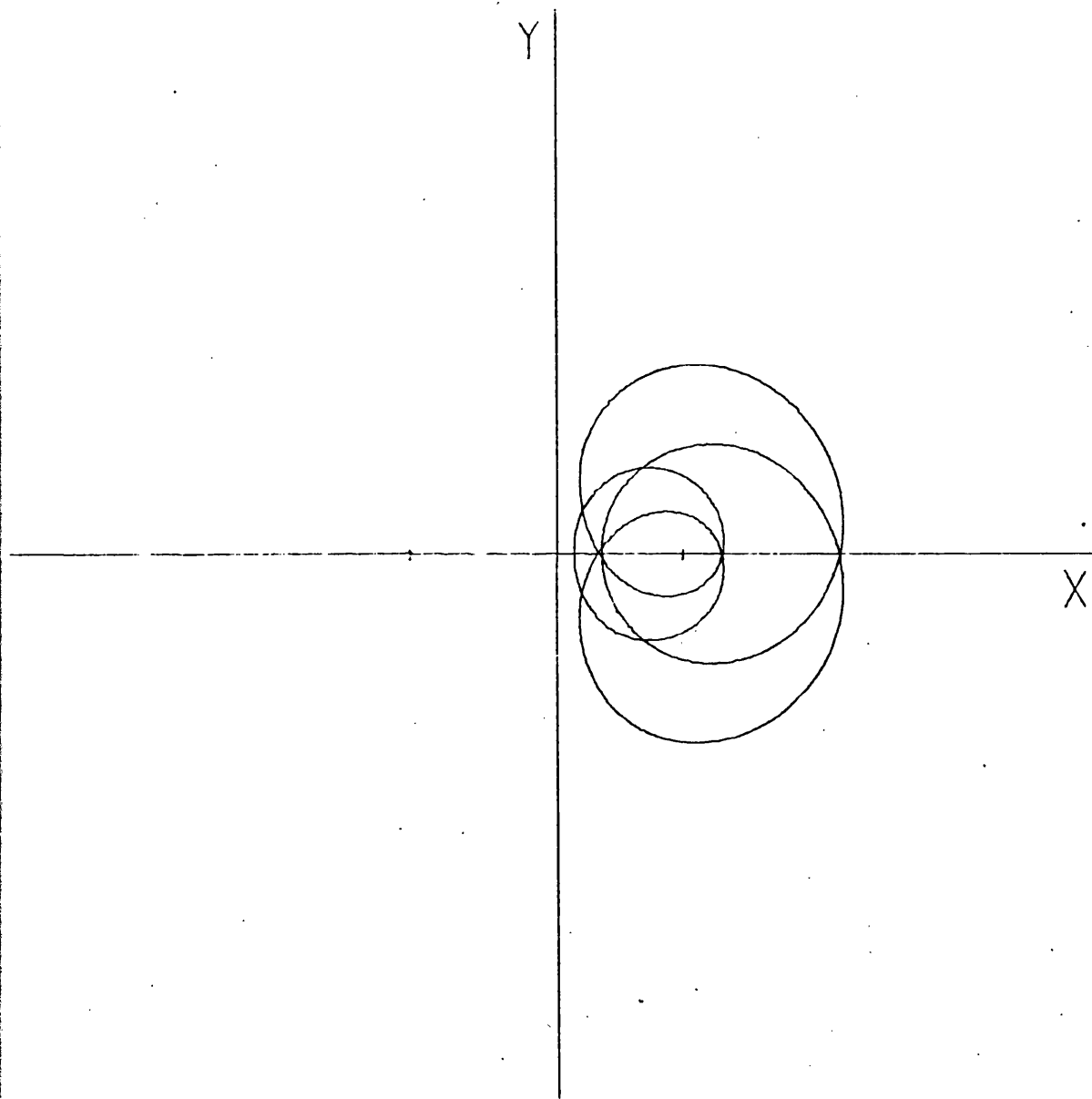


Figure A51

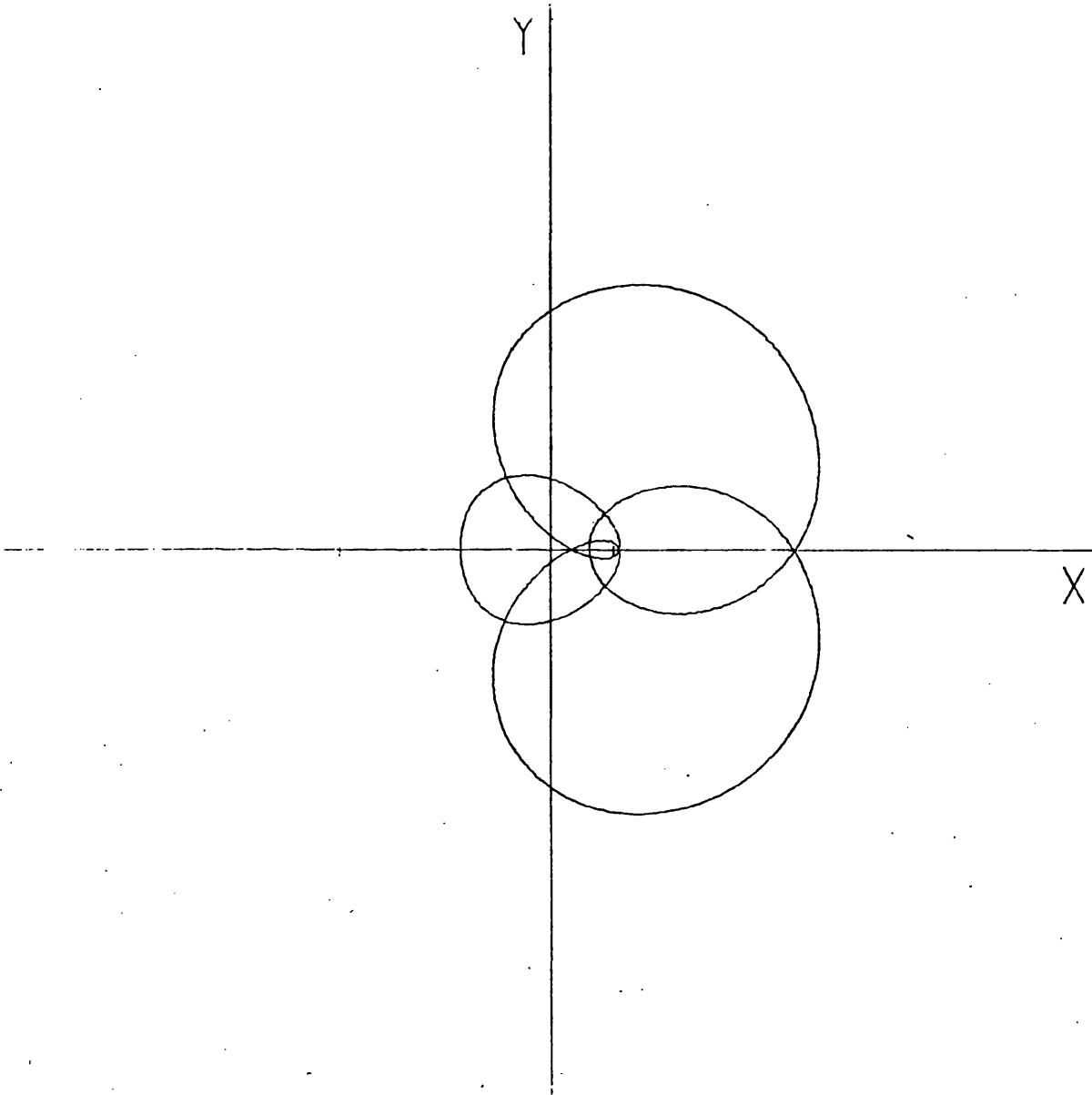


Figure A52

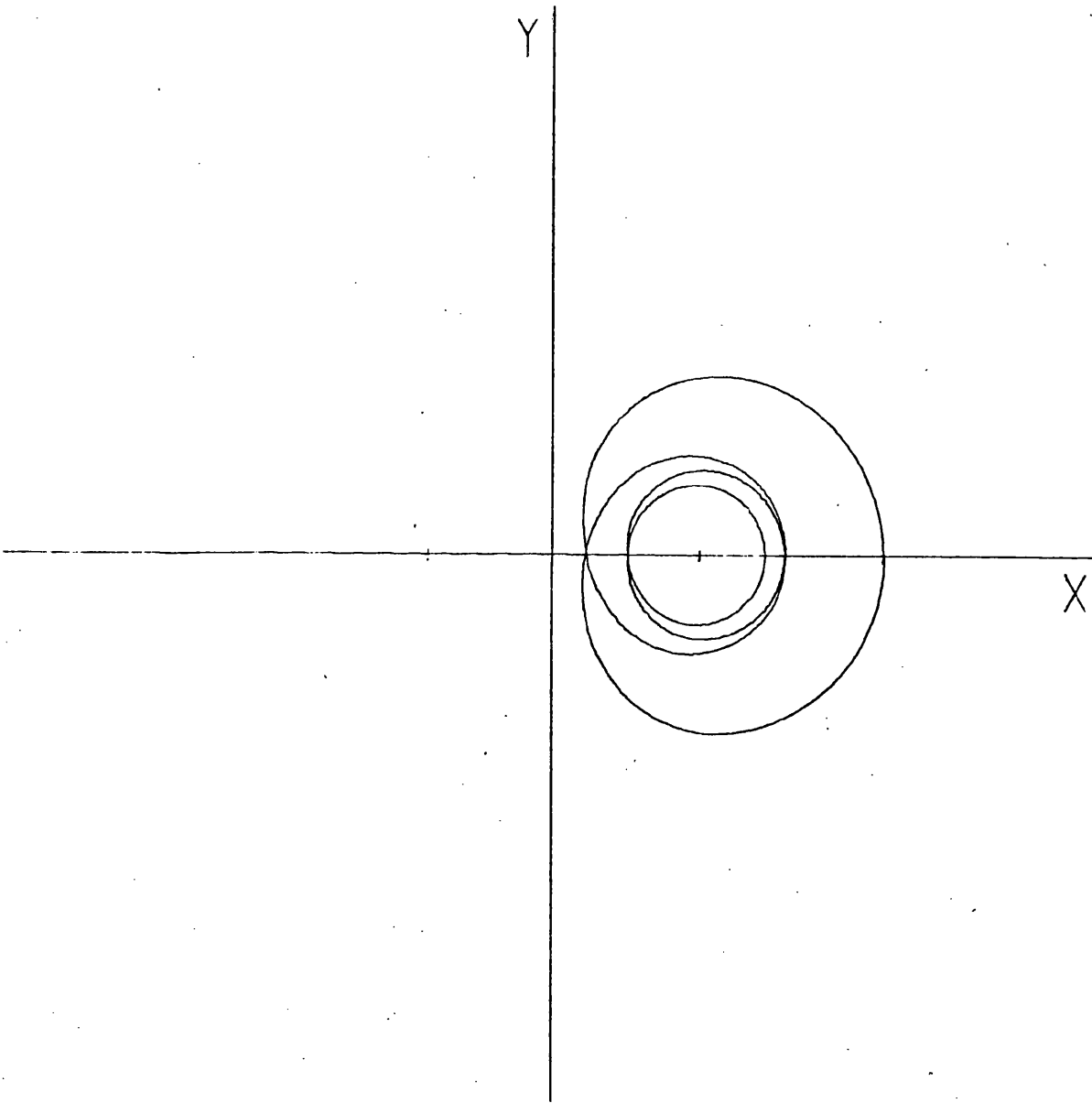


Figure A53

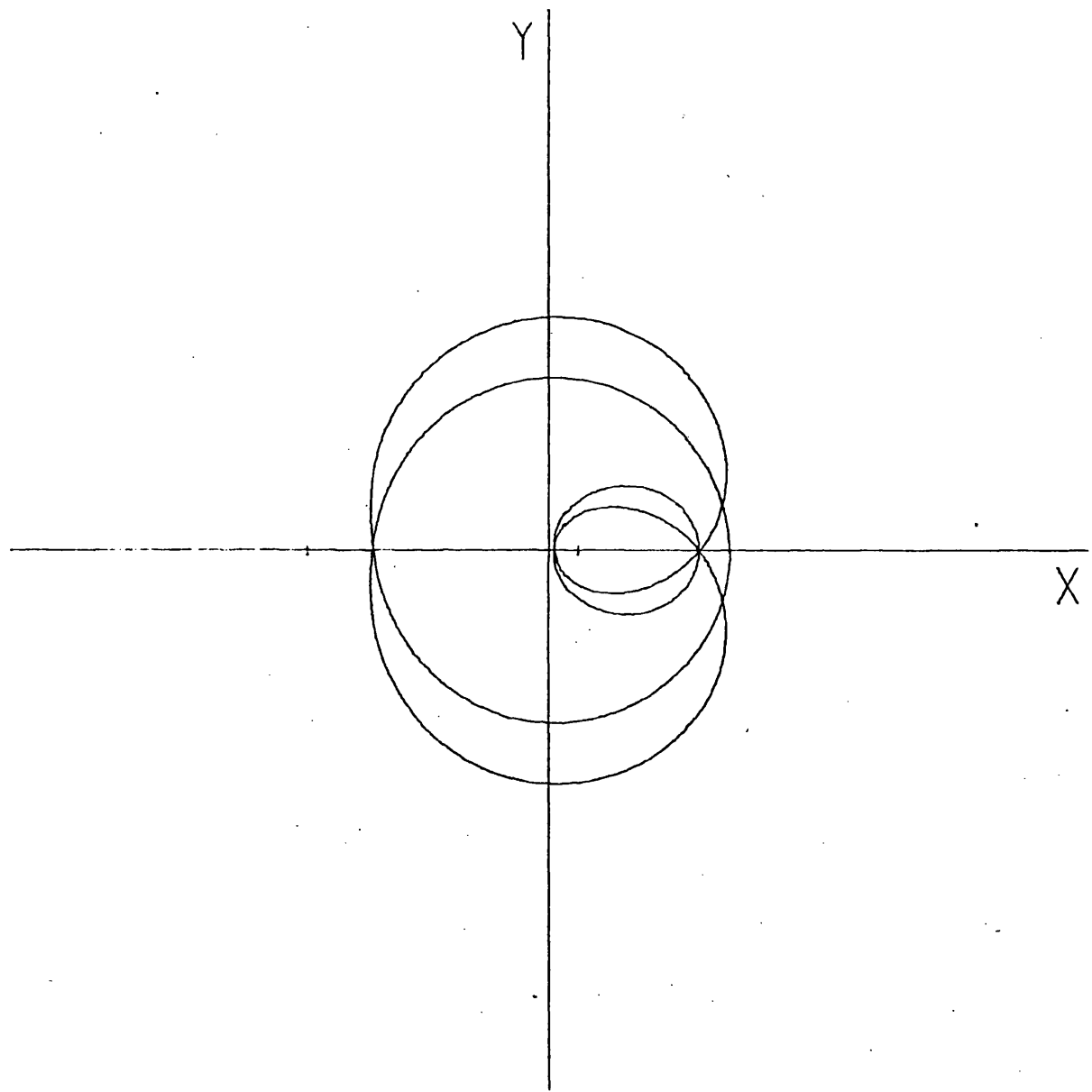


Figure A54

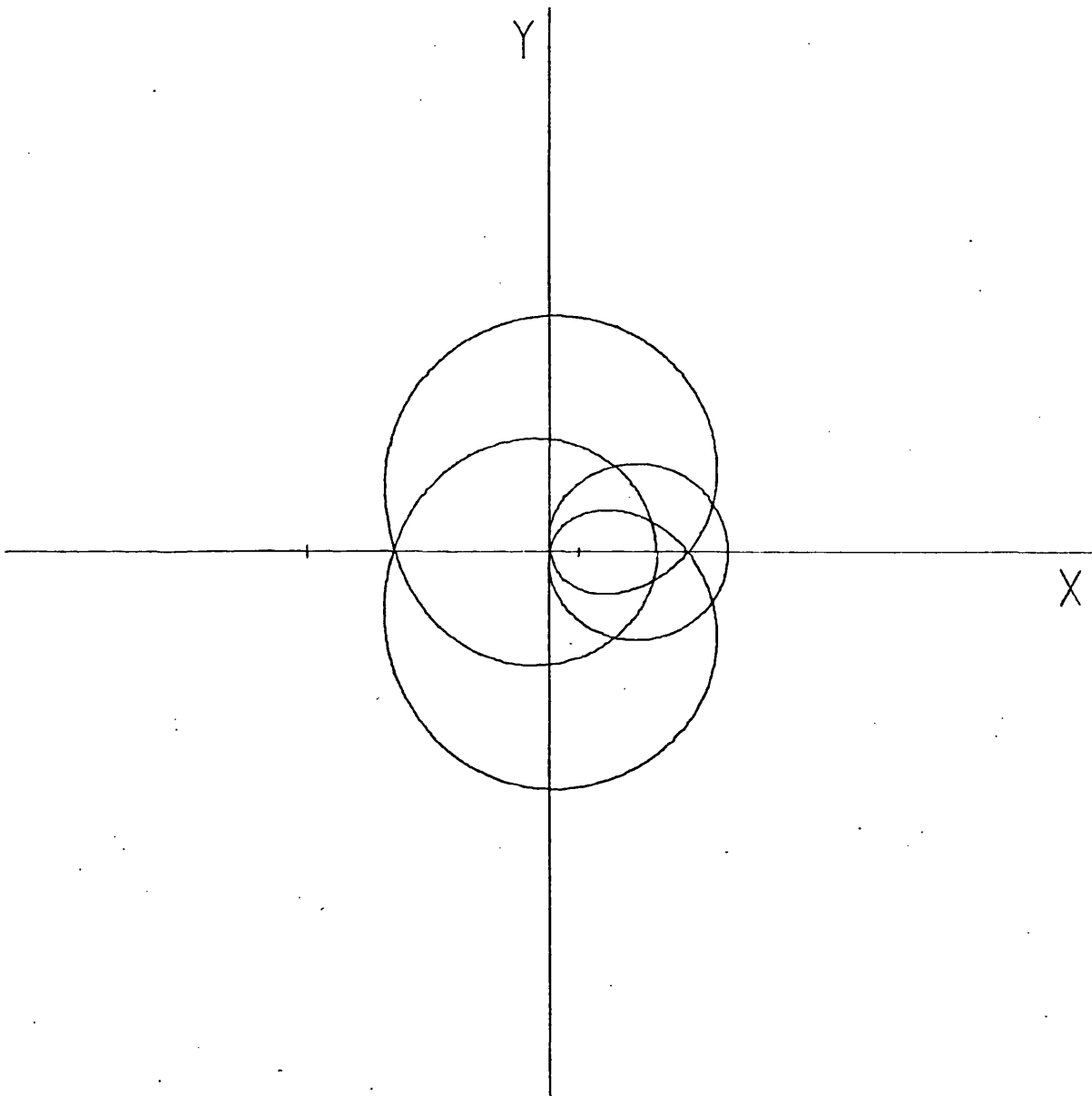


Figure A55

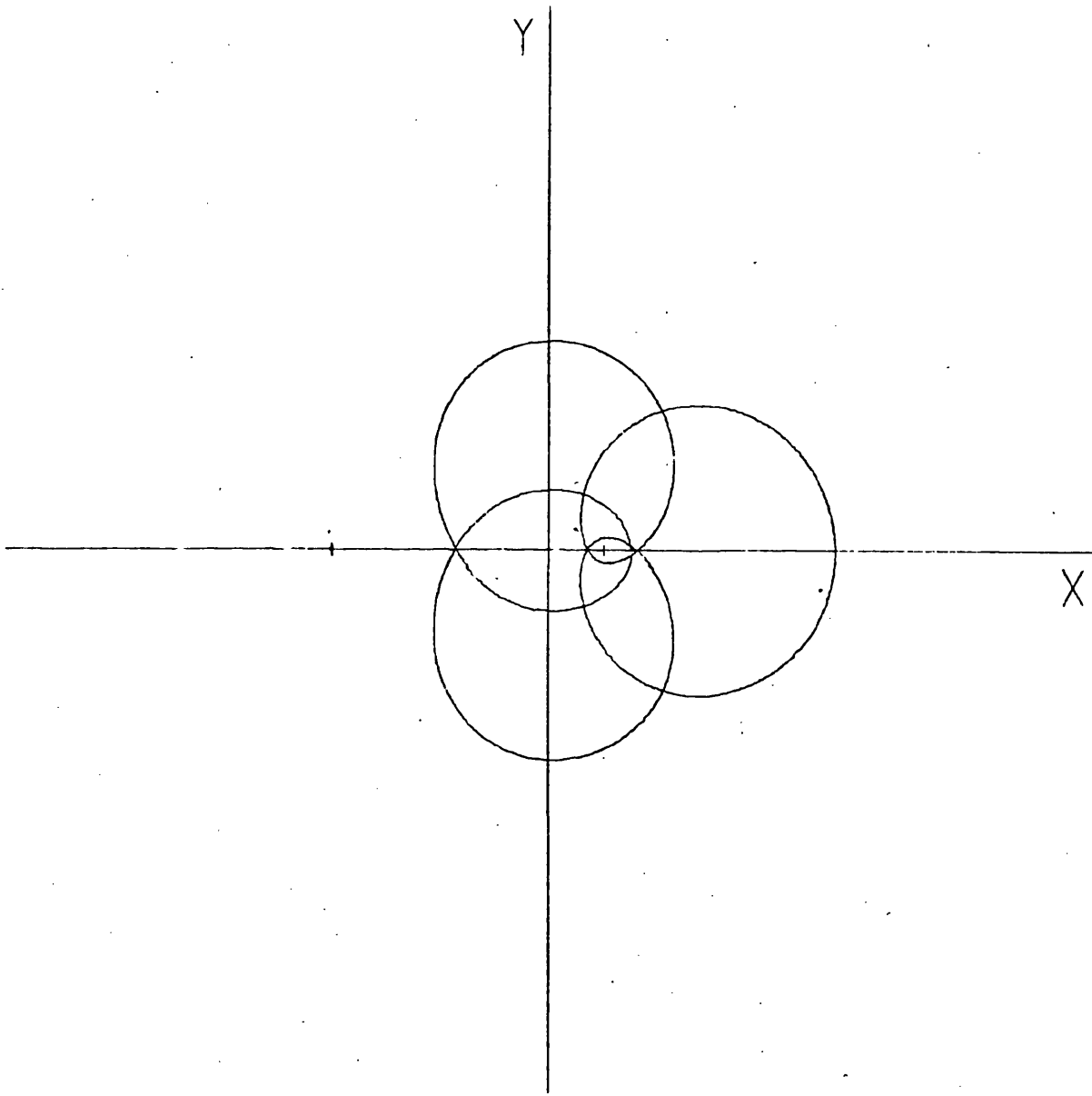


Figure A56

Group (d): Figures A57 - A70

Figures A57 - A69: A series of orbit plots illustrating the evolution of the family of plane symmetric orbits generated from a bifurcation in three dimensions with the family  $A_{1v}$  and terminating in a planar orbit about the primary  $m_1$ , with consecutive collisions with  $m_2$ .

The orbit plotted in Figure A57 is the bifurcation orbit of the vertical branch  $A_{1v}$  from which the family originates; the orbit plotted in Figure A60 is near the bifurcation with the vertical branch  $F_{v15}^{1(p)}$ , and Figure A69 shows an orbit near the termination of the family.

All of the orbits, with the exception of that in Figure A69, are plotted with respect to coordinates centred on the primary  $m_2$  (Jupiter) and rotating with the primaries; in the final plot the origin is shifted to the primary  $m_1$  (Sun). Whenever the other primary is within the scope of the plot, its position is indicated by a tick on the X-axis.

Note that different scales have had to be used because of the large variations in the sizes of the orbits along the family. The following table indicates the scale in terms of the length of the positive half of the Z-axis, in units of the distance between the primaries.

Figures	Scale
A57 - A60	0.1
A61 - A63	0.2
A64 - A66	1.0
A67 - A69	2.0

Figure A70 : Isometric projection of a representative orbit belonging to the family of plane symmetric orbits generated from a quadruple bifurcation in three dimensions with the family  $A_{1v}$ . The parameters of this orbit are given by the final entry of Table 8.3. The origin of the coordinate system is at the primary  $m_2$  (Jupiter), and the scale of the plot is 0.1.

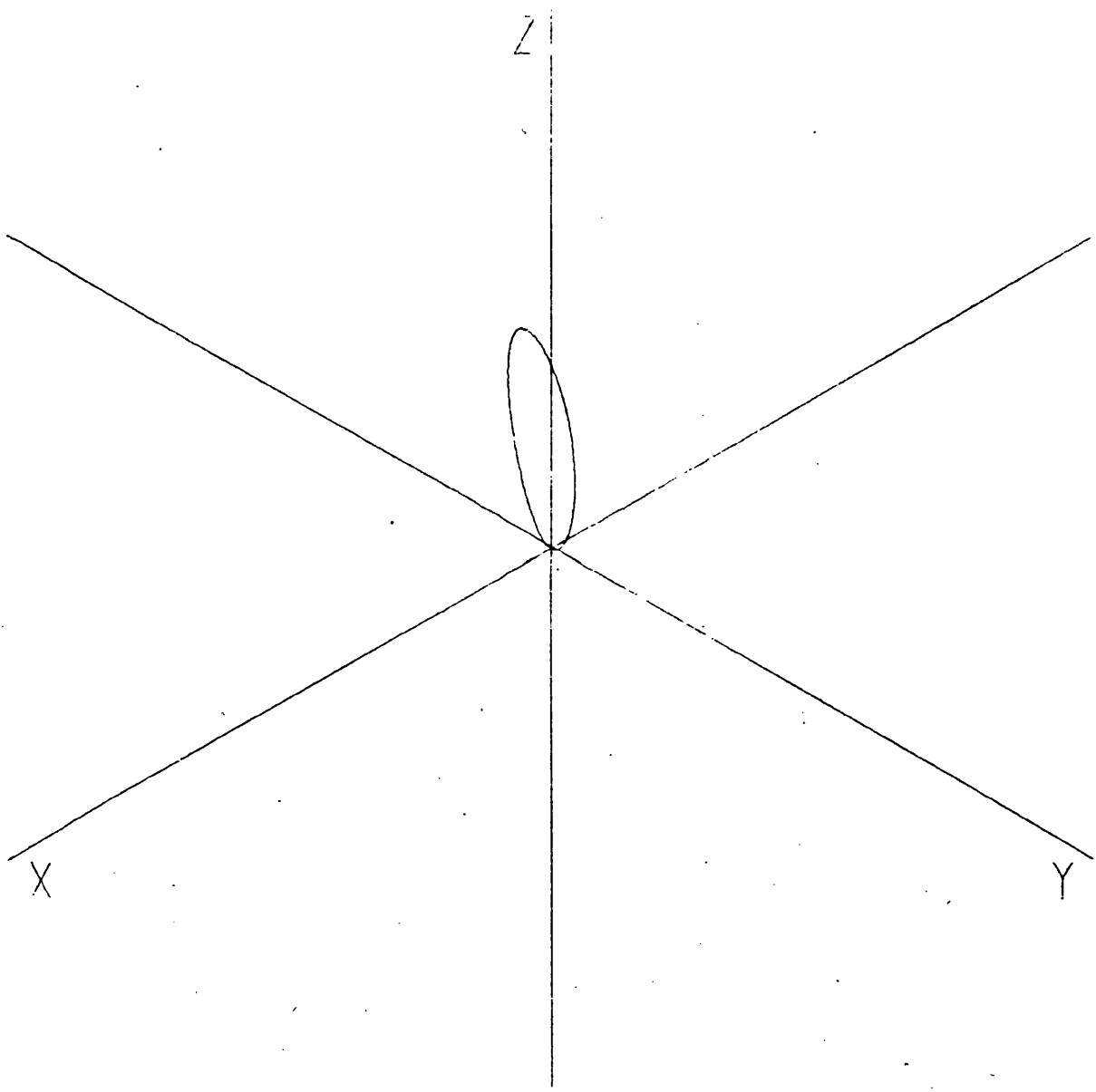


Figure A57

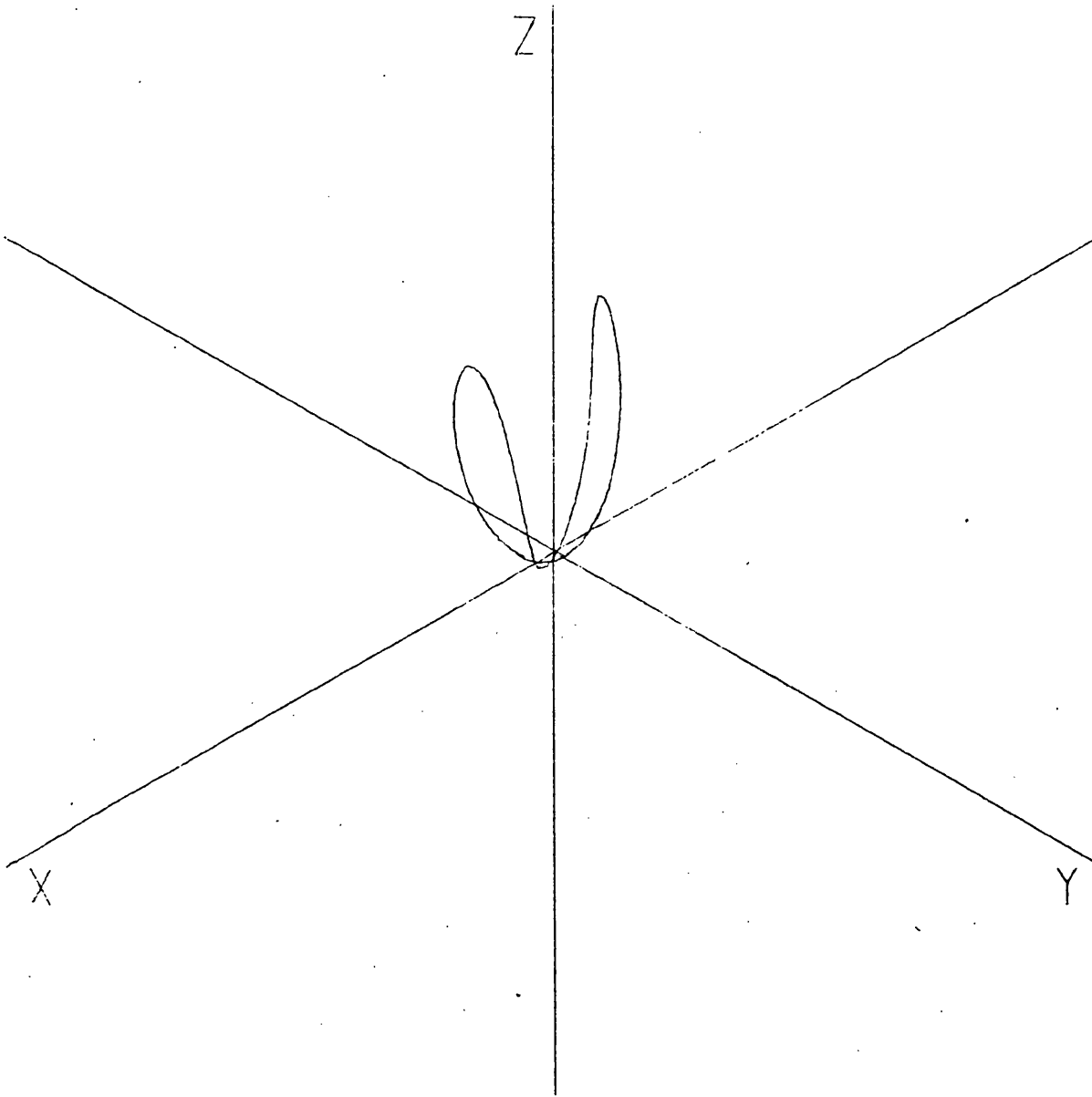


Figure A58

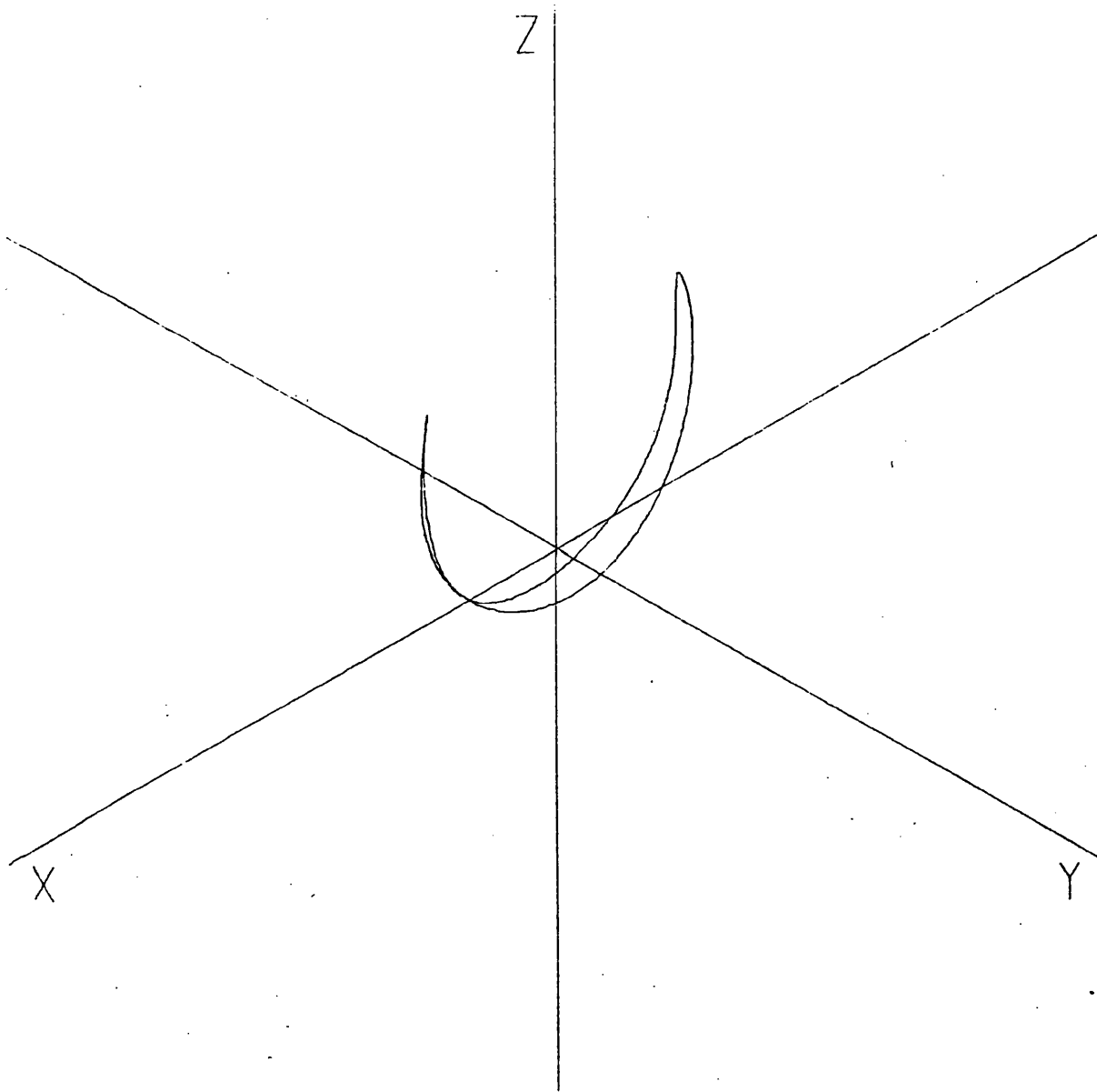


Figure A59

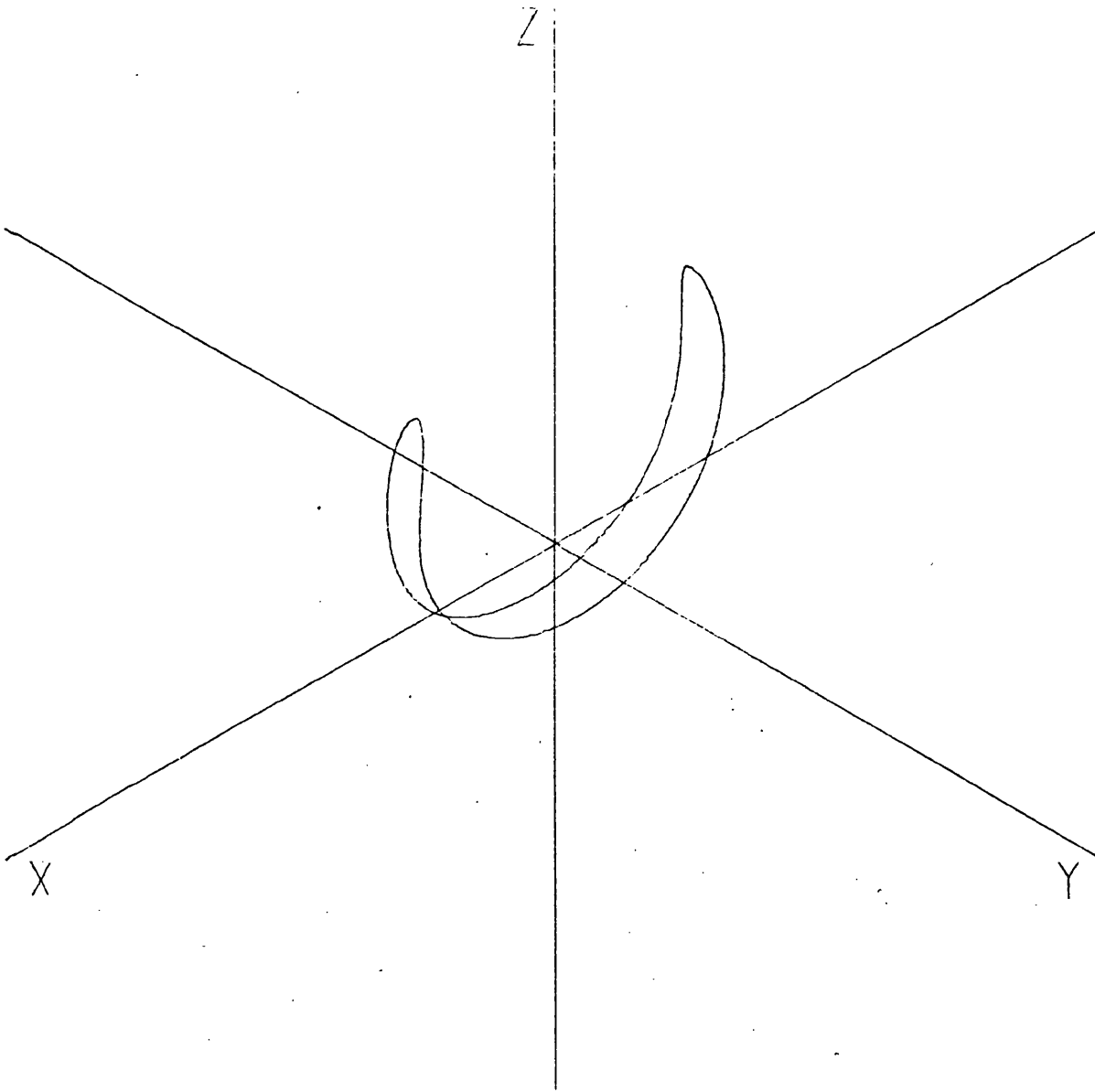


Figure A60

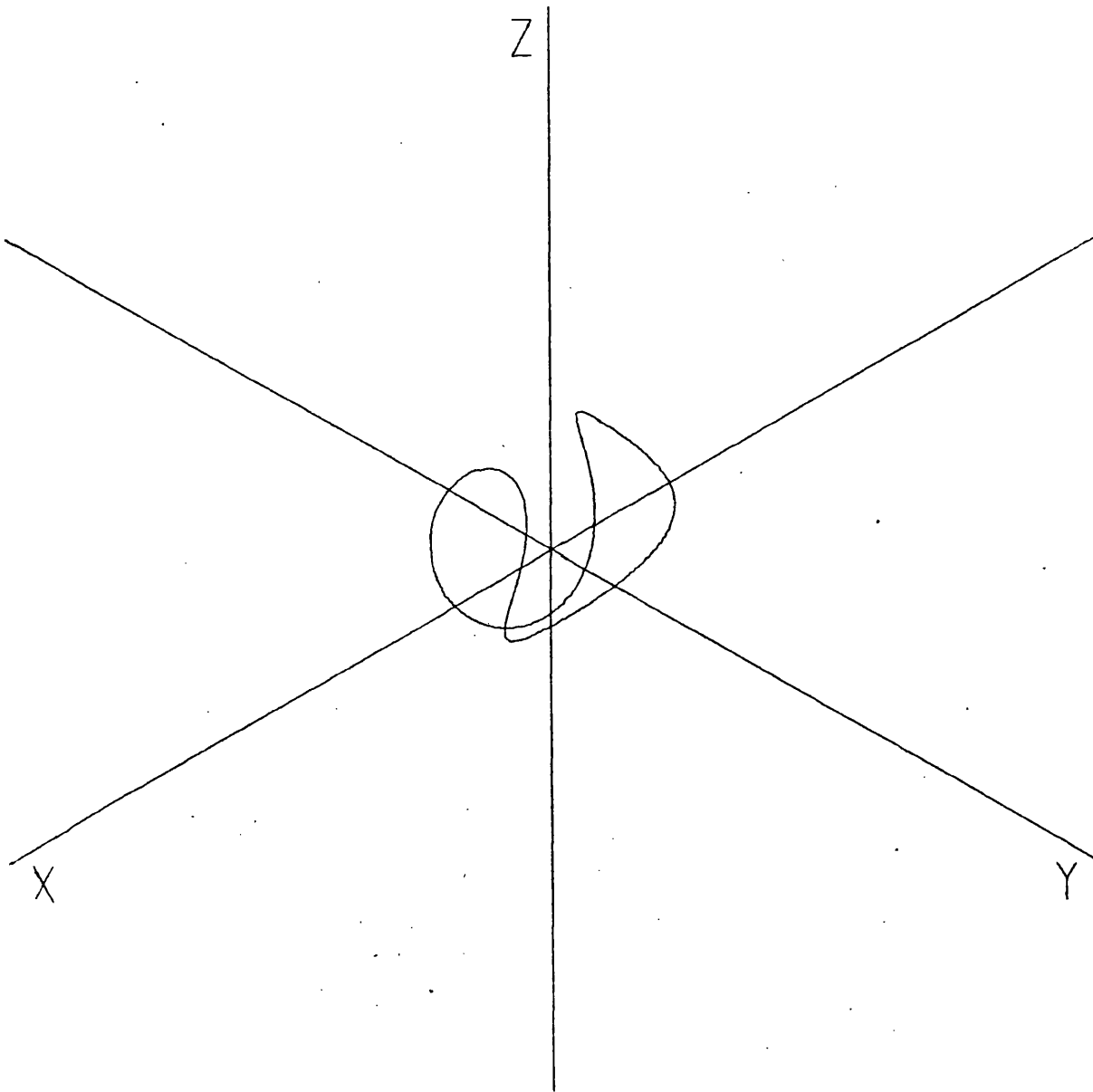


Figure A61

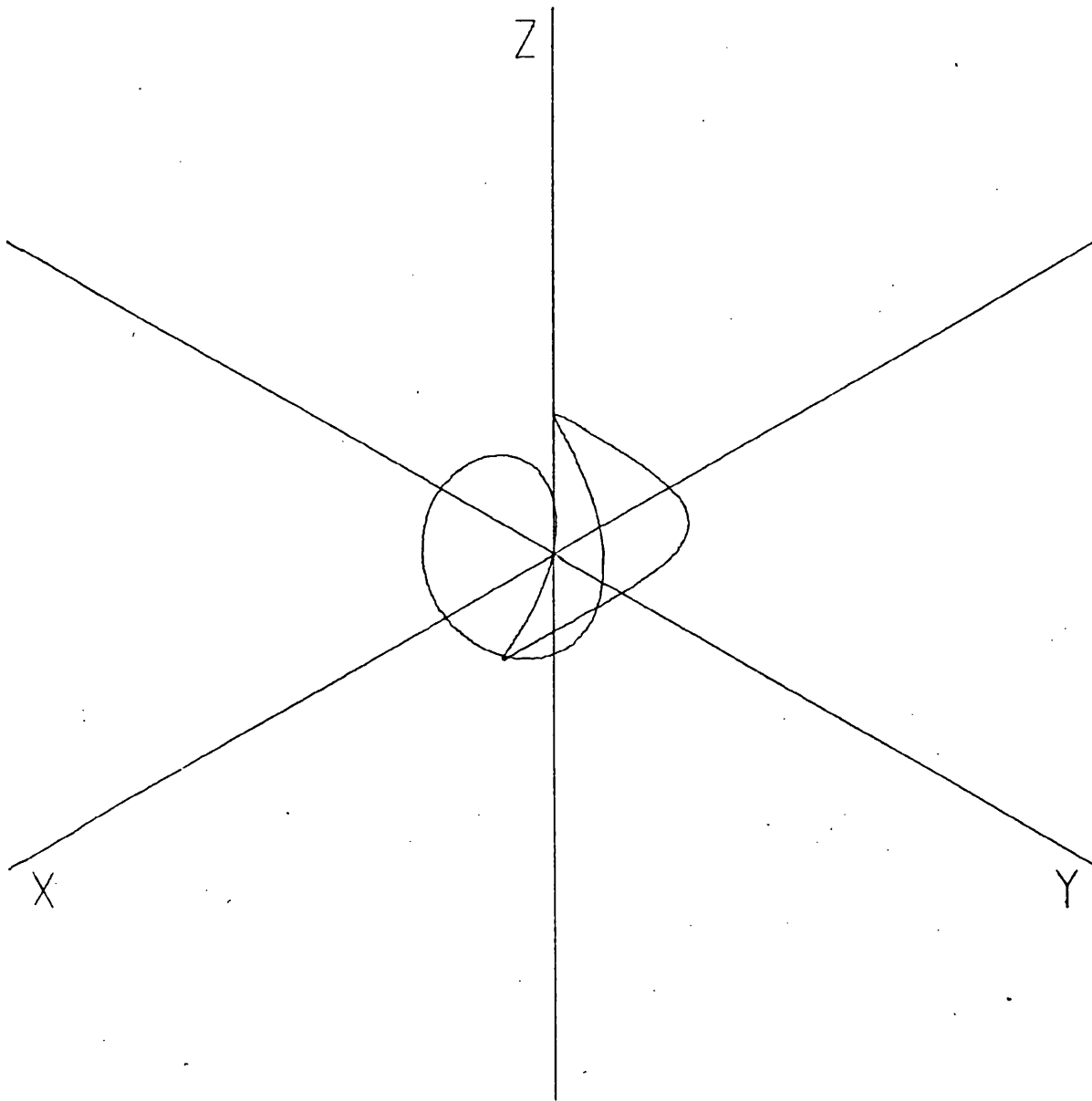


Figure A62

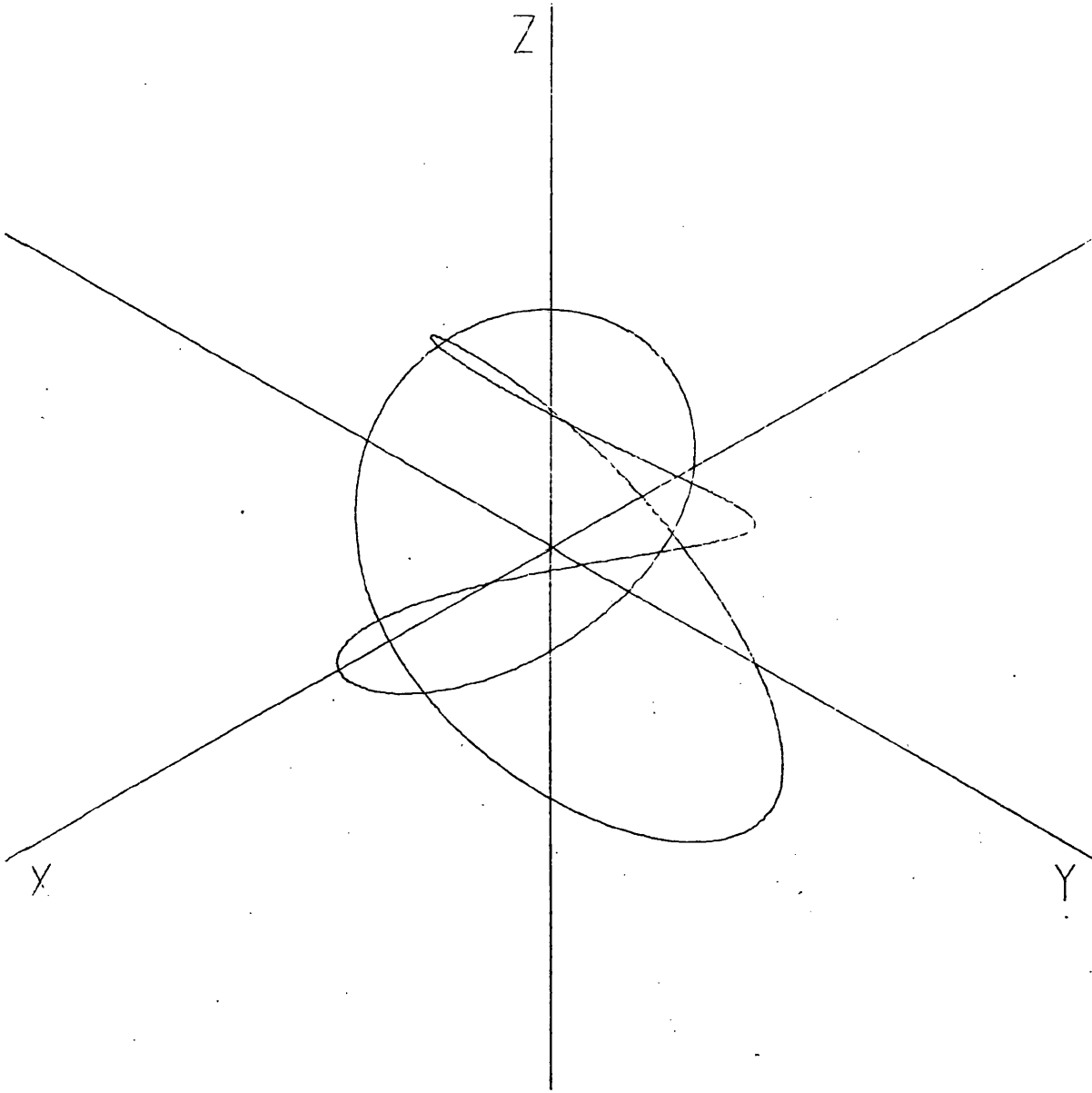


Figure A63

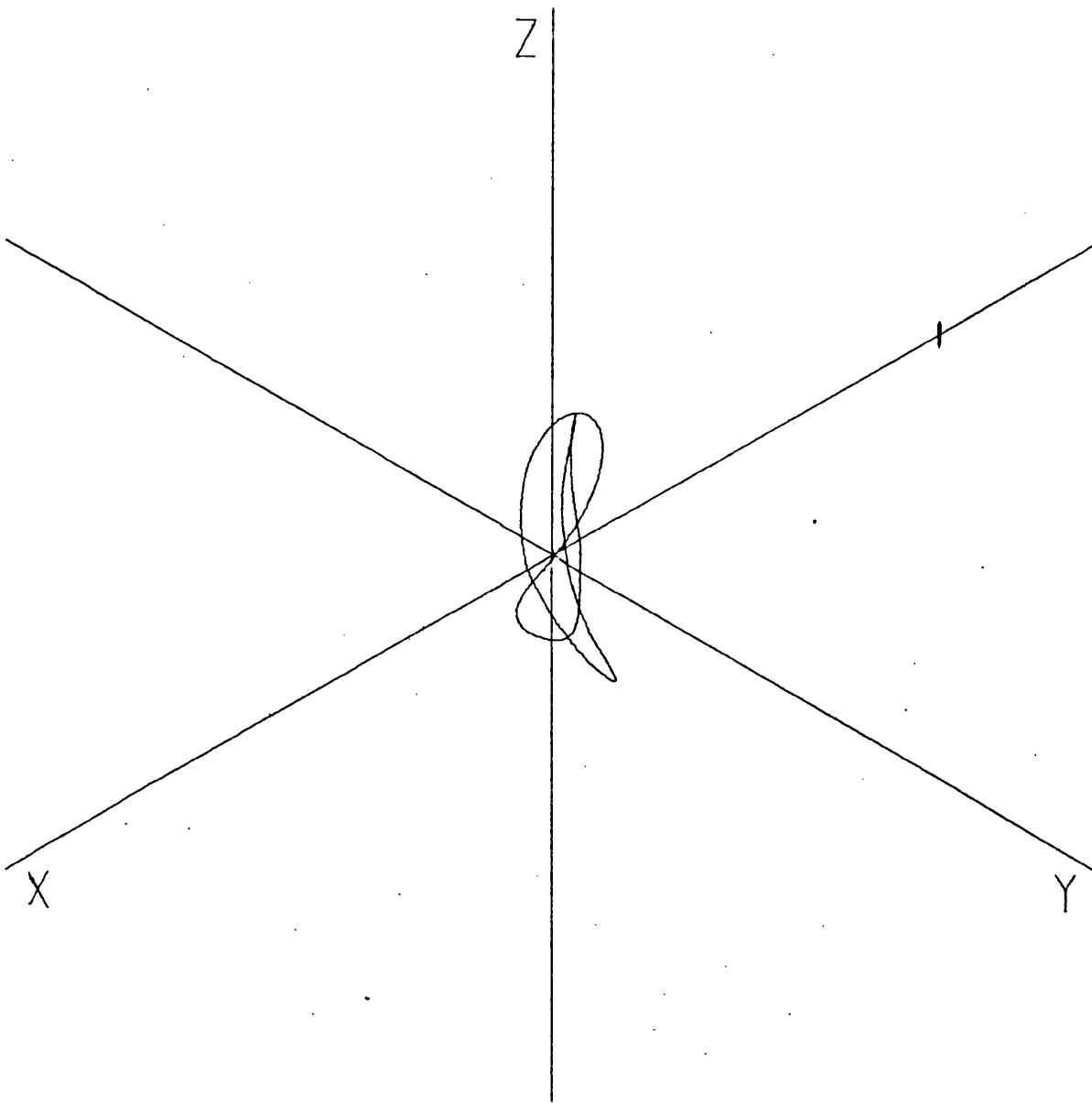


Figure A64

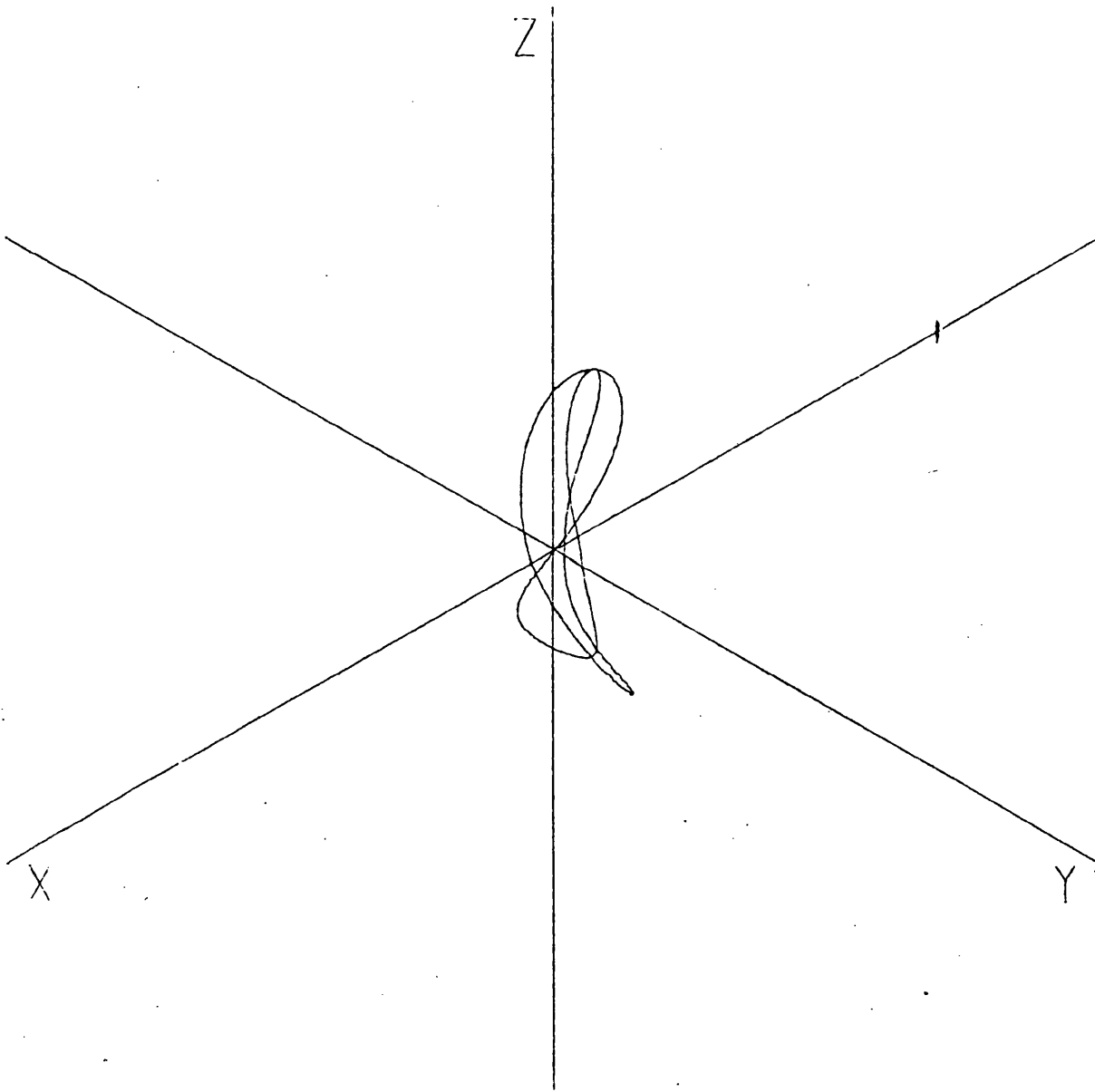


Figure A65

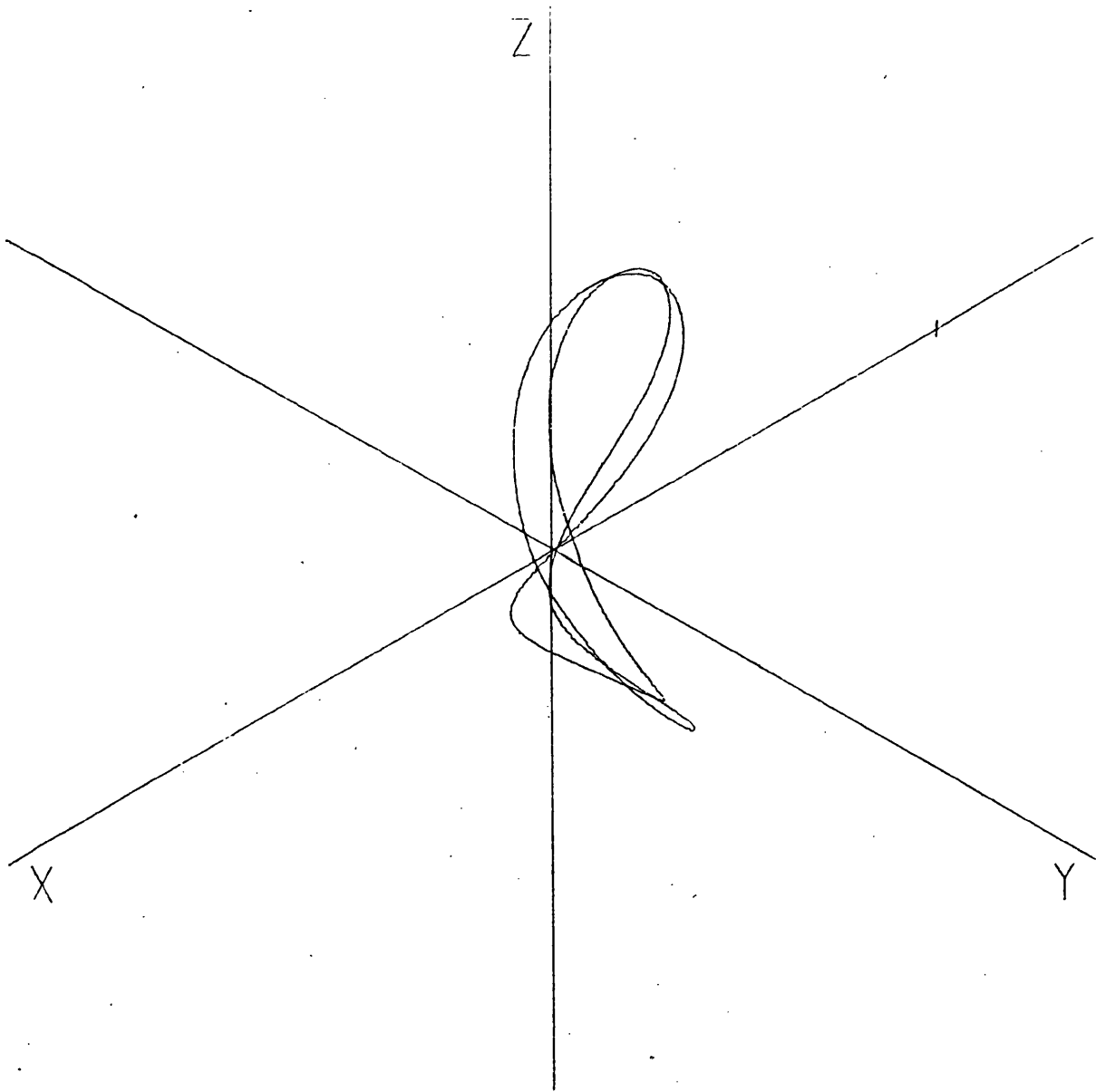


Figure A66

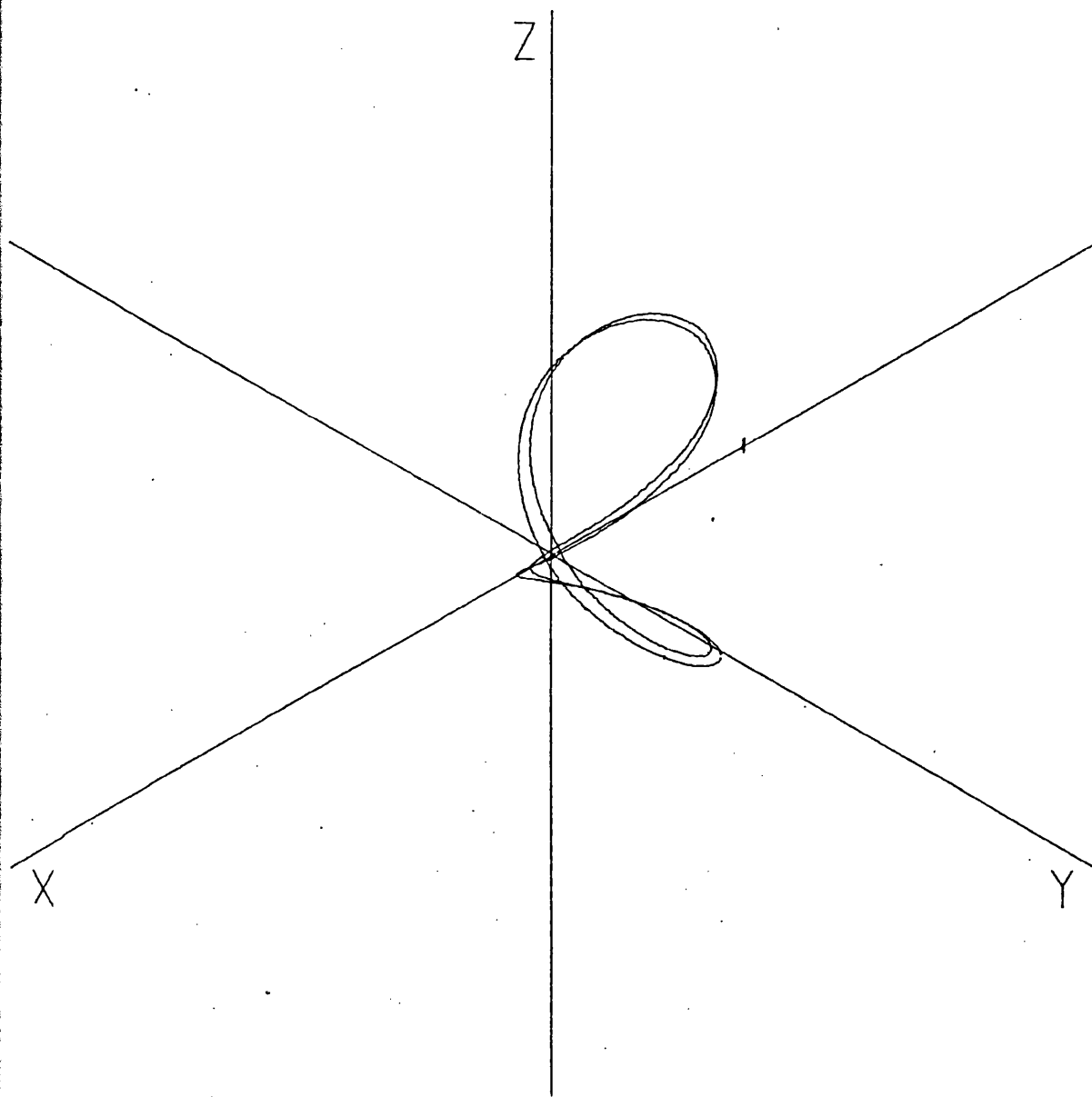


Figure A67

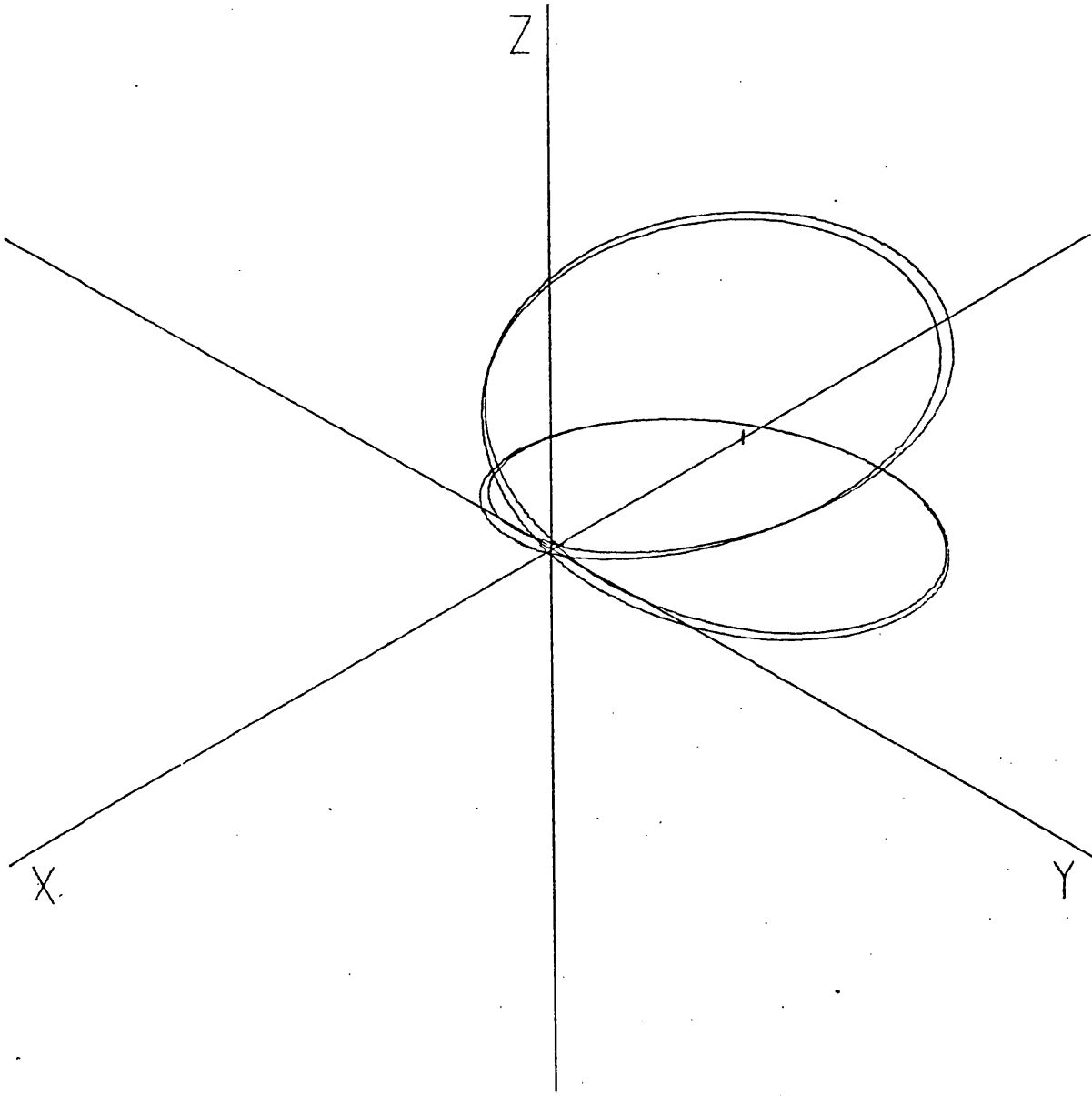


Figure A68

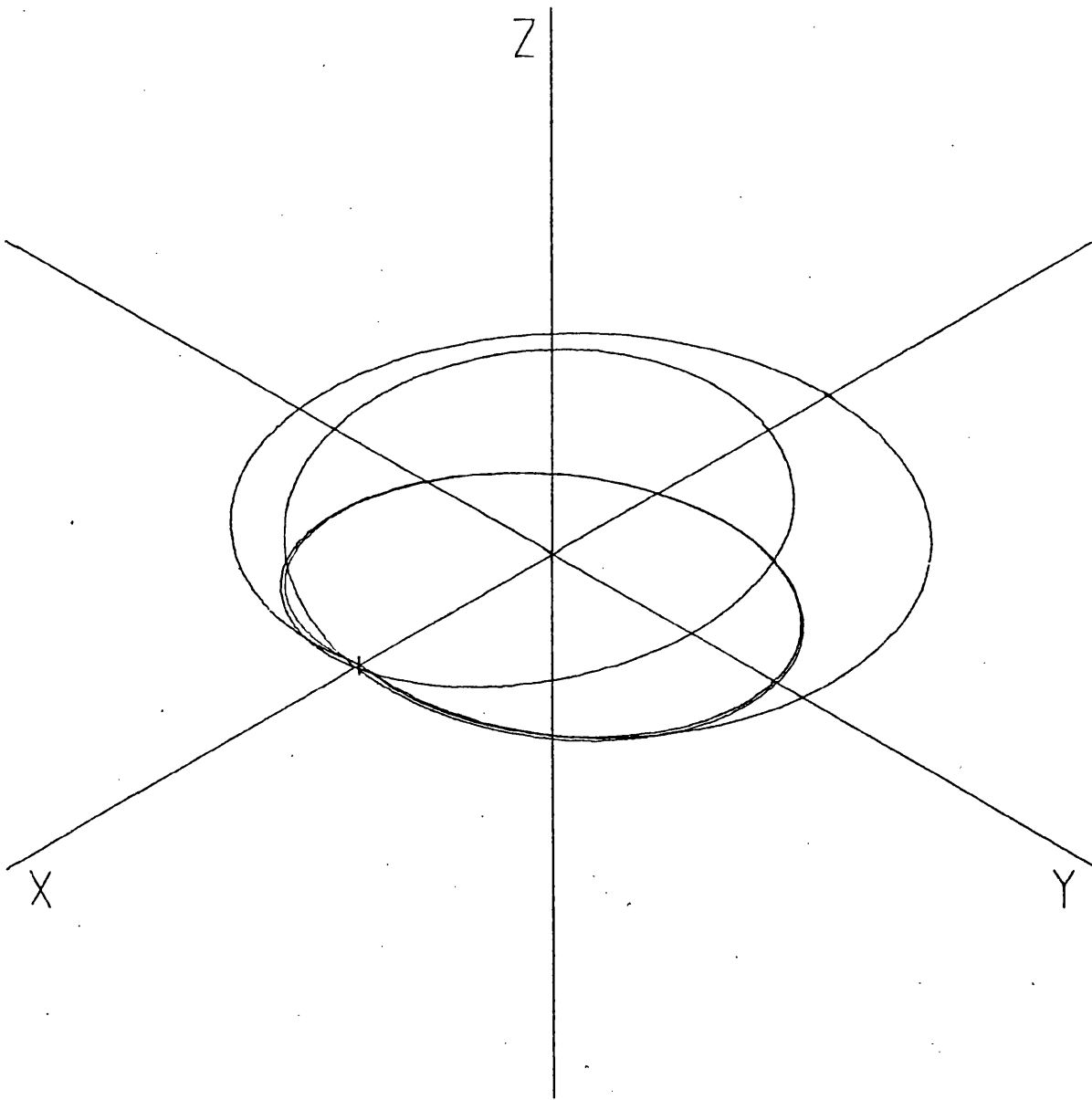


Figure A69

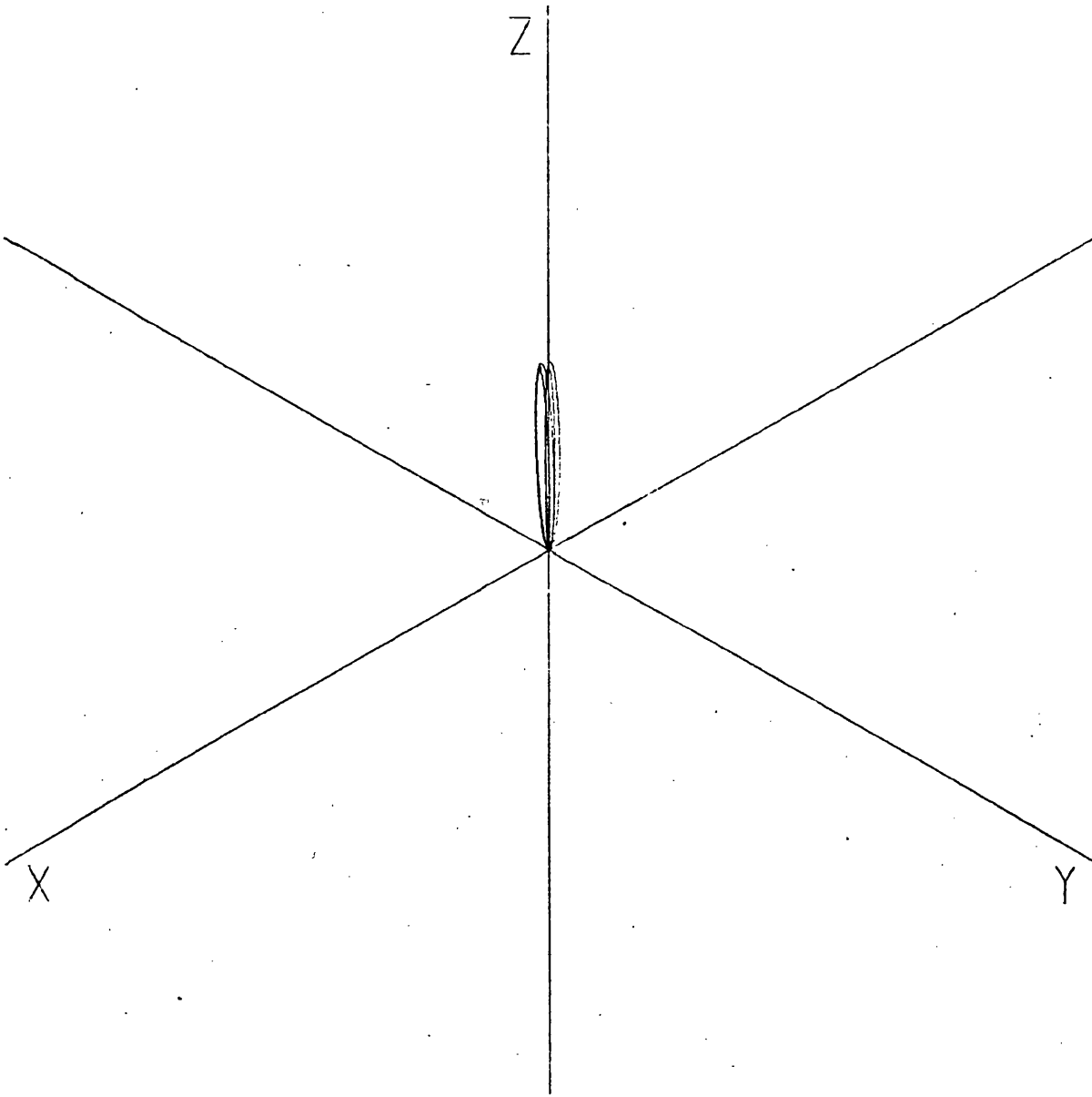


Figure A70



# NUMERICAL DETERMINATION OF THREE-DIMENSIONAL PERIODIC ORBITS GENERATED FROM VERTICAL SELF-RESONANT SATELLITE ORBITS

I. A. ROBIN and V. V. MARKELLOS

*Department of Astronomy, University of Glasgow, Glasgow, Scotland*

(Received 10 May; accepted 18 May, 1979)

**Abstract.** The mechanism by which 'vertical' branches consisting of symmetric, three-dimensional periodic orbits bifurcate from families of plane orbits at 'vertical self-resonant' orbits is discussed, with emphasis on the relationship between symmetry properties and multiplicity, and methods for the numerical determination of such branches are described. As examples, eight new families of all symmetry classes which branch vertically from the family  $f$  of retrograde satellite orbits in the Sun-Jupiter case of the restricted problem ( $\mu = 0.000\ 95$ ), are given in their entirety; these branches are found, as expected, to occur in pairs, each pair arising from the same self-resonant orbit, and their symmetry properties following the predicted pattern. The stability and other properties of the branch orbits are discussed.

## 1. Introduction

In the planar restricted three-body problem, the 'horizontal branches' of a family of symmetric simple-periodic orbits are families of symmetric multiple-periodic orbits of the second generation (Poincaré's '*deuxième genre*') which bifurcate from the generating family of simple orbits. Each horizontal branch intersects the generating family at a horizontal self-resonant orbit, where the horizontal stability parameter  $a$  satisfies the condition  $a = \cos(2\pi n/m)$  for some positive integers  $m$  and  $n$ , the branch consisting of orbits of multiplicity  $m$ . Markellos (1974, 1975) has found many of the horizontal branches of family  $f$  (retrograde satellite orbits around the less-massive primary) for the Sun-Jupiter value  $\mu = 0.000\ 95$  of the mass parameter.

When the restricted problem is extended into three dimensions it is found that the planar families also have 'vertical branches', which bifurcate from the generating families at vertical self-resonant orbits, where the vertical stability parameter  $a_v$  satisfies the condition  $a_v = \cos(2\pi n/m)$ , and which consist of symmetric multiple-periodic orbits. The multiplicity of the branch orbits is initially equal to  $m$ . All the orbits of a given vertical branch have the same type of symmetry; the characteristic symmetry properties of a vertical branch depend solely on the value of  $m$ , and in general vertical branches of all possible types of symmetry (axisymmetric, plane symmetric, doubly-symmetric) may occur. The importance of second-generation solutions in the planar restricted problem is well known, and we may reasonably expect that investigation of the vertical branches of planar families will yield valuable information in the more general case of three-dimensional motion of the massless third body.

This paper deals with the vertical branches of family  $f$  in the vicinity of the less-massive primary (Jupiter) for  $\mu = 0.000\ 95$ . Eight vertical branches in four pairs of initial multiplicities 5, 6, 7 and 8 are presented; these are the lowest-multiplicity vertical branches since as will be seen below family  $f$  possesses no vertical branches of multiplicity four or less in the vicinity of Jupiter. This group of eight vertical branches comprises three-dimensional periodic orbits of all possible symmetry types. Each of the branches is completely determined here, starting with the bifurcation from family  $f$  and finishing at the branch termination orbit, which in every case but one is once again in the horizontal plane.

The dimensionless barycentric rotating coordinate system ( $x_1 = x$ ,  $x_2 = y$ ,  $x_3 = z$ ) with Jupiter at  $x_1 = 1 - \mu = 0.999\ 05$ ,  $x_2 = x_3 = 0$ , is employed, the velocity components along the three axes being denoted by  $x_4 (= \dot{x}_1)$ ,  $x_5 (= \dot{x}_2)$  and  $x_6 (= \dot{x}_3)$ . The unit of time is such that the period of the primaries is  $2\pi$ . The Jacobi constant  $C$  used is that defined by Szebehely (1967) so that  $C = 3$  for a particle at rest at an equilateral triangle equilibrium point. For definitions of the horizontal and vertical stability parameters of a symmetric plane periodic orbit we refer to Hénon (1965, 1973).

## 2. Determination of Vertical Branches

### 2.1. SYMMETRY PROPERTIES AND PERIODICITY CONDITIONS

Methods of tracing families of symmetric three-dimensional periodic orbits have been discussed by various authors (e.g. Zagouras and Markellos, 1977). The search for an orbit belonging to such a family is simplified by applying the well-known Periodicity Theorem of Roy and Ovenden (1955). The theorem is valid in the general  $n$ -body problem and states that any solution in which two mirror configurations occur at distinct epochs is periodic. The problem of determining a symmetric three-dimensional periodic orbit in the restricted three-body problem therefore reduces to that of finding a set of initial conditions ( $x_{01}, x_{02}, x_{03}, x_{04}, x_{05}, x_{06}$ ) satisfying a mirror configuration, which, upon integration of the equations of motion, yields a second mirror configuration at a later epoch.

In the restricted three-body problem there are two possible types of mirror configuration, which we denote by (A) and (P). A type (A) (on-axis) mirror configuration is one in which the massless third body is located on the  $x_1$ -axis, the axis of the primaries, with its instantaneous velocity vector perpendicular to the axis. In a type (P) (in-plane) mirror configuration the particle is located in the  $(x_1, x_3)$ -plane with its instantaneous velocity vector normal to the plane. Various combinations of these two types of mirror configuration occurring at the two epochs result in periodic orbits having different symmetry properties. If the two mirror configurations are of the same type the orbit is simply-symmetric: an orbit in which two type (P) mirror configurations occur successively possesses symmetry with respect to the  $(x_1, x_3)$ -plane (plane symmetric), while an orbit in which two type (A) mirror configurations

occur successively is symmetrical with respect to the  $x_1$ -axis (axisymmetric). If both kinds of mirror configuration occur at different epochs in the same orbit, that orbit is said to be doubly-symmetric, because of its symmetry with respect to both the  $(x_1, x_3)$ -plane and the  $x_1$ -axis.

Clearly in order to find orbits belonging to a vertical branch of a family of plane periodic orbits by making use of the Periodicity Theorem, we need to know which types of mirror configuration have to be satisfied at the initial and final epochs; i.e. we must know the symmetry class to which the branch orbits belong. It is known (Hénon, 1973) that the symmetry properties of a vertical branch consisting initially of simple or double orbits ( $m = 1$  or  $2$ ) may be inferred from the values of the vertical stability parameters  $b_v$  and  $c_v$  of the vertical critical orbit at which the branch bifurcates from the generating family of plane orbits. In a recent paper, Markellos (1980) investigated the mechanism of vertical bifurcation more generally, to include cases where the branch multiplicity is initially greater than two, and reached the following conclusions:

(i) A vertical self-resonant orbit for which  $m = 1$  or  $m = 2$  ( $a_v = \pm 1$ , i.e. a *vertical-critical* orbit) is the point of bifurcation of one and only one vertical branch, which consists of orbits of simple or double symmetry respectively, the exact type of symmetry depending on the values of  $b_v$  and  $c_v$ .

(ii) Exactly two vertical branches bifurcate from the generating family at a vertical self-resonant orbit for which  $m > 2$ . When  $m$  is odd, one branch consists of axisymmetric orbits and the other of planesymmetric orbits; when  $m$  is even, both branches consist of doubly-symmetric orbits.

Owing to the symmetry of the restricted problem with respect to the  $(x_1, x_2)$ -plane, for every vertical branch there is a 'mirror image' consisting of orbits which are the images under reflection in the  $(x_1, x_2)$ -plane of the orbits belonging to the first branch. The above statements are made without regard to this duplicity of vertical branches; we consider only one member of each mirror-image pair.

The relationships between orbital multiplicity, symmetry classes and types of mirror configuration are summarised in Table I.

TABLE I

Case	Multiplicity $m$	Type of mirror configuration at:		Symmetry class	Fraction of the period elapsed	Fraction of the period elapsed	
		Initial Epoch	Final Epoch			$i$	$j$
1	Odd	P	P	plane symmetric	$T/2$	3	6
2	Odd	A	A	axisymmetric	$T/2$	6	3
3	Even	A	P	} doubly symmetric	$T/4$	6	6
4	Even	P	A		$T/4$	3	3

We see from Table I that the interval of time between successive mirror configurations, that is the interval over which we require to perform trial integrations in order

to determine a branch orbit, is equal to half the orbital period  $T$  for orbits of simple symmetry and only a quarter of the period for doubly-symmetric orbits.

In a type (A) mirror configuration the state vector  $\mathbf{x} = (x_1, x_2, x_3, x_4, x_5, x_6)$  has the form

$$\mathbf{x} = (x_1, 0, 0, 0, x_5, x_6) \quad (2.1)$$

where  $x_1$ ,  $x_5$  and  $x_6$  may have any values. In a type (P) mirror configuration the state vector has the form

$$\mathbf{x} = (x_1, 0, x_3, 0, x_5, 0) \quad (2.2)$$

where the components  $x_1$ ,  $x_3$  and  $x_5$  may have any values. Omitting the zero components, the initial conditions of a symmetric periodic orbit starting from a mirror configuration may therefore be written as  $(x_{01}, x_{05}, x_{0i})$ , where the subscript  $i = 3$  for a type (P) and  $i = 6$  for a type (A) mirror configuration at the initial epoch. If we integrate the equations of motion with these initial conditions up to epoch  $t$ , say, the final state vector may be expressed as

$$\mathbf{x} = \mathbf{x}(x_{01}, x_{05}, x_{0i}; t). \quad (2.3)$$

Since the initial conditions have been chosen to satisfy a mirror configuration, the orbit will be periodic if at some epoch  $t \neq 0$  the final conditions also satisfy a mirror configuration. Thus the 'periodicity conditions' are

$$\begin{aligned} x_2(x_{01}, x_{05}, x_{0i}; t) &= 0 \\ x_4(x_{01}, x_{05}, x_{0i}; t) &= 0 \\ x_j(x_{01}, x_{05}, x_{0i}; t) &= 0 \end{aligned} \quad (2.4)$$

where  $j = 3$  for a type (A) and  $j = 6$  for a type (P) mirror configuration at epoch  $t$ . The remaining three final conditions may have any values.

Trial integration up to a specified epoch (as employed in this and later sections) is usually preferable, from the computational point of view, to the alternative method of integration to a specified crossing of the  $(x_1, x_3)$ -plane, when vertical branches such as those described in this paper are being traced. This is because of the frequent occurrence of multiplicity changes as the branches evolve, causing breakdown of predictor-corrector algorithms based on the latter procedure; by contrast with the discrete nature of the multiplicity, the orbital period is a continuous variable along any branch, and by integrating to the epoch using the procedures described below, it is possible to trace an entire family without any interruption.

## 2.2. CORRECTOR ALGORITHM

The periodicity conditions (2.4) present formally the problem of determining a symmetric periodic orbit in three dimensions; the equations can be applied to orbits of any symmetry class by suitable choice of the subscripts  $i$  and  $j$  (see Table I). Equations (2.4) can be solved numerically to an arbitrary accuracy by an iterative

procedure in which the results of trial integrations are used to compute corrections in the initial conditions and the period. The corrector algorithm is derived from the periodicity conditions as follows.

Suppose  $(x_{01}^*, x_{05}^*, x_{0i}^*)$  and  $t^*$  are approximate values of the initial conditions and integration interval of the sought branch orbit, differing from the exact solutions  $(x_{01}, x_{05}, x_{0i}, t)$  of (2.4) by the amounts

$$\begin{aligned}\delta x_{01} &= x_{01} - x_{01}^* \\ \delta x_{05} &= x_{05} - x_{05}^* \\ \delta x_{0i} &= x_{0i} - x_{0i}^* \\ \delta t &= t - t^*\end{aligned}\tag{2.5}$$

which are assumed to be small. We seek an algorithm allowing the ‘corrections’  $\delta x_{01}$ ,  $\delta x_{05}$ ,  $\delta x_{0i}$  and  $\delta t$  to be determined,  $t$  being equal to half or quarter of the period  $T$  depending on the symmetry of the orbit.

Numerical integration from initial conditions  $(x_{01}^*, x_{05}^*, x_{0i}^*)$  up to epoch  $t^*$  yields final conditions

$$\begin{aligned}x_2^* &= x_2(x_{01}^*, x_{05}^*, x_{0i}^*; t^*) \\ x_4^* &= x_4(x_{01}^*, x_{05}^*, x_{0i}^*; t^*) \\ x_j^* &= x_j(x_{01}^*, x_{05}^*, x_{0i}^*; t^*).\end{aligned}\tag{2.6}$$

Using Equations (2.5) we may write the periodicity conditions as

$$\begin{aligned}x_2 &= x_2(x_{01}^* + \delta x_{01}, x_{05}^* + \delta x_{05}, x_{0i}^* + \delta x_{0i}; t^* + \delta t) = 0 \\ x_4 &= x_4(x_{01}^* + \delta x_{01}, x_{05}^* + \delta x_{05}, x_{0i}^* + \delta x_{0i}; t^* + \delta t) = 0 \\ x_j &= x_j(x_{01}^* + \delta x_{01}, x_{05}^* + \delta x_{05}, x_{0i}^* + \delta x_{0i}; t^* + \delta t) = 0.\end{aligned}\tag{2.7}$$

Expanding the right-hand sides of Equations (2.7) in Taylor series, to first order in the corrections, we obtain

$$\begin{aligned}x_2^* + \frac{\partial x_2}{\partial x_{01}} \delta x_{01} + \frac{\partial x_2}{\partial x_{05}} \delta x_{05} + \frac{\partial x_2}{\partial x_{0i}} \delta x_{0i} + \frac{dx_2}{dt} \delta t &= 0 \\ x_4^* + \frac{\partial x_4}{\partial x_{01}} \delta x_{01} + \frac{\partial x_4}{\partial x_{05}} \delta x_{05} + \frac{\partial x_4}{\partial x_{0i}} \delta x_{0i} + \frac{dx_4}{dt} \delta t &= 0 \\ x_j^* + \frac{\partial x_j}{\partial x_{01}} \delta x_{01} + \frac{\partial x_j}{\partial x_{05}} \delta x_{05} + \frac{\partial x_j}{\partial x_{0i}} \delta x_{0i} + \frac{dx_j}{dt} \delta t &= 0.\end{aligned}\tag{2.8}$$

The partial derivatives  $\partial x_k / \partial x_{0l}$  are known as the first-order variations, and are denoted by  $v_{kl}$ . The matrix of first-order variations  $V = (v_{kl})_{6 \times 6}$  is calculated by integrating the equations of variation simultaneously with the equations of motion.

The time derivatives  $dx_k/dt$  are denoted by  $f_k$ . Rewriting Equations (2.8) in terms of these quantities, we have

$$\begin{aligned} v_{21} \delta x_{01} + v_{25} \delta x_{05} + v_{2i} \delta x_{0i} + f_2 \delta t &= -x_2^* \\ v_{41} \delta x_{01} + v_{45} \delta x_{05} + v_{4i} \delta x_{0i} + f_4 \delta t &= -x_4^* \\ v_{j1} \delta x_{01} + v_{j5} \delta x_{05} + v_{ji} \delta x_{0i} + f_j \delta t &= -x_j^* . \end{aligned} \quad (2.9)$$

In these equations the first order variations  $v_{kl}$  and time derivatives  $f_k$  have the values calculated at epoch  $t^*$  in the trial integration from initial conditions  $(x_{01}^*, x_{05}^*, x_{0i}^*)$ .

This system of three simultaneous equations, in the four unknowns  $\delta x_{01}$ ,  $\delta x_{05}$ ,  $\delta x_{0i}$  and  $\delta t$ , is the basic form of the corrector algorithm. The system is underdetermined, with one degree of freedom, allowing a further arbitrary constraint to be applied. This is usually done by setting one of the four corrections to zero and solving for the other three. The choice of which of the corrections to set to zero, i.e. which of the initial parameters to fix in value when the corrector is applied, can have an important effect on the convergence of the solution. This question is connected with the choice of 'family parameter' in the predictor algorithm, and will be discussed in Section 2.3. For the time being, in order to introduce the convention of interchangeable subscripts allowing flexibility in the choice of the fixed parameter, let us rewrite Equations (2.9) in the form

$$\begin{aligned} v_{2K} \delta x_{0K} + v_{2L} \delta x_{0L} + v_{2M} \delta x_{0M} + f_2 \delta t &= -x_2^* \\ v_{4K} \delta x_{0K} + v_{4L} \delta x_{0L} + v_{4M} \delta x_{0M} + f_4 \delta t &= -x_4^* \\ v_{jK} \delta x_{0K} + v_{jL} \delta x_{0L} + v_{jM} \delta x_{0M} + f_j \delta t &= -x_j^* . \end{aligned} \quad (2.10)$$

The three subscripts  $K$ ,  $L$  and  $M$  can be selected as any permutation of 1, 5 and  $i$  (recall that  $i = 3$  or  $6$  depending on the symmetry class of the orbit as in Table I). Since  $K$  can always be selected appropriately we can, without loss of generality, set  $\delta x_{0K} = 0$ , keeping  $x_{0K}^*$  fixed in the corrector process, and then solve for the corrections  $\delta x_{0L}$ ,  $\delta x_{0M}$  and  $\delta t$ . A new integration is started with the corrected initial conditions up to the corrected final epoch and the whole procedure repeated in an iterative fashion until the final conditions satisfy those of exact periodicity within some specified accuracy. A suitable form of periodicity criterion is

$$\sqrt{(x_2^2 + x_4^2 + x_j^2)} < \varepsilon , \quad (2.11)$$

where  $\varepsilon$  is some small constant. (The orbits presented in this paper were computed with a 'periodicity accuracy'  $\varepsilon = 10^{-8}$ ).

### 2.3. PREDICTOR ALGORITHMS

The corrector algorithm described in the previous section allows the initial conditions and period of a three-dimensional branch orbit to be found arbitrarily

accurately in principle, assuming that the values of these parameters are known approximately in the first place. The use of a corrector alone is sufficient to allow a series of orbits at intervals along the branch to be found, by incrementing one of the parameters  $(x_{01}, x_{05}, x_{0i}; t)$  by a fixed amount between successive orbits and taking the values of the other three parameters for the orbit just found as estimates for those of the next orbit. The whole process is started with the known initial conditions and period of the vertical self-resonant orbit from which the branch bifurcates (the period of a branch orbit close to the bifurcation point being approximately  $m$  times that of the vertical self-resonant orbit). This ‘zeroth order predictor’, however, is inefficient, requiring many iterations of the corrector for the periodicity criterion to be satisfied; and the interval between successive orbits along the branch usually has to be made quite small to ensure convergence of the corrector. At little cost in program complexity, a first or second order predictor can be set up to produce accurate estimates of the initial conditions and period of the next orbit on the family. Predictors of higher order than the second result in more accurate estimates of these parameters, reducing and sometimes eliminating the need for a corrector step, but have the disadvantage of requiring either higher-order variations to be calculated, or more complex starting procedures to be devised. In this section, the first and second order predictors used in obtaining the results given in this paper are described. In addition, a simple criterion is given for selecting the most suitable ‘family parameter’ at any point along a family of symmetric three-dimensional orbits.

The linear predictor algorithm, like the corrector, is based on first-order Taylor series expansion of the periodicity conditions. Let us assume that the initial conditions  $x_{01}^1, x_{05}^1, x_{0i}^1$  and period  $T^1$  of an orbit satisfying the periodicity criterion (2.11) are known. Then, to accuracy  $\varepsilon$ , we have

$$\begin{aligned} x_2^1 &= x_2(x_{01}^1, x_{05}^1, x_{0i}^1; t^1) = 0 \\ x_4^1 &= x_4(x_{01}^1, x_{05}^1, x_{0i}^1; t^1) = 0 \\ x_j^1 &= x_j(x_{01}^1, x_{05}^1, x_{0i}^1; t^1) = 0 \end{aligned} \quad (2.12)$$

where  $t^1$  is the epoch of the second mirror configuration (i.e.  $t^1 = T^1/2$  or  $T^1/4$  depending on the orbital symmetry). Let  $(x_{01}^2, x_{05}^2, x_{0i}^2; t^2)$  be the corresponding parameters of another orbit of the same family in the neighbourhood of the known orbit, such that the quantities

$$\begin{aligned} \Delta x_{01} &= x_{01}^2 - x_{01}^1 \\ \Delta x_{05} &= x_{05}^2 - x_{05}^1 \\ \Delta x_{0i} &= x_{0i}^2 - x_{0i}^1 \\ \Delta t &= t^2 - t^1 \end{aligned} \quad (2.13)$$

are small. The periodicity conditions for the second orbit can be written

$$\begin{aligned}x_2^2 &= x_2(x_{01}^1 + \Delta x_{01}, x_{05}^1 + \Delta x_{05}, x_{0i}^1 + \Delta x_{0i}; t^1 + \Delta t) = 0 \\x_4^2 &= x_4(x_{01}^1 + \Delta x_{01}, x_{05}^1 + \Delta x_{05}, x_{0i}^1 + \Delta x_{0i}; t^1 + \Delta t) = 0 \\x_j^2 &= x_j(x_{01}^1 + \Delta x_{01}, x_{05}^1 + \Delta x_{05}, x_{0i}^1 + \Delta x_{0i}; t^1 + \Delta t) = 0.\end{aligned}\tag{2.14}$$

Expanding in Taylor series to first order in the  $\Delta$ 's and using Equations (2.12), we obtain the basic form of the linear predictor algorithm:

$$\begin{aligned}v_{21} \Delta x_{01} + v_{25} \Delta x_{05} + v_{2i} \Delta x_{0i} + f_2 \Delta t &= 0 \\v_{41} \Delta x_{01} + v_{45} \Delta x_{05} + v_{4i} \Delta x_{0i} + f_4 \Delta t &= 0 \\v_{j1} \Delta x_{01} + v_{j5} \Delta x_{05} + v_{ji} \Delta x_{0i} + f_j \Delta t &= 0.\end{aligned}\tag{2.15}$$

The values of the first-order variations  $v_{ki}$  and time derivatives  $f_k$  appearing as coefficients in the equations are those for the known orbit.

The system of three simultaneous Equations (2.15) is formally very similar to the corrector algorithm (2.9); in particular, like the corrector, it has one degree of freedom, allowing an arbitrary constraint to be applied, for example by assigning a value to one of the  $\Delta$ 's. The trivial solution  $\Delta x_{01} = \Delta x_{05} = \Delta x_{0i} = \Delta t = 0$  merely reflects the property of periodicity of the known orbit. The parameter to which a fixed increment is given is termed the 'family parameter'. The choice of this parameter from  $x_{01}$ ,  $x_{05}$ ,  $x_{0i}$  and  $t$  can be important; if the selected family parameter has an extremum over the branch being traced, the predictor-corrector scheme will break down completely and will require to be restarted with a new choice of family parameter.

To overcome this difficulty, we rewrite Equations (2.15) in terms of the variable subscript notation introduced in the previous section:

$$\begin{aligned}v_{2K} \Delta x_{0K} + v_{2L} \Delta x_{0L} + v_{2M} \Delta x_{0M} + f_2 \Delta t &= 0 \\v_{4K} \Delta x_{0K} + v_{4L} \Delta x_{0L} + v_{4M} \Delta x_{0M} + f_4 \Delta t &= 0 \\v_{jK} \Delta x_{0K} + v_{jL} \Delta x_{0L} + v_{jM} \Delta x_{0M} + f_j \Delta t &= 0.\end{aligned}\tag{2.16}$$

As before, the subscripts  $K$ ,  $L$  and  $M$  can be any permutation of the set  $(1, 5, i)$ . By suitable definition of  $K$  we can, without loss of generality, specify the value of the increment  $\Delta x_{0K}$  and solve for  $\Delta x_{0L}$ ,  $\Delta x_{0M}$  and  $\Delta t$  from

$$\begin{aligned}v_{2L} \Delta x_{0L} + v_{2M} \Delta x_{0M} + f_2 \Delta t &= -v_{2K} \Delta x_{0K} \\v_{4L} \Delta x_{0L} + v_{4M} \Delta x_{0M} + f_4 \Delta t &= -v_{4K} \Delta x_{0K} \\v_{jL} \Delta x_{0L} + v_{jM} \Delta x_{0M} + f_j \Delta t &= -v_{jK} \Delta x_{0K}.\end{aligned}\tag{2.17}$$

A criterion for selecting the family parameter on a 'local' basis, i.e. for selecting  $K$  from the set  $(1, 5, i)$  each time the predictor is to be applied, can be established in

terms of the determinants

$$D_1 = \begin{vmatrix} v_{2i} & v_{25} & f_2 \\ v_{4i} & v_{45} & f_4 \\ v_{ji} & v_{j5} & f_j \end{vmatrix} \tag{2.18a}$$

$$D_5 = \begin{vmatrix} v_{21} & v_{2i} & f_2 \\ v_{41} & v_{4i} & f_4 \\ v_{j1} & v_{ji} & f_j \end{vmatrix} \tag{2.18b}$$

$$D_i = \begin{vmatrix} v_{25} & v_{21} & f_2 \\ v_{45} & v_{41} & f_4 \\ v_{j5} & v_{j1} & f_j \end{vmatrix}. \tag{2.18c}$$

It can be shown that these determinants are proportional to the direction cosines of the tangent to the family characteristic in the space of initial conditions  $(x_{01}, x_{05}, x_{0i})$  at the point  $(x_{01}^1, x_{05}^1, x_{0i}^1)$ , and thus the parametric equation of the tangent can be written as

$$\begin{aligned} x_{01}(s) &= x_{01}^1 + sD_1 \\ x_{05}(s) &= x_{05}^1 + sD_5 \\ x_{0i}(s) &= x_{0i}^1 + sD_i. \end{aligned} \tag{2.19}$$

In principle we could arrange, by assigning an appropriate value to the parameter  $s$ , that the predicted initial conditions  $(x_{01}^2, x_{05}^2, x_{0i}^2)$  be the coordinates of a point some specified interval along the tangent from the point representing the known orbit. This choice of arbitrary constraint on the system (2.15) would ensure that the branch orbits determined by application of the predictor and corrector algorithms were in a geometrical sense evenly spaced on the family characteristic. Another method would be to fix the increment  $\Delta t$  in the parameter  $t$ , to generate orbits equally spaced in terms of the orbital period; this suffers from the disadvantage that the method breaks down at an extremum in the period.

The strategy adopted by the authors was to select as the local family parameter the initial condition  $x_{0K}$  corresponding to the determinant  $D_K$  having the largest absolute value among the set  $(D_1, D_5, D_i)$ . This is equivalent to specifying a fixed increment in the most rapidly-varying initial condition, thus ensuring that difficulties associated with extrema in the initial conditions along the branch are avoided. Having chosen the value of the subscript  $K$  according to this criterion,  $\Delta x_{0K}$  is assigned an appropriate value and Equations (2.17) solved for  $\Delta x_{0L}$ ,  $\Delta x_{0M}$  and  $\Delta t$  (the subscripts  $L$  and  $M$  being defined as the remaining two from the set  $(1, 5, i)$ ).

Solving Equations (2.17) we obtain

$$\begin{aligned} \Delta x_{0L} &= \Delta x_{0K} D_L / D_K \\ \Delta x_{0M} &= \Delta x_{0K} D_M / D_K \\ \Delta t &= \Delta x_{0K} D / D_K \end{aligned} \tag{2.20}$$

where

$$D = \begin{vmatrix} v_{21} & v_{25} & v_{2i} \\ v_{41} & v_{45} & v_{4i} \\ v_{j1} & v_{j5} & v_{ji} \end{vmatrix}. \quad (2.21)$$

The predicted values of the parameters  $(x_{01}^2, x_{05}^2, x_{0i}^2)$  and  $t^2$  are then obtained from Equations (2.13). When the corrector algorithm is applied to improve the accuracy of these parameters, the local family parameter  $x_{0K}$  is kept fixed,  $K$  having been selected on the basis of the predictor criterion. This ensures that the corrector will converge successfully to the sought orbit. By testing the relative absolute magnitudes of the three determinants defined in Equations (2.18a–c) every time the predictor is used, and redefining  $K$ ,  $L$  and  $M$  as necessary, we can proceed along the branch identifying orbits at roughly equal intervals without the interruptions caused by extrema when the family parameter is fixed.

The quadratic predictor differs from the linear predictor described above in that it requires that two orbits of a branch are known, in order to predict the initial conditions of a third.

Suppose  $(x_{01}^0, x_{05}^0, x_{0i}^0; t^0)$ ,  $(x_{01}^1, x_{05}^1, x_{0i}^1; t^1)$  are the parameters of the two known branch orbits, such that

$$\Delta x_{0K} = x_{0K}^1 - x_{0K}^0 \quad (2.22)$$

is equal to the fixed increment in the family parameter, the subscript  $K$  being one of  $(1, 5, i)$  as usual. Let  $v_{kl}$  and  $f_k$  be respectively the first-order variations and time derivatives of the final conditions for the orbit indicated by the superscript '1'.

The equation of the branch characteristic in the space of parameters  $(x_{0L}, x_{0M}, t)$  may be written in parametric form with  $x_{0K}$  as the (local) family parameter:

$$\begin{aligned} x_{0L} &= x_{0L}(x_{0K}) \\ x_{0M} &= x_{0M}(x_{0K}) \\ t &= t(x_{0K}). \end{aligned} \quad (2.23)$$

It can be shown by means of second-order Taylor series expansions of the periodicity conditions for orbits 0 and 2 with respect to orbit 1 that if

$$x_{0K}^2 - x_{0K}^1 = x_{0K}^1 - x_{0K}^0 = \Delta x_{0K} \quad (2.24)$$

then

$$\begin{aligned} x_{0K}^2 &= x_{0K}^0 + 2 \Delta x_{0K} \\ x_{0L}^2 &= x_{0L}^0 + 2 \Delta x_{0L} \\ x_{0M}^2 &= x_{0M}^0 + 2 \Delta x_{0M} \\ t^2 &= t^0 + 2 \Delta t \end{aligned} \quad (2.25)$$

where  $\Delta x_{0L}$ ,  $\Delta x_{0M}$  and  $\Delta t$  are given by Equations (2.20).

Equations (2.25) are correct to the second order in  $\Delta x_{0K}$ , higher orders in the Taylor series expansions being neglected. The quadratic predictor is therefore more accurate than the linear one and the requirement for smallness of  $\Delta x_{0K}$  is not as severe. It cannot be used, however, either (a) at the beginning of a branch when we seek to predict the parameters of the second orbit with only one previous orbit known, or (b) immediately following a change of family parameter, when Equation (2.24) is not satisfied due to unequal intervals in the initial conditions between the two pairs of orbits. In both these circumstances the linear predictor is used.

The criterion described above for selecting the local family parameter can still be applied when the quadratic predictor algorithm is in use. If the criterion indicates that a change of family parameter is required, the subscripts  $K$ ,  $L$  and  $M$  can be suitably redefined so that the new value of  $K$  corresponds to the new family parameter; by means of appropriate program logic the next orbit is predicted linearly rather than quadratically, the quadratic predictor being applied for subsequent orbits until another change of family parameter becomes necessary to take account of variations in the relative rates of change of the initial conditions along the branch.

It has been found by the authors that by combining integration to a specified epoch with automatic selection of the family parameter based on the criterion described in this section, difficulties in tracing families of three-dimensional orbits arising from multiplicity changes, and extrema in the initial conditions, are avoided. As a rule an entire family of three-dimensional periodic orbits, from its beginning at a plane self-resonant orbit to its termination at another such orbit, is obtained from a single run of the computer program.

### 3. Vertical Branches of Family $f$

Having dealt with the general problem of numerical determination of the vertical branches of families of plane periodic orbits, we now confine our attention to one particular value of the mass parameter,  $\mu = 0.000\ 95$ , one particular family of planar periodic orbits, family  $f$ , and one particular part of that family, that for which  $x_1$  is greater than about 0.93 at the conjunction crossing of the axis of the primaries. We refer to this part of family  $f$  as being 'in the vicinity of Jupiter'. The significance of this part of the family in relation to the vertical branches can be seen from Figure 1, in which the vertical stability parameter  $a_v$  for family  $f$  is plotted against  $x_{01}$ , the  $x_1$ -coordinate at conjunction, for  $\mu = 0.000\ 95$ . The vertical stability curve reaches a minimum value  $a_v \approx 0.08$  at  $x_{01} \approx 0.93$ ; to the right of this minimum,  $a_v$  increases monotonically, approaching the limit  $a_v = +1$  at the singularity  $x_{01} = 1 - \mu = 0.999\ 05$ , where the retrograde orbits of family  $f$  shrink to zero size. Between these two points  $a_v$  assumes all intermediate values and consequently a manifold of vertical branches representative of all multiplicities  $m \geq 5$  (and all types of symmetry) is generated from this part of the family. The vertical branches of family  $f$  in the vicinity of Jupiter are interesting because it is in this region that

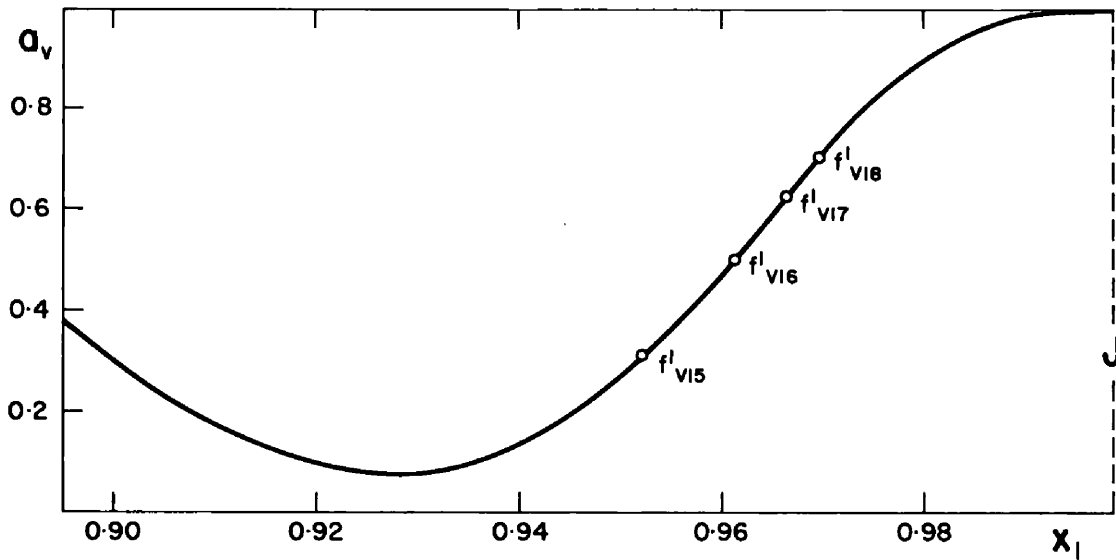


Fig. 1. Vertical stability curve of family  $f$  near the less massive primary (Jupiter) for  $\mu = 0.000\ 95$ .

three-dimensional periodic motion most closely resembling the motion of the natural satellites is to be expected.

Since  $a_v$  never quite reaches zero at any point in Figure 1, no vertical branches of family  $f$  of multiplicity four or less occur in this part of the family, although all multiplicities higher than four are represented. This paper deals with vertical branches of multiplicities 5, 6, 7 and 8, the four 'simplest' cases; these occur in four pairs bifurcating from the four vertical self-resonant orbits for which  $a_v = \cos 2\pi/5$  ( $\approx 0.309\ 02$ ),  $a_v = \cos \pi/3$  ( $= 0.5$ ),  $a_v = \cos 2\pi/7$  ( $\approx 0.623\ 49$ ), and  $a_v = \cos \pi/4$  ( $\approx 0.707\ 11$ ). These four orbits are represented by points marked on the vertical stability curve (Figure 1), and by pairs of points, corresponding to the two intersections of each orbit with the  $x_1$ -axis, on the family characteristic in the  $(C, x_1)$ -plane (Figure 2). Each vertical self-resonant orbit is designated according to the formula  $f^i_{vnm}$ . The letter ' $f$ ' indicates the generating family according to Strömgen's classification, the subscript ' $v$ ' is to distinguish vertical from horizontal self-resonant orbits, and the integers  $m$  and  $n$  define the value  $a_v = \cos(2\pi n/m)$  of the vertical stability parameter. The superscript ' $i$ ' is necessary to distinguish between self-resonant orbits having the same value of  $a_v$ ; it is assigned the value  $i = 1$  for the first orbit having a given value of  $a_v$  as the family evolves from its point of origin, subsequent orbits having the same value of vertical stability being labelled  $i = 2, 3 \dots$  etc. For the part of family  $f$  in the vicinity of Jupiter ( $x_{01} > 0.93$ ) we have the  $i = 1$  branches.

This notation for the vertical self-resonant orbits can be extended to allow the vertical branches themselves to be classified. Since the vertical branches of family  $f$  are of quintuple or higher multiplicity, we can conclude from Markellos' results on vertical bifurcations (Section 2.1) that these occur in pairs bifurcating (or more accurately, 'trifurcating') from the same plane orbit. Any vertical branch of family  $f$  can therefore be uniquely specified by identifying the vertical self-resonant orbit

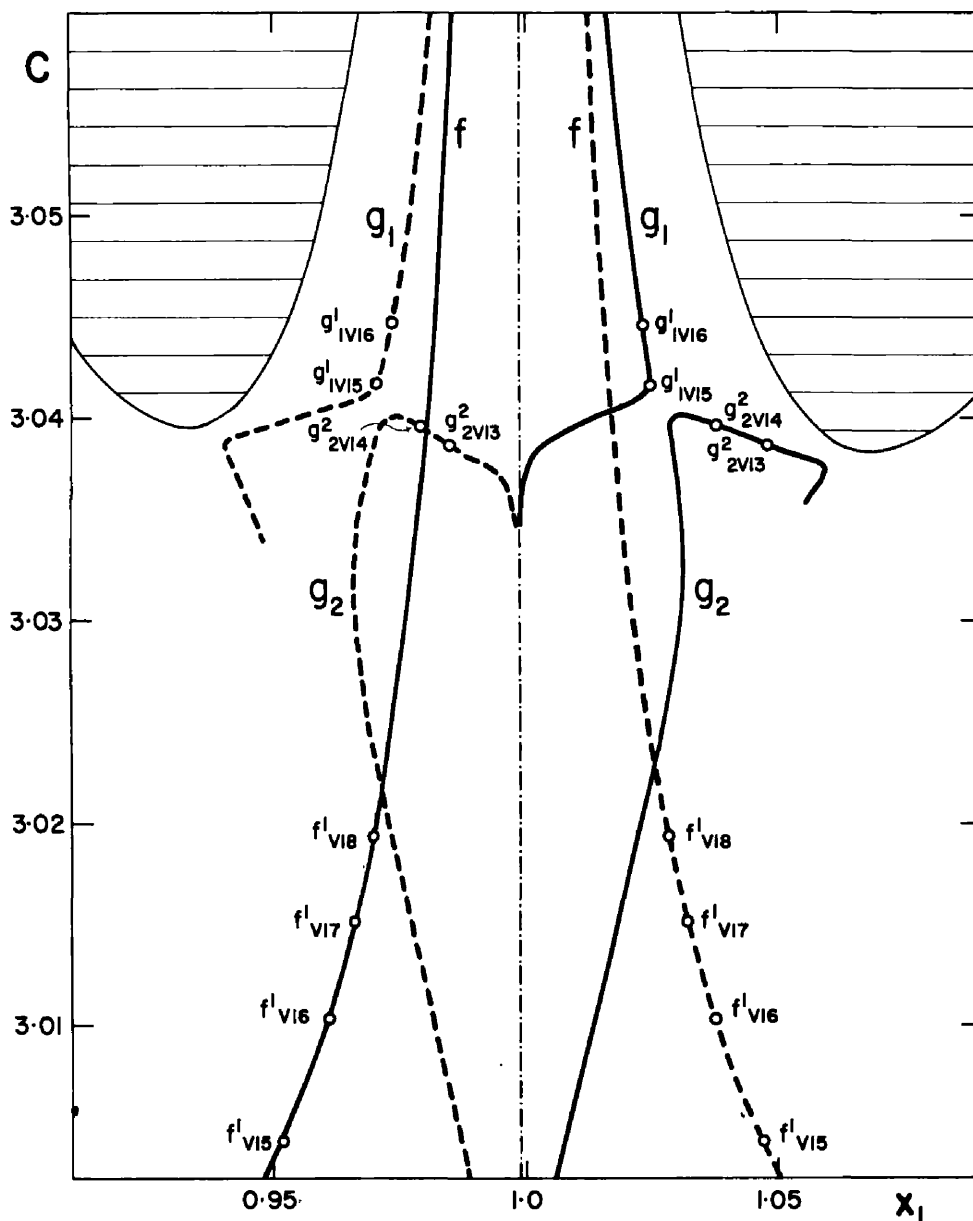


Fig. 2. Characteristics in the  $(C, x_1)$ -plane of the families  $f, g_1$  and  $g_2$  of plane periodic orbits in the vicinity of Jupiter. The continuous heavy lines correspond to the positive crossings of the axis of the primaries. The broken lines correspond to the negative crossings. The hatched areas are the 'forbidden regions' bounded by the zero-velocity curves. The points marked on the family characteristics represent the vertical self-resonant orbits at which the vertical branches of family  $f$  intersect the plane families. The line  $-\cdot-\cdot-$  indicates the position of Jupiter at  $x_1 = 1 - \mu = 0.99905$ .

from which it bifurcates out of the plane, and distinguishing it from the other member of the pair. The superscripts  $(p)$  and  $(a)$  are added to the designation  $F^i_{vnm}$  of the self-resonant orbit in the cases where  $m$  is odd, to distinguish between the plane symmetric and the axisymmetric branches bifurcating therefrom, and the capital letter  $F$  is used instead of  $f$  to clearly indicate the three-dimensionality of the orbits of the branch. When  $m$  is even both the branches consist of doubly-symmetric orbits; one branch consists of orbits which intersect the  $x_1$ -axis at conjunction, and the other of orbits which intersect the axis at opposition. The superscripts  $(c)$  and  $(o)$  can

therefore be used to distinguish between the two branches according to this property, which is invariant along any branch as long as collisions with Jupiter do not occur.

The four pairs of branches presented in this paper fall naturally into two groups depending on the symmetry class. Group (i) comprises the four families  $F_{v15}^{1(a)}$ ,  $F_{v15}^{1(p)}$ ,  $F_{v17}^{1(a)}$  and  $F_{v17}^{1(p)}$ ; these are all of simple symmetry, and are discussed in Section 4. Group (ii) comprises the four doubly-symmetric families  $F_{v16}^{1(c)}$ ,  $F_{v16}^{1(o)}$ ,  $F_{v18}^{1(c)}$  and  $F_{v18}^{1(o)}$ . This group is dealt with in Section 5. The stability properties of all of these vertical branches are discussed in Section 6.

## 4. Results: Odd-Multiplicity Branches

### 4.1. FAMILY $F_{v15}^{1(a)}$

This family of axisymmetric orbits branches from family  $f$  at the vertical self-resonant orbit  $f_{v15}^1$  for which  $x_{01} \approx 0.952$  and  $C \approx 3.0044$ . The nonzero initial conditions  $(x_{01}, x_{05}, x_{06})$ , period  $T$ , Jacobi constant  $C$  and multiplicity  $m$  of representative orbits belonging to this branch are listed in Table 1 (see the Appendix). It is seen that as the family branches upward from the plane and the initial 'z-velocity' ( $x_{06}$ ) increases, the orbits contract inwards towards Jupiter ( $x_{01}$  increasing) and the 'y-velocity' at the axis crossing ( $x_{05}$ ) decreases monotonically. The initial velocity vector, decreasing slowly in magnitude, becomes progressively more steeply inclined to the horizontal plane. This behaviour is maintained as  $x_{05}$  decreases towards zero,  $x_{06}$  increases steadily, the period  $T$  increases, the Jacobi constant increasing monotonically and the orbits continuing to become smaller. Eventually the vertical component of velocity  $x_{06}$  reaches a maximum value of about 0.173 and begins to decrease. When  $x_{05}$  reaches zero one of the loops of the orbit vanishes, and the orbital multiplicity (defined as half the number of crossings of the  $(x_1, x_3)$ -plane occurring in the full period) is reduced from 5 to 4. After a short interval the final 'y-velocity'  $x_5$  also passes through zero from negative to positive values, resulting in the loss of another loop at the second perpendicular crossing of the axis, and a further reduction in the orbital multiplicity  $m$  from 4 to 3. As we trace the family further the size of the orbit (indicated by the value of  $x_{01}$ ) continues to decrease, and the angle of inclination of the initial velocity vector also decreases steadily as  $x_{05}$  becomes more and more negative while  $x_{06}$  continues to become smaller in value. The multiplicity remains unchanged at  $m = 3$  over the remainder of the family as  $x_{06}$  decreases towards zero and the orbits become 'flatter' in character, the sense of orbital motion, originally retrograde with respect to rotating axes, having become direct. The branch terminates back in the horizontal plane at the vertical self-resonant orbit  $g_{2v13}^2$  of family  $g_2$ , for which  $a_v = \cos 2\pi/3 = -0.5$ ,  $x_{01} \approx 0.935$  and  $C \approx 3.0387$ . This orbit is marked on the characteristic of family  $g_2$  in the  $(C, x_1)$ -plane in Figure 2.

From this identification of the termination orbit of the vertical branch  $F_{v15}^{1(a)}$  we conclude that the family is also the vertical branch  $G_{2v13}^{2(a)}$  of family  $g_2$ . Classification of the family as either  $F_{v15}^{1(a)}$  or  $G_{2v13}^{2(a)}$  is arbitrary since there is no obvious

boundary where the two branches meet; there is a kind of ‘no man’s land’ segment where a short bridge of quadruple orbits, which cannot be definitely assigned to either branch, joins together the quintuple ‘retrograde’ and triple ‘direct’ regimes. The safest course would perhaps be to designate the entire family as “ $F_{v15}^{1(a)}/G_{2v13}^{2(a)}$ ”.

The phenomenon of the direct linking together of two planar families (such as, in this case,  $f$  and  $g_2$ ) by a family of three-dimensional orbits which branches vertically from the two generating families, is most common, though not universal. As will be seen below, all the families given in this paper, with one exception, begin and terminate in the horizontal plane at intersections with planar families. A vertical branch may, however, effectively terminate in three dimensions, as will be seen in the next section. Typical orbits of  $F_{v15}^{1(a)}$  are given in Figures 4(a)–(i).

#### 4.2. FAMILY $F_{v15}^{1(p)}$

This is the other member of the pair of branches which bifurcate from the vertical self-resonant orbit  $f_{v15}^1$ , and consists of plane symmetric orbits. Representative orbits of the branch are given in Table 2 of the Appendix. The branch exhibits generally more complicated behaviour as it evolves than any of the other branches discussed in this paper. The orbital period  $T$  and Jacobi constant  $C$  do not vary monotonically along the branch, both of these parameters possessing two turning points. The branch has altogether four different multiplicity regimes. The characteristic of family  $F_{v15}^{1(p)}$  which distinguishes it from the other branches given in this paper, however, is that it effectively terminates in three dimensions, rather than back in the horizontal plane.

The initial condition  $x_{03}$ , which (for plane symmetric 3D orbits) confers the property of three-dimensionality on the branch orbits, increases monotonically as the branch evolves from its bifurcation with family  $f$ . At the same time  $x_{05}$  decreases monotonically, although never becoming negative, so that the branch consists entirely of what might loosely be termed ‘synodically retrograde’ orbits (insofar as the term can be applied to the complicated motion involved in the majority of cases). The initial condition  $x_{01}$  shows a general trend towards higher values, passing through first a maximum and then a minimum in the early stages of the branch. The trends in  $T$  and  $C$  are respectively towards decreased and increased values as the branch evolves, a pattern common to all the branches given in this paper.

The bulk of the family retains the initial multiplicity of five; this drops to three, briefly increases to four, and finally decreases again to two. The reductions of two in the multiplicity (from 5 to 3 and from 4 to 2) occur when two loops of the orbit, images of one another with respect to the plane of symmetry (the  $(x_1, x_3)$ -plane) migrate away from the plane so that they no longer intersect it. The increase in multiplicity from 3 to 4 occurs through the formation of a cusp with its vertex in the plane of symmetry. This cusp occurs at the final epoch when the final ‘y-velocity’  $x_5$  passes through zero from negative to positive values; consequently at the vertex the instantaneous velocity with respect to the rotating coordinate system is zero.

As the branch evolves towards the effective termination point in three dimensions along the final double-periodic ( $m = 2$ ) phase, the two perpendicular crossings of the  $(x_1, x_3)$ -plane move more and more closely together, until they eventually coincide exactly at the termination orbit. This orbit, whose parameters are approximately those given for the last orbit of Table 2, is a plane symmetric simple-periodic orbit described twice, and is a member of a family of such orbits which bifurcates with the branch  $F_{v15}^{1(p)}$  in three dimensions. (This family of simple orbits has not been identified). The intersection orbit also represents a 'point of reflection' of  $F_{v15}^{1(p)}$  since as we continue to trace the branch with any choice of family parameter, we simply retrace the branch in the opposite direction. One interesting feature of the family  $F_{v15}^{1(p)}$ , a short interval over which the orbits are distinctly stable, is described in Section 6. Typical orbits of family  $F_{v15}^{1(p)}$  are given in Figures 5(a)–(g).

#### 4.3. FAMILY $F_{v17}^{1(a)}$

Family  $F_{v17}^{1(a)}$  bifurcates from its generating family ( $f$ ) at the vertical self-resonant orbit  $f_{v17}^1$  for which  $x_{01} \approx 0.9661$ ,  $C \approx 3.0151$ . Its general features are very similar to those of the family  $F_{v15}^{1(a)}$  described above. Representative orbits are given in Table 5. The branch consists of axisymmetric orbits, the multiplicity being initially  $m = 7$ . As the branch evolves out of the horizontal plane the orbits shrink ( $x_{01}$  increases) and the initial velocity vector, decreasing gradually in magnitude, becomes more and more inclined to the horizontal. The period decreases monotonically and the Jacobi constant increases monotonically from beginning to end of the family. Shortly after the initial 'z-velocity'  $x_{06}$  reaches a maximum value of about 0.186 and begins to decrease, the initial 'y-velocity' passes through zero from positive to negative values. When this happens the multiplicity changes from 7 to 6 as one of the orbit loops disappears. At this stage the final 'y-velocity'  $x_5$  has a small negative value and is approaching zero. As  $x_5$  passes through zero and becomes increasingly positive, the multiplicity again drops from 6 to 5, as another loop vanishes. From here the initial velocity vector, still decreasing in magnitude and now corresponding to direct orbital motion, becomes less inclined to the horizontal, while the orbits continue to become smaller. Just before the family returns to the plane, however,  $x_{01}$  reaches a maximum value of about 0.972 and starts to decrease. The orbital multiplicity remains unchanged at  $m = 5$  as the branch evolves, and eventually terminates back in the horizontal plane at the vertical self-resonant orbit  $g_{1v15}^1$  of family  $g_1$ , for which  $a_v = \cos 2\pi/5 \approx 0.30902$ ,  $x_{01} \approx 0.971$  and  $C \approx 3.0417$ . This orbit is marked on the characteristic of family  $g_1$  in the  $(C, x_1)$ -plane in Figure 2. Family  $F_{v17}^{1(a)}$  therefore acts as a three-dimensional link between the planar families  $f$  and  $g_1$  and is identical with the vertical branch  $G_{1v15}^{1(a)}$  of family  $g_1$ . Note that the branches  $F_{v15}^{1(a)}$  and  $F_{v17}^{1(a)}$  terminate on different planar families,  $g_2$  and  $g_1$  respectively. While both  $g_1$  and  $g_2$  consist of direct satellite orbits around the less massive primaries, they are quite distinct (Markellos *et al.*, 1975) for all values of the mass parameter except in Hill's case ( $\mu = 0$ ) of the restricted problem, when they intersect (Hénon, 1969).

#### 4.4. FAMILY $F_{v17}^{1(p)}$

This is the plane symmetric branch which, together with  $F_{v17}^{1(a)}$ , bifurcates from family  $f$  at the vertical self-resonant orbit  $f_{v17}^1$ . Numerical data for the family are given in Table 6. As the family branches vertically out of the plane, and the initial 'z-coordinate'  $x_{03}$  increases, the orbits become 'smaller' ( $x_{01}$  increases) while  $x_{05}$ , the initial 'y-velocity', decreases. The multiplicity retains its initial value  $m = 7$  throughout the first part of the branch; the period decreases monotonically and the Jacobi constant increases monotonically over the whole branch. The perpendicular crossing of the plane at the initial epoch migrates upwards and towards Jupiter in the  $x_{01}$ -direction, until  $x_{03}$  reaches a maximum of about 0.029 almost directly above Jupiter (at  $x_1 = 0.999\ 05$ ), and then begins to curve back down towards the horizontal plane on the other side of Jupiter, i.e. the opposition side. Shortly after the extremum in  $x_{03}$  has been reached, the multiplicity drops from 7 to 5, this value being maintained as the branch evolves and  $x_{03}$  decreases towards zero;  $x_{01}$  continues to increase while  $x_{05}$  reaches a minimum of about 0.170 and then begins to increase. The branch terminates in the horizontal plane at the vertical self-resonant orbit  $g_{1v15}^1$  of family  $g_1$ , which is also the termination orbit of the branch  $F_{v17}^{1(a)}$  (Section 4.3).

### 5. Results: Even-Multiplicity Branches

#### 5.1. FAMILY $F_{v16}^{1(c)}$

This family is one of the pair of doubly-symmetric branches which bifurcate from family  $f$  at the branch orbit  $f_{v16}^1$ , for which  $a_v = \cos 2\pi/6 = 0.5$  and the Jacobi constant  $C \approx 3.0103$ . The two intersections of the branch orbit occur at  $x_1 \approx 0.961$  (conjunction crossing) and  $x_1 \approx 1.038$  (opposition crossing), and the two branches consist of orbits which have their type (A) mirror configuration, or crossing of the  $x_1$ -axis, at conjunction (family  $F_{v16}^{1(c)}$ ) or at opposition (family  $F_{v16}^{1(o)}$ ). In establishing the doubly-symmetric branches of family  $f$  it was found most convenient to integrate the orbits starting from the axis; thus the initial conditions of representative orbits from each family are those for a type (A) mirror configuration, although in-plane initial conditions could equally well have been used. The data for family  $F_{v16}^{1(c)}$  are given in Table 3.

The initial conditions ( $x_{01}, x_{05}, x_{06}$ ) evolve in much the same way as those for branches  $F_{v15}^{1(a)}$  and  $F_{v17}^{1(a)}$ . As the initial 'z-velocity'  $x_{06}$  increases to a maximum value of about 0.179,  $x_{01}$  increases steadily (with the result that the orbits become smaller overall) and  $x_{05}$  decreases monotonically, passing through zero after the maximum in  $x_{06}$  and becoming negative. Associated with this change of sign of the initial 'y-velocity' there is a drop in the orbital multiplicity from 6 to 4. This arises through the simultaneous disappearance of two loops cutting the  $(x_1, x_3)$ -plane; owing to the double symmetry of the orbits these two loops are images of one another with respect to the  $(x_1, x_3)$ -plane. The orbital multiplicity remains  $m = 4$  as the branch evolves back towards the horizontal plane,  $x_{01}$  continuing to increase and  $x_{05}$  becoming more

negative. As with other vertical branches, the period is a monotonic decreasing, and the Jacobi constant a monotonic increasing function, as the family evolves. The branch terminates in the horizontal plane at the vertical self-resonant orbit  $g_{2v14}^2$  of family  $g_2$ , for which  $a_v = 0$ ,  $x_{01} \approx 0.979$  and  $C \approx 3.030\ 97$ ; we therefore conclude that the vertical branches  $F_{v16}^{1(c)}$  and  $G_{2v14}^{2(c)}$  are identical. The termination orbit  $g_{2v14}^2$  is marked on the characteristic of family  $g_2$  in the  $(C, x_1)$ -plane in Figure 2. Typical orbits of  $F_{v16}^{1(c)}$  are given in Figures 6(a)–(f).

### 5.2. FAMILY $F_{v16}^{1(o)}$

This is the other member of the pair of branches of doubly-symmetric orbits bifurcating from family  $f$  at  $f_{v16}^1$ . The initial conditions at the perpendicular crossing of the  $x_1$ -axis (occurring at opposition throughout the branch) and other parameters of representative orbits are listed in Table 4. The orbital multiplicity is initially  $m = 6$  and maintains this value as the initial ‘z-velocity’  $x_{06}$  increases to a maximum of about 0.178 and starts to decrease, while  $x_{01}$  decreases slightly and  $x_{05}$  increases steadily from its maximum negative value at the beginning of the branch. The orbits become quadruple when  $x_{05}$  passes through zero to take on increasingly positive values. The branch returns to the horizontal plane as  $x_{06}$  decreases towards zero;  $x_{01}$  reaches a minimum value of about 1.030 and starts to increase until the branch terminates at the vertical self-resonant orbit  $g_{2v14}^2$  (the orbit being started from the opposition rather than the conjunction crossing). We conclude that the pair of branches  $F_{v16}^{1(c)}$  and  $F_{v16}^{1(o)}$  not only start from the same vertical self-resonant orbit of family  $f$ , but finish at the same orbit of family  $g_2$ ; we can also identify  $F_{v16}^{1(o)}$  with the branch  $G_{2v14}^{2(o)}$ . As usual, the period is monotonic decreasing and the Jacobi constant monotonic increasing along the branch, starting from family  $f$  and ending on family  $g_2$ . Typical orbits of family  $F_{v16}^{1(o)}$  are given in Figures 7(a) and (b).

### 5.3. FAMILY $F_{v18}^{1(c)}$

This family has many characteristics in common with  $F_{v16}^{1(c)}$ . It is one of a pair of doubly-symmetric branches bifurcating from family  $f$  at  $f_{v18}^1$ , for which  $a_v = \cos 2\pi/8 \approx 0.707\ 11$  and  $C \approx 3.0194$ , the crossings of the  $x_1$ -axis occurring at  $x_1 \approx 0.970$  (conjunction),  $x_1 \approx 1.028$  (opposition). As indicated by the superscript (c), the branch with which we are concerned here is the one whose orbits all intersect the  $x_1$ -axis at conjunction. Numerical data for the family are given in Table 7. The usual pattern is found in the evolution of the initial velocity vector:  $x_{05}$  decreases monotonically from positive to negative values, a drop in the multiplicity from 8 to 6 occurring as the sign of  $x_{05}$  changes;  $x_{06}$  rises to a maximum of about 0.194 just before  $x_{05}$  reaches zero, and then decreases towards zero. This rotation of the initial velocity vector through half a revolution about the  $x_1$ -axis changes the sense of motion from synodically retrograde to direct (although these terms can only be applied meaningfully to orbits at either end of the branch where the motion is more nearly confined to a common plane). The initial condition  $x_{01}$  increases to a maximum value of about 0.974 just before the branch terminates, and then decreases

slightly. The familiar monotonic behaviour of the period and Jacobi constant is apparent. The branch terminates at the vertical self-resonant orbit  $g_{1v16}^1$  of family  $g_1$ , for which  $a_v = \cos 2\pi/6 = -0.5$ , the Jacobi constant  $C \approx 3.0447$ , and the conjunction crossing occurs at  $x_1 \approx 0.974$ . Thus family  $F_{v18}^{1(c)}$  is identical to the vertical branch  $G_{1v16}^{1(c)}$  of  $g_1$ . The orbit  $g_{1v16}^1$  is marked on the characteristic of family  $g_1$  in Figure 2.

#### 5.4. FAMILY $F_{v18}^{1(o)}$

This is the family of doubly-symmetric orbits starting from the  $x_1$ -axis at opposition, which together with  $F_{v18}^{1(c)}$  forms a pair of branches bifurcating from family  $f$  at the vertical self-resonant orbit  $f_{v18}^1$ . Representative orbits are listed in Table 8. Owing to the fact that both branches consist of relatively ‘small’ orbits, they are almost mirror images of one another with respect to the plane parallel to the  $(x_2, x_3)$ -plane passing through Jupiter, and this is apparent in the comparison of the various orbital parameters listed in Tables 7 and 8. It can be seen from Figure 1 that as the branch multiplicity  $m$  increases and  $a_v$  approaches unity, the vertical self-resonant orbits become smaller and, as a result, more nearly symmetrical with respect to the axis passing through Jupiter parallel to the  $x_2$ -axis. We would therefore expect greater symmetry between the two members of a pair of even-multiplicity branches as the multiplicity increases.

The initial ‘z-velocity’  $x_{06}$  increases to a maximum value of about 0.193, then starts to decrease just before  $x_{05}$  passes through zero and becomes increasingly positive; the change of sign of  $x_{05}$  is marked, as in family  $F_{v18}^{1(c)}$ , by a drop in the orbital multiplicity from  $m = 8$  to  $m = 6$ . Throughout the branch,  $x_{01}$  decreases steadily, while  $T$  and  $C$  also vary monotonically. The branch terminates at the same orbit,  $g_{1v16}^1$ , as its ‘twin’  $F_{v18}^{1(c)}$ . Thus the three pairs of branches of multiplicities 6, 7 and 8 form twofold connections between three vertical self-resonant orbits of family  $f$  ( $f_{v16}^1, f_{v17}^1, f_{v18}^1$ ) and the three self-resonant orbits  $g_{2v14}^2, g_{1v15}^1, g_{1v16}^1$  of families  $g_2$  and  $g_1$ .

## 6. Stability

### 6.1. CALCULATION OF THE STABILITY PARAMETERS

In order to calculate the stability parameters  $p$  and  $q$  of a periodic orbit in the three-dimensional circular restricted problem, the matrix of first-order variations  $V(T)$ , computed at the full period  $T$  of the orbit, is used. The stability parameters are then given by

$$p = \frac{1}{2}(\alpha + \sqrt{\Delta}); \quad q = \frac{1}{2}(\alpha - \sqrt{\Delta}) \tag{6.1}$$

where

$$\begin{aligned} \Delta &= \alpha^2 - 4(\beta - 2) \\ \alpha &= 2 - \text{Tr}(V) \\ \beta &= \frac{1}{2}(\alpha^2 + 2 - \text{Tr}(V^2)) \end{aligned} \tag{6.2}$$

(e.g. Zagouras and Markellos, 1977). The criterion for stability can then be stated in terms of  $p$  and  $q$ ; three conditions must be satisfied:

- (i)  $p$  and  $q$  both real ( $\Delta \geq 0$ )
- (ii)  $|p| < 2$ .
- (iii)  $|q| < 2$ .

We note that in the three-dimensional case  $p$  and  $q$  are determined indiscriminately as the two roots of the quadratic

$$\nu^2 - \alpha\nu + (\beta - 2) = 0 ; \quad (6.3)$$

if the orbit is plane the variational equations decouple into two sets, one referring to 'horizontal' variations and the other referring to 'vertical' variations, and each of the two roots is now determined uniquely from the linear equation arising from the corresponding submatrix of the variational matrix. If the roots arising from the 'horizontal' and 'vertical' submatrices are called  $\rho_h$  and  $\rho_v$  respectively, then the following relations with the horizontal and vertical stability parameters  $a$  and  $a_v$  are easily seen to hold:

$$\rho_h = -2a, \quad \rho_v = -2a_v. \quad (6.4)$$

When we are dealing, as in this paper, with symmetric orbits, it is not necessary to integrate the equations of variation for the full period in order to determine  $p$  and  $q$ . By making use of the symmetry properties of an orbit it is possible to relate the variational matrix  $V(T)$  at the full period  $T$ , to its value at  $T/2$  or  $T/4$ , according to whether the orbit is of simple or double symmetry; that is, at the epoch of the second mirror configuration. Defining the  $6 \times 6$  diagonal matrices  $L$  and  $M$  by

$$\begin{aligned} L &= \text{diag} \{1, -1, 1, -1, 1, -1\} \\ M &= \text{diag} \{1, -1, -1, -1, 1, 1\} \end{aligned} \quad (6.5)$$

we obtain the following formulae for  $V(T)$  for each of the four cases listed in Table I.

$$\text{Case 1 (Plane Symmetric Orbits):} \quad V(T) = LV^{-1}(T/2)LV(T/2) \quad (6.6a)$$

$$\text{Case 2 (Axisymmetric Orbits):} \quad V(T) = MV^{-1}(T/2)MV(T/2) \quad (6.6b)$$

$$\text{Case 3 (Doubly Symmetric Orbits, starting from axis):} \quad V(T) = [MV^{-1}(T/4)LV(T/4)]^2 \quad (6.6c)$$

$$\text{Case 4 (Doubly Symmetric Orbits, starting from plane):} \quad V(T) = [LV^{-1}(T/4)MV(T/4)]^2 \quad (6.6d)$$

These relationships result in an economy of computing effort in the determination of the stability of an orbit.

6.2. STABILITY OF THE VERTICAL BRANCHES OF FAMILY  $f$

In this section we deal briefly with the stability of the orbits belonging to the vertical branches of family  $f$  given in Sections 4 and 5.

It was found that, in general, the bulk of the vertical branch orbits are unstable according to the criterion of Section 6.1, although there exist intervals where the conditions are marginally satisfied: that is, both stability parameters are real, one lying distinctly within the ‘stable zone’ between  $\pm 2$ , and the other very close to the limit of this zone. Since no numerical checks were made on the accuracy of calculations of the stability parameters, we have marked as ‘stable’ (by the letter  $S$  appearing on the right-hand side of the entries in Tables 1–8) only those orbits which certainly satisfy all three of the conditions of Section 6.1. The absence of the letter ‘ $S$ ’ from a given entry in one of the tables should not therefore be taken to imply that the corresponding orbit is necessarily unstable, although any stable orbits not so marked would possess only marginal stability.

Only two of the vertical branches given in this paper contain definitely stable orbits: these are  $F_{v15}^{1(p)}$  and  $F_{v16}^{1(c)}$  (Tables 2 and 3). In the latter case the stability is still somewhat marginal; while  $p$  varies between about  $-1.36$  and  $+1.86$ , clearly within the limits of condition (ii),  $q$  is never further from the boundary value  $-2$  than  $-1.995$ . In the former case (family  $F_{v15}^{1(p)}$ ), however, there exists a definitely stable part represented by one orbit in Table 2. This part of  $F_{v15}^{1(p)}$  has been surveyed in more detail, and a plot of  $q$  versus  $p$  for a part of the branch including the stable segment is shown in Figure 3. In this figure the hatching marks the part of the diagram in which the stability criterion is satisfied.

We conclude, therefore, that apart from marginal cases where one of the stability parameters is very close to the stability limit, the vertical branches of family  $f$  given in this paper are generally unstable. This is particularly true of those orbits which involve significant departures from the horizontal plane (i.e. large values of  $x_{03}$  or  $x_{06}$ ).

7. Remarks

- (1) The following table lists the vertical self-resonant orbits of families  $f$ ,  $g_1$  and  $g_2$  at which the vertical branches of family  $f$  given in this paper start and finish:

TABLE II

Branch	Starting orbit	Termination orbit
$F_{v15}^{1(a)}$ :	$f_{v15}^1$	$g_{2v13}^2$
$F_{v16}^{1(c)}, F_{v16}^{1(o)}$ :	$f_{v16}^1$	$g_{2v14}^2$
$F_{v17}^{1(p)} : F_{p17}^{1(p)}$ :	$f_{v17}^1$	$g_{1v15}^1$
$F_{v18}^{1(o)} : F_{p18}^{1(o)}$ :	$f_{v18}^1$	$g_{1v16}^1$

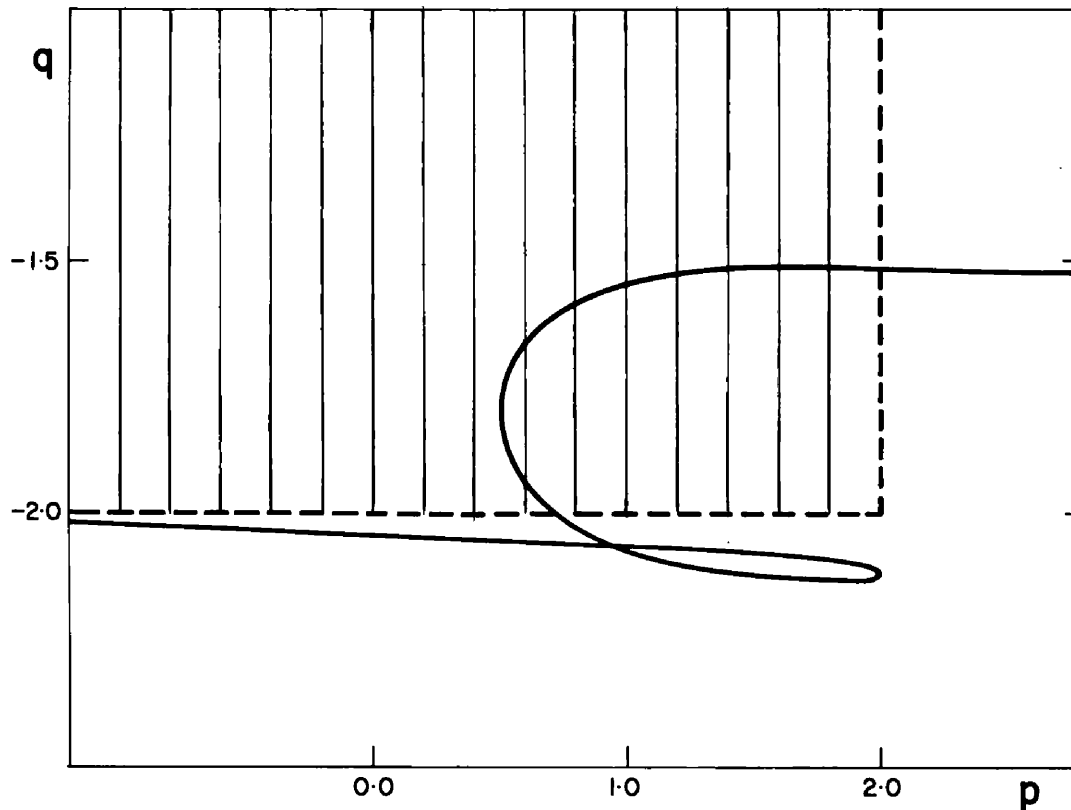


Fig. 3. Stability curve in the  $(p, q)$ -plane of part of the vertical branch  $F_{v15}^{1(p)}$  containing distinctly stable orbits. The hatching marks part of the stable region defined by  $|p| < 2, |q| < 2$ .

We see from this table that the multiplicity of the termination orbit is two less than that of the starting orbit. This pattern has been found to apply also to higher-multiplicity branches of family  $f$  not discussed in this paper. This appears to be a general feature of the three-dimensional branches which connect the retrograde family  $f$  with the direct families  $g_1$  and  $g_2$ .

(2) As can also be seen from Table II, the multiplicity 5 and 6 branches of family  $f$  (with the exception of  $F_{v15}^{1(p)}$ ) terminate on  $g_2$ , while those of multiplicity 7 and 8 terminate on  $g_1$ . Figure 2 shows that this sequence of termination orbits occurs in the sense of increasing  $C$ , the jump between families  $g_2$  and  $g_1$  taking place in the vicinity of the narrow 'neck' where the two family characteristics in the  $(C, x_1)$  plane approach most closely (and where the two curves actually intersect in Hill's case,  $\mu = 0$ ). There seems to be a general trend in the termination points of vertical branches of  $f$  in the vicinity of Jupiter, indicated by the four multiplicity cases examined, whereby those branches starting from the neighbourhood of  $f_{v15}^1$  and  $f_{v16}^1$  connect with  $g_2$ , while those beyond  $f_{v17}^1$  end up on  $g_1$ .

(3) As many authors have pointed out, the circular restricted problem may not be an adequate model for studies of certain astronomical systems, such as the Earth-Moon or outer Jovian satellite systems, in which the non-zero eccentricity of the orbit of the primaries may have important dynamical consequences (particularly with regard to capture and escape mechanisms). It may therefore be desirable to investigate such systems in the framework of the elliptic restricted problem. The

determination of vertical branches in the circular problem is a useful starting point for finding symmetric periodic orbits in the three-dimensional elliptic problem, for these branches contain isolated orbits whose periods are commensurable with the period of the primaries, and can therefore be used to establish families of periodic orbits in the elliptic problem with either the mass parameter  $\mu$ , or eccentricity  $e$  of the primaries, as the family parameter. A natural continuation of the present work would be to use commensurable orbits of the vertical branches of family  $f$  to obtain three-dimensional symmetric periodic orbits in the elliptic problem for the Sun-Jupiter case ( $\mu = 0.000\ 95$ ) in the vicinity of Jupiter, with a view to application to the problem of the outer retrograde satellites of Jupiter.

(4) It must be stressed that the generation of three-dimensional periodic orbits from the vertical-critical orbits ( $a_v = \pm 1$ ) of simple-periodic plane orbits is a special case providing the simpler form of three-dimensional periodic orbits, namely the cases of multiplicity 1 or 2, and these forms occur in a finite and relatively small number of instances. The present work describes the mechanism of generation of three-dimensional periodic orbits in the general case where the generating plane orbit is vertically self-resonant and the multiplicity of the resulting orbits can be any integer  $m > 2$ . Thus, this work exemplifies the behaviour of the great abundance of the three-dimensional periodic orbits of the problem. For, even if we restrict ourselves to the vertically stable segments of simple-periodic (one-revolution) plane orbits, there are many infinities of families of three-dimensional periodic orbits of arbitrary multiplicity that can be found to bifurcate therefrom in the way described.

(5) The numerical procedures described here are not only efficient for the determination of entire families of three-dimensional periodic orbits, but can easily be modified to be applicable in the case of asymmetric plane periodic orbits which present, in so far as numerical determination is concerned, the same degree of complexity as the symmetric three-dimensional orbits.

### Appendix Tables 1–8 and Figures 4–7

In Figures 4–7, orbits representing various parts of the families described in Sections 4 and 5 are plotted with respect to coordinates  $(X, Y, Z)$  defined by

$$X = x_1 - (1 - \mu) = x_1 - 0.999\ 05$$

$$Y = x_2$$

$$Z = x_3 .$$

Thus the origin of this coordinate system is at Jupiter ( $x_1 = 1 - \mu$ ). The scale of the plots is such that the length of the positive half of each axis is 0.1 (in units of the Sun-Jupiter distance). The orbits are projected orthogonally on the  $(X, Y)$ ,  $(X, Z)$  and  $(Y, Z)$  planes. Figure 5(g) is an orthogonal projection on a plane perpendicular to the vector  $(1, 1, 1)$ .

TABLE 1  
Family  $F_{v15}^{1(a)}/G_{2v13}^{2(a)}$

$x_{01}$	$x_{05}$	$x_{06}$	$T$	$C$	$m$
0.951 982	0.199 771	0.005	8.527 992	3.004 444	5
0.952 009	0.199 526	0.01	8.516 937	3.004 482	5
0.952 116	0.198 545	0.02	8.473 496	3.004 633	5
0.952 528	0.194 587	0.04	8.311 018	3.005 226	5
0.954 000	0.178 091	0.08	7.790 756	3.007 485	5
0.956 194	0.146 902	0.12	7.177 642	3.011 175	5
0.959 557	0.084 317	0.16	6.521 408	3.017 354	5
0.962 546	0.013 698	0.173 014	6.126 857	3.023 174	5
0.963 138	-0.001 302	0.172 406	6.066 102	3.024 294	4
0.964 178	-0.026 302	0.169 123	5.976 432	3.026 075	3
0.969 812	-0.086 302	0.165 598	5.717 008	3.029 878	3
0.973 415	-0.116 302	0.167 475	5.531 260	3.031 697	3
0.978 654	-0.176 302	0.160 732	5.255 900	3.034 653	3
0.980 581	-0.206 302	0.150 640	5.159 574	3.035 809	3
0.983 336	-0.261 302	0.114 048	5.028 337	3.037 521	3
0.984 528	-0.291 332	0.073 921	4.973 970	3.038 283	3
0.984 849	-0.300 254	0.053 921	4.959 584	3.038 491	3
0.985 052	-0.306 108	0.033 921	4.950 533	3.038 623	3
0.985 157	-0.309 211	0.013 921	4.945 854	3.038 691	3
0.985 177	-0.309 783	0.003 921	4.944 999	3.038 704	3

TABLE 2  
Family  $F_{v15}^{1(p)}$

$x_{01}$	$x_{03}$	$x_{05}$	$T$	$C$	$m$
0.952 359	0.005	0.199 526	8.505 618	3.004 521	5
0.953 530	0.01	0.198 536	8.427 558	3.004 796	5
0.958 379	0.02	0.194 222	8.117 607	3.005 996	5
0.956 833	0.039 158	0.169 505	8.985 683	3.005 174	5
0.970 833	0.044 457	0.161 227	8.584 528	3.007 524	5
0.985 833	0.048 168	0.150 268	8.229 079	3.010 729	5
0.992 672	0.049 434	0.143 539	8.120 409	3.012 304	5
1.002 156	0.051 581	0.129 539	8.002 749	3.014 539	5
1.005 978	0.052 804	0.121 539	7.947 346	3.015 475	5
1.011 451	0.054 889	0.107 539	7.837 344	3.016 912	5
1.013 858	0.055 859	0.100 539	7.774 735	3.017 596	5
1.017 957	0.057 473	0.087 539	7.649 209	3.018 836	5
1.019 708	0.058 138	0.081 539	7.589 944	3.019 390	5
1.023 205	0.059 455	0.068 539	7.467 896	3.020 501	3
1.024 923	0.060 127	0.061 539	7.409 845	3.021 026	3
1.027 838	0.061 359	0.048 539	7.322 457	3.021 820	3
1.029 281	0.062 022	0.041 539	7.287 356	3.022 143	3
1.031 590	0.063 145	0.029 539	7.246 401	3.022 524	3
1.032 321	0.063 510	0.025 539	7.237 926	3.022 603	4
1.034 422	0.064 553	0.013 547	7.227 158	3.022 704	2

TABLE 3  
Family  $F_{v16}^{1(c)}/G_{2v14}^{2(c)}$

$x_{01}$	$x_{05}$	$x_{06}$	$T$	$C$	$m$	
0.960 903	0.202 786	0.005	7.768 097	3.010 288	6	
0.960 912	0.202 563	0.01	7.763 612	3.010 314	6	
0.960 949	0.201 669	0.02	7.745 780	3.010 414	6	
0.961 095	0.198 055	0.04	7.676 075	3.010 816	6	
0.961 705	0.182 945	0.08	7.419 880	3.012 447	6	
0.962 793	0.154 532	0.12	7.051 156	3.015 313	6	
0.964 290	0.110 066	0.155	6.652 516	3.019 381	6	
0.965 770	0.057 581	0.175	6.334 946	3.023 697	6	
0.966 509	0.027 342	0.178 983	6.196 464	3.026 002	6	
0.966 890	0.010 568	0.179 040	6.129 494	3.027 233	6	
0.967 344	-0.010 570	0.176 928	6.053 228	3.028 740	4	
0.967 729	-0.029 511	0.172 892	5.991 444	3.030 054	4	
0.968 179	-0.052 960	0.164 851	5.922 218	3.031 634	4	
0.968 547	-0.073 149	0.154 851	5.868 134	3.032 958	4	S
0.969 324	-0.117 005	0.119 851	5.765 421	3.035 716	4	S
0.976 955	-0.198 339	0.082 300	5.553 752	3.038 516	4	S
0.978 980	-0.228 014	0.04	5.470 898	3.039 450	4	S
0.979 326	-0.233 753	0.02	5.456 139	3.039 621	4	S
0.979 408	-0.235 142	0.01	5.452 629	3.039 662	4	S
0.979 431	-0.235 528	0.004	5.451 658	3.039 673	4	S

TABLE 4  
Family  $F_{v16}^{1(o)}/G_{2v14}^{2(o)}$

$x_{01}$	$x_{05}$	$x_{06}$	$T$	$C$	$m$	
1.037 500	-0.201 469	0.003 632	7.768 784	3.010 285	6	
1.037 478	-0.201 174	0.010 909	7.762 293	3.010 321	6	
1.037 404	-0.200 162	0.021 919	7.740 325	3.010 445	6	
1.037 168	-0.196 806	0.040 779	7.670 487	3.010 849	6	
1.036 220	-0.181 203	0.082 771	7.394 357	3.012 624	6	
1.035 071	-0.156 718	0.118 252	7.069 467	3.015 152	6	
1.033 255	-0.100 918	0.160 394	6.583 780	3.020 217	6	
1.032 780	-0.081 762	0.168 295	6.463 212	3.021 809	6	
1.032 321	-0.061 049	0.174 096	6.349 708	3.023 468	6	
1.031 877	-0.038 705	0.177 471	6.242 791	3.025 197	6	
1.031 447	-0.014 654	0.177 948	6.142 026	3.026 998	6	
1.031 030	0.011 181	0.174 840	6.047 014	3.028 871	4	
1.030 724	0.031 774	0.169 549	5.979 317	3.030 325	4	
1.030 425	0.053 441	0.161 001	5.914 524	3.031 821	4	
1.029 780	0.108 779	0.120 015	5.772 498	3.035 518	4	
1.033 248	0.111 504	0.080 294	5.670 506	3.037 257	4	
1.036 641	0.105 860	0.040 743	5.513 805	3.038 963	4	
1.037 492	0.104 951	0.019 207	5.465 535	3.039 512	4	
1.037 667	0.104 783	0.010 102	5.455 374	3.039 630	4	
1.037 713	0.104 740	0.005 605	5.452 675	3.039 662	4	

TABLE 5  
Family  $F_{v17}^{1(a)}/G_{1v15}^{1(a)}$

$x_{01}$	$x_{05}$	$x_{06}$	$T$	$C$	$m$
0.966 244	0.207 918	0.005	7.405 761	3.015 110	7
0.966 248	0.207 708	0.01	7.403 231	3.015 130	7
0.966 267	0.206 867	0.02	7.393 133	3.015 208	7
0.966 342	0.203 465	0.04	7.353 133	3.015 521	7
0.966 659	0.189 246	0.08	7.198 740	3.016 810	7
0.967 249	0.162 700	0.12	6.956 258	3.019 124	7
0.968 262	0.114 524	0.16	6.622 982	3.023 049	7
0.969 173	0.066 281	0.18	6.377 806	3.026 683	7
0.969 630	0.039 683	0.185	6.267 931	3.028 580	7
0.969 953	0.019 683	0.186 245	6.194 281	3.029 964	7
0.970 259	-0.000 317	0.185 372	6.127 086	3.031 314	6
0.970 333	-0.005 317	0.184 819	6.111 187	3.031 647	5
0.970 547	-0.020 317	0.182 336	6.065 443	3.032 634	5
0.971 295	-0.080 317	0.158 320	5.906 783	3.036 443	5
0.971 633	-0.119 810	0.124 564	5.817 877	3.038 876	5
0.971 604	-0.147 330	0.079 564	5.757 591	3.040 642	5
0.971 229	-0.157 420	0.039 564	5.728 629	3.041 462	5
0.971 019	-0.158 999	0.019 564	5.720 388	3.041 669	5
0.970 953	-0.159 287	0.009 564	5.718 166	3.041 721	5
0.970 936	-0.159 349	0.004 564	5.717 612	3.041 734	5

TABLE 6  
Family  $F_{v17}^{1(p)}/G_{1v15}^{1(p)}$

$x_{01}$	$x_{03}$	$x_{05}$	$T$	$C$	$m$
0.966 260	0.001	0.207 973	7.405 867	3.015 110	7
0.966 313	0.002	0.207 929	7.403 649	3.015 127	7
0.966 525	0.004	0.207 751	7.394 761	3.015 195	7
0.967 118	0.007	0.207 254	7.370 149	3.015 387	7
0.969 377	0.013	0.205 373	7.278 304	3.016 130	7
0.971 136	0.016	0.203 922	7.208 931	3.016 721	7
0.973 431	0.019	0.202 045	7.121 124	3.017 509	7
0.979 342	0.024 217	0.197 311	6.908 370	3.019 629	7
0.985 342	0.027 356	0.192 654	6.710 559	3.021 919	7
0.991 342	0.029 017	0.188 152	6.529 215	3.024 351	7
0.997 342	0.029 439	0.183 815	6.362 710	3.026 932	7
1.000 342	0.029 205	0.181 714	6.284 558	3.028 281	7
1.003 342	0.028 665	0.179 662	6.209 571	3.029 669	5
1.009 342	0.026 575	0.175 737	6.068 402	3.032 569	5
1.012 342	0.024 933	0.173 894	6.001 847	3.034 086	5
1.018 292	0.019 974	0.170 676	5.876 512	3.037 246	5
1.022 407	0.013 974	0.169 591	5.792 046	3.039 625	5
1.024 434	0.007 974	0.171 352	5.743 972	3.041 039	5
1.024 816	0.004 974	0.173 296	5.728 817	3.041 458	5
1.024 913	0.001 974	0.175 150	5.719 411	3.041 692	5
1.024 917	0.000 974	0.175 489	5.717 933	3.041 726	5

TABLE 7  
Family  $F_{v18}^{1(c)}/G_{1v16}^{1(c)}$

$x_{01}$	$x_{05}$	$x_{06}$	$T$	$C$	$m$
0.969 965	0.213 616	0.005	7.188 209	3.019 407	8
0.969 968	0.213 416	0.01	7.186 556	3.019 423	8
0.969 979	0.212 616	0.02	7.179 954	3.019 487	8
0.970 025	0.209 384	0.04	7.153 648	3.019 745	8
0.970 218	0.195 906	0.08	7.049 825	3.020 811	8
0.970 580	0.170 971	0.12	6.879 715	3.022 734	8
0.971 207	0.127 298	0.16	6.635 554	3.025 953	8
0.971 727	0.089 138	0.18	6.463 596	3.028 622	8
0.972 165	0.054 864	0.19	6.333 291	3.030 919	8
0.972 689	0.010 452	0.193 566	6.190 106	3.033 770	8
0.972 914	-0.010 152	0.191 774	6.131 537	3.035 051	6
0.973 024	-0.020 647	0.19	6.103 327	3.035 694	6
0.973 355	-0.054 550	0.18	6.018 741	3.037 734	6
0.973 671	-0.091 943	0.16	5.935 203	3.039 927	6
0.973 932	-0.134 017	0.12	5.850 409	3.042 355	6
0.973 991	-0.157 386	0.08	5.805 840	3.043 716	6
0.973 970	-0.169 632	0.04	5.782 423	3.044 451	6
0.973 957	-0.172 506	0.02	5.776 826	3.044 629	6
0.973 952	-0.173 213	0.01	5.775 439	3.044 673	6
0.973 951	-0.173 389	0.005	5.775 093	3.044 684	6

TABLE 8  
Family  $F_{v18}^{1(o)}/G_{1v16}^{1(o)}$

$x_{01}$	$x_{05}$	$x_{06}$	$T$	$C$	$m$
1.028 278	-0.212 692	0.005	7.188 201	3.019 407	8
1.028 273	-0.212 500	0.01	7.186 528	3.019 423	8
1.028 254	-0.211 730	0.02	7.179 844	3.019 488	8
1.028 180	-0.208 619	0.04	7.153 270	3.019 749	8
1.027 891	-0.195 597	0.08	7.049 182	3.020 818	8
1.027 424	-0.171 335	0.12	6.880 437	3.022 726	8
1.026 854	-0.135 225	0.155 135	6.673 746	3.025 409	8
1.026 348	-0.096 225	0.177 582	6.492 206	3.028 151	8
1.025 908	-0.056 225	0.189 787	6.337 656	3.030 838	8
1.025 709	-0.036 225	0.192 514	6.269 615	3.032 141	8
1.025 520	-0.016 225	0.193 155	6.206 672	3.033 421	8
1.024 340	0.003 775	0.191 739	6.148 217	3.034 679	6
1.024 996	0.043 775	0.182 521	6.042 852	3.037 135	6
1.024 610	0.088 775	0.160 395	5.939 737	3.039 803	6
1.024 190	0.132 711	0.121 170	5.852 337	3.042 298	6
1.023 876	0.158 774	0.081 170	5.806 242	3.043 704	6
1.023 658	0.173 219	0.041 170	5.782 597	3.044 446	6
1.023 598	0.176 794	0.021 170	5.776 967	3.044 624	6
1.023 581	0.177 715	0.011 170	5.775 530	3.044 670	6
1.023 577	0.177 962	0.006 170	5.775 146	3.044 682	6

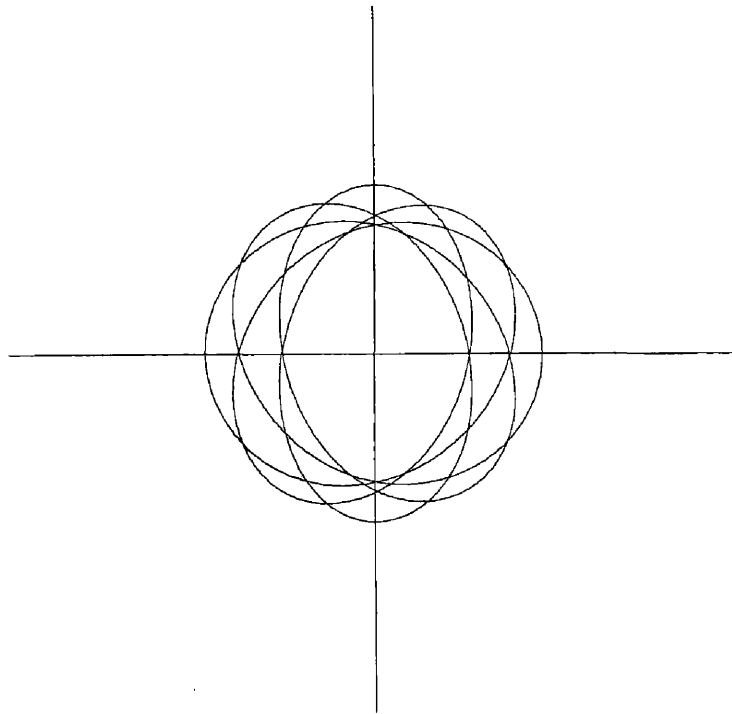


Fig. 4(a).

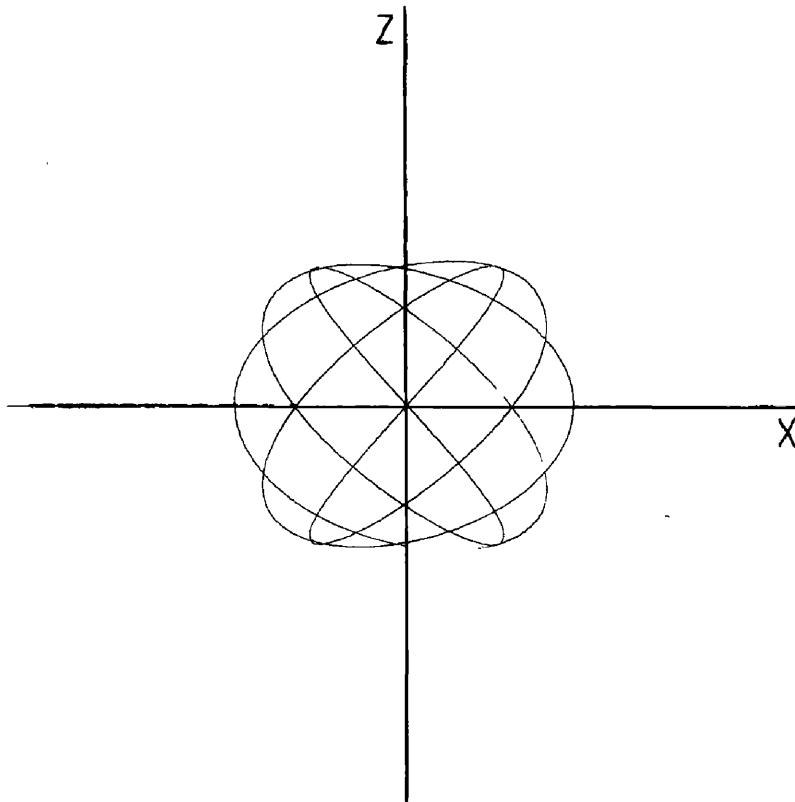


Fig. 4(b).

Figs. 4(a)–(i). Typical orbits of family  $F_{v15}^{1(a)}$ . Figures 4(a)–(c) are projections, in the  $(X, Y)$ ,  $(X, Z)$  and  $(Y, Z)$  planes, of an orbit belonging to the  $m = 5$  segment of the family; Figures 4(d)–(f) are the three projections of a representative quadruple ( $m = 4$ ) member, and Figures 4(g)–(i) the projections of a representative triple-periodic ( $m = 3$ ) member.

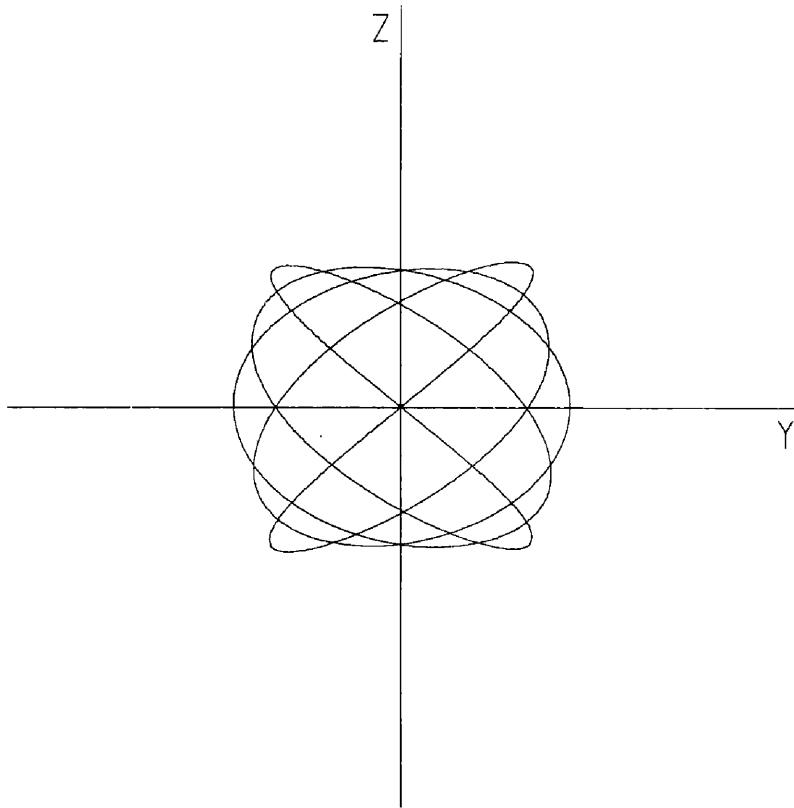


Fig. 4(c).

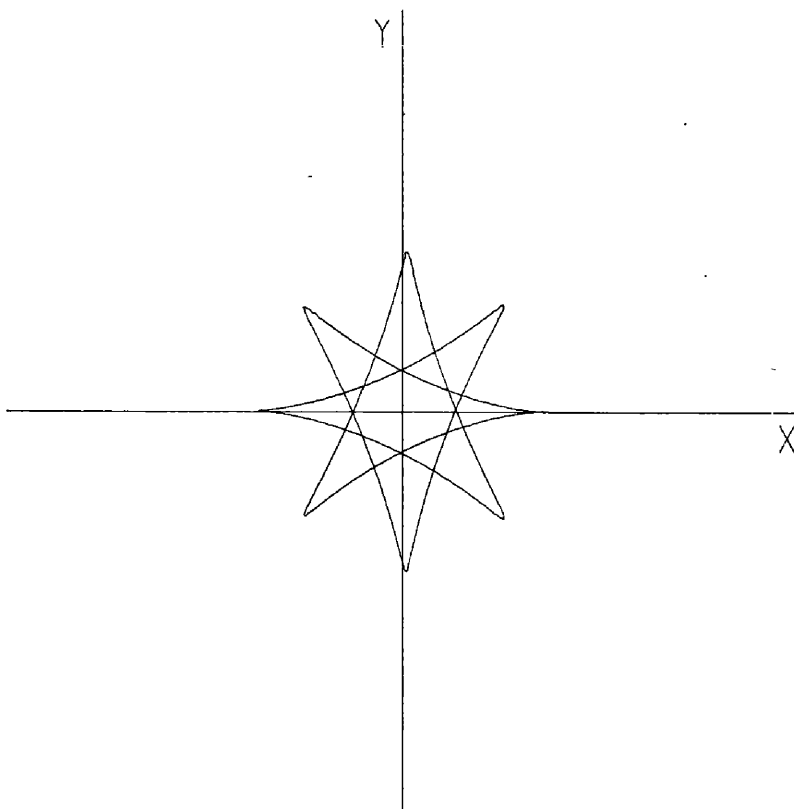


Fig. 4(d).

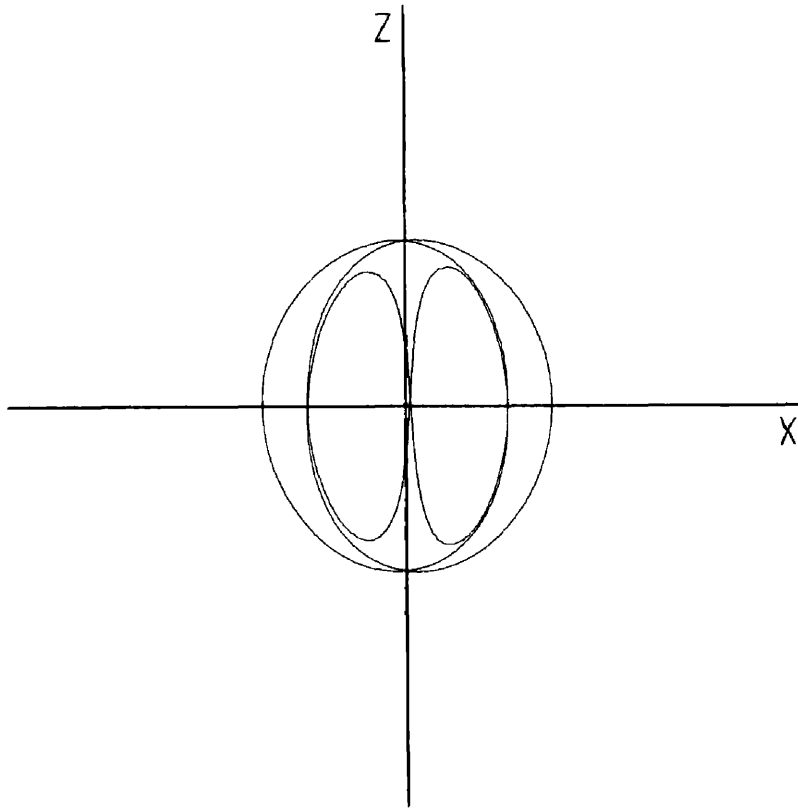


Fig. 4(e).

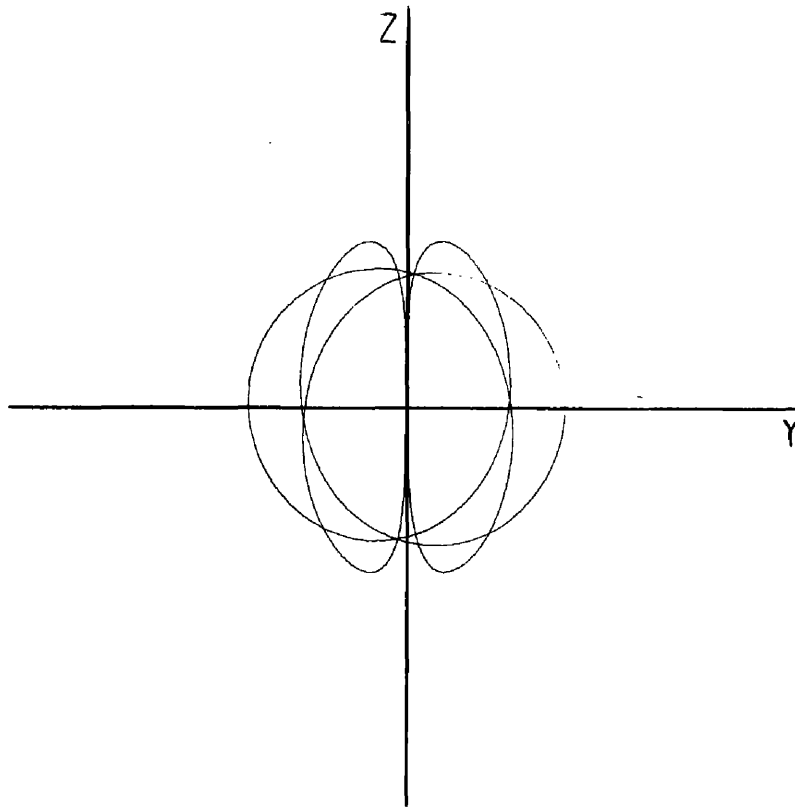


Fig. 4(f).

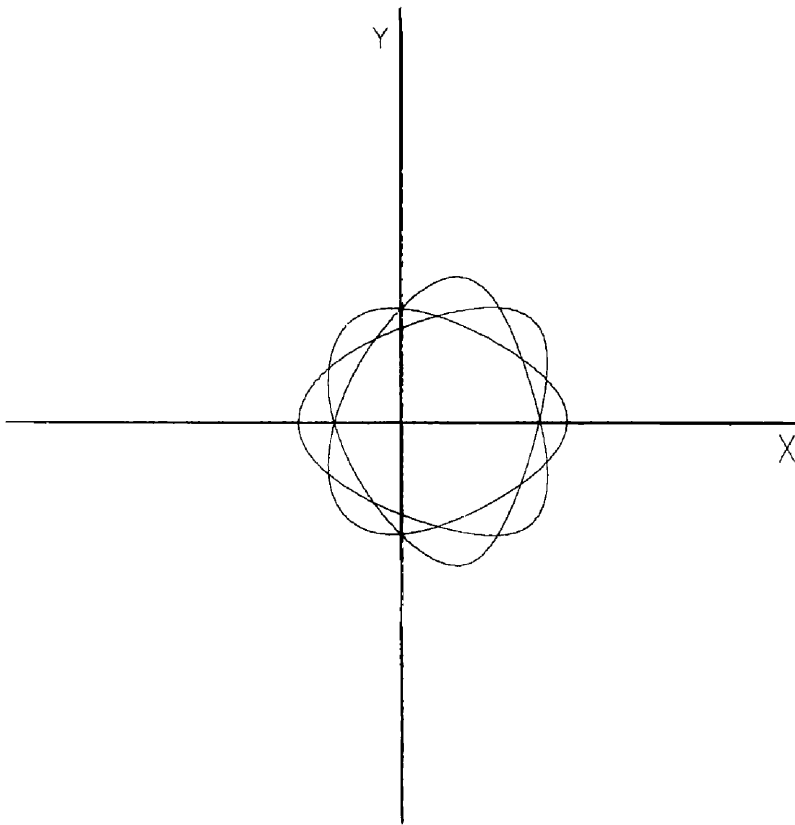


Fig. 4(g).

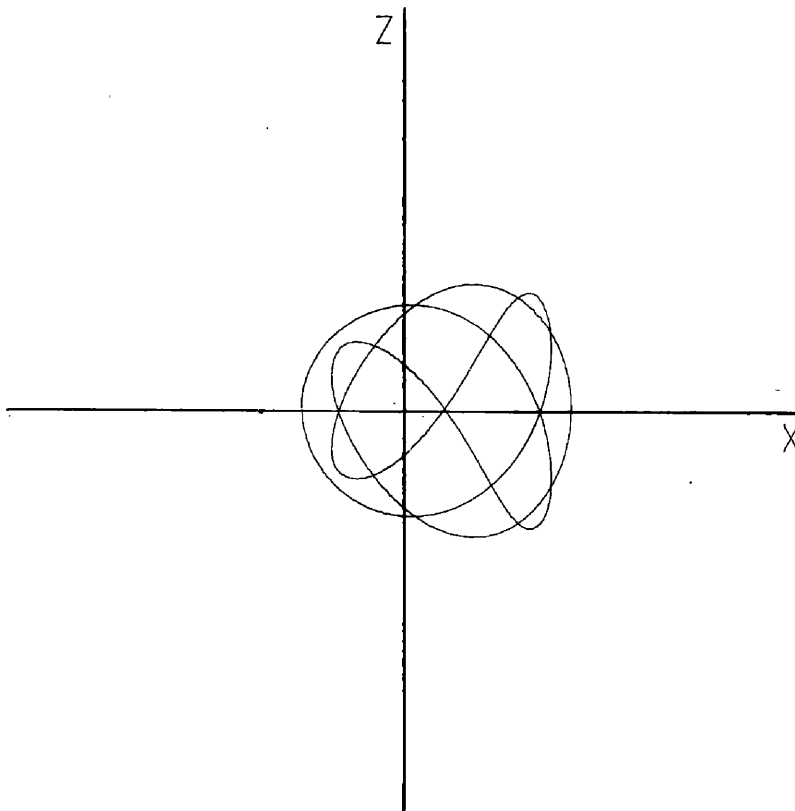


Fig. 4(h).

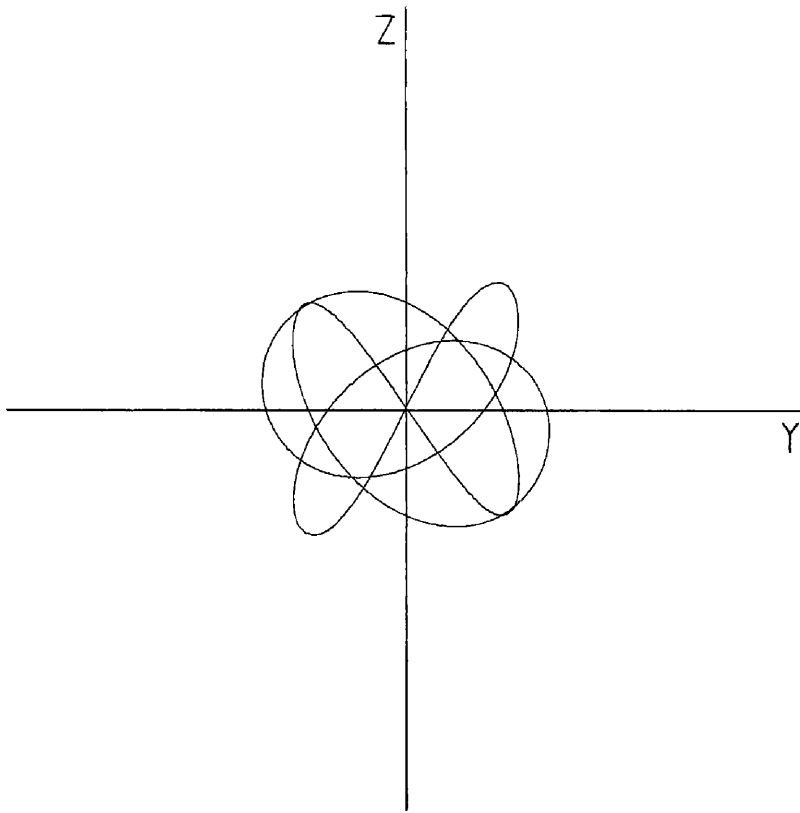


Fig. 4(i).

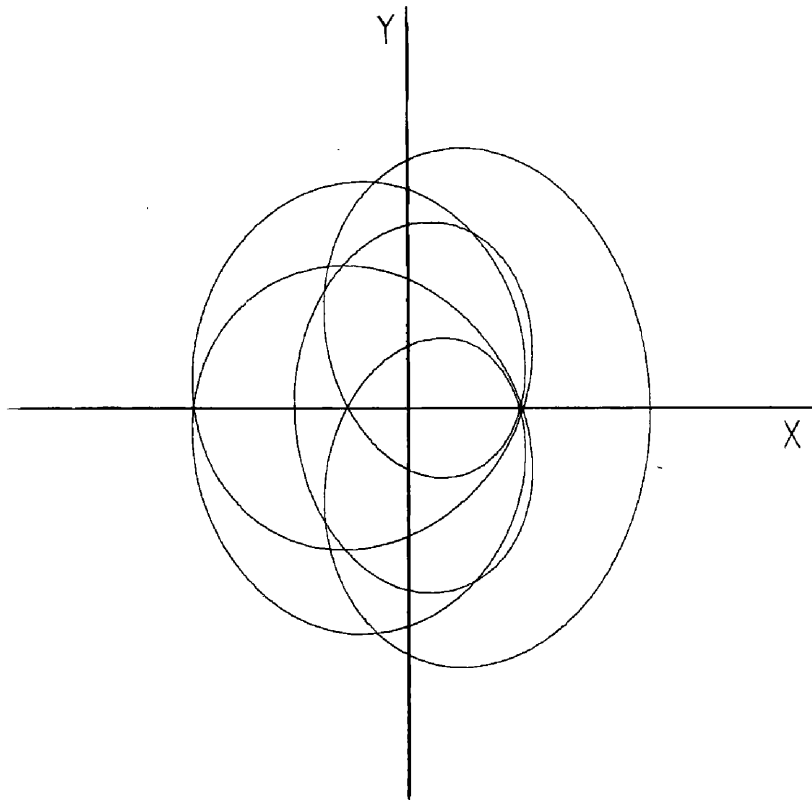


Fig. 5(a).

Figs. 5(a)–(g). Typical orbits of family  $F_{v15}^{1(p)}$ . Figures 5(a)–(c) are the  $(X, Y)$ ,  $(X, Z)$  and  $(Y, Z)$  projections of an orbit belonging to the  $m = 5$  segment, and Figures 5(d)–(f) are the projections of a representative orbit of the  $m = 3$  segment. Figure 5(g) is a ‘three-dimensional’ projection of a double-periodic orbit near the termination of the family.

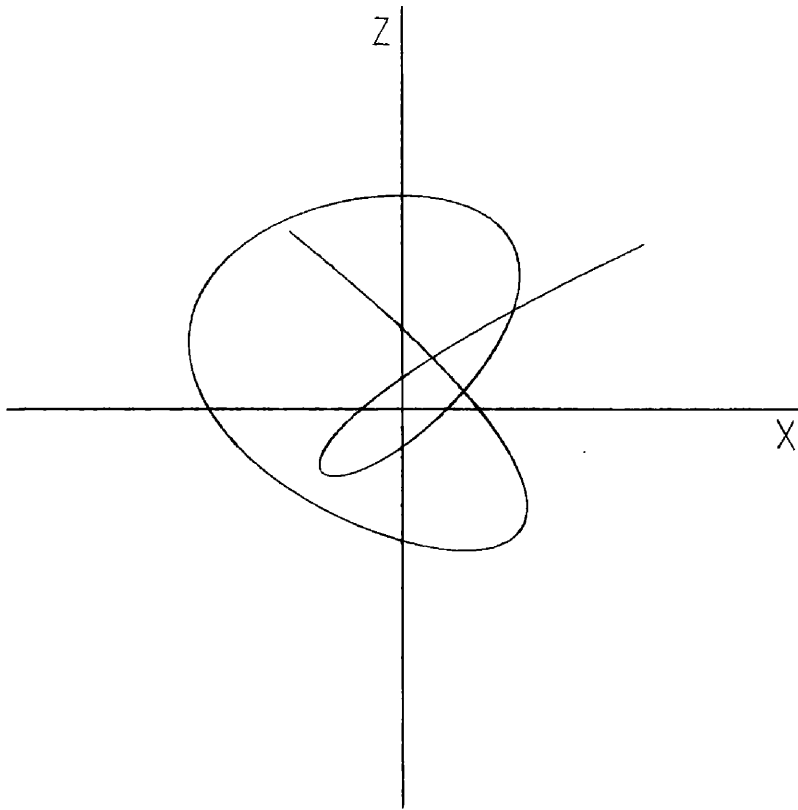


Fig. 5(b).

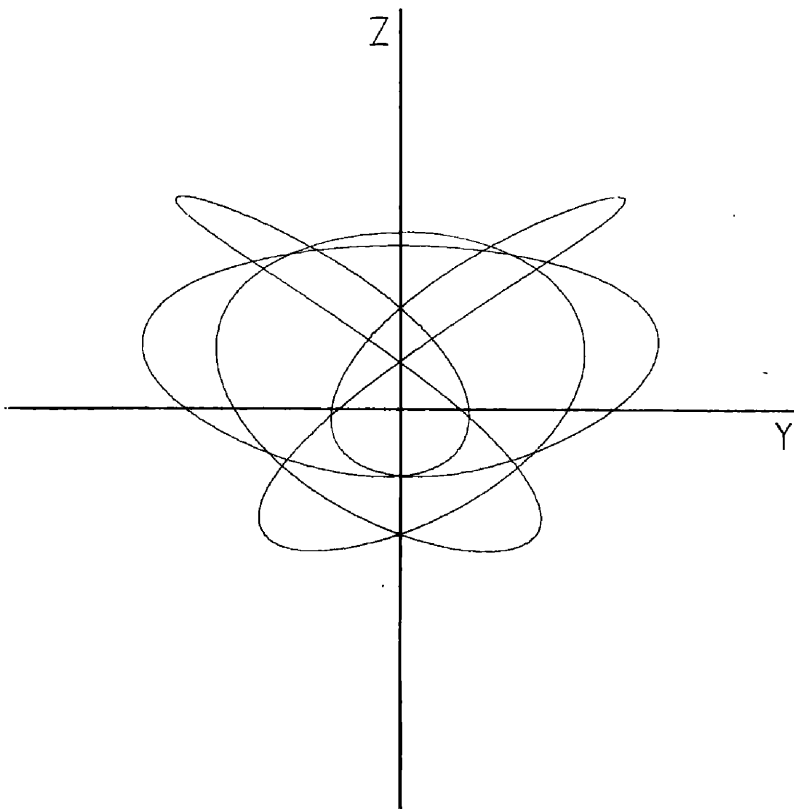


Fig. 5(c).

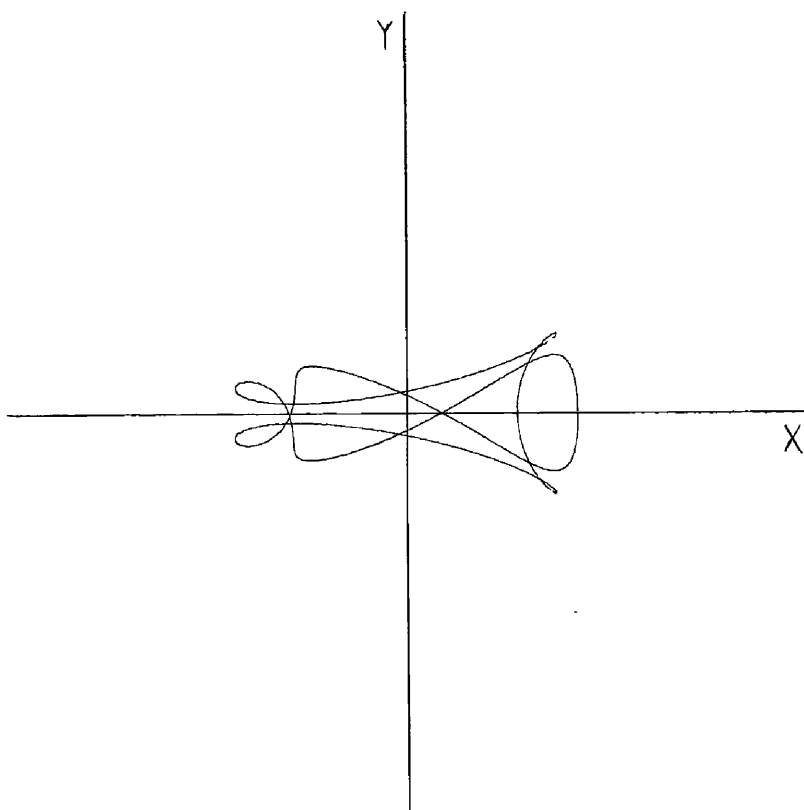


Fig. 5(d).

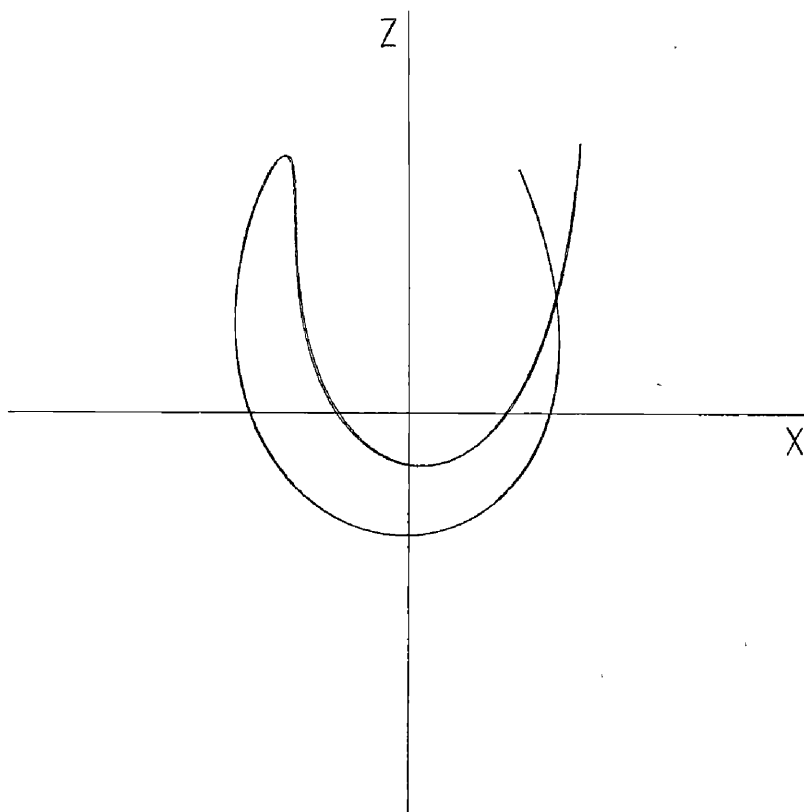


Fig. 5(e).

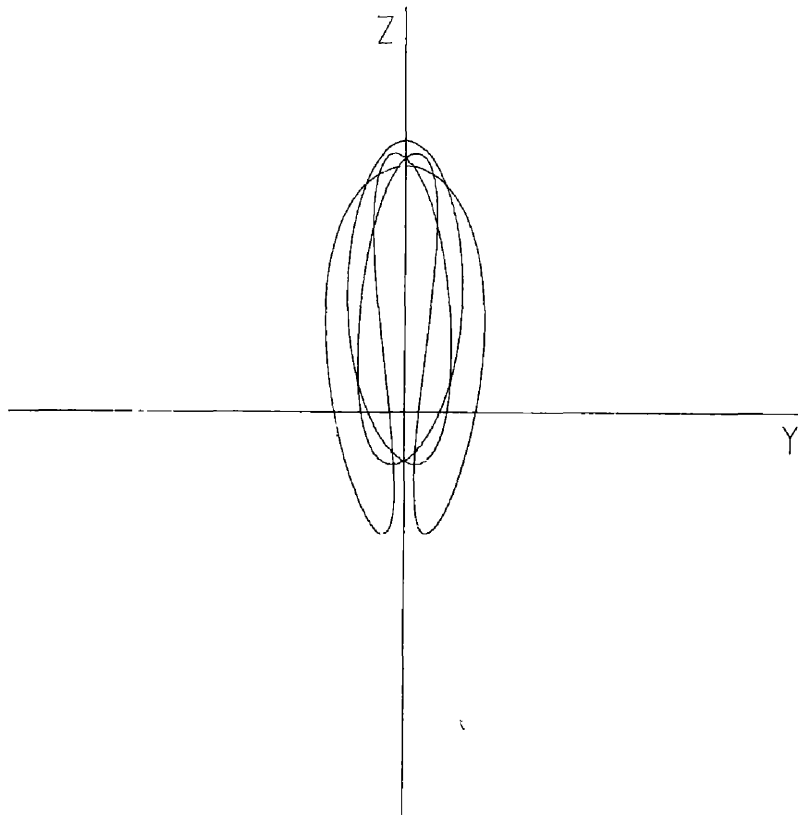


Fig. 5(f).

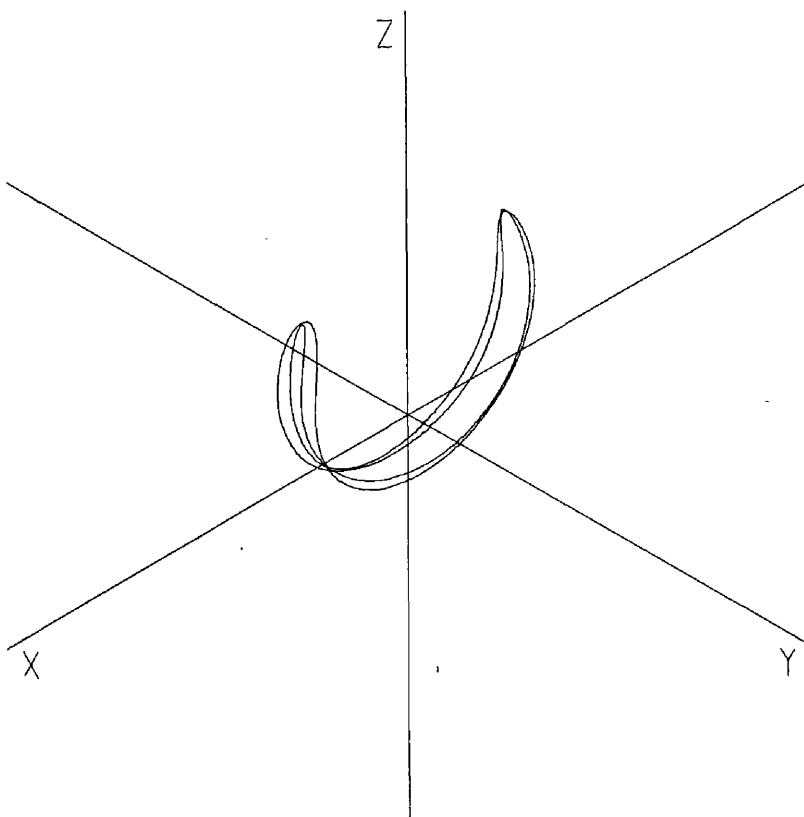


Fig. 5(g).

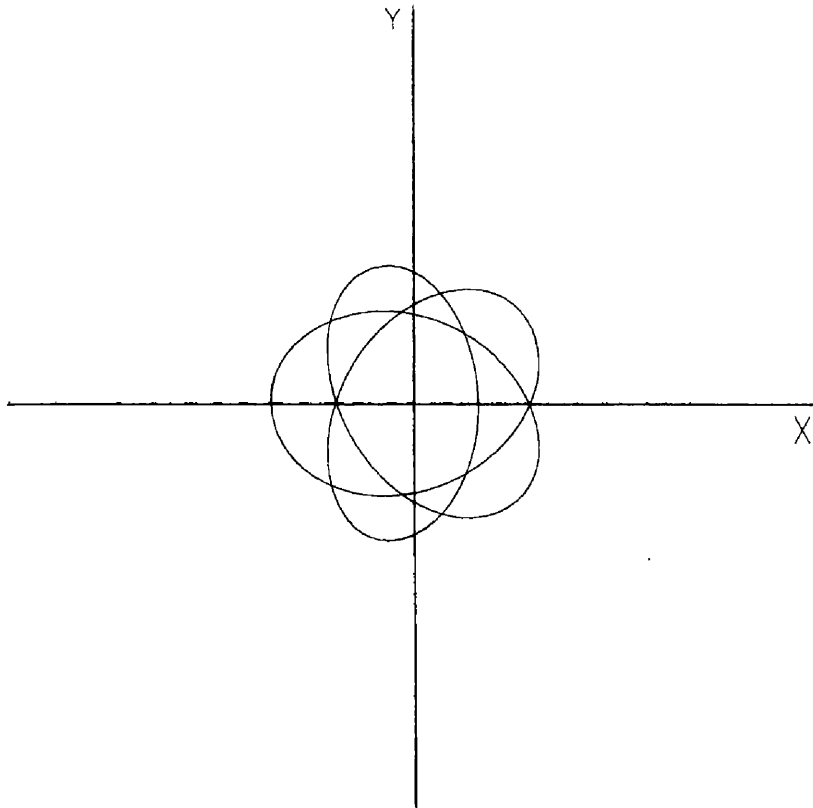


Fig. 6(a).

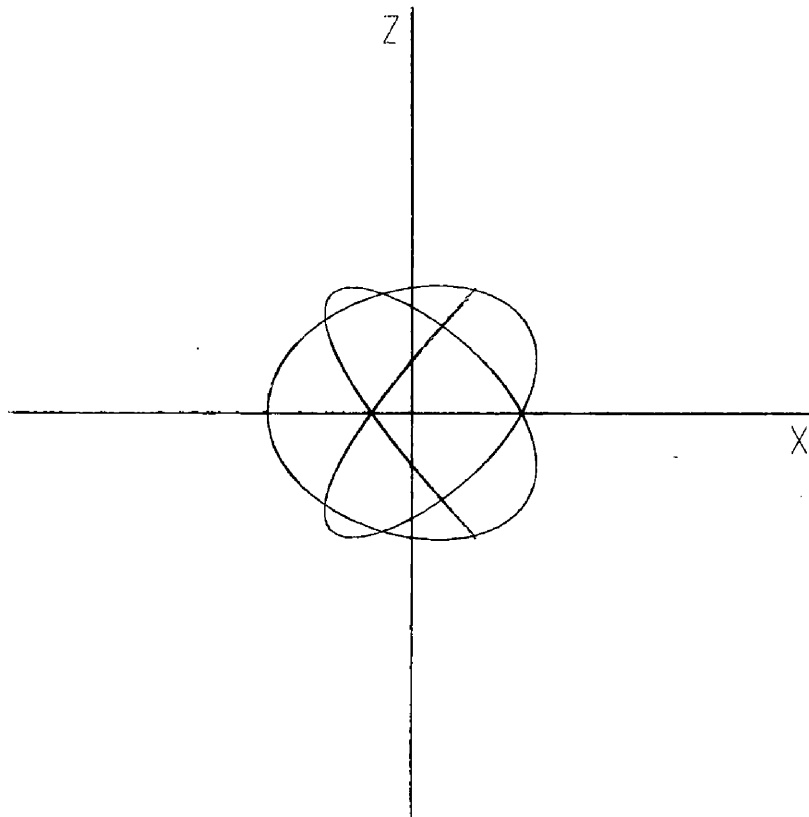


Fig. 6(b).

Figs. 6(a)–(f). Typical orbits of family  $F_{016}^{1(c)}$ . Figures 6(a)–(c) and 6(d)–(f) are the three plane projections of orbits representing the  $m = 6$  and  $m = 4$  segments of the family, respectively.

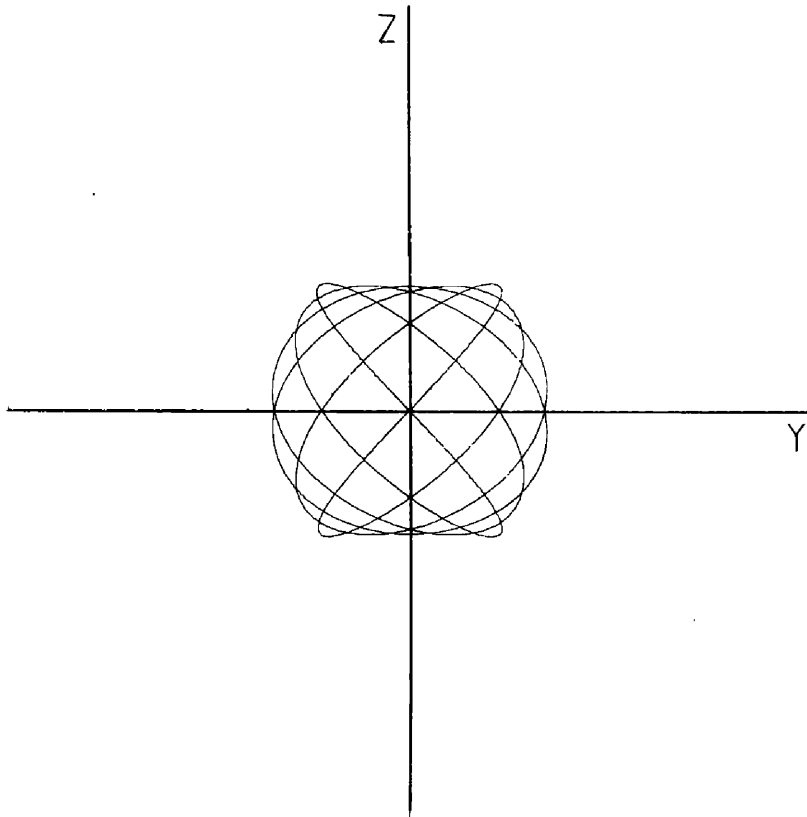


Fig. 6(c).

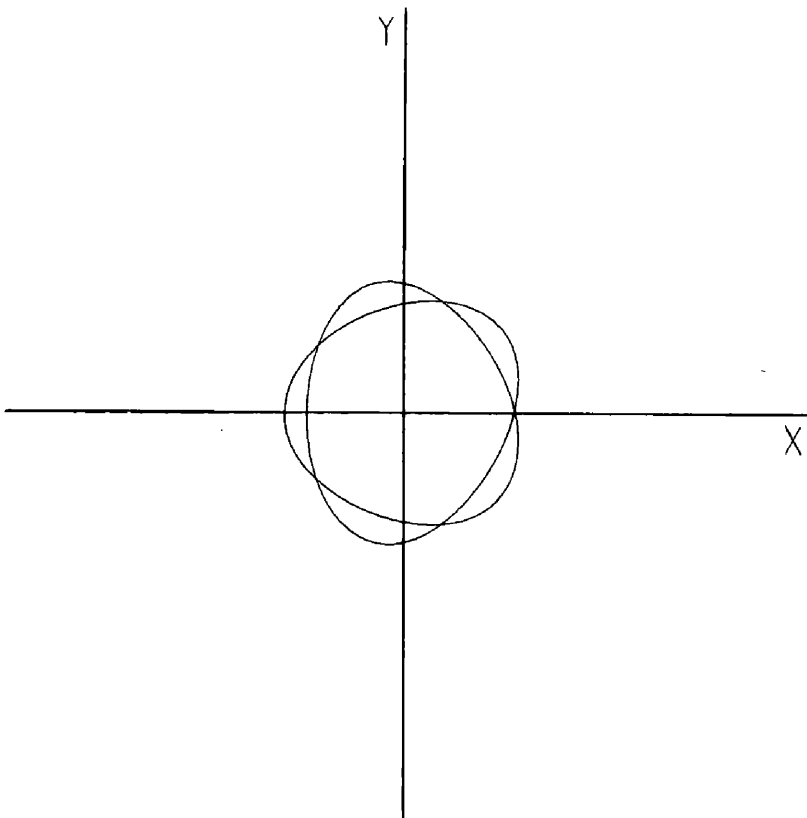


Fig. 6(d).

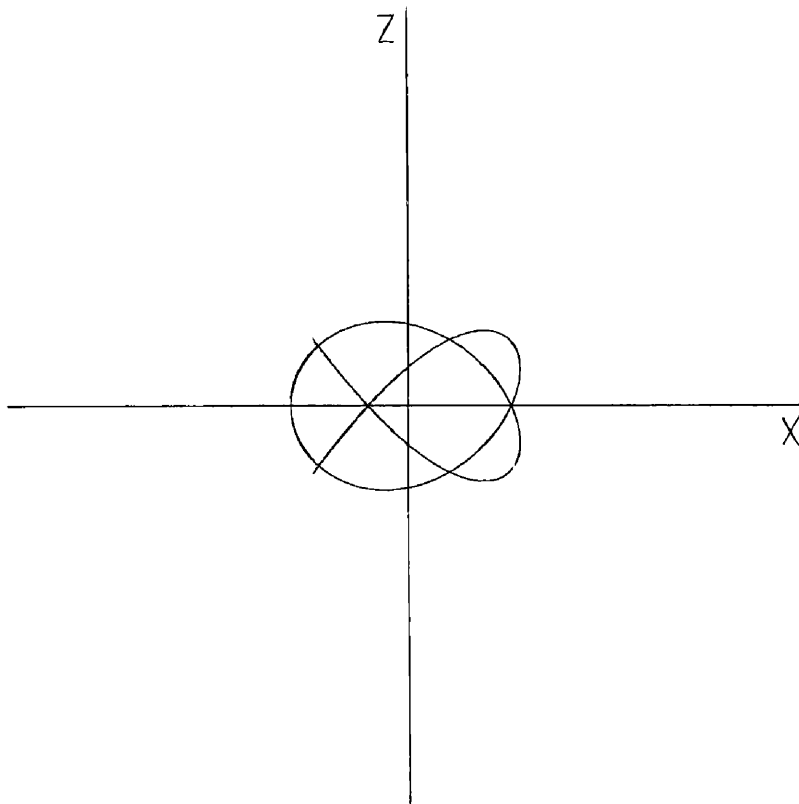


Fig. 6(e).

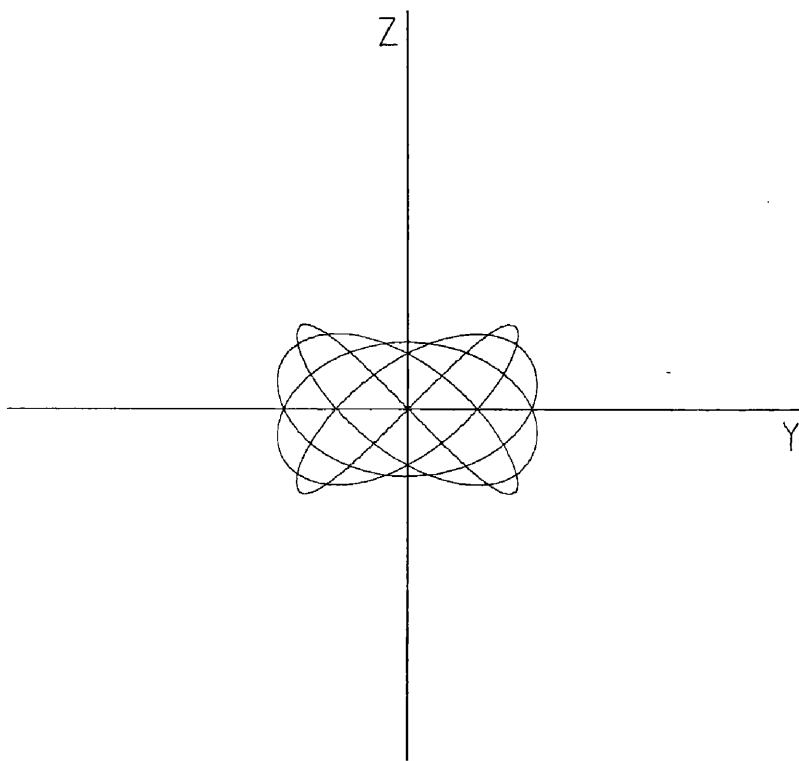


Fig. 6(f).

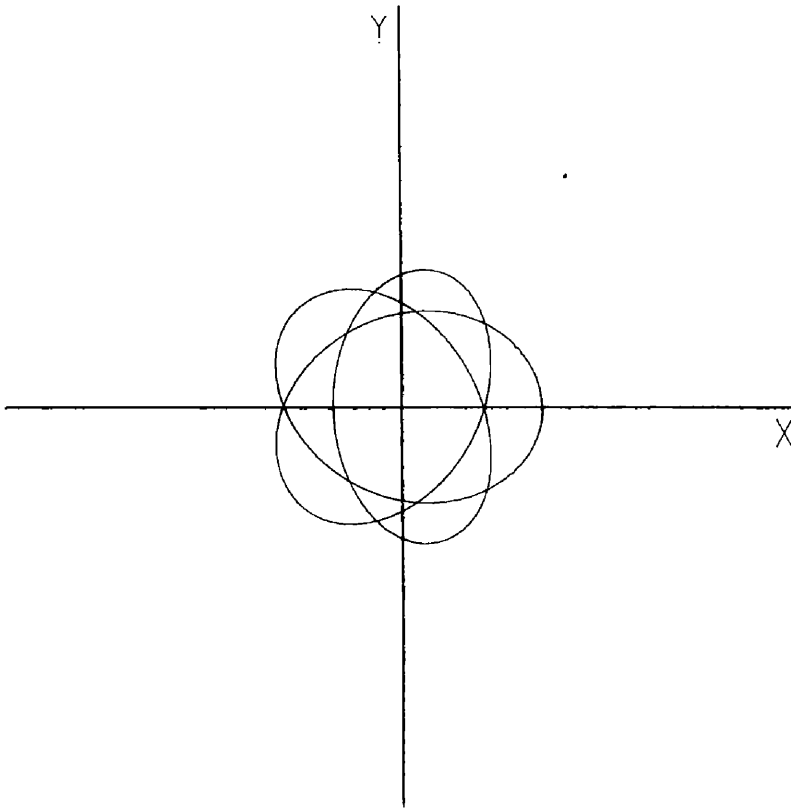


Fig. 7(a).

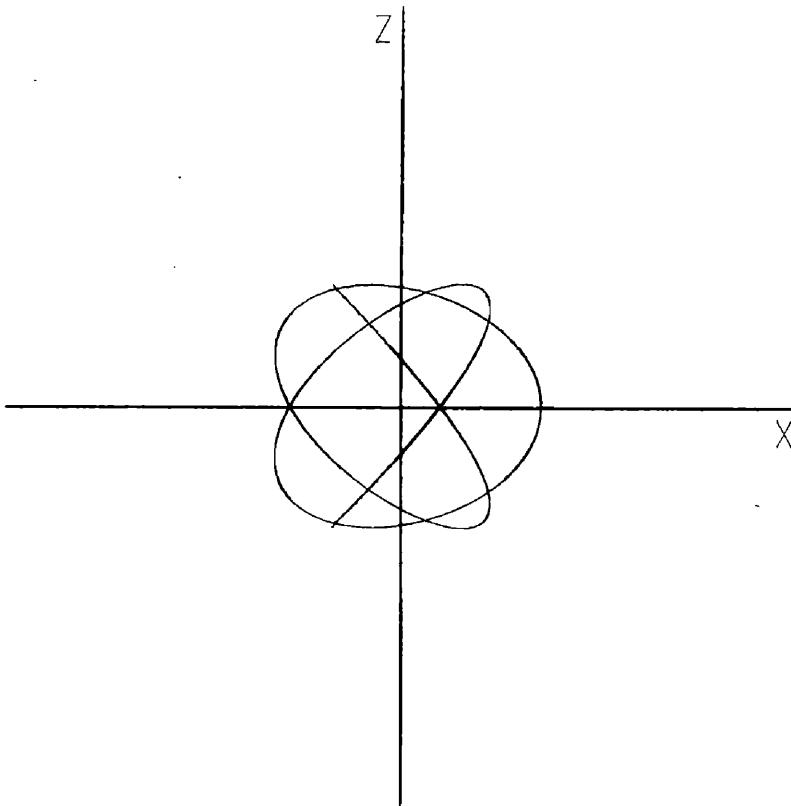


Fig. 7(b).

Figs. 7(a)–(b). A typical orbit of the  $m = 6$  segment of family  $F_{v16}^{1(o)}$ , in  $(X, Y)$  and  $(X, Z)$  projections. This orbit is almost the mirror image in the  $(Y, Z)$  plane of the orbit belonging to  $F_{v16}^{1(c)}$  plotted in Figures 6(a)–(c). The orbits of the quadruple segment of  $F_{v16}^{1(o)}$ , not plotted here, are similarly almost mirror-images of those belonging to the corresponding part of  $F_{v16}^{1(c)}$ .

### Acknowledgment

During the course of this work, one of the authors (IAR) was in receipt of an SRC studentship.

### References

- Hénon, M.: 1965, *Ann. Astrophys.* **28**, 992.  
Hénon, M.: 1969, *Astron. Astrophys.* **1**, 223.  
Hénon, M.: 1973, *Astron. Astrophys.* **28**, 415.  
Markellos, V. V.: 1974, *Celes. Mech.* **10**, 87.  
Markellos, V. V.: 1975, *Celes. Mech.* **12**, 215.  
Markellos, V. V.: 1980, *Astrophys. Space Sci.*, in press.  
Markellos, V. V., Moran, P. E., and Black, W.: 1975, *Astrophys. Space Sci.* **33**, 385.  
Roy, A. E. and Ovenden, M. W.: 1955, *Mon. Not. R. Astr. Soc.* **115**, 296.  
Szebehely, V.: 1967. *Theory of Orbits*, Academic Press, New York.  
Zagouras, C. G. and Markellos, V. V.: 1977, *Astron. Astrophys.* **59**, 79.